



Development and Assessment of Lightweight Walkable Pavement Slabs with Integrated Solar Panels

by

Sirwan Faraj

**BTEC, DIP, Construction Eng and the Built Environ, BSc, Civil Eng,
MSc, Structural Eng with Materials**

This thesis is submitted to fulfil the requirements for the Doctor of Philosophy degree at Nottingham Trent University, School of Architecture, Design, and the Built Environment.

October 2024

DECLARATION

This thesis has been submitted to Nottingham Trent University (NTU) to pursue a PhD degree. I hereby affirm that the research conducted in this thesis adhered to the regulations set forth by NTU and that it is entirely original, except any explicitly referenced sources. The study presented in this thesis was conducted at Nottingham Trent University from October 2020 to July 2024. The points of view in this thesis only reflect the author's perspective and do not represent the views of the university.

Sirwan Faraj (October 2024)

LIST OF PUBLICATIONS

PUBLISHED PAPER:

- Sirwan Faraj & Amin Al-Habaibeh. Investigating the Utilisation of Waste Sand from Sand Casting Processes for Concrete Products for Environmental Sustainability.

[Check the link: Energy and Sustainable Futures: Proceedings of the 3rd ICESF, 2022 | SpringerLink](#)

CONFERENCE PAPERS:

ADBE School Research Conference July 2022, Nottingham Trent University City Campus

1. Use of Recycled Materials within Concrete for Product Design Applications

Energy and Sustainable Futures: Proceedings of the 3rd ICESF conference, 2022

2. Investigating the Utilisation of Waste Sand from Sand Casting Processes for Concrete Products for Environmental Sustainability.

ABSTRACT

Sustainability plays a vital role in modern engineering, particularly in urban pavement design. This research explores the integration of solar energy with recycled materials to develop a durable and eco-friendly pavement solution. Existing solar pavement systems often struggle with durability and inefficient energy storage, limiting their practical use. To address these challenges, a novel solar pavement slab was developed, incorporating photovoltaic panels, batteries, and LED lighting within a lightweight concrete base enhanced with recycled materials.

A comprehensive experimental study was conducted to optimise the mechanical properties of foamed concrete (FC) for walkable pavement slabs. Various recycled materials, including waste foundry sand, recycled tyre steel fibres, and polystyrene, were incorporated to improve strength, reduce self-weight, and enhance sustainability. Waste foundry sand was partially replaced for normal sand, creating a more environmentally friendly concrete mix while minimising dependence on virgin materials. Results indicate that replacing 25% of fine aggregates with waste foundry sand increased compressive strength by 100% while reducing overall weight. Additionally, incorporating steel fibres and controlled quantities of recycled materials further enhanced structural performance. The final prototype, measuring $400 \times 400 \times 50$ mm, featured a tempered glass or acrylic optical layer over a photovoltaic module and was successfully tested under different environmental conditions. The findings confirm the feasibility of using lightweight foamed concrete with recycled materials to develop efficient and resilient solar pavements. This approach not only enhances the sustainability of construction materials but also supports environmental conservation by reducing carbon emissions. In situ testing demonstrated reliable LED lighting and battery charging performance during summer, with battery voltages averaging 4.19 volts overnight. However, reduced sunlight in winter led to minor declines in performance, highlighting the need for further optimisation. This study contributes to sustainable infrastructure development by integrating renewable energy into urban paving solutions and encouraging the use of recycled materials. Future research could focus on improving battery efficiency and extending applications to snow-melting systems and street lighting.

Keywords: Solar Panel Design, Pavement Slab, Sustainable Development, Mechanical and Electrical Investigation, Energy Efficiency, Recycled Material, Foam Concrete.

ACKNOWLEDGEMENT



In the name of ALLAH, the Most Gracious and the Most Merciful

First and foremost, I offer all praise to Allah for bestowing upon me health, patience, strength, countless blessings, and the opportunity and knowledge to successfully complete this PhD. I am deeply grateful to my beloved family, especially my mother and my wife, to whom I owe a great debt for their care, support, prayers, and patience throughout my studies. Completing this journey would have been impossible without them. I am fortunate to have a family that consistently cared for me, encouraged me, and provided guidance, endless love, and comforting hands, preparing me for my future. May Allah bless you all with joy and happiness.

This thesis was only completed with the support and encouragement of many people. I express my sincere gratitude to all who have helped me succeed. First and foremost, I acknowledge and thank my supervisor, Professor Amin Al-Habaibeh, for his exceptional supervision, encouragement, continuous guidance, feedback, freedom, and constant interest in my research area. I hope this partnership has been as memorable and enjoyable for you as it has been for me.

I also extend my sincere gratitude and appreciation to my supervisor, Dr. Amrit Sagoo, for his valuable feedback and kindness. Additionally, I am thankful to the technical laboratory staff members who supported my entire project effortlessly. A massive thanks to Matthew Garlick, Carl Smith, James Cooper, Truman Kerry, Quinn Emily, William Zindoga, and Hutton Ben for their assistance with material preparation and testing in the laboratory. Special thanks also go to Dr. Bubaker Shakmak and Sohaib Naseer for their help in formatting and organising the project using MATLAB. Finally, I would like to thank all my fellow PhD researchers in the School of ADDE.

Table of Contents

DECLARATION	II
LIST OF PUBLICATIONS	III
ABSTRACT	IV
ACKNOWLEDGEMENT	V
TABLE OF CONTENTS	VI
LIST OF FIGURES.....	XII
LIST OF TABLES.....	XVI
LIST OF ABBREVIATIONS	XVII
LIST OF NOTATIONS.....	XIX
CHAPTER 1: INTRODUCTION.....	20
1.1 RESEARCH MOTIVATION	20
1.2 SOLAR WALKABLE PAVEMENT SLABS	20
1.3 THE ROLE OF CONCRETE IN PAVEMENTS	22
1.4 THE ROLE OF RECYCLED MATERIALS WITHIN CONCRETE.....	24
1.5 AERATED CONCRETE	27
1.6 PROBLEM DEFINITION	28
1.7 AIM AND OBJECTIVES	29
1.7.1 Aim.....	29
1.7.2 Objectives	29
1.8 SCOPE OF THE RESEARCH.....	30
1.9 THESIS OUTLINE.....	31
CHAPTER 2: LITERATURE REVIEW	35
2.1 INTRODUCTION.....	35
2.2 ALTERNATIVE AND SUSTAINABLE MATERIALS IN THE CIVIL SECTOR	35
2.2.1 Expanded Polystyrene (EPS).....	38
2.2.2 Recycled Steel Tyre Fibre	40
2.2.3 Waste Foundry Sand (WFS).....	41
2.2.4 Superplasticizers.....	42
2.3 FOAMED CONCRETE.....	44
2.4 MODERN APPLICATIONS AND SUSTAINABILITY.....	47

2.5	MECHANICAL PROPERTY AND DENSITY OF LIGHTWEIGHT CONCRETE (LWC)	48
2.6	DEVELOPMENT AND INNOVATION OF LIGHTWEIGHT CONCRETE.....	49
2.6.1	<i>Types of Lightweight Concrete</i>	49
2.6.2	<i>Aerated Concrete</i>	50
2.6.3	<i>Specification</i>	52
2.6.4	<i>Foamed Concrete Development</i>	54
2.7	FOAMED CONCRETE CURRENT APPLICATIONS	56
2.8	PRODUCTION OF FOAMED CONCRETE	59
2.9	FOAMED CONCRETE METHODS	60
2.9.1	<i>Pre-Foaming Method</i>	60
2.9.2	<i>Mix-Foaming Method</i>	61
2.9.3	<i>Foaming Agent</i>	61
2.9.4	<i>Water</i>	63
2.9.5	<i>Ordinary Portland Cement</i>	64
2.9.6	<i>Fine Aggregate</i>	66
2.10	CONSIDERATIONS	67
2.11	TYPICAL PROPERTIES OF FOAMED CONCRETE	67
2.11.1	<i>Wet Density</i>	67
2.11.2	<i>Dry Density</i>	68
2.11.3	<i>Thermal Conductivity</i>	69
2.11.4	<i>Workability</i>	70
2.11.5	<i>Durability</i>	71
2.11.6	<i>Fire Resistance</i>	72
2.11.7	<i>Compressive Strength</i>	73
2.11.8	<i>Flexural Strength</i>	75
2.12	RENEWABLE ENERGY	76
2.13	PHOTOVOLTAIC SOLAR PANELS	77
2.13.1	<i>Types of Solar Panels</i>	79
2.13.2	<i>Benefits of Solar Panels</i>	80
2.14	SOLAR PAVEMENTS	81
2.15	SOLAR PAVEMENT STRUCTURE.....	82
2.16	EXISTING RESEARCH ON SOLAR PAVEMENTS.....	83
2.16.1	<i>Benefits of Solar Walkable Pavements</i>	93
2.16.2	<i>Solar Paving Bricks</i>	94
2.16.3	<i>Current Application of Solar Bricks</i>	95
2.17	SOLAR GARDEN LIGHTS	96
2.17.1	<i>Current Application of Solar Garden Lights</i>	96

2.18	CONCRETE.....	97
2.19	THE USE OF CONCRETE IN PAVEMENTS.....	98
2.19.1	<i>Benefits and Challenges of Using Alternative Materials in Concrete Pavements</i>	100
2.19.2	<i>Benefits of Using New Materials in Walkable Pavement Slabs</i>	100
2.19.3	<i>Challenges of Using New Materials in Walkable Pavement Slabs</i>	101
2.20	REFLECTION ON THE LITERATURE REVIEW	103
2.21	SUMMARY	108
CHAPTER 3: THESIS METHODOLOGY		110
3.1	INTRODUCTION.....	110
3.2	RESEARCH DESIGN AND RATIONALE.....	112
3.2.1	<i>Phase 1: Research and Material Development</i>	112
3.2.2	<i>Phase 2: Prototype Development, Experimental, and Numerical Validation</i>	114
3.2.3	<i>Phase 3: Construction, Integration, and Testing</i>	116
3.3	ETHICAL CONSIDERATIONS	118
3.4	SUMMARY	119
CHAPTER 4: FOAMED CONCRETE DESIGN AND EXPERIMENTAL STUDY		120
4.1	INTRODUCTION.....	120
4.2	MATERIAL SELECTION	121
4.2.1	<i>Standard Material</i>	121
4.2.2	<i>Fine Aggregate (Sand)</i>	121
4.2.3	<i>Ordinary Portland Cement (OPC)</i>	122
4.2.4	<i>Water</i>	123
4.2.5	<i>Foaming Agent</i>	124
4.2.6	<i>Waste Foundry Sand</i>	125
4.2.7	<i>Polystyrene</i>	126
4.2.8	<i>Recycled Steel Tyre Fibre</i>	126
4.2.9	<i>Superplasticisers</i>	127
4.3	EXPERIMENTAL DESIGN	127
4.3.1	<i>Foamed Concrete Mixing Design</i>	131
4.3.2	<i>Foamed Concrete Calculation</i>	131
4.3.3	<i>Material Selection to Produce Foamed Concrete</i>	132
4.3.4	<i>Mix Design</i>	133
4.3.5	<i>Examine Flowability</i>	134
4.3.6	<i>Density</i>	136
4.3.7	<i>Foamed Concrete Samples Production</i>	139
4.3.8	<i>Mechanical Analysis</i>	142

4.3.9	Summary	147
CHAPTER 5: FOAMED CONCRETE – RESULTS AND DISCUSSION		148
5.1	INTRODUCTION.....	148
5.2	EXPERIMENTAL DESIGN	148
5.3	RESULT ANALYSIS	149
5.3.1	<i>Compressive Strength</i>	149
5.3.2	<i>Effect of Replaced Recycled Materials on Compressive Strength</i>	151
5.3.3	<i>Effect of Density on Compressive Strength</i>	153
5.3.4	<i>Effect of Additives on Compressive Strength</i>	155
5.3.5	<i>Effect of Density with Various Recycled Materials on Compressive Strength</i>	156
5.3.6	<i>Flexural Strength</i>	158
5.3.7	<i>Flexural Strength of Normal and Foamed Concrete</i>	159
5.3.8	<i>Effect of Waste Foundry Sand (WFS)</i>	161
5.3.9	<i>Effect of Polystyrene</i>	163
5.3.10	<i>Relationship Between Compressive and Flexural Strength</i>	165
5.3.11	<i>Cracks Propagation</i>	168
5.4	PROPOSED SAMPLE SELECTION FOR FURTHER INVESTIGATION.....	171
5.5	SUMMARY	172
CHAPTER 6: DESIGN AND DEVELOPMENT OF SOLAR SLAB PROTOTYPE		174
6.1	INTRODUCTION.....	174
6.2	SOLAR PAVEMENT SLAB TRIAL ASSEMBLY DIAGRAM.....	175
6.3	TRAIL PROTOTYPE DESIGN AND FABRICATION	177
6.3.1	<i>Component System Design</i>	177
6.3.2	<i>Electrical Requirements</i>	177
6.3.3	<i>Electrical System Design</i>	178
6.3.4	<i>Trial Design of the Structural and Electrical Prototype</i>	186
6.3.5	<i>Walkable Solar Pavement Slab Trial Prototype</i>	187
6.4	SUMMARY	188
CHAPTER 7: EXPERIMENTAL AND NUMERICAL DESIGN OF SOLAR SLAB BASE		190
7.1	INTRODUCTION.....	190
7.2	STAGE 1: EXPERIMENTAL DESIGN.....	191
7.2.1	<i>Stage 1: Production and Fabrication</i>	192
7.2.2	<i>Solar Slab Construction</i>	192
7.2.3	<i>Profile Fabrication</i>	193
7.2.4	<i>Plywood</i>	193

7.2.5	<i>Grey Foam</i>	194
7.3	FOAMED CONCRETE SLAB MANUFACTURE	195
7.3.1	<i>Experimental Work Preparation</i>	195
7.3.2	<i>Flexural Analysis</i>	199
7.4	STAGE 2: NUMERICAL MODELLING.....	201
7.4.1	<i>ABAQUS Overview</i>	201
7.4.2	<i>Linear Finite Element Method (FEM)</i>	202
7.4.3	<i>Modelling Concrete Elastic Behaviour</i>	203
7.4.4	<i>Load Stepping Using (ABAQUS)</i>	205
7.4.5	<i>Method for Leaner Analysis Solution</i>	205
7.4.6	<i>Element Types in ABAQUS</i>	206
7.4.7	<i>Concrete Modelling</i>	206
7.4.8	<i>Embedded Model</i>	208
7.4.9	<i>Geometry</i>	210
7.4.10	<i>Loading and Boundary Conditions</i>	211
7.4.11	<i>Meshing</i>	213
7.5	SUMMARY	215
CHAPTER 8: EXPERIMENTAL AND NUMERICAL RESULTS AND DISCUSSION.....		216
8.1	INTRODUCTION.....	216
8.2	EXPERIMENTAL RESULTS AND DISCUSSION	216
8.3	NUMERICAL VALIDATION	220
8.3.1	<i>Linear Analysis Method</i>	220
8.3.2	<i>Load Deflection Analysis</i>	221
8.3.3	<i>Deflection Comparison</i>	223
8.3.4	<i>Stress and Strain of Concrete Slabs</i>	226
8.4	RATIONALE FOR SELECTING A SLAB WITH 50% WASTE FOUNDRY SAND	229
8.5	SUMMARY	230
CHAPTER 9: FINAL DESIGN AND EVALUATION OF SOLAR WALKABLE SLAB		232
9.1	INTRODUCTION.....	232
9.2	STRUCTURAL DEVELOPMENT.....	233
9.2.1	<i>Material Analysis</i>	234
9.2.2	<i>Traditional Slab Analysis</i>	234
9.2.3	<i>Mechanical and Functionality</i>	235
9.2.4	<i>Solar Pavement Slab Structural Design</i>	237
9.2.5	<i>Actual Prototype Design</i>	237
9.2.6	<i>Solar Walkable Slabs Assembly</i>	242

9.2.7	<i>Final Design of Solar Walkable Pavement Slab</i>	243
9.3	PHASE 2: ELECTRICAL ANALYSIS AND DISCUSSION	245
9.3.1	<i>Performance of the Solar Slab in Summer</i>	245
9.3.2	<i>Solar Panel Performance</i>	245
9.3.3	<i>Performance of LED Strip Lights</i>	246
9.3.4	<i>Battery Performance</i>	247
9.3.5	<i>Humidity and Temperature</i>	248
9.4	PERFORMANCE OF THE SOLAR SLAB IN WINTER	249
9.4.1	<i>Solar Panel Performance</i>	249
9.4.2	<i>LED Strip Light Performance</i>	250
9.4.3	<i>Battery Performance</i>	251
9.4.4	<i>Humidity and Temperature</i>	252
9.5	COMPARISON OF SOLAR PAVEMENT DESIGN WITH EXISTING MARKET PRODUCTS.....	254
9.6	SUMMARY	255
CHAPTER 10:	CONCLUSIONS.....	257
10.1	OVERVIEW	257
10.2	CONCLUSIONS	257
10.3	CONTRIBUTION TO THE KNOWLEDGE.....	260
10.4	RECOMMENDATIONS FOR FUTURE WORK	261
REFERENCES	263
APPENDIX A	287
APPENDIX B	289
APPENDIX C	290
APPENDIX D	292

List of Figures

Figure 1-1: (a) Solar Cycle Path in the Netherlands, (b) Solar Road Prototype Panel (Northmore, 2014)	21
Figure 1-2: Aerated Concrete Block (Bradfords Building Supplies, 2024).....	27
Figure 1-3: Thesis Structure.....	31
Figure 2-1: (a) Plastic Waste, (b) Recycled Rubber Tyre Fibre, (c) Glass Fibre, (d) Carbon Fibre, (e) Recycled Aggregate, (f) Fly Ash.....	38
Figure 2-2: (a) Polystyrene, (b) Waste foundry sand, (c) Recycle steel tyre fibre	42
Figure 2-3: Foam Generation Process (Raj, Sathyan, & Mini, 2019).....	46
Figure 2-4: Types of Foamed Concrete (Thakur et al., 2022)	50
Figure 2-5: The Components of Foamed Concrete (Raj, Sathyan & Mini, 2019).....	51
Figure 2-6: Lightweight Foamed Concrete Applications (www.dr-luca.com, 2009).....	57
Figure 2-7: Applications of Foamed Concrete (Beng, 2021)	58
Figure 2-8: Foam Production from Foam Generator (EAB Associates, 2001)	60
Figure 2-9: Density for Different Cement-to-Sand (C/S) Ratios (Nambiar & Ramamurthy, 2006)	74
Figure 2-10: Types of Solar Panels (Northmore, 2015)	78
Figure 2-11: Types of Solar Panels on the Market (The Eco Experts, n.d.).....	79
Figure 2-12: Layers of Solar Roadways (Rahman et al., 2017&Northmore & Tighe, 2016)	83
Figure 2-13: Solar Roadways (Scott Brusaw)	84
Figure 2-14: Hollow-Plate Solar Pavement Layers (Zha et al., 2016).....	85
Figure 2-15: Platino Solar Pavement (PLATIO Solar Paver) (https://www.smartpaverrenewableenergy.com/platio-solar-pavers/)	86
Figure 2-16: Solar Roadways (TNO, 2013).....	87
Figure 2-17: Netherlands Solar Cycle Path (SolaRoad, 2014)	88
Figure 2-18: Walkable Solar Pavement System (Onyx Solar)	89
Figure 2-19: Solar Highway in China ((Hossain et al., 2021)	91
Figure 2-20: (a) Solar Roadway, (b) Solar Concrete Slab Prototype (IFSTTAR).....	92
Figure 2-21: Examples of Solar Paving Bricks (https://www.exteriorlights.co.uk/product/Paverlight-solar-brick-light).....	94

Figure 2-22 Solar Brick (Solar Centre).....	95
Figure 2-23: Solar Garden Lights Available in the UK (Solar Centre)	97
Figure 2-24: Walkable Pavement Slab, (University of Leicester, 2023).....	99
Figure 3-1: The Project’s Methodology and the Research Stages.....	111
Figure 4-1: (a) River Washed Sand, (b) Ordinary Portland Cement	122
Figure 4-2: Normal Water.....	123
Figure 4-3: Foaming Agent and Foam Generator.....	124
Figure 4-4: Waste Foundry Sand, (b) Polystyrene, (c) Recycle Steel Tyre Fibre, (d) Superplasticiser	127
Figure 4-5: Foam Production Process for Foamed Concrete – (a) Foam Generator, (b) Foam, (c) Rotary Drum Mixer.....	134
Figure 4-6: Dimensions of Modified Marsh Cone.....	136
Figure 4-7: Designed Wet, Measured Wet, and Fully Dried Densities of Foamed Concrete.....	139
Figure 4-8: (a) Cube Moulds, (b) Prism Mould.....	140
Figure 4-9: Foamed Concrete Production and Moulds, (b) Rotary Drum Mixer	140
Figure 4-10: Experimental Samples in Moulds and During Curing.....	141
Figure 4-11: Examples of Weighing Samples – (a) Cube, (b) Prism	141
Figure 4-12: Examples of Weighing Cubes and Prisms	142
Figure 4-13: Cube Compression Test Using Hydraulic Compression Machine.....	143
Figure 4-14: Prisms Flexural Test Using Hydraulic Flexural Testing Machine.....	145
Figure 5-1: Compressive Strength vs. Density of Mortar Concrete and Foamed Concrete	151
Figure 5-2: Compressive Strength of Concrete Mixes with Varying Densities and Sand Ratios	152
Figure 5-3: Compressive Strength versus Density of Cubes with Recycled Materials	154
Figure 5-4: The Impact of Additives on Compressive Strength.....	156
Figure 5-5: Average Density of Samples with Lightweight Recycled Materials Replacement .	158
Figure 5-6: Applied Load versus Deflection for Control (Normal Mortar) and NFC Prisms ...	160
Figure 5-7: Maximum Applied Load versus Deflection for WFS Prisms	162
Figure 5-8: Maximum Load and Deflection of Prisms with Different Polystyrene Ratios	164
Figure 5-9: Applied Load versus Deflection for All Prisms.....	165
Figure 5-10: Relationship Between Compressive Strength and Flexural Strength	167

Figure 5-11: Mixture Components with Foundry Waste Sand – (a) 25%, (b) 50%, (c) 75%, (d) 100%	169
Figure 5-12: The Components of the Mixture: (e) Recycled Steel Tyre Fibre, (f) Polystyrene.	170
Figure 6-1: Base Design of the Prototype Solar Slab	174
Figure 6-2: Schematic Diagram of Devices Installed Within the Trial Sample Made with Grey Foam Base.....	176
Figure 6-3: Selected Solar Panel for the Prototype.....	179
Figure 6-4: Solar Panel and Its Specifications, Voltaic Systems (2017).....	179
Figure 6-5: (a) Solar Lithium Charger, (b) Lithium-Ion Rechargeable Battery(RS Components Ltd., 2023).....	181
Figure 6-6: Adafruit Trinket 3.3V MCU (RS Components Ltd., 2023).....	182
Figure 6-7: (a) LED Strip Light, (b) Mini PIR Sensor (RS Components Ltd., 2023)	184
Figure 6-8: Solar Slab with Transparent Top Layer	185
Figure 6-9: Assembly of Electronics and Data Loggers in Solar Slab Prototype Base	187
Figure 6-10: Solar walkable Pavement Slab Prototype	188
Figure 7-1: Solar Slab Production – (a) Slab Geometry, (b) Mold Fabrication, (c) Solar Slab Structure	191
Figure 7-2: Solar Pavement Slab with Profiled Base.....	193
Figure 7-3: Grey Foam Profile.....	194
Figure 7-4: (a) Preparation of Materials, (b) Concrete Mixture Drum	197
Figure 7-5: Casting of Slab Samples	197
Figure 7-6: De-moulding of the Slabs	198
Figure 7-7: Curing of Slabs in a Water Container	198
Figure 7-8: Removal of Grey Foam from Slab Cavity	199
Figure 7-9: Solar Slab Under Hydraulic Testing Machine	200
Figure 7-10: ((a) Plane Stress Quadrilateral Four-Node Element, (b) Eight-Node Linear Brick Element	207
Figure 7-11: Embedded Formulations for Concrete Mortar	208
Figure 7-12: Step-by-Step Process in ABAQUS Simulation	209
Figure 7-13: Solar Prototype Geometry.....	211
Figure 7-14: Boundary Conditions of the Solar Slab.....	212

Figure 7-15: Meshing of the Slab Base Model	214
Figure 8-1: Experimental Results for Concrete Slab	218
Figure 8-2: Flexural Test Under Universal Testing Machine (UTM)	219
Figure 8-3: Solar Slab Deflection Analysis – (a) Normal Concrete Mortar, (b) Foamed Concrete	222
Figure 8-4: Solar Slab Deflection Analysis Presented from Different Angles	223
Figure 8-5: Experimental Comparison of the Control Slab and the Slab with 50% WFS.....	224
Figure 8-6: ABAQUS vs Experimental Analysis for Control Sample	225
Figure 8-7: ABAQUS vs Experimental Analysis for Sample Made with WFS	225
Figure 8-8: ABAQUS vs Experimental Analysis Comparison.....	226
Figure 8-9: Numerical Stress Value, (a) Normal Concrete Slab, (b) Foamed Concrete Slab	227
Figure 8-10: Numerical Strain Value, (a) Normal Concrete Mortar, (b)Foamed Concrete	229
Figure 9-1: Final Product Solar Slab Design Made from Concrete-Based Material	233
Figure 9-2: Installation of Electrical Devices onto the Concrete Base.....	238
Figure 9-3: Data Loggers for Voltage and Temperature/Humidity Monitoring.....	241
Figure 9-4: Schematic Diagram Showing the Installation of Electrical Devices for Performance Monitoring	242
Figure 9-5: Final Prototype Prepared for Testing	243
Figure 9-6: Solar Pavement Slab Placed for Testing in Leicester, UK	244
Figure 9-7: Solar Panel Device Analyzed in August 2023 (Leicester, UK).....	248
Figure 9-8: Devices Analyzed in December 2023 (Leicester, UK).....	253

List of Tables

Table 2-1: Published Specification of Foamed Concrete in the UK (Beng, 2021).....	53
Table 2-2: Leading UK Researchers' Developments in Foamed Concrete (Hulusi et al., 2020) .	55
Table 2-3: Surfactant Types and Properties (Thakur et al., 2022).....	63
Table 2-4: Mechanical Properties of Foamed Concrete (Hamad, 2014)	74
Table 4-1: Design Mix for Standard Concrete Mortar.....	128
Table 4-2: Foamed Concrete Mix Design for Cubes with a Target Density of 1400 kg/m ³	129
Table 4-3: Foamed Concrete Design for Prisms with a Target Density of 1400 kg/m ³	130
Table 4-4: Experimental Calculations for Foamed Concrete	132
Table 4-5: Flow Time and Behaviour Classification (Jones et al., 2003).....	135
Table 4-6: Wet Plastic Density and Corresponding Dried Density	138
Table 4-7: Compressive and Flexural Test According to British Standard (BS)	146
Table 5-1: Compressive Strength of Foamed Concrete vs. Normal Concrete Cubes.....	150
Table 5-2: Compressive Strength of Concrete Cubes with Varying Densities and Sand Ratios	150
Table 5-3: Comparison of Measured Density Against Target Density of Sample	157
Table 5-4: Maximum Load and Deflection for Prisms with Various Recycled Materials	159
Table 5-5: Compressive and Flexural Strength Calculations for Cubes and Prisms	166
Table 7-1: Slab Design Incorporating Different Percentages of Recycled Materials and Additives	196
Table 7-2: Modulus of Elasticity of Normal and Foamed Concrete (Beng, 2021).....	204
Table 8-1: Flexural Strength and Deflections of Slabs.....	217
Table 9-1: Mechanical Properties of Traditional Slab Material (Neville, 2011).....	235
Table 9-2: Mechanical Properties of the Current Solar Pavement Slab	236
Table 9-3: Acrylic Plastic Technical Data (PPMA, Technical Datasheet).....	237
Table 9-4: Comparison of Market Products with the Developed Solar Slab.....	255

List of Abbreviations

AC	Aerated concrete
ACI	American Concrete Institute
AEA	Air-entraining agent
ASTM	The American Society for Testing and Materials
BCA	British Cement Association
BEIS	Business, Energy, and Industrial Strategy
BS	British Standard Institution
CO	Control
CSP	Concentrated Solar Power
CTU	Concrete Technology Unit
DC	Direct Current
EPS	Expanded Polystyrene
FC	Foam Concrete
FEA	Finite Element Analysis
GHGs	Greenhouse Gases
GW	George Washington University
HAUC	Highway Authorities and Utilities Committee's
IEA	International Energy Agency
IRENA	International Renewable Energy Agency
LAC	Lightweight Aggregate Concrete
LCA	Life Cycle Analysis
LED	Light-Emitting Diode
LWC	Lightweight concrete
LWFC	Lightweight foamed concrete
MPPT	Maximum Power Point Tracking
NC	Normal concrete
NFC	Normal foam concrete
OPC	Ordinary Portland Cement's
PMMA	Polymethyl Methacrylate

PO	Polystyrene
PV	Photovoltaics
RSTF	Recycled Steel Tire Fibre
SPs	Superplasticizer
SR	Solar Roadways
TNO	The Netherlands Organization
WFS	Waste Foundry Sand

List of Notations

A_c	The cross-sectional area of the specimen
B	Width of the slab
D	Effective depth of the slab
D_{dry}	Density of foamed concrete
D_{wet}	Density of foamed concrete
E	Modulus of elasticity
F	Maximum load at the time of failure
F_{cd}	Design compressive strength of concrete
F_{ck}	Characteristic value of concrete cylinder compressive stress
f_r	Flexural strength of concrete
L	Length of specimen
M_1	Mass of the container and the foamed concrete sample in kilograms,
M_2	Mass of the empty container in kilograms,
V	Volume of the container in cubic meters
W/C	Water to cement ratio
w_{ct}	Weight of cement in the batch, in kilograms
w_{da}	Weight of dry aggregate in the batch, in kilograms
ρ_m	Target plastic density in kg/m ³
ρ_{dry}	Target dry density in kg/m ³
ρ_{wet}	Measured wet density in kg/m ³

Chapter 1: Introduction

1.1 Research Motivation

For years, most of the materials currently used on roads and highways have remained unchanged. Solar pavement is a new technology with significant potential for making transportation and energy production more environmentally friendly. Scott and Julie first proposed this concept in (2006) leading to the formation of the company Solar Roadways (SR), according to Hu et al., (2021a). This innovation suggests the possibility of turning our roads into energy-generating assets, which could help balance electricity use and alleviate stress on traditional power grids.

Recent advancements have focused on making pavements more sustainable in various ways. Increasingly, recycled materials such as glass, asphalt shingles, recycled asphalt pavements, recycled rubber tyres, and other additives in asphalt mixes, as well as recycled materials within concrete, are being incorporated into pavements.

A study by Thompson et al. (2021) examined the durability and efficiency of solar cells in photovoltaic pavements. The research concluded that it is possible to achieve acceptable efficiency levels with solar cells integrated into pavement surfaces without significantly compromising the pavement's structural integrity. However, issues such as temperature fluctuations, surface wear, and load-bearing capacity remain major challenges. Additionally, solar cells are more expensive and require more complex installation compared to conventional road surfaces, resulting in higher

1.2 Solar Walkable Pavement Slabs

Solar pavement represents a significant development in utilising solar energy by integrating photovoltaic cells directly into pavement materials, allowing roads and pathways to generate electricity from sunlight. Solar pavement was first introduced in the early 2010s to utilise vast areas of pavement surfaces for energy production, particularly in urban and heavily populated areas (Erdiwansyah et al., 202). Solar energy, a key component of renewable energy sources, is expanding in applications ranging from basic rooftop panels to urban infrastructure. This advancement is best illustrated by the development of solar pavements, which demonstrate the synergy between energy technology and civil engineering. Harvesting solar energy from the pavement is a novel approach that combines the utility of road surfaces with renewable energy technology (Northmore & Tighe, 2012a).

Solar pavements embed photovoltaic cells within a robust, transparent surface material capable of withstanding vehicle and pedestrian traffic stresses. The electricity generated can be used for various purposes, such as powering streetlights and traffic signals, charging electric vehicles, providing energy to surrounding buildings, and feeding into the electrical grid (Baiju and Yarema, 2022). The main challenges for solar pavements include maintaining solar cell efficiency in varying weather conditions, ensuring longevity, and achieving cost-effectiveness (Ardani et al., 2021).

Solar Road is an experimental cycling path in the Netherlands that generates sustainable energy using solar panels on the pavement surface. A 70-meter stretch of cycle path was completed in November 2014 (Renewable Energy World, 2014). The roadway consists of a 2.5 by 3.5-meter prefabricated sandwich panel with a top one-centimetre layer of rugged, textured, tempered glass over crystalline silicon solar cells and a base layer made of concrete. The road is designed to avoid soil damage expansion, and contraction caused by temperature changes. It includes a skid-resistant coating and is tilted slightly to ensure rain washes off dirt, mud, ice, and snow (Shekhar et al., 2015a). The Netherlands Organization (TNO) research institutions developed a solar road panel for cycling paths (see Figure 1-1c). The panel they built was 1.5 by 2.5 meters, consisting of a glass surface layer, crystalline silicon solar cells, and a concrete block housing. The trail installation in North Holland was expected to be completed in 2012, but it has yet to be finished (TNO, 2013; Northmore, 2014a). See Figure 1-1a for examples of concrete-based solar paving panels.



Figure 1-1: (a) Solar Cycle Path in the Netherlands, (b) Solar Road Prototype Panel (Northmore, 2014)

Despite the promising potential of solar pavement slabs in generating renewable energy, several notable limitations restrict their broader application. One significant limitation is that these solar slabs are typically constructed with concrete bases, making them heavy and difficult to handle. The installation process requires the use of very heavy machinery, which not only increases the complexity of the installation but also drives up costs due to the need for specialised equipment and labour. This logistical challenge can make the arrangement of solar pavement slabs impossible, especially in areas where access to heavy machinery is limited or where such machinery costs are prohibitive (Northmore & Tighe, 2012).

Another key limitation is the cost-effectiveness of solar pavement slabs. At the same time, they offer the dual functionality of serving as both pavement and a source of renewable energy, the high costs associated with their production and installation. Based on available information, the 70-meter stretch of the Solar Road cycling path in the Netherlands, which includes prefabricated solar panels embedded within the pavement, cost approximately €3 million to build. The high costs are largely due to the advanced materials used, including rugged, tempered glass and the integration of photovoltaic cells into the concrete base. This translates to around €43,000 per meter of solar road, making it a significant investment compared to traditional road construction (Erdiwansyah et al., 2020).

1.3 The Role of Concrete in Pavements

Concrete is one of the most essential construction materials globally, renowned for its strength, durability, and versatility. Composed mainly of cement, aggregates, and water, concrete provides excellent compressive strength, making it ideal for a wide range of construction applications, including buildings, bridges, and pavements. Its ability to be moulded into various shapes and sizes before hardening makes it a preferred choice for complex architectural designs and large-scale infrastructure projects.

In the context of paving, concrete is particularly valued for its durability and capacity to withstand heavy loads and harsh environmental conditions. Concrete pavements are known for their long lifespan, often exceeding 30 years with proper maintenance, and their resistance to deterioration from vehicular traffic. This makes them especially suitable for high-traffic areas, highways, and urban roads. Concrete's reflective properties also help reduce urban heat islands, contributing to more sustainable urban environments (Neville, 2011).

However, traditional concrete poses several challenges, particularly its significant weight and environmental impact. The production and transportation of conventional concrete require substantial energy and resources, and the process of cement manufacturing is a major contributor to carbon dioxide emissions. These factors have driven the exploration of more sustainable alternatives within the construction industry.

Researchers have extensively explored the use of recycled and composite materials in concrete to enhance sustainability and address some of these challenges. By incorporating recycled materials into new concrete mixes, the demand for virgin materials is reduced, and waste is diverted from landfills. Recycled concrete has shown comparable performance to traditional aggregates in various applications, including paving (Pacheco-Torgal et al., 2013).

Another innovative approach is the development of lightweight concrete, such as aerated concrete, which incorporates air bubbles or lightweight aggregates to reduce the material's overall density. This type of concrete is helpful in pavement applications where weight reduction is beneficial, such as in areas with less load-bearing requirements or where ease of handling and transportation are priorities. Lightweight concrete also offers improved thermal insulation and reduces heat transfer through pavement surfaces (Narayanan & Ramamurthy, 2000).

When these approaches are combined using recycled materials within lightweight concrete formulations, a more sustainable and efficient pavement solution emerges. Such concrete reduces the environmental footprint of construction and maintains the structural integrity and durability required for pavement applications. This makes it a promising option for creating solid pavement bases that are both environmentally friendly and capable of supporting the necessary loads for various types of traffic.

This combination of recycled and lightweight materials is particularly relevant for solar installations, where integrating solar panels with concrete bases made from these innovative materials can address issues such as the heavy weight of conventional solar slabs. By using lighter, more sustainable concrete alternatives, the logistical challenges and costs associated with the installation of heavy solar slabs can be mitigated. Similarly, in the case of solar bricks, which are often made of plastic, incorporating recycled or composite materials could address durability concerns. Using more robust and environmentally friendly materials can overcome plastic bricks' limitations, such as their susceptibility to damage under heavy loads. This approach enhances the

structural integrity of solar bricks and contributes to the overall sustainability of solar energy projects.

When these approaches are combined, using recycled materials within lightweight concrete formulations, a more sustainable and efficient pavement solution emerges. Such concrete reduces the environmental footprint of construction and maintains the structural integrity and durability required for pavement applications. This makes it a promising option for creating solid pavement bases that are both environmentally friendly and capable of supporting the necessary loads for various types of traffic.

Researchers have extensively explored the use of recycled and composite materials in concrete to enhance sustainability and address some of the challenges associated with traditional construction methods. This is particularly relevant for solar installations, where integrating solar panels with concrete bases that incorporate recycled materials can mitigate issues such as the heavy weight of conventional solar slabs. Using lighter, more sustainable concrete alternatives can reduce the logistical challenges and costs associated with installing heavy solar slabs.

Similarly, in the case of plastic solar bricks, which are often made of plastic, incorporating recycled or composite materials could address durability concerns. By using more robust and environmentally friendly materials, it may be possible to overcome the limitations of plastic bricks, such as their susceptibility to damage under heavy loads. This approach enhances the structural integrity of solar bricks and contributes to the overall sustainability of solar energy projects.

Solar pavement, which incorporates solar panels onto road surfaces, represents a creative innovation for researchers. This chapter investigates renewable energy innovations, focusing on the role of solar pavement systems in modern energy technology. Incorporating solar pavements into urban infrastructure signifies a move towards a more sustainable and integrated approach to urban design and development, marking progress in renewable energy technology.

1.4 The Role of Recycled Materials Within Concrete

Researchers have extensively explored the use of recycled and composite concrete materials to enhance construction sustainability. This approach is particularly relevant when integrating solar panels with concrete bases that incorporate recycled materials, addressing both environmental concerns and the durability challenges associated with solar installations. By combining recycled materials with concrete in the foundations of solar panels, it is possible to reduce waste, lower

production costs, and improve the overall sustainability of solar energy projects within the construction industry.

Concrete is one of the most widely used building materials on earth, known for its excellent mechanical properties, particularly its compressive strength. It is composed of cement, water, sand, and coarse aggregate. Its applications range from structural uses to pavers, curbs, pipes, and drains. Despite its advantages in terms of strength and stability, the heavy weight of concrete presents challenges in transportation, handling, and load-bearing requirements for underlying structures.

The primary aim of these investigations is to understand the properties of recycled and composite materials compared to conventional materials, focusing on their strengths and weaknesses (Bolden, Abu-Lebdeh & Fini, 2013). Achieving sustainability in the construction industry is increasingly vital, with recycled materials gaining popularity as sustainable components in concrete production. While durable and useful, traditional concrete has a high carbon footprint due to the energy-intensive manufacturing process of Portland cement. Incorporating recycled materials such as steel tyre fibre, polystyrene, and foundry sand can reduce concrete's environmental impact while retaining its structural integrity. The development of lightweight concrete, exemplified by foamed concrete, represents a significant advancement in construction materials. By introducing air pockets into the concrete mix, foamed concrete achieves reduced density, enhancing its insulation properties and ease of handling while also reducing the use of raw materials and the overall weight of structures.

Researchers are exploring ways to reduce the weight of concrete without significantly compromising its structural integrity by introducing recycled materials. This approach reduces the burden on global landfills and provides economically sustainable solutions. Using recycled elements such as expanded polystyrene (EPS), fly ash, and rubber from disposed tyres has significantly reduced the overall weight of concrete. With their lower density, these materials can replace typical aggregates, contributing to a lighter overall product (Makul, 2020).

Using lightweight concrete as the base material for solar slabs is central to this development. Lightweight concrete, with its low density but appropriate structural strength, is an excellent choice for solar pavement applications. It simplifies installation and reduces stress on the underlying infrastructure. Recycling waste construction materials conserves natural resources and energy, reduces solid waste, decreases air and water contaminants, and lowers greenhouse gas emissions. The construction industry can recognise and benefit from using recycled waste and composite

materials within concrete to produce lightweight concrete for various applications. Several recycled materials were investigated to be utilised in this reach, including:

1. Waste foundry sand

Metal foundries widely use metal casting, which requires a substantial amount of foundry sand. This sand is recycled and reused multiple times in these foundries before ultimately being disposed of through landscaping. Utilising foundry sand in other engineering applications can help address disposal challenges by repurposing the material (Bhardwaj & Kumar, 2017). Foundry sand is primarily composed of silica sand coated with burnt carbon and dust. Incorporating it into concrete can improve strength and other durability characteristics. (Ganesh Prabhu, Hyun and Kim, 2014) Foundry sand can be used as a partial or complete replacement for fine aggregates, promoting sustainable infrastructure by repurposing industrial waste. This approach reduces the concrete's density and contributes to more effective management of industrial waste. This research explores the potential civil engineering applications of foundry sand, demonstrating that they are both technically feasible and environmentally safe. This study examines the effect of foundry sand as a replacement for fine particles on compressive and flexural strength in concrete mixtures. Using waste foundry sand in the concrete mix for the solar base is a noteworthy aspect of this innovation.

2. Polystyrene

Expanded polystyrene (EPS) is an innovative material used to develop lightweight concrete composites. Incorporating EPS in concrete offers environmental benefits, such as recycling polystyrene waste and producing lightweight concrete structures that reduce material consumption and carbon footprint. Additionally, the enhanced thermal insulation properties of EPS concrete contribute to energy-efficient buildings, significantly improving thermal insulation, structural efficiency, and environmental sustainability in line with construction industry goals (Cadere et al., 2018). Using recycled EPS in concrete prevents the material from ending up in landfills and helps create sustainable building materials. However, the environmental impact of producing EPS, a petroleum-based product, and the potential for microplastic pollution are critical factors that require careful management and further investigation (Kharun & Svintsov, 2017).

3. Recycle Steel Tire Fiber

The use of recycled steel tyre fibres in concrete is an innovative technique for enhancing the mechanical properties and durability of concrete while addressing environmental issues related to tyre waste (Aghaee et al., 2015). Steel fibres extracted from recycled tyres serve as reinforcing components in concrete mixtures, significantly improving various mechanical properties due to steel's high tensile strength. According to Thomas and Ramaswamy, incorporating 1.5% steel tyre fibre into the cement ratio of a concrete mixture increases tensile strength by 38% compared to standard concrete. Additionally, adding 1.5% steel fibres increases the modulus of elasticity by 8.3% in normal-strength concrete, 9.2% in moderately high-strength concrete, and 8.2% in high-strength concrete. These fibres act as micro-reinforcement, providing resistance against crack propagation and enhancing the tensile strength and toughness of the composite material.

1.5 Aerated Concrete

Aerated Concrete is made of sand, cement, and foaming agents and does not contain coarse aggregate. Typically, aerated concrete is produced by incorporating air into a slurry of cement and fine aggregate during mixing, resulting in random air pockets. This lightweight cellular concrete has a density between 400 and 1,850 kg/m³ (Amran, Farzadnia & Ali, 2015a). Aerated concrete, also known as foamed concrete, is recognised for its lower density, superior flowability, minimal cement requirement, and remarkable thermal insulation properties. Figure 1-2 indicates the examples of aerated concrete.

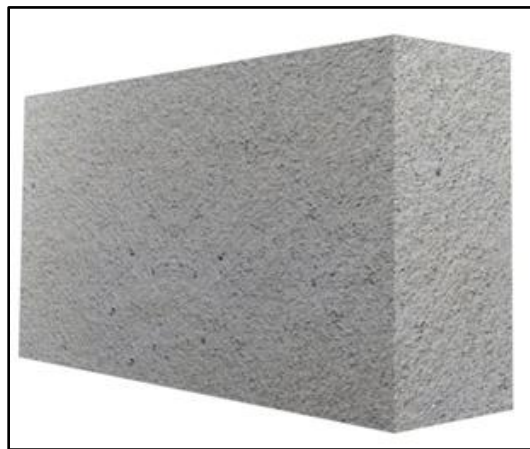


Figure 1-2: Aerated Concrete Block (Bradford's Building Supplies, 2024)

The infusion of air bubbles into the concrete reduces its weight, making it especially useful in applications where heavy machinery is not required for installation. Foamed concrete is a cost-effective option for fabricating large-scale, lightweight construction materials and components, such as structural elements, pavements, foundations, walls, filling gaps, foundry sand, a byproduct of the metal casting industry, has been used in this research as an alternative material to replace fine aggregates within the foam concrete. Previously considered a waste product, this sand can be repurposed, reducing landfill waste and providing a cost-effective alternative to natural sand in concrete mixes. Its use not only aids in waste minimisation but also contributes to the circular economy, where materials are reused and recycled to reduce environmental impact. and road embankment infill. Its efficient production process enhances its appeal for extensive use. Countries such as Germany, the United Kingdom, the Philippines, Turkey, and Thailand have extensively adopted foamed concrete in construction (Thienel, Haller & Beuntner, 2020).

Waste

1.6 Problem Definition

The existing solar pavement materials, such as concrete, are inherently heavy, imposing significant structural loads that can lead to subsidence and increased maintenance costs in urban areas. Their production and transportation generate substantial carbon emissions, while their reliance on virgin materials, such as natural aggregates, leads to resource environmental degradation. Additionally, existing solar pavements do not incorporate recycled materials or contribute to sustainable construction practices. Existing solar pavements, such as those installed in the Netherlands, are also limited by the use of heavy concrete bases embedded with photovoltaic (PV) cells, making them difficult to transport and install. These bases are primarily manufactured from virgin materials, raising further environmental concerns. While some solar pavement solutions, such as PLATIO Solar Pavers and Solar Brick Lights, integrate recycled materials, they remain limited in functionality and scalability, failing to provide a comprehensive solution for large-scale sustainable urban infrastructure. The construction industry, as a major consumer of raw materials, has a crucial role in addressing these challenges by adopting lightweight, recyclable materials to reduce environmental impact and enhance efficiency in urban development. In response to these limitations, this research proposes the creation of a solar pavement slab incorporating recycled materials and built-in electronic components to enhance durability, ease of installation, and energy

efficiency. This approach aims to provide a practical and scalable alternative to conventional and existing solar pavements, contributing to more sustainable urban infrastructure.

1.7 Aim and Objectives

1.7.1 Aim

The aim of this research is to develop sustainable, lightweight solar walkable pavement slabs using a foamed concrete base incorporating various percentages of recycled materials. The study includes experimental, numerical, and electrical analyses to evaluate the mechanical performance and feasibility of the proposed solution.

1.7.2 Objectives

To achieve the aim of this research, the following objectives will be undertaken to ensure the project is carried out accurately:

- 1.** To manufacture a range of foamed concrete cubes with target densities between 800 and 1400 kg/m³ incorporating different mix designs.
- 2.** To investigate the compressive and flexural behaviour of cubes and prisms containing various percentages of recycled materials such as waste foundry sand, polystyrene, and recycled steel tyres within foamed concrete.
- 3.** To investigate the deflections of the solar pavement slab base through experimental testing, analysing its structural response under a hydraulic testing machine to assess its performance.
- 4.** To investigate the deflection of the solar concrete slab numerically by simulating models with Finite Element Analysis (ABAQUS).
- 5.** To monitor the energy absorption and performance of the solar panels, battery, LED lights, and sensors integrated with the solar pavement slab, using data loggers to record and analyse variations in energy generation and consumption during winter and summer conditions.
- 6.** To monitor the humidity levels within the solar panel using an integrated humidity data logger, analysing variations in environmental conditions during both winter and summer to assess their impact on performance.
- 7.** To analyse the performance of the electrical components integrated into the solar pavement slab using MATLAB, based on data recorded via data loggers, evaluating their efficiency, functionality, and response under varying environmental conditions.

1.8 Scope of the Research

This research focuses on developing a walkable solar pavement slab by integrating photovoltaic (PV) technology into lightweight concrete. The project follows a structured process that includes design, material selection, manufacturing, and performance evaluation.

The first stage involves creating a draft design of the solar pavement slab using CAD software. This ensures that the structural layout accommodates embedded solar components without compromising functionality.

Next, mechanical testing is conducted on foamed concrete samples containing different recycled materials, including waste foundry sand, polystyrene, recycled tyre fibres, and superplasticisers. These tests determine the impact of material combinations on strength, self-weight, and durability, leading to the selection of an optimal mix design.

Once the best composition is identified, the manufacturing stage begins, where the solar pavement slabs are cast and prepared for testing. Experimental and numerical analysis is then performed to evaluate mechanical behaviour and structural performance. The numerical validation is carried out using Abaqus, where finite element analysis (FEA) is used to model and predict the structural response under applied loads. The experimental analysis includes physical load testing of the slabs to measure deflection and compare results with the numerical model. The deflection results from both methods are then compared to ensure the accuracy of the mechanical analysis and validate the reliability of the numerical simulations.

The final stage includes in-situ testing of the electrical performance of the slabs. Solar panels, batteries, sensors, LED lights, and data loggers are integrated into the design to monitor energy generation and efficiency under real environmental conditions during summer and winter.

This research provides a structured approach to developing a functional and durable solar pavement slab, ensuring its feasibility for urban applications.

1.9 Thesis Outline

Figures 1-3 explain the outline structure, which is evenly split into nine chapters, allowing for a more explicit focus on specific aspects of the research.

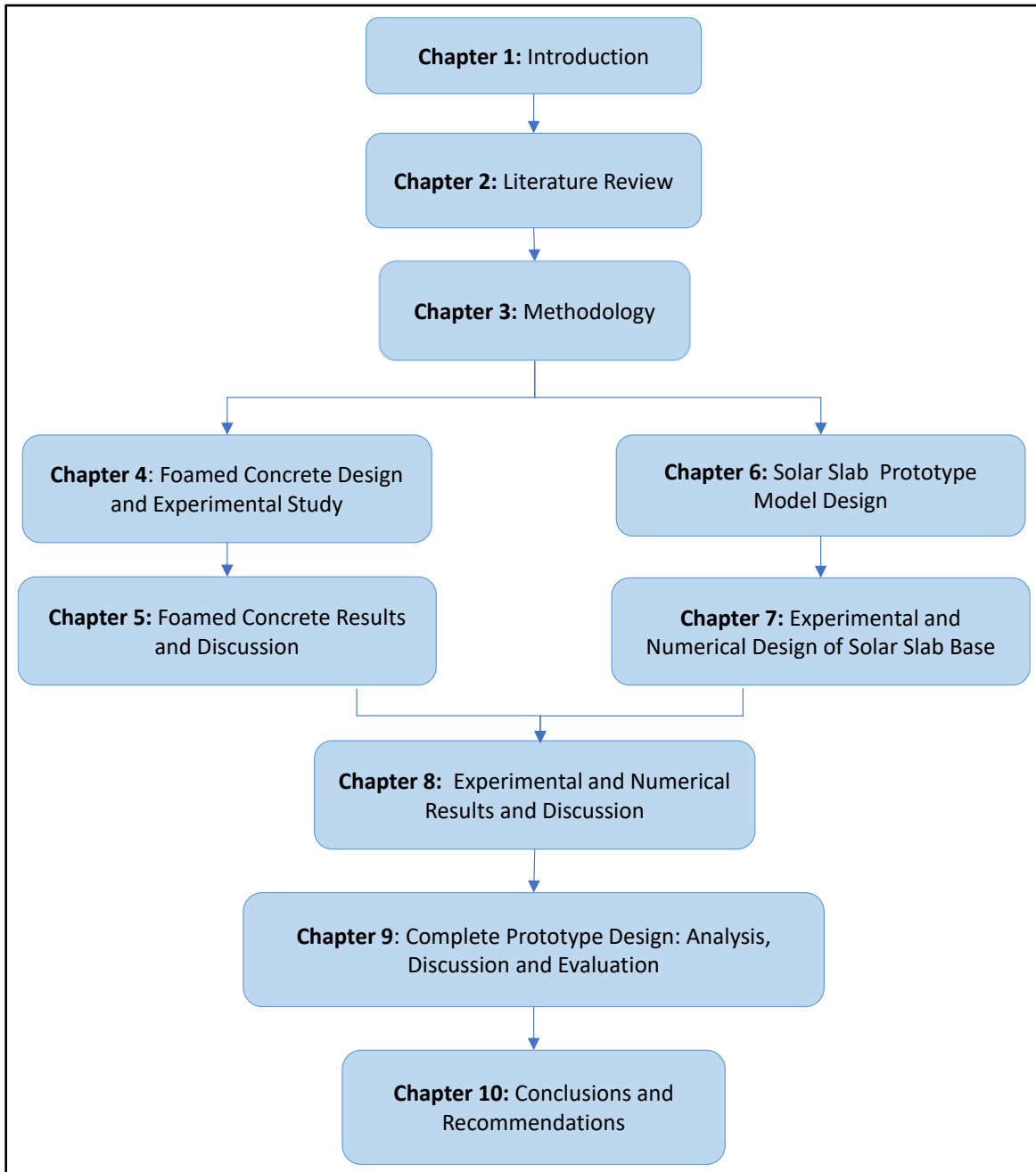


Figure 1-3: Thesis Structure

Chapter 1: Introduction

This chapter provides a foundation for the research by discussing the global need for renewable energy, mainly focusing on solar energy solutions. The chapter introduces the solar pavement concept, explaining the motivations behind the development of solar walkable slabs and the benefits of using recycled materials and foamed concrete. It outlines the overall objectives, aims, and significance of the research. Additionally, it provides a summary of the thesis outline and scope of the study, setting the stage for the upcoming chapters.

Chapter 2: Literature Review

This chapter explores existing technologies related to solar pavements and energy-harvesting infrastructure. It reviews relevant studies on solar energy integration, the use of recycled materials in construction, and the mechanical properties of foamed concrete. The literature provides insights into design principles, material selection, and structural challenges, establishing the theoretical framework for the thesis. The review identifies gaps in the current research, specifically in the application of solar pavements using recycled and lightweight materials. These gaps highlight the need for innovative approaches to address both sustainability and functionality, forming the basis for the current research.

Chapter 3: Methodology

This chapter outlines the methodology used to develop the solar pavement slab. It includes a detailed description of the CAD modelling and the design phase for both the foamed concrete and the solar slab. The chapter explains the step-by-step process of prototype development, material selection, and mechanical analysis. Both experimental and numerical testing methods are presented, with a focus on Finite Element Analysis (FEA) using ABAQUS to assess structural integrity and performance under various conditions.

Chapter 4: Foamed Concrete Design and Experimental Study

This chapter delves into the design of foamed concrete incorporating recycled materials, examining its mechanical properties such as strength, thermal insulation, and weight. The experimental procedure includes casting foamed concrete slabs and conducting tests to determine their performance under different loads and conditions. The goal is to establish an optimal mix of recycled materials and lightweight concrete for use in the solar pavement slab. The results of the

foamed concrete design are discussed, providing insight into its feasibility for solar pavement construction.

Chapter 5: Foamed Concrete Results and Discussion

This chapter presents the experimental results from the foamed concrete tests. It analyses the mechanical properties, durability, and overall performance of the foamed concrete under applied loads. The discussion explores the implications of these findings for the solar pavement slab design and compares them with the expected performance based on the literature. If the foamed concrete fails to meet performance expectations, potential modifications are considered.

Chapter 6: Solar Slab Prototype Model Design

This chapter focuses on the design of the solar slab prototype, integrating solar cells and electrical components into the foamed concrete base. It covers the CAD modelling and construction of the prototype, ensuring that all mechanical and electrical elements are properly embedded and function as intended. The process of constructing the model is described, including details of how solar cells, LED lights, and batteries are positioned within the slab.

Chapter 7: Experimental and Numerical Design of Solar Slab Base

This chapter covers both experimental tests and numerical simulations using Finite Element Analysis (FEA) in ABAQUS. It evaluates the mechanical performance of the solar slab base under different loads and operational conditions. If the slab exhibits early failure, alternative materials are considered to improve the design. The chapter concludes with a discussion of the test and simulation results, including any necessary design adjustments.

Chapter 8: Experimental and Numerical Results and Discussion

Detailed Analysis: This chapter presents the combined results of the experimental and numerical tests conducted on the solar slab. It evaluates the overall performance, structural integrity, and energy efficiency of the slab. The results are compared with benchmarks from existing literature, and their implications for the broader field of solar pavement technology are discussed.

Chapter 9: Complete Prototype Design: Analysis, Discussion, and Evaluation

Final Design Evaluation: The complete prototype is analysed based on all previous tests and simulations. The final design includes adjustments based on both mechanical performance and

energy generation capabilities. The chapter discusses the success of the design and evaluates whether the slab meets the project's objectives for sustainability, functionality, and durability.

Chapter 10: Conclusions and Recommendations

Summary of Findings: The final chapter summarises the research findings, highlighting the successful aspects of the solar pavement slab design and the challenges encountered. Recommendations for future research and improvements to the solar slab design are presented, along with suggestions for broader applications in urban infrastructure.

Chapter 2: Literature Review

2.1 Introduction

This chapter provides a comprehensive review with regards to the utilise of renewable energy and solar panels in the civil engineering sector, including the different types of solar panel applications for various purposes. Next, it examines the role of solar panels in pavement systems, analysing their benefits, challenges, and feasibility. The chapter then shifts focus to recycled materials in construction, exploring their mechanical properties and suitability for pavement applications. Finally, the review evaluates foamed concrete as a lightweight, sustainable solution in pavement engineering, emphasising its potential when combined with recycled materials. Through this structured review, the chapter aims to provide a thorough understanding of the latest advancements in integrating renewable energy and sustainable materials into civil engineering, inspiring future research and innovative applications in infrastructure development.

2.2 Alternative and sustainable materials in the civil sector

The construction industry has long been a cornerstone of urban development, facilitating the growth of modern infrastructure. However, its operations heavily depend on finite natural resources, leading to environmental concerns such as resource depletion, escalating carbon emissions, and increasing construction waste. These issues have driven a global shift toward sustainable practices in civil engineering, focusing on the adoption of innovative and eco-friendly materials. Pavements, pedestrian walkways, and structural components can significantly benefit from these alternative materials, which offer both environmental and structural advantages. The construction industry is a significant contributor to greenhouse gas emissions, primarily due to cement manufacturing, which accounts for roughly 8% of global carbon dioxide output. Addressing these challenges requires innovative solutions that not only conserve resources but also reduce environmental degradation and encourage waste recycling.

Incorporating sustainable materials into civil industry practices offers multiple environmental and economic benefits. For instance, fly ash and recycled aggregates reduce dependency on virgin resources and curtail emissions, while lightweight concrete and polystyrene contribute to energy-efficient buildings. These materials collectively minimise construction waste, lower production

costs, and enhance structural longevity, making them viable solutions for future infrastructure projects.

Lightweight concrete is increasingly employed in pedestrian pathways and pavement systems due to its low density and superior insulation properties. Formulated with lightweight aggregates such as expanded clay, shale, or polystyrene beads, this type of concrete decreases the overall weight of structures, enhancing their seismic resistance and reducing transportation expenses (Chandra & Berntsson, 2002). Additionally, lightweight concrete provides better thermal performance, resulting in improved energy efficiency, and is particularly advantageous in regions with weak soil conditions as it lessens the load on the foundation.

Fly ash, generated from coal combustion, is a widely recognised pozzolanic material that enhances the durability and workability of concrete. Substituting a portion of cement with fly ash lowers greenhouse gas emissions, mitigates heat of hydration, and improves resistance to sulfate attack (Pacheco-Torgal et al., 2011). Fly ash-based concrete is increasingly preferred in pavement construction and pedestrian-friendly infrastructure due to its cost-efficiency and long-term structural performance.

Recycled aggregates, sourced from demolished concrete and construction debris, offer a sustainable substitute for natural aggregates. Their application in road construction and pedestrian pathways reduces material costs and minimises waste disposal challenges (Tam et al., 2018). Although recycled aggregates may require stringent quality checks to match the performance of natural aggregates, they contribute to the conservation of raw materials and support the development of environmentally conscious infrastructure.

Recycled tyre fibre, extracted from waste tyres, enhances concrete's toughness and impact resistance. It is particularly beneficial in pedestrian walkways and pavement applications, improving slip resistance and reducing the risk of cracking under dynamic loads (Gupta et al., 2014). This material supports sustainable waste management and promotes eco-friendly construction. The flexibility of tyre fibre-modified concrete makes it suitable for areas subjected to frequent thermal fluctuations and heavy foot traffic (Gupta et al., 2014). It is particularly beneficial in pedestrian walkways and pavement applications, improving slip resistance and reducing the risk of cracking under dynamic loads (Gupta et al., 2014). This material supports sustainable waste management and promotes eco-friendly construction. The flexibility of tyre

fibre-modified concrete makes it suitable for areas subjected to frequent thermal fluctuations and heavy foot traffic.

Recycled tyre rubber is another innovative material in sustainable construction. Ground rubber particles can be incorporated into concrete to improve elasticity and reduce brittleness. Rubber-modified concrete enhances shock absorption and reduces surface noise, making it ideal for pedestrian pathways, playgrounds, and sports courts. It also diverts significant amounts of waste tyres from landfills, contributing to better waste management practices (Ganjian et al., 2009). Ground rubber particles can be incorporated into concrete to improve elasticity and reduce brittleness. Rubber-modified concrete enhances shock absorption and reduces surface noise, making it ideal for pedestrian pathways, playgrounds, and sports courts. It also diverts significant amounts of waste tyres from landfills, contributing to better waste management practices.

Recycled plastic is emerging as a viable alternative material in the construction industry. Plastic waste, including polyethene and polypropylene, can be processed into plastic aggregates or fibres and incorporated into concrete mixtures. Recycled plastic concrete exhibits improved durability, resistance to cracking, and reduced permeability. It is particularly suitable for non-structural applications such as footpaths, cycle lanes, and urban landscaping. Moreover, using plastic waste reduces environmental pollution and conserves natural resources (Saikia & de Brito, 2012). Plastic waste, including polyethene and polypropylene, can be processed into plastic aggregates or fibres and incorporated into concrete mixtures. Recycled plastic concrete exhibits improved durability, resistance to cracking, and reduced permeability. It is particularly suitable for non-structural applications such as footpaths, cycle lanes, and urban landscaping. Moreover, using plastic waste reduces environmental pollution and conserves natural resources. Glass fibre-reinforced concrete (GFRC) is valued for its tensile strength, lightweight nature, and resistance to cracking. This composite material is often employed in architectural cladding, pedestrian pathways, and structural repairs (Bentur & Mindess, 2007). GFRC minimises the need for steel reinforcement, reducing the risk of corrosion and lowering long-term maintenance costs. Additionally, its versatility and aesthetic appeal make it an ideal choice for urban landscaping projects.

Carbon fibre composites, though costly, offer unparalleled strength-to-weight ratios, corrosion resistance, and durability. Increasingly utilised in bridge decks, pedestrian walkways, and structural retrofitting, carbon fibre reinforcement extends the lifespan of infrastructure while minimising maintenance requirements (Hollaway, 2010). Carbon fibre-reinforced concrete

(CFRC) is also gaining traction in the development of ultra-thin pavements and lightweight pedestrian bridges, highlighting its potential to revolutionise future construction methodologies. The integration of alternative and sustainable materials in the civil engineering sector is pivotal in mitigating environmental impacts and promoting resource efficiency. Lightweight concrete, recycled steel tyre fibre, polystyrene, waste foundry sand, fly ash, recycled aggregate, recycled tyre fibre, superplasticisers, glass fibre, and carbon fibre exemplify innovative solutions that align with the principles of green construction.



Figure 2-1: (a) Plastic Waste, (b) Recycled Rubber Tyre Fibre, (c) Glass Fibre, (d) Carbon Fibre, (e) Recycled Aggregate, (f) Fly Ash

By embedding these materials into pavements and pedestrian infrastructure, the construction industry can reduce waste generation, lower carbon emissions, and contribute to a circular economy. Future research should emphasise optimising the composition of these materials and exploring hybrid combinations to further enhance their structural and environmental performance.

2.2.1 Expanded Polystyrene (EPS)

Polystyrene, a synthetic polymer known for its versatility, is frequently incorporated into concrete production as a lightweight aggregate and insulation agent. Expanded polystyrene (EPS) beads, when used as a replacement for traditional aggregates, notably decrease concrete density while enhancing its thermal insulation capabilities (Alengaram et al., 2011). These properties make EPS concrete especially suitable for pedestrian walkways, non-load-bearing structures, and recreational

surfaces where shock absorption and improved comfort are desirable, such as in parks and playgrounds. By integrating EPS beads, concrete achieves a significant reduction in weight while retaining adequate compressive strength, making it a practical choice for energy-efficient buildings and lightweight construction projects (Cadere et al., 2018).

From a sustainability perspective, incorporating recycled EPS into concrete supports waste reduction efforts by diverting non-biodegradable materials from landfills. This practice also promotes the efficient use of resources; however, environmental concerns arise from the potential release of microplastics and the reliance on petroleum-based production processes for EPS, necessitating proper management strategies to mitigate these risks (Kharun & Svintsov, 2017).

The mechanical performance of EPS concrete is closely tied to the proportion of EPS beads in the mix. Increasing the EPS content generally weakens the compressive and tensile strength due to the lower stiffness of EPS compared to conventional aggregates (Vandhiyan et al., 2016). Nonetheless, carefully optimised mix proportions can achieve a balance between reduced weight, thermal insulation, and structural performance, making EPS concrete adaptable for both structural and non-structural applications (Karolina et al., 2019).

The introduction of EPS as a key material has greatly benefited the development of lightweight concrete composites. Aside from reducing material usage and lowering the carbon footprint associated with concrete production, recycling polystyrene waste into concrete helps address disposal issues, aligning with broader environmental sustainability goals (Kharun & Svintsov, 2017).

The influence of polystyrene on concrete's mechanical properties becomes evident as the EPS bead content increases. Research by Vandhiyan et al. (2016) indicates that substituting 10% of coarse aggregates with EPS beads slightly reduces concrete strength, whereas a 50% replacement results in a significant decrease in density, transforming the material into lightweight concrete. Their findings revealed that concrete density decreased between 3.5% and 23.5% as the EPS content varied from 10% to 50%. The suitability of EPS concrete for non-structural applications, such as wall panels and partitions, was highlighted in this study.

Further data support these trends. According to Nader et al. (2022), introducing 10% polystyrene led to a reduction in compressive strength from 14.09 MPa to 9.41 MPa, while the density declined by approximately 42%. Tensile strength experienced a comparable reduction, decreasing from 3.57 MPa to 0.22 MPa. These reductions occur because the presence of soft, deformable EPS beads

interrupts the continuity of the concrete matrix, diminishing both compressive and tensile performance. Depending on the specific mix and EPS proportion, compressive strength values in EPS concrete can range from as low as 1 MPa to over 17 MPa (Karolina et al., 2019). This highlights the necessity for precise mix designs to meet performance demands across different applications (Nader et al., 2022).

2.2.2 Recycled Steel Tyre Fibre

Recycled steel tyre fibres, recovered from end-of-life tyres, serve as a valuable reinforcement material in concrete, enhancing its toughness, tensile strength, and resistance to cracking under load. These fibres are particularly effective in high-traffic pedestrian zones and pavements, where they improve impact resistance and minimize surface wear and slip hazards. Incorporating tyre fibres into concrete not only boosts mechanical performance but also supports sustainable waste management by reducing the accumulation of discarded tyres in landfills.

The use of steel tyre fibres helps to reduce dependence on conventional steel reinforcements, leading to potential cost savings and a lower carbon footprint associated with steel production. Their ability to increase fatigue resistance and prevent crack propagation makes them especially suitable for pavements, bridge decks, and other load-bearing surfaces exposed to heavy or dynamic loads. Research by Thomas et al. (2016) demonstrated that recycled tyre fibres improve tensile strength, crack resistance, and impact durability, offering a sustainable approach to strengthening concrete while addressing environmental concerns.

Experimental investigations have shown that adding 1.5% steel tyre fibre by cement ratio can enhance the tensile strength of concrete by up to 38% and increase the modulus of elasticity by approximately 8% compared to conventional concrete (Thomas & Ramaswamy, 2020). In addition, tests involving crumb rubber and tyre steel fibres have indicated that optimal results were achieved with 12.5% crumb rubber replacing fine sand and steel fibres added in proportions ranging from 0.3% to 1.2% by mass. According to Ndayambaje et al. (2017), the combination of 12.5% crumb rubber and 1.2% steel fibres provided the best impact resistance, particularly at the points of initial cracking and ultimate failure, making it a suitable mix for road pavements and other applications requiring enhanced durability.

Steel fibres act as micro-reinforcements within the concrete matrix, bridging cracks and distributing stress more evenly throughout the material. Their presence significantly improves ductility, impact strength, and load-bearing capacity after cracking, which reduces the likelihood

of sudden structural failures (Aghaee et al., 2015). These properties make steel fibre-reinforced concrete highly effective in structures subjected to heavy loads and dynamic stresses.

From an environmental perspective, recycling steel tyre fibres helps mitigate the disposal challenges posed by used tyres while also reducing the need for energy-intensive virgin steel production, which is a major source of greenhouse gas emissions (Zhang et al., 2022). However, achieving uniform dispersion of steel fibres in concrete can be challenging, requiring careful mix design and proper handling techniques to prevent clumping and ensure consistent mechanical performance across the structure (Zia et al., 2022).

2.2.3 Waste Foundry Sand (WFS)

Waste foundry sand, a by-product of metal casting, presents an eco-friendly alternative to natural fine aggregates. Integrating foundry sand into concrete mixtures enhances compressive strength and minimises shrinkage while alleviating pressure on natural sand resources (Singh & Siddique, 2012). Utilising this industrial by-product fosters circular economy principles by repurposing waste materials and reducing environmental strain associated with sand mining. Foundry sand has demonstrated remarkable performance in both rigid and flexible pavement applications under diverse climatic conditions. Waste foundry sand (WFS) is an industrial by-product from metal casting processes, offering an environmentally friendly alternative to natural sand in concrete production (Sahare, 2019). Due to its fine particle size and chemical composition, WFS has been found to enhance concrete strength, durability, and resistance to aggressive environmental conditions (Rashid & Nazir, 2018).

The mechanical performance of WFS-containing concrete varies based on the replacement ratio and material properties. While high WFS content may slightly reduce compressive and tensile strength, optimised replacement levels can maintain or even enhance concrete performance (Etxeberria et al., 2007). Research by Siddique et al. (2011) found that replacing 20% of natural sand with WFS maintained comparable compressive strength, while higher replacement levels required mix modifications.

Beyond mechanical performance, WFS has shown improvements in concrete workability and durability. However, some studies indicate that the irregular shape of WFS particles may reduce workability, necessitating the use of water-reducing admixtures to optimise mix performance (Guney et al., 2010). Durability studies indicate that WFS improves resistance to freeze-thaw cycles, sulfate attack, and chloride ion penetration, making it a promising material for long-term

infrastructure applications (Siddique & Naik, 2004). Additionally, using WFS reduces the reliance on natural sand extraction, contributing to sustainable aggregate consumption and reduced environmental impact (Tittarelli, 2018).



Figure 2-2: (a) Polystyrene, (b) Waste foundry sand, (c) Recycle steel tyre fibre

The integration of alternative and sustainable materials in civil engineering is crucial for reducing the industry's environmental footprint while maintaining structural efficiency, cost-effectiveness, and durability. The use of polystyrene, waste foundry sand, and recycled steel tyre fibres offers viable solutions for pavement and structural applications, reducing resource consumption, improving mechanical performance, and minimizing landfill waste.

As the demand for sustainable construction solutions increases, further research is required to optimise material performance and expand applications in pavement engineering, lightweight structures, and energy-efficient buildings. By embracing alternative materials, the civil engineering sector can significantly lower its carbon footprint, reduce waste, and support circular economy principles, contributing to long-term sustainability and innovation in construction practices (Sohail et al., 2013).

2.2.4 Superplasticisers

Superplasticisers, also called high-range water reducers, play a vital role in enhancing the workability of concrete mixtures without increasing the water content. These chemical admixtures enable the production of high-performance concrete (HPC) and self-compacting concrete (SCC), which demand superior flowability and self-consolidating characteristics without segregating the mix components (Okamura, 1997). By promoting ease of placement and compaction, particularly in complex formworks and reinforced structures, superplasticisers simplify construction processes and contribute to achieving denser, more durable concrete (Mehta & Monteiro, 2006).

The use of superplasticisers significantly reduces the water-to-cement ratio by dispersing fine particles throughout the concrete matrix. This reduction in water content leads to denser concrete with fewer voids, improving compressive strength and long-term durability (Neville, 2011). According to Nwoye (2020a), these additives create a cohesive mix, enhancing the concrete's structural integrity while maintaining desirable workability levels. Additionally, the slump level of the concrete increases, allowing for easier placement and consolidation (Nwoye, 2020b).

Research indicates that incorporating superplasticisers can reduce water requirements by up to 30% without compromising workability (Eckert & Carrasquillo, 2020). Lower water-to-cement ratios are associated with higher strength and reduced permeability, leading to concrete that withstands harsh environmental conditions, including freeze-thaw cycles and chemical exposure (Neville, 2011). Alsadey and Omran (2022) further highlight that precise water reduction optimises cement hydration, enhancing strength while reducing porosity.

Superplasticisers contribute to accelerating early strength development in concrete, enabling quicker formwork removal and earlier structural loading (Mehta & Monteiro, 2001). These admixtures facilitate better cement particle dispersion, reducing the need for excess water and improving the compactness of the concrete matrix (Nwoye, 2020). As a result, the final concrete product exhibits enhanced mechanical properties and increased resistance to wear and environmental stressors (Neville, 2011).

The environmental benefits of superplasticisers are equally notable. By decreasing cement and water consumption, these admixtures contribute to reducing the carbon footprint associated with cement production, which is a significant source of CO₂ emissions (H et al., 2020; Nwoye & Obele, 2020). Thus, superplasticisers not only improve concrete performance but also promote sustainability in construction practices.

Further research continues to explore advanced formulations of superplasticisers to improve their compatibility with various cement types and other admixtures. This ongoing development is expected to expand their application in innovative concrete technologies, such as ultra-high-performance concrete (UHPC) and self-compacting concrete, fostering further improvements in construction efficiency and material performance (He et al., 2020).

The present study adopted a 1% superplasticiser dosage relative to the cement content to optimise both the mechanical properties and workability of the foamed concrete samples under investigation. Additionally, alternative cement types, including high-strength and rapid-setting

Portland cement conforming to BS 915:1983 standards, were considered to enhance the overall performance of the concrete mix. Figure 4-4 outlines the specific recycled materials and additives incorporated in this study. According to MPA Mortar (2021), adhering to guidelines from BS EN 998-1 and BS EN 998-2 ensures that additives are effectively integrated into the mix, improving particle dispersion and reducing the water-to-cement ratio, ultimately contributing to a robust and durable concrete structure.

2.3 Foamed Concrete

Foamed concrete is an innovative and sustainable construction material that offers lightweight properties, enhanced thermal insulation, and resource efficiency, making it a viable alternative in modern civil engineering applications. It is produced by introducing air voids into a cementitious matrix, resulting in low-density concrete with improved workability and reduced material consumption (Jones & McCarthy, 2005). Due to its self-compacting nature, foamed concrete eliminates the need for extensive vibration during placement, contributing to lower labour costs and energy consumption in construction projects (Kearsley & Wainwright, 2002).

One of the major environmental benefits of foamed concrete is its potential for incorporating recycled materials, such as waste foundry sand, polystyrene, and steel tyre fibres, thereby reducing dependency on natural resources (Mohammed et al., 2020). Additionally, its high porosity and air content contribute to better thermal and acoustic insulation, making it suitable for energy-efficient buildings and sustainable infrastructure (Amran et al., 2015). The absence of coarse aggregates in foamed concrete production further reduces mining activities and environmental degradation, promoting eco-friendly construction solutions (Ramamurthy et al., 2009).

Despite its lower compressive strength compared to conventional concrete, foamed concrete demonstrates adequate mechanical performance for non-structural applications, lightweight partitions, pavement sub-bases, and void filling (Jones & McCarthy, 2006). However, advancements in mix design and material optimisation have enabled the development of higher-strength foamed concrete suitable for load-bearing applications and infrastructure projects (Gholampour & Ozbakkaloglu, 2018).

This chapter provides a comprehensive overview of foamed concrete's mechanical, durability, and sustainability characteristics, analysing its potential as an alternative material in pavement and civil engineering applications. A detailed evaluation of its performance when combined with recycled materials is presented in later sections, offering insights into its feasibility for modern

sustainable construction practices. The chapter concludes with a thorough discussion of the role of foamed concrete in sustainable civil engineering, addressing both its benefits and limitations, along with future research directions for enhancing its structural performance and environmental impact. Foamed concrete, often termed lightweight cellular concrete, has become increasingly significant in modern construction due to its low density, high thermal insulation properties, and ease of application. This innovative material consists primarily of a cementitious binder, fine sand, water, and a foaming agent, which collectively create a porous structure. Hamad (2014) characterises foamed concrete as a material containing evenly distributed air voids introduced through the addition of stable foam. The American Concrete Institute (ACI) outlines the importance of foam uniformity in their guidelines (ACI 523.3R-14, 2003), while the performance and reliability of foaming agents are evaluated according to standards like ASTM C869-91 and ASTM C796-97. Typically, the air content in foamed concrete ranges between 6% and 35% by volume, influencing both its density and mechanical performance.

The production process involves combining a pre-formed foam, created by mixing a foaming agent with water and compressed air, with a cementitious slurry. The uniform dispersion of foam is crucial to ensure stability and avoid segregation, directly impacting strength and load-bearing capacity (Mydin & Wang, 2012). Foaming agents are categorised into protein-based and synthetic types. Protein-based agents, such as the Propump 26 used in this research, are favoured for their ability to produce small, uniform, and stable bubbles, leading to denser, more robust cellular structures. They are also biodegradable and derived from natural proteins, making them an environmentally preferable choice compared to synthetic counterparts (Jones & McCarthy, 2005). Density variations in foamed concrete span from as low as 200 kg/m³ to 1700 kg/m³, allowing customisation to suit diverse applications, including non-structural fill, roof insulation, and lightweight structural elements (Kearsley & Wainwright, 2001).

Parallel to foamed concrete, Lightweight Concrete (LWC) represents another class of low-density construction materials valued for reducing dead loads, improving thermal efficiency, and enhancing seismic resilience. LWC can be produced either by using lightweight aggregates such as expanded clay, shale, or pumice or by incorporating air voids using admixtures or foaming processes (Newman & Owens, 2005). These reductions in mass yield significant structural and economic advantages. The lower self-weight decreases the load on foundations and structural

members, enabling more slender and efficient designs in high-rise buildings and long-span bridge constructions (Neville, 2011; Kan & Demirboğa, 2009). Figure 2-3 illustrates the foam production.

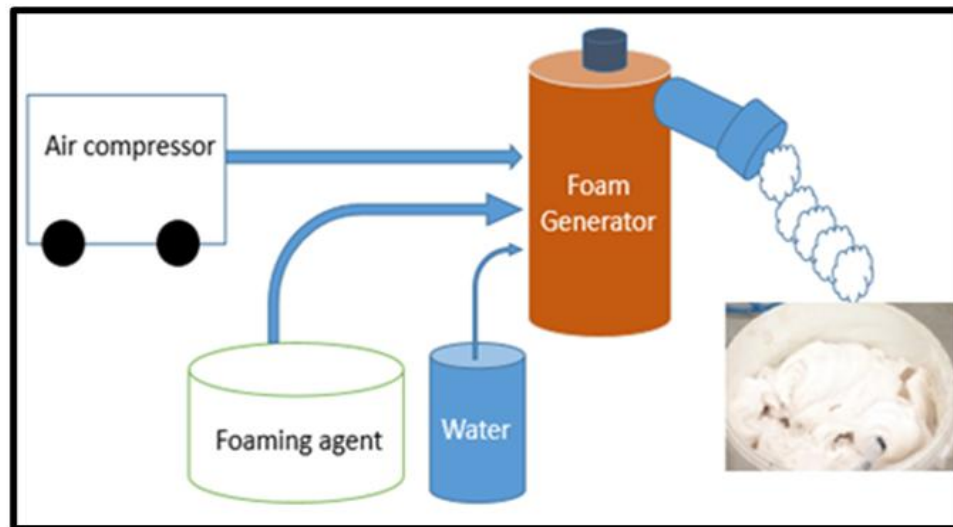


Figure 2-3: Foam Generation Process (Raj, Sathyan, & Mini, 2019)

Beyond structural efficiency, LWC exhibits improved insulation properties and increased fire resistance due to its porous structure, attributes that enhance its suitability for both residential and industrial applications, according to Raj, Sathyan, & Mini (2019) (Neville, 2011). Additionally, its sound absorption characteristics improve acoustic performance in buildings, further amplifying its functional appeal (ACI 213R-14, 2014). Innovative developments in lightweight concrete, such as high-performance, lightweight concrete (HPLWC), have pushed the boundaries of strength and durability, bridging the gap between conventional concrete and lightweight alternatives (Thienel et al., 2020).

The historical trajectory of LWC reveals its longstanding utility in construction. Kan and Demirboğa (2009) and Thienel et al. (2020) note that ancient civilisations, including the Romans, employed natural lightweight aggregates like volcanic pumice to construct monumental structures. A remarkable example is the Pantheon in Rome, built around 128 AD, which incorporated lightweight materials in its dome to reduce structural loads, enabling its remarkable span and durability (Bremner, 2008). The decline of the Roman Empire saw a reduction in LWC usage, attributed to the scarcity of suitable lightweight aggregates (Thienel et al., 2020).

The resurgence of LWC in the 19th and 20th centuries coincided with industrial advancements, leading to the development of artificial lightweight aggregates such as expanded clay and sintered

fly ash (Holm, 1983). These innovations revitalised LWC's potential, aligning with contemporary demands for sustainable construction materials. The reduced consumption of raw materials and lower transportation costs associated with LWC contribute to its environmental benefits, reinforcing its role in modern green construction practices (Chandra & Berntsson, 2002).

2.4 Modern Applications and Sustainability

The modern development of LWC began in the early 20th century when industrial processes were introduced to create artificial lightweight aggregates and aerated concrete as an alternative sustainable civil industry material. These innovations marked the beginning of lightweight concrete's journey towards becoming a fundamental part of the construction industry.

In recent years, the focus on sustainable and energy-efficient construction has further elevated the importance of LWC. According to Junaid et al., its ability to reduce the overall weight of structures leads to savings in foundation costs. It also contributes to reducing greenhouse gas emissions through lower transportation and materials used.(2022)Additionally, the thermal insulation properties of LWC play a crucial role in reducing energy consumption in buildings, which aligns with global sustainability purposes.

The literature analysis highlights an increasing interest in developing more sustainable building materials, particularly those incorporating raw, natural ingredients. The emphasis is on developing materials such as Lightweight Concrete (LWC) that not only have improved physical and mechanical qualities but also have lower density. Such advancements in material science are not only targeted at enhancing the efficiency and performance of construction materials but also at minimising their environmental impact, as mentioned by Junaid et al.(2022).

This shift towards sustainability reduces an awareness that the building sector contributes significantly to environmental degradation, mainly through the extraction and consumption of vast amounts of natural resources. The sector may drastically reduce its dependency on natural resources by emphasising the reuse of waste materials and industrial byproducts. This strategy not only improves waste management but also helps to conserve natural resources, resulting in a more sustainable development trajectory for the construction industry.

Using such materials is consistent with global sustainability goals, providing a pathway for decreasing the carbon footprint of new projects and encouraging the circular economy in the building industry. The shift to employing sustainable building materials, including LWC, reflects a broader commitment to environmental management and is a viable route for innovation and

growth in construction technologies. Lightweight foam concrete (LWC) has emerged as a highly sought-after material in the construction industry, owing to its versatility and the increasing demand for sustainable and efficient building solutions. LWC can be differentiated into various categories, each defined by its unique production technique and the materials used in its composition. These classifications provide a broad spectrum of applications, from thermal insulation to structural components, reflecting the adaptability of lightweight concrete in meeting diverse construction needs.

2.5 Mechanical Property and Density of Lightweight Concrete (LWC)

According to Kohail et al. (2018), concrete can be classified into three types based on its unit weight and compressive strength: low-strength concrete (less than 20 MPa and up to 1800 kg/m³), moderate-strength concrete (between 20 and 40 MPa and densities between 1800 and 3500 kg/m³), and high-strength concrete (more than 40 MPa). Moderate-strength concrete, often plain concrete, is the foundation for most structural engineering projects due to its strength and workability. High-strength concrete, on the other hand, is used in specialised applications that require exceptional performance under high loads or in harsh circumstances. The creation of lightweight concrete (LWC), which ranges in strength from low to moderate depending on its composition and intended purpose, uses natural and artificial lightweight aggregates.

Furthermore, according to Kohail et al. (2018) and Thienel et al. (2020b), natural materials such as shales, clays, pumice, diatomite, volcanic cinders, and slates have an inherent quality that reduces the overall weight of the concrete without significantly affecting structural integrity. Alternatively, by-products such as iron blast furnace slag, clay, sintered fly ash, and shale serve as artificial sources of lightweight aggregates, providing a sustainable solution by recycling industrial waste into valuable construction materials. These lightweight aggregates are critical for making LWC with desirable qualities such as reduced density, enhanced thermal insulation, and acceptable strength for diverse construction applications, as Chandra and Berntsson (2002) emphasised.

According to (Kumar, Lakhani and Tomar, 2018), Lightweight Concrete (LWC) can have densities ranging from 350 to 1800 kg/m³ and compressive strengths between 1 and 30 MPa. LWC is known for its excellent thermal insulation properties, and some varieties, such as lightweight aggregate concrete, are used as structural materials.

According to (Hilal, 2015), the modern construction industry has seen a significant increase in demand for LWC in structural applications due to its benefits, such as lower thermal conductivity

and a higher strength-to-weight ratio. According to (Hama, 2017), structurally, LWC with densities ranging from 1350 to 1850 kg/ kg/m³ can achieve compressive strengths that are more significant than 17 MPa after 28 days, comparable to conventional-weight concrete. This makes it especially useful for reducing dead loads on concrete structures. Lightweight concrete can be prepared either by injecting air into its composition or by omitting the finer sizes of the aggregate or even replacing them with a hollow, cellular, or porous aggregate.

2.6 Development and Innovation of Lightweight Concrete

Throughout the 20th century, advancements in technology and materials science pushed the development of various forms of LWC. Innovations such as expanded clay and shale aggregates, as well as synthetic foaming agents, have developed the applications of lightweight concrete, explained by (Fathi, et.al., (2004) and Junaid et al., 2022). These developments improved the material's structural properties and enhanced its thermal insulation, fire resistance, and sound absorption capabilities.

2.6.1 Types of Lightweight Concrete

Lightweight concrete can be broadly classified into three main categories according to Fathi, M, et al., (2004) and (Kan and Demirboğa, 2009), based on its production method and the materials used:

1. Lightweight Aggregate Concrete (LAC): Utilizes lightweight aggregates like expanded clay, shale, or slate, which have a lower density compared to traditional aggregates. LAC is known for its structural strength, thermal insulation, and reduced weight, making it suitable for a wide range of applications, from residential buildings to bridges.

2. Foamed Concrete: Also known as cellular or aerated concrete, this type is produced by incorporating air bubbles into the concrete mix through chemical or mechanical means. Foamed concrete is characterised by its low density, excellent thermal insulation, and fire resistance, making it ideal for insulation panels, void filling, and lightweight blocks.

3. No Fines Concrete: This variety excludes the use of fine aggregates, relying solely on course aggregates. The result is concrete with large void spaces, offering unique permeability and lightweight characteristics. Fines concrete is often used in applications requiring drainage or reduced weight without high structural demands.

2.6.2 Aerated Concrete

Aerated concrete type as it does not contain coarse aggregate and can be considered aerated mortar. Typically, aerated concrete is made by introducing air or other gas into a cement slurry and fine sand. In commercial practice, the sand is replaced by pulverised fuel ash or other siliceous material, and lime may be used instead of cement. Aerated concrete is classified into two types: air-entrained concrete and foam concrete (Thakur et al., 2022).

1. Air-entraining method: this method involves adding gas-forming chemicals to the mortar, which react during mixing to form a porous structure. Examples include aluminium powder, calcium carbide, and hydrogen peroxide.

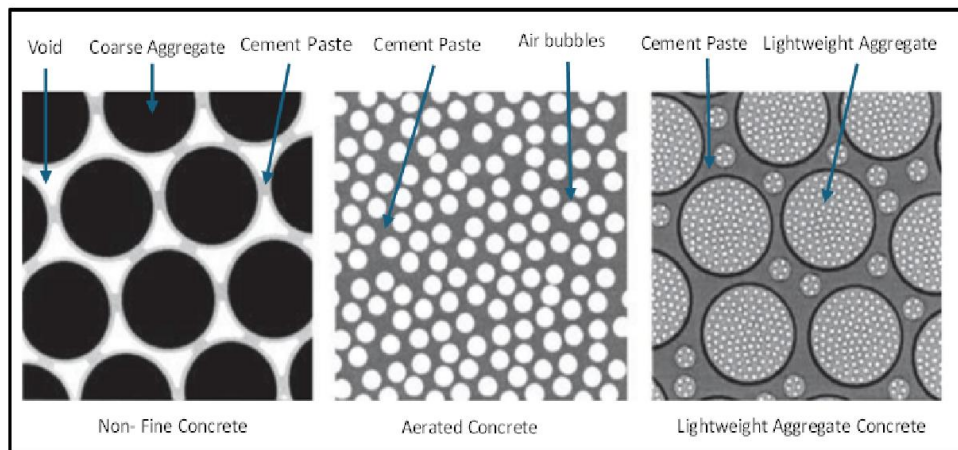


Figure 2-4: Types of Foamed Concrete (Thakur et al., 2022)

2. Alternatively, the foaming method: this method creates pores mechanically through a pre foaming process, where the foaming agent is combined with water before mixing, or a mixed foaming process, where the foaming agent is directly mixed with the mortar.

The first method is usually used in precast concrete factories where the precast units are subsequently sterilised in order to produce concrete with reasonably high strength and low drying shrinkage. The second method is mainly used for in-situ concrete and is suitable for insulation roof screeds or pipe lagging. Figure 2-4 shows the aerated concrete.

This research has focused on aerated concrete, which is a useful construction material characterised by its lightweight, porous structure. As explained by Hamad (2014), foamed concrete is made by mixing a cementitious material (usually Portland cement, fine sands, and a foaming agent). This foam agent is introduced into the mix to create many tiny air bubbles throughout the

material, significantly reducing its density compared to traditional concrete. As Okay (2010) and Ramamurthy et al.(2009a) highlighted that the density of foamed concrete typically ranges from 400 kg/m^3 to 1800 kg/m^3 , which is considerably lighter than standard concrete, which usually has a density of about 2400 kg/m^3 . The concept of incorporating air bubbles into concrete to reduce its density and improve specific properties dates back to the early 20th century. However, the systematic development of foamed concrete began in the 1950s and 1960s, with its applications initially focused on insulation and soundproofing due to its inherent thermal and sound-insulating properties (Raj, Sathyan and Mini, 2019).

The Romans developed concrete's workability and durability by incorporating animal blood into a mixture of small stones, sand, hot lime, and water, resulting in small air pockets in the mix.

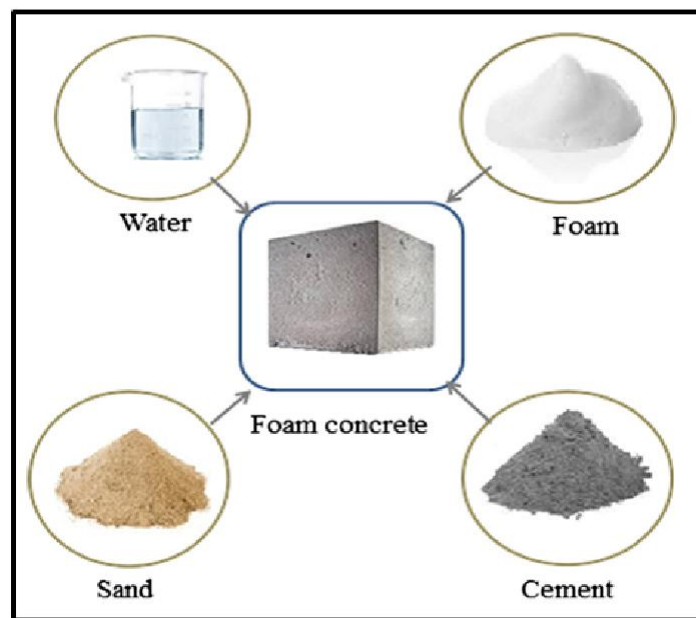


Figure 2-5: The Components of Foamed Concrete (Raj, Sathyan & Mini, 2019)

However, Axel Eriksson's patent in 1923 officially documented the invention of Portland cement-based foamed concrete. Figures 2-5 explain the foamed concrete components.

Abd & Jassam, (2019) demonstrated the production of foamed concrete, which involves creating a stable foam using a foam generator, which is then mixed with a cement-based slurry. The foam introduces a controlled amount of air into the mix, creating a matrix of evenly distributed air voids. The result is a material that can be easily pumped and moulded into desired shapes, offering significant advantages in handling and construction efficiency. Raj et al. (2019) also mentioned that foamed concrete's low density is achieved without significantly compromising strength,

making it an attractive option for many construction projects. Its cellular structure also provides excellent thermal insulation, making buildings more energy efficient. Furthermore, its porous nature allows for better sound absorption. In terms of sustainability, foamed concrete is considered an eco-friendly construction material. Its ability to incorporate industrial by-products like fly ash and slag as partial cement replacements reduces cement production's environmental impact. Additionally, its lightweight nature leads to lower transportation costs and reduced emissions.

2.6.3 Specification

The British Cement Association (BCA) established a precedent in 1991 with its first report outlining specifications for foamed concrete in the UK, which sparked a series of subsequent publications between 1992 and 1995. These documents contributed to the construction industry's understanding of foamed concrete by focusing on its benefits, characteristics, and application guidelines, particularly emphasising its use in ground stabilisation and void filling. This period it marked the initial recognition of the practical applications of foamed concrete in groundwork and trench replacement. (OZLUTAS, 2015a).

The Highway Authorities and Utilities Committee's (HAUC) 1992 introduction of a specification for the reinstatement of highway openings was a watershed moment. After its approval as a Code of Practice, this specification was supplemented with an appendix that addressed the use of foamed concrete in reinstatement. This code, which was formally enforced in January 1993, made a substantial contribution to the standardisation of foamed concrete usage in the maintenance of highways. (Beng, 2021).

In 2001, with assistance from Dundee University's Concrete Technology Unit (CTU), the Highways Agency and the Transport Research Laboratory released an application guide, AG39, titled "Specification for foamed concrete." This publication offered comprehensive insights into quality control, material properties, potential applications, and acceptance criteria, further advancing the industry's knowledge base. (Hilal et al., 2015).

Table 2-1: Published Specification of Foamed Concrete in the UK (Beng, 2021)

Published specifications for foamed concrete in the UK		
Publishing Body/year	Title of the specification	Contents
BCA /1991	Foamed concrete	Definition, properties, advantages
BCA /1994	Foamed concrete composition and properties Specification	Definition, properties, advantages, and potential applications
UKWIR /1995	Specification of foamed concrete	Use as a reinstatement material
HAUC (2010) 1st & 2nd Publications / 1992 & 2002	Specification for the reinstatement of openings in highways	General requirements for foamed concrete as an alternative reinstatement material
TRL- Brady et. al with contributions of University of Dundee /2001	TRL Report AG39 – Specification for foamed concrete	Constituents, production, properties, uses, a guideline for specifications, uses and quality control
WRAP /2005	Recycled and secondary aggregates in foamed concrete	Specification on the use of recycled and secondary aggregates in the production
WRAP /2007	Specification and quality control of foamed concrete incorporating RSA	Constituent materials, requirements, production control, and end-of-life and recycling of RSA foamed concrete
Concrete Society /2009 Title	Concrete Guide 7 - Foamed concrete: application & specification	Case studies, practicalities, properties, quality control

Additionally, the UK Water Industry in 1995 expanded the scope of foamed concrete applications, including its use as a reinstatement material. By 2004, specifications were also put forward for its application in insulated building foundations, indicating a broadening approval for the material's adaptability.

Internationally, Japan contributed to standardisation efforts by publishing an industrial standard, JIS A 1162:1973, which focuses on testing methods for cellular concrete volume change, recognising the importance of foamed concrete in construction.

Despite these advances and the growing body of guidelines and specifications, it is worth noting that a unified standard or code of practice specific to foamed concrete as a structural material has yet to be developed. This gap highlights an area of future development, emphasising the need for comprehensive standards that address the properties, quality control, and broader applications of foamed concrete in structural engineering (OZLUTAS, 2015). See Table 2-1, published specification of foamed concrete in the UK

2.6.4 Foamed Concrete Development

Over recent years, significant developments have occurred in the field of foamed concrete (FC), including advancements in materials, manufacturing techniques, quality control, and properties. These improvements have broadened the range of FC applications in construction. M. Amran et al. (2020) explained that FC technology and materials have expanded their uses to include a wide range of applications due to their strength, making them an appropriate construction material in the industrialised building system. Its ability to fill cavities and voids over long distances without requiring vibration or impact is a significant advantage. This material allows for quick, settlement-free construction, providing excellent thermal insulation, superior freeze/thaw properties, and substantial fire resistance.

According to Raj and Mini (2019), FC is utilised for many applications, including sound and thermal insulation for floors, thermal protection for various roof types, well backfilling, cavity filling, masonry grouting, the manufacture of building blocks and wall panels, the construction of monolithic low-rise and individual houses, road sub-base maintenance, and bridge abutment and ground stabilisation. Its development has been driven by continuous research and innovation, focusing on improving its mechanical properties, durability, and environmental footprint. Foamed concrete is praised for its adaptability, offering solutions to various construction challenges while supporting the industry's move towards more sustainable practices (Ashrafian et al., 2020; Hashim, 2014). Technological advancements have significantly facilitated the successful application of foamed concrete, enabling more precise examinations of its properties.

One of the critical areas of innovation in foamed concrete technology involves optimising its mix design. Raj, Sathyan, and Mini (2019) have stated that research using various admixtures and supplementary cementitious materials aims to improve the strength-to-weight ratio and durability of foamed concrete. For instance, incorporating fly ash, silica fume, superplasticisers, and other industrial by-products as partial replacements for cement in foamed concrete mixes has been shown to improve the material's mechanical properties and sustainability profile (Jones and McCarthy, 2005). The UK universities' progress in the development of foamed concrete is detailed in Table 2-2.

Table 2-2: Leading UK Researchers' Developments in Foamed Concrete (Hulusi et al., 2020)

Researcher/University	Main Development
Jones, M.R. and McCarthy (2004) / The University of Dundee	Development of thermally insulating foundations and evaluating several fresh properties of FC with plastic densities range from 1000 to 1400 kg/m ³ .
Rao (2008) / The University of Dundee	Characterising 1000 and 1400 kg/m ³ foamed concretes produced with a wider range of recycled secondary aggregates (RSA) than fly ash and demolition fines. Developed foamed concrete with no/minimal primary aggregates with a plastic density of 500 kg/m ³ .
Yerramala, (2008) / The University of Dundee	Evaluated the energy absorption potential of foamed concrete. Explored the recycling potential of RSA foamed concrete for utilising it as fine aggregate in new foamed concrete.
Othuman, (2010) The University of Manchester	Evaluate the thermal and mechanical properties of FC at high temperatures and structural performance of composite walling system with FC core.
Mohammad (2011) / The University of Dundee	Attempted to solve the stability issues in 300 kg/m ³ foamed concrete and gained further understanding of instability.
Hilal, (2015) / The University of Nottingham	A comprehensive study on Properties and microstructure of pre-formed foamed concretes.
Shawnim and Mohammad, (2018)/Nottingham Trent University	Foamed concrete development for structural purposes: An investigation to the viability of using alternative materials.

Moreover, the development of advanced manufacturing techniques is another crucial aspect of current research. Innovations in foam generation and mixing methods are aimed at producing more uniform and stable foams, resulting in foamed concrete with better consistency and quality (Nambiar and Ramamurthy, 2006). Additionally, the use of preformed foam and synthetic surfactants has been explored to control the bubble size distribution and density of foamed concrete more effectively, enabling the production of materials tailored to specific applications.

Sustainability is a significant driver of recent developments in foamed concrete technology. The industry is focusing on reducing the carbon footprint of foamed concrete by optimising the use of raw materials and incorporating waste materials as aggregates or fillers (Kearsley and Wainwright, 2001). The potential for recycling foamed concrete is also being investigated, with research into the material's life cycle assessment and end-of-life reuse options. This aligns with the broader construction industry's shift towards more environmentally responsible materials and practices. Nottingham Trent University and other research institutions have conducted intensive investigations into FC, examining its prospects and characteristics from various angles, resulting in substantial progress. The ongoing development of foamed concrete aims to enhance its

mechanical properties, durability, and environmental sustainability, making it an area of keen research interest.

2.7 Foamed Concrete Current Applications

Lightweight foamed concrete (LFC) has gained significant interest in the construction industry due to its unique properties, including lower density, good thermal insulation, and reduced material cost. This material, characterised by its inclusion of air bubbles, has found a broad field of applications ranging from structural elements to geotechnical fillings.

One notable application of LFC is in the construction of structural and non-structural elements. According to Kearsley and Wainwright (2001), LFC is particularly advantageous for producing lightweight blocks and panels due to its excellent workability and thermal insulation properties. The reduced weight of LFC elements eases handling and transportation, leading to faster construction times and lower overall costs (Kearsley and Wainwright, 2001)

In the realm of infrastructure, LFC has been applied in the construction of bridge abutments, where its lightweight nature minimises settlements and reduces the loads imposed on underlying soils. Jones and McCarthy (2005) highlighted the use of LFC in bridge construction, demonstrating its capability to improve project sustainability while ensuring structural integrity. (Jones and McCarthy, 2005a)

LFC is also widely used in geotechnical applications, such as backfill material for tunnels and retaining walls. Its self-compacting nature and ability to flow into narrow spaces without requiring mechanical compaction make it an ideal choice for such applications. Nambiar and Ramamurthy (2006) explored its use as a filling material, emphasising its potential to enhance the stability of underground structures while providing thermal and acoustic insulation. (Nambiar and Ramamurthy, 2007). Figures 2-6 and 2-7 are examples of lightweight foamed concrete applications. Furthermore, LFC's thermal insulation properties have led to its use in flooring systems and roofing slabs, contributing to energy-efficient buildings. The material's inherent ability to reduce heat transfer can significantly decrease heating and cooling demands, as discussed by Mydin and Wang (2012), who assessed the energy-saving potential of LFC in building applications (Mydin and Wang, 2012). In conclusion, the versatility and beneficial properties of lightweight foamed concrete have facilitated its adoption in a wide array of construction applications. From structural elements to geotechnical solutions and energy-efficient building components, LFC continues to play a pivotal role in advancing sustainable construction practices.



Figure 2-6: *Lightweight Foamed Concrete Applications* (www.dr-luca.com, 2009)

Despite its limited use in structural applications due to its low compressive strength, foamed concrete has a wide range of applications in the construction industry due to its unique properties. These applications primarily focus on non-structural and semi-structural roles, taking advantage of the material's lightweight properties, thermal insulation, and ease of installation (MD Jalal, A Tanveer, 1991). Consider the following applications in greater detail:

1. **Thermal Insulation:** foamed concrete is an excellent conductor because of its high porosity and air content. It is used in roofs, floors, and walls to increase a building's energy efficiency by lowering the need for heating and cooling.
2. **Void Filling:** because foamed concrete is fluid, it can be easily pumped into difficult-to-reach places, which makes it perfect for filling gaps. This includes mine shafts, abandoned pipes, and tunnels where placing them does not require the use of compacting machinery.
3. **Soil Stabilization:** loose soil can be stabilised with foamed concrete, which increases the soil's strength and bearing capacity. This application is especially helpful for laying the groundwork for pathways, roads, and lightweight buildings.
4. **Precast Wall Elements/Panels:** Foamed concrete is used to make precast wall panels and components because of its lightweight and insulating properties. These panels provide quick assembly and energy-efficient options for building construction.

5. Slope Protection: Because of the material's moldability and adherence to various surfaces, it can be used for landscaping and slope protection, preventing erosion and stabilising embankments.

Application	Dry Density Range (kg/m ³)		Advantages	Site Images
Roof Insulation Screed http://alliedfoamtech.com			Has excellent thermal insulation properties and Does not add significantly to the overall weight of the roof	
Road Sub-Base https://compositecellularconcrete.com	300-1000	1.0 – 3.5	Reduce loads on weak underlying soils	
Raising Floor Level (Prabha et al., 2017)	400-1200	1.0 – 4.5	No compaction needed, less weight, High-performance void-filling, used for skin friction piles - Reduced foundation cost	
Decorative Panels www.fsiwi.com	>1000	3.5 - 5.5	Enhance the appearance of buildings without adding much extra loading to the structure	
Trench Reinstatement www.rusmarinc.com/cellularconcrete	>1200	4.5 - 5.5	Self-levelling, filling small cavities, easily to pump with low pressure over long distances	
Ground Stabilisation www.greenbuildingadviser.com	600 - 1000	2.0 - 5.5	Reducing loading on burden soil imposes a little vertical stress on the substructure -	
Building blocks www.indiamart.com	400 - 1000	2.0 – 8.0	Foamed blocks are lightweight with excellent sound and thermal insulation properties	
Void fill www.rusmarinc.com/cellularconcrete	300 - 1600	1.0 - 10.0	loading reduction on the basement floor and roof column piers	
Harbour fill www.greenbuildingadviser.com	400 - 1600	1.0 - 10.0	Used as impact layer due to its energy-absorbing properties	
Floor Slabs (Mohamad et al., 2014)	1200 - 1600	4.5 - 10.0	It can be pre-cast or cast in-situ. It is solid and light in weight.	
Bridge Abutments www.fsiwi.com	400 - 1650	1.5 - 10.0	Less overburden on the structure and underlying soils--dropping the thickness of the walls and the size of the foundations, thus huge cost savings can be achieved	
Non-Structural Walls www.greenbuildingadviser.com	800 - 1600	3.0 - 10.0	Foamed concrete walls are both lightweight and low in cost	
Semi-Structural Walls www.fsiwi.com	1200 - 1600	6.5 - 12.0	It is possible to build walls from pre-cast reinforced foamed concrete elements. It is lightweight and strong enough to take some load.	

Figure 2-7: Applications of Foamed Concrete (Beng, 2021)

6. Road Sub-bases: Foamed concrete is a lightweight fill material used in road construction, and it is especially effective at reducing settlements on weaker soils. It provides a solid foundation for the road structure without adding significant load.
7. Bridge Abutment Backfill: Foamed concrete is the best material for backfilling in bridge construction projects because of its lightweight nature, which reduces lateral loads on bridge abutments.
8. Sound Insulation: Foamed concrete's cellular structure offers superior sound-absorbing capabilities, which makes it a good choice for acoustic panels and sound barriers.

2.8 Production of Foamed Concrete

Foamed concrete, a material recognised for its lightweight and insulating properties, integrates air bubbles into a cementitious mixture. This unique construction material is produced by combining cement, water, fine aggregate, and a foaming agent, resulting in a mix that offers both structural integrity and thermal insulation. (Hashim and Tantray, 2021). The initial step in the production of foamed concrete is to prepare the base mix. This typically requires combining cement, water, and any additional fine aggregates or additives needed for the specific application. The consistency and composition of the base mix are critical factors determining the final properties of the foamed concrete, such as density, strength, and thermal conductivity. (Döpfner, Schmeck and Berner, 1994)

Following the preparation of the base mixture, a foaming agent is added. This agent is typically a surfactant that lowers the surface tension of the mixture, allowing air bubbles to form and stabilise within it. The foaming agent can be added in a pre-formed manner, where foam is generated using a foam generator and then mixed into the slurry. Alternatively, it can be added directly to the mix, where the air is entrained mechanically. The incorporation of air bubbles is an important step that has a direct impact on the density and insulating properties of the resulting material, as illustrated in Figures 2-8. (Jones and McCarthy, 2005b) The consistency of the foamed concrete mixture allows it to be easily poured into moulds or directly onto construction sites, making it a versatile option for a wide range of applications. Foamed concrete is much lighter than regular concrete and has a cellular structure that, once set, offers superior thermal insulation. This feature enhances a building's energy efficiency while also lessening the strain on foundations and structures.

Moreover, the production process of foamed concrete allows for incorporating several additives and waste materials, such as plasticisers, slag or fly ash, which can increase its mechanical

properties and sustainability. (Othuman Mydin et al., 2014), emphasised the environmental benefits of using such materials, mentioning that they can reduce the carbon footprint of foamed concrete and contribute to the construction industry's sustainability areas. (Lin, Deng and Chen, 2022).

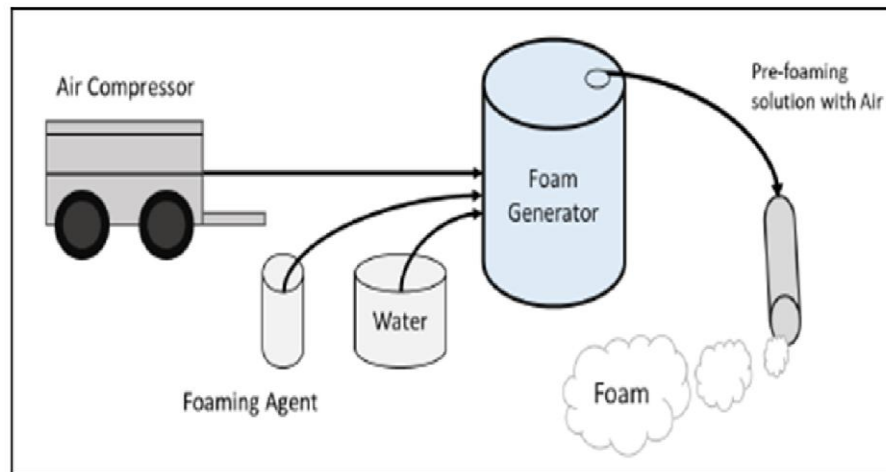


Figure 2-8: Foam Production from Foam Generator (EAB Associates, 2001)

2.9 Foamed Concrete Methods

Foamed concrete, an adaptable construction material known for its lightweight and insulating properties, is made using two main methods: pre-foaming and mix-foaming. As explained by M. Amran et al., (2020) and Hamad, (2014), Each method is crucial for controlling the mixing process and ensuring the quality of the final product.

2.9.1 Pre-Foaming Method

The pre-foaming method consists of two significant steps: creating the base mix and stabilising the preformed liquid foam separately. The pre-formed foam, which is essential to this method, can be made using either dry or wet methods:

1. **Dry Foam** is developed by forcing a foam agent solution through a series of high-density screens while compressed air is injected into a mixing chamber. Dry foam is distinguished by its stability and the formation of bubbles less than 1 mm in diameter, allowing for a stable and uniform mixture with the base material. This produces pumpable foamed concrete with consistent quality and structure.
2. **Wet Foam:** In contrast, wet foam is created by spraying the foam agent solution through a

fine mesh, resulting in bubbles ranging in size from 2 to 5 mm. Although the process is similar, the resulting foam is less stable than dry foam, affecting the uniformity and stability of the foamed concrete.

2.9.2 Mix-Foaming Method

The mix-foaming method involves mixing the surface-active agent directly with the base-mix ingredients, such as the cement slurry while mixing. This integration forms a cellular structure within the foamed concrete, critical for its lightweight and insulating properties. To ensure the success of this method, the foam generated must be consistent and able to withstand the pressure of the mortar until the cement begins to set. This stability ensures that a solid concrete matrix forms around the air voids, contributing to the foamed concrete's structural integrity. As explained by M. Amran et al. (2020), Hama (2017) and Hamad (2014), Pre-foaming and mix-foaming are required for producing preferable foamed concrete, and each has advantages and applications. The technique used will be determined by the equipment available, the desired properties of the foamed concrete, and the construction specifications. The foam must be stable during the mixing and setting phases to ensure foamed concrete's ideal structural and insulating properties.

2.9.3 Foaming Agent

Foaming agents made from broken-down proteins come from both animal parts (like blood, horns, and hooves) and plants. This process splits protein molecules into smaller pieces, which makes them more reactive and better at acting like detergents. Ramamurthy et al. (2009b) observed that these protein pieces naturally act like detergents, reducing the surface tension of water and helping to create and stabilise air bubbles in a liquid.

Indicated by Othuman Mydin et al., (2014), that mixing a foaming agent with water creates a stable foam that produces foamed concrete. This foam, when introduced to the cementitious mix, enables the protein-based surfactants to maintain the stability of air bubbles. The endurance of these bubbles throughout the mixing, placing, and curing stages is crucial, as it ensures the formation of consistent air voids within the concrete, contributing to its lightweight and thermal insulation properties.

Rasheed & Prakash (2015) explain that protein foaming agents work by arranging surfactant molecules at the air-water boundary. The water-attracting ends go into the water, and the water-repelling ends stick outwards. This arrangement lowers the surface tension of the water, making it

easier to form stable air bubbles. The protein molecules also create a flexible film around the bubbles, preventing them from merging and collapsing.

Mydin & Wang (2012) mention that foaming agents are crucial in determining the density of concrete. They do this by controlling the formation of air bubbles within the cement mixture. These bubbles act as trapped air pockets, forming when foam agents are added to the mix. As reported by OZLUTAS, (2015b) and Thakur, S., Goyal, M., Gupta, M., & Siddique, R. (2022), two primary categories of foam agents are synthetic and protein-based, each playing a significant role in crafting foamed concrete.

1. Protein-based agents form a denser, more durable bubble structure with closed cells, allowing for the incorporation of more air and resulting in a strong network of stable air voids.
2. Synthetic agents, on the other hand, cause more significant expansion, resulting in a lower concrete density,

Using protein-based foaming agents is particularly beneficial in applications requiring high stability and uniformity of air voids, such as in lightweight concrete and insulation materials. Their natural origin and biodegradability make them an environmentally friendly choice compared to synthetic surfactants.

The amount of foaming agent added has a significant impact on the properties of the concrete, both when fresh and after it has hardened. It has been observed that using too much foam reduces the flowability of concrete. However, mixing duration has a significant impact on flow; longer mixing times can increase air entrapment, but excessively long mixing may reduce air content by allowing bubbles to escape. Furthermore, the use of water-reducing chemicals can destabilise the foam, so they are generally avoided in foam concrete mixtures (OZLUTAS, 2015b).

The effectiveness and serviceability of foam agents for concrete should be evaluated using the standards outlined in ASTM C 869-91 and ASTM C 796-97. In the case of foamed concrete, the air void content ranges from 6% to 35% of the total volume. According to (ACI 523.3R-14, 2014) and (Committee 2003) guidelines, foam is created by combining the foaming agent with water and water-compressed air (from an air compressor) in specific proportions. This mixture is then passed through a foam generator, which sets a specific discharge rate. Taylor, (1967) introduced an alternative foam production method. Their method emphasises the importance of the foam agent's dilution ratio, the formation process, the pressure of the compressed air, its density, and the techniques used for incorporating and mixing the foam with the mortar, all of which influence the

quality of the resulting foam. The quality of the foam is important because it determines the stability of the foamed concrete, which influences its strength and rigidity. Unlike traditional concrete, where the water-cement ratio has a significant impact on compressive strength, foamed concrete's strength is primarily determined by the amount of foam added to the mix. The type of foam agent used is essential; protein-based agents, for example, tend to increase compressive strength more effectively than synthetic agents. Table 2-3 details the various surfactant types and properties.

Table 2-3: Surfactant Types and Properties (Thakur et al., 2022)

Surfactant type	Example composition	Properties	Characteristics of foam produced	Applications in foamed concrete
Synthetic	Alkyl sulfates	Consistent, Stable and easy to formulate	Larger with opened cells due to lower strength & higher expansion	In higher FCs density, good for fast & and large placing
Protein	keratin and Hydrolysed animal proteins	Stabilised, variable & highly refined	Firm texture, Stable, more substantial, and smaller closed-cell bubbles	In low FC density, when waterproofing and high strength are required

Experimental and theoretical analysis conducted by (Wee et al., 2006) revealed that including air bubbles in foamed concrete significantly affects its compressive strength rather than its stiffness. For optimal results, it is recommended that the foam be incorporated into the mix immediately after its creation while it is still in a viscous state to ensure its stability. Adding foam-stabilizing agents, such as fluorinated surfactants, can improve the foam's stability within the concrete mixture. Propump developed the protein foaming agent Propump 26, which is used in this experiment and is suitable for incorporation into mixture designs ranging from 200kg/m³ to 1700kg/m³.

2.9.4 Water

The amount of water required for foamed concrete depends on the mix's components, including any admixtures used. The water content is critical for achieving the desired level of uniformity, consistency, and stability. According to (Nambiar and Ramamurthy, 2006), insufficient water causes the mix to become too rigid, breaking bubbles while mixing and increasing the mix's

density. In contrast, too much water creates a slurry that is too fluid to keep the bubbles in place, causing them to separate from the mix and increase the final density. The recommended water-to-cement ratio is usually between 0.4 and 1.25, corresponding to 6.5% to 14% of the target density. Water quality is also important when producing foamed concrete; according to ACI 523.3R-93 guidelines, it should be clean, fresh, and potable. According to the British Cement Association, the presence of organic contaminants can negatively impact the quality of protein-based foam agents and the formation of foamed concrete mixes.

Non-potable water can still be used for foamed concrete if it allows the concrete to reach 90% strength within 7 to 28 days, as observed with municipal water sources. Highlighted the significance of modifying the sand content in proportion to the increase in the water/cement ratio (Valore, 1954). Rather than strictly following a preset water/cement ratio, Valore encouraged estimating the correct amount of water based on the consistency of the mix. This approach ensures that the mix remains workable in fresh-foamed concrete designs. An incorrect water level could cause the cement to draw water from the foam, causing the foam to degrade rapidly. The British Cement Association recommends keeping the water/cement ratio between 0.5 and 0.6 for best results. Plasticisers play an essential role in improving the workability and stability of foamed concrete. They act as water-reducing agents to improve fresh concrete performance by making it easier to handle and shape without causing segregation. Super plasticisers have a significant effect on foamed concrete because of their ability to reduce the need for water mixing and thus accelerate the strength development of the concrete. The recommended proportion of plasticiser is between 0.45% and 5% of the foam agent's volume, providing a strategic way to improve the concrete's characteristics and performance.

2.9.5 Ordinary Portland Cement

Cement is a fundamental binding agent in the construction industry, serving as a key ingredient in concrete, which is the most widely used building material globally. It is produced through the controlled processing of raw materials such as limestone, clay, shale, and other substances, which are heated in a kiln to form clinker. This clinker is subsequently ground into a fine powder, with gypsum added to regulate setting times, resulting in cement. Cement's hydraulic properties allow it to set and harden upon mixing with water, enabling it to bond with other materials and provide structural strength (Neville, n.d.; Mehta, 2014; Piggin, 2006).

In the United Kingdom, Ordinary Portland Cement (OPC) is manufactured in accordance with British Standard BS EN 197-1:2011. This standard, part of the broader European Norm (EN) framework, outlines the composition, properties, and conformity requirements for OPC and other cement types, ensuring product quality and performance consistency across the construction industry (EN, 2011; ACI 523.3R-14, 2014). The OPC employed in this experimental investigation was classified as CEM I 32.5N, meeting the requirements of BS EN 197: Part 1: 2000. This specific grade of cement is commonly used in foamed concrete production due to its balanced performance characteristics.

The chosen cement-to-sand ratio for this investigation was 1:2, in accordance with relevant British Standards. This mix proportion was consistently applied across both mortar and foamed concrete samples to ensure uniformity in mechanical properties. In foamed concrete production, OPC is particularly valued for its compatibility with foaming agents. Its fine particle size and reactivity facilitate the formation of a stable cellular matrix, crucial for achieving the target density, strength, and durability.

Foamed concrete mixtures typically incorporate cement quantities ranging between 250-500 kg/m³. However, as noted by Meera and Gupta (2020), increasing the cement content beyond 500 kg/m³ can further enhance compressive strength for certain applications. Alternative cement types, such as high-strength and rapid-setting Portland cement conforming to BS 915:1983, have also been explored to improve the performance of foamed concrete, particularly in terms of early strength development (Awang et al., 2014). The selection of cement type is guided by specific project requirements and desired performance characteristics, highlighting the adaptability of foamed concrete for diverse construction applications.

The ongoing advancements in cement technology underscore the importance of optimising cement content and type in foamed concrete to enhance its mechanical and structural performance. Tailoring these properties enables engineers to broaden the application range of foamed concrete, from non-structural fills to load-bearing elements (Jones and McCarthy, 2005c). Adjustments to the mix design, including water-to-cement ratio, choice of foaming agents, and incorporation of supplementary materials like fly ash or silica fume, further refine the performance of OPC-based foamed concrete (Ramamurthy, Kunhanandan Nambiar, and Indu Siva Ranjani, 2009b).

2.9.6 Fine Aggregate

Fine aggregate, typically sand, plays a crucial role in conventional concrete by providing bulk, strength, and stability to the mix. However, its utilisation within foamed concrete presents a different scenario. Foamed concrete, known for its lightweight and insulating properties, primarily relies on incorporating air voids rather than traditional aggregates for its structure. This characteristic significantly influences the role and necessity of fine aggregate in its composition. Studies have shown that while fine aggregate is a fundamental component of standard concrete mixes, its presence in foamed concrete can be minimised or entirely omitted. According to (Kearsley and Wainwright, 2001), the density and thermal conductivity of foamed concrete are directly affected by the inclusion of fine aggregates. Their research suggests that reducing the content of fine aggregate in foamed concrete can enhance its thermal insulation properties while maintaining structural integrity (Jones and McCarthy, 2005d). In the production of foamed concrete, the choice of aggregates is critical due to its impact on the material's structure, density, and overall performance. The use of natural siliceous sand with a particle size of up to 4 mm, in compliance with BS EN 12620, is a standard practice for creating the fine aggregate component of foamed concrete. This specification ensures that the sand meets quality standards that are suitable for achieving the desired properties in the final product. The absence of coarse aggregates in foamed concrete formulations is deliberate, as the material's characteristic fine air void structure is incompatible with larger aggregate sizes. (Nambiar and Ramamurthy, 2007)

The inclusion of bigger aggregates could compromise the integrity of the air voids, leading to issues such as segregation, which would adversely affect the material's uniformity and strength. Exploring sustainable alternatives to traditional fine aggregates has identified a range of materials that can be incorporated into foamed concrete to enhance its environmental friendliness without compromising its structural properties. These alternatives include chalk, lime, incinerator bottom ash, crushed concrete, recycled glass, and Lytag fines. Using such materials not only contributes to reducing the overall density of foamed concrete but also aligns with sustainable construction practices by repurposing waste products as valuable resources in concrete production. This approach not only mitigates the environmental impact associated with the extraction and processing of virgin materials but also offers a pathway to addressing waste management challenges by integrating by-products into the construction materials cycle. (Mohd Sari and Mohammed Sani, 2017).

The exploration of these alternative fine aggregates underscores the ongoing evolution in foamed concrete technology towards more sustainable and environmentally considerate formulations. By employing waste or by-products as raw materials, the construction industry can significantly reduce its carbon footprint and resource consumption, making foamed concrete an even more attractive option for a wide range of applications, from lightweight structural elements to insulation and void filling. This shift towards incorporating alternative materials reflects a broader trend in construction towards sustainability and environmental stewardship, emphasising the role of innovative material science in achieving these goals.

2.10 Considerations

Density: Target densities for foamed concrete can range from 400 kg/m³ to 1600 kg/m³, affecting both the thermal and mechanical properties.

Strength: While foamed concrete is not typically used for high-strength structural applications, the mix design can be tailored to meet specific strength requirements.

Thermal Insulation: One of the critical advantages of foamed concrete is its excellent thermal insulation properties, making it ideal for insulation layers on floors and roofs.

To achieve the desired characteristics, designing and producing foamed concrete requires careful consideration of the mix design, material properties, and production techniques. Tailoring the mix to specific applications allows for the optimisation of strength, density, and thermal properties, making foamed concrete a versatile construction material.

2.11 Typical Properties of Foamed Concrete

Foamed concrete, or cellular lightweight concrete, is a versatile material characterised by its lightweight, high porosity, and thermal insulation properties. Its unique properties are primarily due to the incorporation of stable air bubbles within the cementitious matrix. Here are some of the typical properties of foamed concrete, supported by academic literature:

2.11.1 Wet Density

The wet density of foamed concrete significantly influences its overall properties and is an essential factor in its formulation. As highlighted by Neville (2011), almost all characteristics of foamed concrete are closely linked to its designed density, which is directly impacted by the water content used in the mix. Additionally, various studies have indicated that other factors, such as the

type of fine aggregate, aggregate size, foam type, and sand-cement ratio, also affect the density of foamed concrete.

A notable finding by Ramamurthy and Nambiar (2009) demonstrates that substituting sand with fly ash in the concrete mix not only reduces its density but also enhances its strength. To maintain a specific design density when using fly ash, adjustments in the volume of foam used are necessary, ensuring that the foamed concrete achieves the target density.

In the field of foamed concrete research, empirical relationships have been developed to estimate the density of foam concrete. A method proposed by Jones and McCarthy (2005) provides a practical approach for calculating the approximate fully dry unit weight of foamed concrete; details are shown in equation 2-1, as follows:

$$W_{dry} = \frac{W_{da} + 1.2W_{ct}}{V} \quad \text{Equation 2-1}$$

Where:

W_{da} - Weight of dry aggregate in the batch, in kilograms

W_{ct} - Weight of cement in the batch, in kilograms

V - Volume of concrete produced by the batch, in litres

The term $1.2W_{ct}$ accounts for the combined weight of cement and the water of hydration, considering that the water of hydration constitutes about 20% of the cement weight. This formula provides a foundational guideline for professionals in the construction industry to predict and adjust the density of foamed concrete effectively, enabling the optimisation of its structural and insulating properties.

2.11.2 Dry Density

Foam concrete, an adaptable construction material, is distinguished by its low-density characteristics, primarily due to the incorporation of tiny air bubbles, known as entrained air, into the mortar or Portland cement paste. The density of foam concrete can vary widely, from 300 kg/m³ to 1900 kg/m³, allowing for a broad range of applications, from non-structural fillings to structural components. Mohammed and Hamad (2014) elucidate that Structural Foamed Concrete (SFC), designed for load-bearing applications, typically features densities between 1200 kg/m³ and

1900 kg/m³. This contrasts with normal-weight concrete, which possesses densities ranging from 2240 kg/m³ to 2400 kg/m³, underscoring foam concrete's lightweight advantage.

For structural applications, the American Concrete Institute's ACI 213R Committee (2003) mandates that the concrete's strength should exceed 17.0 MPa, ensuring its capacity to support structural loads effectively. This stipulation ensures that structural foam concrete maintains adequate strength for building applications despite its lower density.

A pivotal aspect of foam concrete's behaviour, as highlighted by Babbitt et al. (2014), is the difference between its wet density (freshly mixed concrete density) and dry density. Notably, the wet density increases and decreases upon drying in an oven at a controlled temperature of 105±2 °C until a constant weight is achieved. This phenomenon is represented mathematically by the equation 2-2.

$$D_{dry} = D_{wet} - \frac{105}{1.05} \quad \text{Equation 2-2}$$

Where:

D_{dry} - The dry density of foamed concrete (kg/m³).

D_{wet} - The wet density of foamed concrete (kg/m³).

This equation applies specifically to foamed concrete with densities ranging from 1400 kg/m³ to 1900 kg/m³, providing a valuable tool for accurately determining the material's density post-drying. This property is essential for precisely calculating material requirements and assessing structural integrity in construction projects utilising foamed concrete.

Foamed concrete exhibits a wide range of densities, typically from 400 kg/m³ to 1600 kg/m³, which can be adjusted based on the application requirements. The variation in density is directly related to the volume of air bubbles introduced into the mix. Lower densities are favoured for thermal insulation and fire resistance, while higher densities are used for structural applications (Nambiar and Ramamurthy, 2006).

2.11.3 Thermal Conductivity

The thermal conductivity of foamed concrete is a critical property that defines its efficiency as an insulating material in construction applications. The unique structure of foamed concrete,

characterised by its air-entrained voids, contributes significantly to its low thermal conductivity, making it an excellent material for thermal insulation purposes.

Foamed concrete's thermal conductivity typically ranges from 0.1 to 0.3 W/(m·K), depending on its density and the size of the entrained air voids. The presence of air voids within the matrix significantly reduces heat transfer through the material, as air is a poor conductor of heat. This property is advantageous in building construction, where foamed concrete can be used to improve energy efficiency by minimising heat gain or loss through walls, floors, and roofs.

According to Jones and McCarthy (2005), the relationship between the density of foamed concrete and its thermal conductivity is inversely proportional; as the density decreases, the thermal conductivity also decreases. This relationship is attributed to the increased volume of air voids in lower-density foamed concrete, which enhances its insulation properties.

Kearsley and Wainwright (2001) conducted extensive research on the thermal properties of foamed concrete. They found that by adjusting the density and composition, foamed concrete can be tailored to meet specific thermal performance requirements. Their findings underscore the material's versatility in construction, mainly when thermal insulation is a priority.

The adaptability and thermal efficiency of foamed concrete make it suitable for various construction applications, from residential to commercial buildings, where energy conservation and thermal comfort are essential. Its low thermal conductivity, lightweight nature, and mechanical properties position foamed concrete as a sustainable building material that contributes to the energy efficiency of structures.

2.11.4 Workability

The workability of foamed concrete is a fundamental characteristic that affects its handling, mixing, placing, and finishing properties. Workability refers to the ease with which a concrete mix can be manipulated to fill the formwork correctly and encapsulate reinforcements without segregation or bleeding. For foamed concrete, workability is paramount due to its unique composition and the presence of air voids.

Foamed concrete exhibits naturally high workability due to its cellular structure, which is comprised of dispersed air bubbles throughout the cementitious matrix. This characteristic makes it highly flowable and suitable for various applications, including void filling, insulation, and lightweight construction. According to Kearsley and Wainwright (2002), the inclusion of foam in the concrete mix increases the fluidity of the mix, allowing it to conform to the shapes of moulds

and formworks easily and to flow into and around intricate reinforcements without the need for excessive compaction efforts.

The viscosity and stability of the foam-concrete mix are crucial for maintaining workability. Jones and McCarthy (2006) have highlighted that the stability of the foam within the mix is essential to prevent the air voids from collapsing during mixing, transporting, and placing, which could adversely affect the uniformity and structural integrity of the final product. The optimal consistency ensures that the foamed concrete can be pumped over long distances or to great heights without losing its homogeneous nature.

Furthermore, the workability of foamed concrete can be adjusted by modifying the mix design, such as altering the water-to-cement ratio and foam content, or by incorporating additives like superplasticisers. Ramamurthy et al. (2009) demonstrated that by carefully selecting and balancing these components, the workability of foamed concrete can be tailored to meet specific application requirements, whether for ease of placement in complex forms or for achieving a desired surface finish. Foamed concrete possesses high workability due to its fluid nature, allowing it to be easily pumped and filled into moulds or cavities without the need for compaction. This property facilitates its use in complex forms and hard-to-reach areas (Ramamurthy et al., 2009).

The inherent workability of foamed concrete, combined with the ability to fine-tune its properties through mixed design adjustments, makes it a versatile and user-friendly material for construction projects. Its ease of application enhances productivity and opens possibilities for innovative architectural and structural designs.

2.11.5 Durability

The durability of foamed concrete, like that of conventional concrete, is a measure of its ability to resist weathering action, chemical attack, abrasion, or any other deterioration process while maintaining its original form, quality, and serviceability when exposed to its environment. Durability is crucial for ensuring the longevity and integrity of structures made from foamed concrete.

Foamed concrete's unique structure, characterised by a matrix of air voids, impacts its durability in several ways. The presence of air voids within the material can influence its permeability, water absorption, and resistance to freeze-thaw cycles, which are key factors in determining the material's durability. According to Kearsley and Wainwright (2001), the closed-cell structure of foamed concrete significantly reduces its permeability compared to conventional concrete, thereby

enhancing its resistance to water ingress and the diffusion of harmful substances that could lead to deterioration.

Jones and McCarthy (2005) have noted that the durability of foamed concrete is also influenced by its mix design, particularly the type and quantity of cement used, the density of the foam, and the addition of any pozzolanic materials such as fly ash or silica fume. These components can enhance the microstructure of foamed concrete, improving its resistance to chemical attack and reducing its susceptibility to degradation processes like carbonation and chloride ingress.

Moreover, the freeze-thaw resistance of foamed concrete is another critical aspect of its durability. Lightweight foamed concrete with a sufficiently closed-cell structure can exhibit excellent resistance to freeze-thaw cycles, as the air voids within the material act as buffers to accommodate the expansion of freezing water, thereby reducing internal stresses. Mydin and Wang (2012) have highlighted the importance of optimising the air void distribution within foamed concrete to maximise its freeze-thaw durability, especially in cold climates.

The durability of foamed concrete can be further enhanced through surface treatments and the use of protective coatings that shield the material from harsh environmental conditions. Such treatments can mitigate the effects of UV exposure, moisture, and chemical attacks, extending the service life of foamed concrete structures.

Studies have shown that foamed concrete has good durability, exhibiting resistance to freeze-thaw cycles, water absorption, and sulphate attack, which is essential for maintaining its structural integrity and longevity (Kunhanandan Nambiar and Ramamurthy, 2007).

2.11.6 Fire Resistance

The fire resistance of foamed concrete is a significant attribute, contributing to its applicability in various construction scenarios, especially in contexts where fire safety is paramount. Due to its fundamental properties and composition, foamed concrete exhibits commendable fire resistance characteristics. This resistance is primarily due to its low thermal conductivity and air voids within its structure, which help insulate the material against heat transfer during fire exposure. According to studies by Hager (2013), the porous structure of foamed concrete contributes to its thermal insulation properties, reducing the heat transfer rate through the material and thereby slowing the rise of temperature on the unexposed side of a fire barrier.

Moreover, the composition of foamed concrete, predominantly consisting of incombustible materials like Portland cement and aggregates, further enhances its fire resistance. When exposed

to fire, the material does not emit toxic fumes or smoke, a critical consideration in assessing building materials' fire performance.

Research by Mydin and Wang (2012) indicates that foamed concrete can maintain its structural integrity and continue to provide insulation in high temperatures typical of building fires. The performance of foamed concrete in fire tests, including those measuring integrity, insulation, and load-bearing capacity, demonstrates its suitability for use in fire-rated applications.

It is also noteworthy that adding certain pozzolans and fire retardants can improve the fire resistance of foamed concrete. These additives can enhance the material's ability to resist spalling, increase its thermal stability, and reduce heat conductivity, making foamed concrete an even more effective barrier against fire spread.

Due to its air voids and low density, foamed concrete has excellent fire resistance properties. It can withstand high temperatures without significant degradation, making it suitable for fire-rated applications (Mydin and Wang, 2012).

2.11.7 Compressive Strength

The compressive strength of foamed concrete is a fundamental property indicating its ability to withstand loads without failure. This characteristic is crucial for evaluating the material's suitability for various construction applications, ranging from non-load-bearing walls to structural components in buildings. The compressive strength of foamed concrete largely depends on its density, controlled by the volume of air bubbles introduced during manufacturing.

The compressive strength of foamed concrete generally ranges from 1 MPa to 25 MPa, depending on the density and mix design. Higher densities result in greater strength, making the material suitable for various structural and non-structural applications (Kearsley and Wainwright, 2001).

Studies by Jones and McCarthy (2005) have demonstrated that the compressive strength of foamed concrete can vary significantly, typically ranging from as low as 1 MPa for very low-density mixes (around 400 kg/m³) to over 25 MPa for higher-density variants (approaching 1600 kg/m³). This wide range allows foamed concrete to be tailored to specific requirements, whether for lightweight insulation or structural applications with higher strength.

Table 2-4, as outlined by Hamad (2014), presents typical properties of foamed concrete, including its compressive strength. With minimum strengths reaching 25 N/mm², foamed concrete demonstrates potential for use in structural applications. See Figure 2-9 for the density design of cement with different mixing ratios. This data suggests that with careful mix design and quality

control, foamed concrete can be optimised to meet various structural requirements, expanding its applicability in the construction industry.

Table 2-4: Mechanical Properties of Foamed Concrete (Hamad, 2014)

Dry density (kg/m^3)	Compressive strength (MPa)	Modulus of elasticity E (GPa)
400	0.25-1.0	0.25-1.0
600	0.5-1.5	0.5-1.5
800	1.0-2.0	1.0-2.0
1000	2.0-4.0	1.5-2.5
1200	3.0-6.0	2.0-4.0
1400	4.0-8.0	3.0-6.0
1600	7.0-12.0	5.0-8.0
1800	10.0-15.0	7.0-12.0

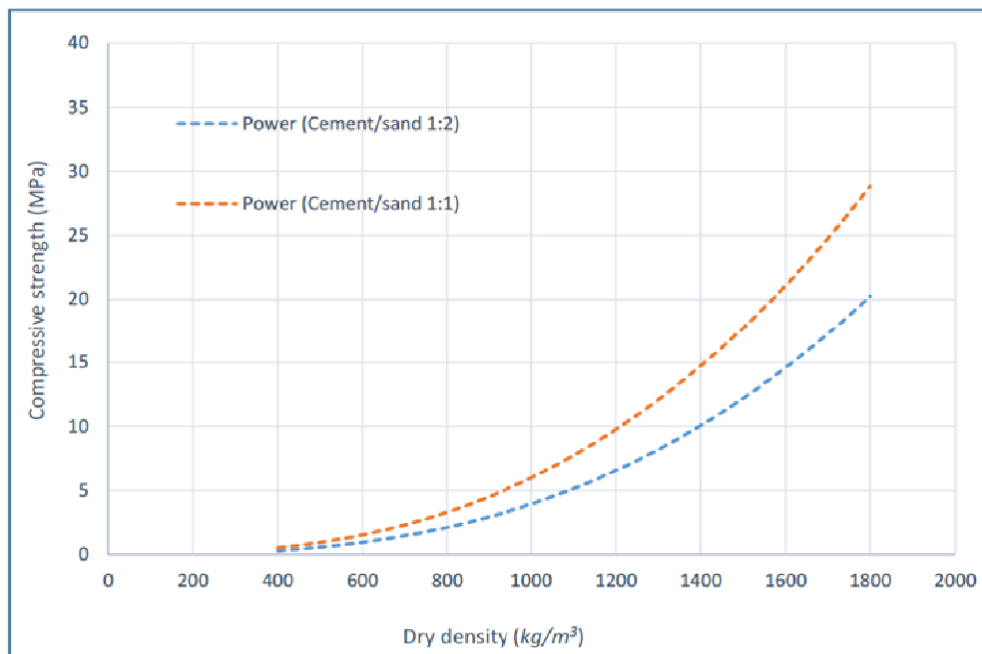


Figure 2-9: Density for Different Cement-to-Sand (C/S) Ratios (Nambiar & Ramamurthy, 2006)

Further research by Ramamurthy, Kunhanandan Nambiar, and Indu Siva Ranjani (2009) has highlighted the impact of mix design on the compressive strength of foamed concrete. They found that factors such as the water-to-cement ratio, type of foaming agent, and incorporating additives

like silica fume or fly ash can significantly affect compressive strength. By optimising these parameters, the mechanical properties of foamed concrete can be enhanced to meet or even exceed those of conventional concrete for specific applications. Hamad (2014) further explores the relationship between compressive strength and density in foamed concrete, indicating that specific formulations of this material can achieve the required durability and strength needed for structural roles.

2.11.8 Flexural Strength

Flexural strength refers to the ability of a material to resist bending under load. Flexural strength is vital in the context of foamed concrete because it indicates the material's capacity to withstand service loads and impacts without failing. The flexural strength of foamed concrete is influenced by its density, with higher densities generally exhibiting higher strengths. Studies by Kearsley and Wainwright (2002) found that the flexural strength of foamed concrete can range from 0.5 to 3.5 MPa, depending on its density and mix composition. Including fibres or other reinforcing materials can further enhance the flexural strength of foamed concrete, making it more resistant to cracking and deformation under load.

Design codes of practice typically emphasise compressive strength as a foundational metric, using it to infer other mechanical properties such as tensile strength, modulus of elasticity, and Poisson's ratio. Various empirical models and theories have been crafted to estimate the splitting tensile strength of foamed concrete based on its known compressive strength. According to Resan et al. (2020), while the American Concrete Institute (ACI) model does not specifically address lightweight concrete, subsequent studies leveraging ACI guidelines suggest a square root relationship between cylinder compressive strength and splitting tensile strength. Furthermore, research indicates that the power of compressive strength in these calculations typically ranges from 0.4 to 0.6 (ASTM C496-96, 1996). Lee et al. (2017) have noted that the splitting tensile strength of foamed concrete generally represents about 10% of its cylinder compressive strength, while its flexural strength accounts for approximately 10-15% of the same. The modulus of rupture can be calculated using several formulas, one of which is provided in ACI 318-05 (2004), shown as Equation 2-3:

$$f_r = 0.62 \sqrt{f'_c}$$

Equation 2-3

Where:

f_r - represents the flexural strength (MPa)

f'_c - signifies the compressive strength (MPa)

It's noted that the splitting tensile strength of foamed concrete is generally lower compared to that of equivalent lightweight aggregate concrete and normal-weight concrete. However, foamed concrete formulations that use a cement-sand base tend to exhibit higher tensile strength than those containing superplasticisers. This increased tensile strength enhances the shear capacity between the paste phase and sand particles, contributing to overall structural integrity (Babbitt et al., 2014). Such insights are crucial for developing and refining applications of foamed concrete in construction, ensuring they meet required specifications and performance expectations.

2.12 Renewable Energy

Renewable energy plays a crucial role in reducing carbon emissions and promoting environmental sustainability in the construction and transportation sectors. Among various renewable energy sources, solar energy is one of the most widely utilised due to its abundance and efficiency (Gao et al., 2021). Solar panels, which convert sunlight into electricity through photovoltaic (PV) technology, have significantly advanced over the years, with various types of solar cells now available, including monocrystalline, polycrystalline, and thin-film solar cells (Sharma et al., 2020). Each type offers different efficiencies, costs, and applications, making them suitable for various engineering solutions, including infrastructure development (Kalogirou, 2019).

One of the emerging applications of solar energy in civil engineering is solar pavement, which integrates PV technology into road surfaces, walkways, and other transportation infrastructure. Solar pavements offer a dual function—providing structural support while generating renewable electricity (Chen et al., 2022). This innovative approach contributes to smart and sustainable urban infrastructure, reducing dependency on non-renewable energy sources (Zhang et al., 2021). Various prototypes and pilot projects worldwide have demonstrated the potential of solar pavement, highlighting challenges such as efficiency, durability, and economic feasibility (Tuffner et al., 2020). For instance, the Solar Roadways project in the United States and the SolaRoad in the Netherlands have provided key insights into the real-world performance of solar pavements (Huang et al., 2020).

2.13 Photovoltaic Solar Panels

Photovoltaic (PV) solar panels are devices designed to capture sunlight and convert it into electricity, playing a crucial role in renewable energy generation. These panels consist of multiple photovoltaic cells arranged in a grid-like pattern, which generate electricity through the photovoltaic effect (Liu et al., 2012). Made from semiconductor materials, typically silicon, these cells produce direct current (DC) electricity when exposed to sunlight, which can be used directly, stored in batteries, or converted into alternating current (AC) for residential, commercial, and industrial applications (Ritchie and Roser, 2018b). Over the years, continuous advancements in solar technology have led to greater efficiency and affordability, making PV systems more accessible and widely adopted.

Solar panels provide a sustainable, clean, and reliable source of energy. Unlike fossil fuels, they operate without emitting greenhouse gases, significantly reducing carbon footprints and contributing to environmental sustainability (Ziemińska-Stolarska, Pietrzak, and Zbiciński, 2021). Even when considering emissions from manufacturing and installation, solar energy has a considerably lower environmental impact than conventional energy sources (Kostopoulos et al., 2018). Technological advancements have led to solar panels achieving efficiencies exceeding 22%, marking a significant milestone in the industry (Smith et al., 2021).

Among renewable energy sources, solar power stands out due to its abundance, adaptability, and cost-effectiveness. The International Energy Agency (IEA, 2020) has recognised solar photovoltaics as the cheapest source of electricity in history, accelerating its global deployment. As of 2020, solar PV accounted for approximately 3% of global electricity generation, with projections indicating rapid growth in the coming years (IRENA, 2021). This expansion is driven by declining production costs, improvements in efficiency, and government incentives supporting renewable energy adoption (Ranabhat et al., 2016).

Currently, the three most common types of PV solar panels are monocrystalline, polycrystalline, and thin-film. Each type varies in efficiency, cost, and application suitability, allowing for flexibility in different energy systems (Energy Saving Trust, 2020). The scalability of solar technology has enabled its integration into various sectors, from large-scale solar farms to small rooftop installations, making it a key component of the global transition toward renewable energy (IEA, 2021).

Monocrystalline Solar Panels: These panels are made of single-crystal silicon, making them extremely efficient at converting solar energy into electricity. They are distinguished by their uniform dark colouration and rounded edges. Their efficiency can range between 15% and 20%, which is higher than other types. However, this efficiency comes at a higher cost, making them a premium choice in the market (Northmore, 2015).

Polycrystalline Solar Panels: Made up of multiple silicon crystals, these panels have a distinctive blue, speckled appearance. They have a slightly lower efficiency (13% to 16%) than monocrystalline panels but are more cost-effective. This makes them a popular option for residential and commercial installations without space constraints (Nayak et al., 2019).

Thin-film solar Panels: Created by depositing one or more layers of photovoltaic material (such as amorphous silicon, cadmium telluride, or copper indium gallium selenide) on a substrate, thin-film solar panels are lightweight and flexible, with an efficiency range of approximately 10% to 13%. They are less susceptible to high temperatures and shading than crystalline silicon panels. While they require more space due to their lower efficiency, their manufacturing process is simpler and potentially less expensive (Northmore, 2015).

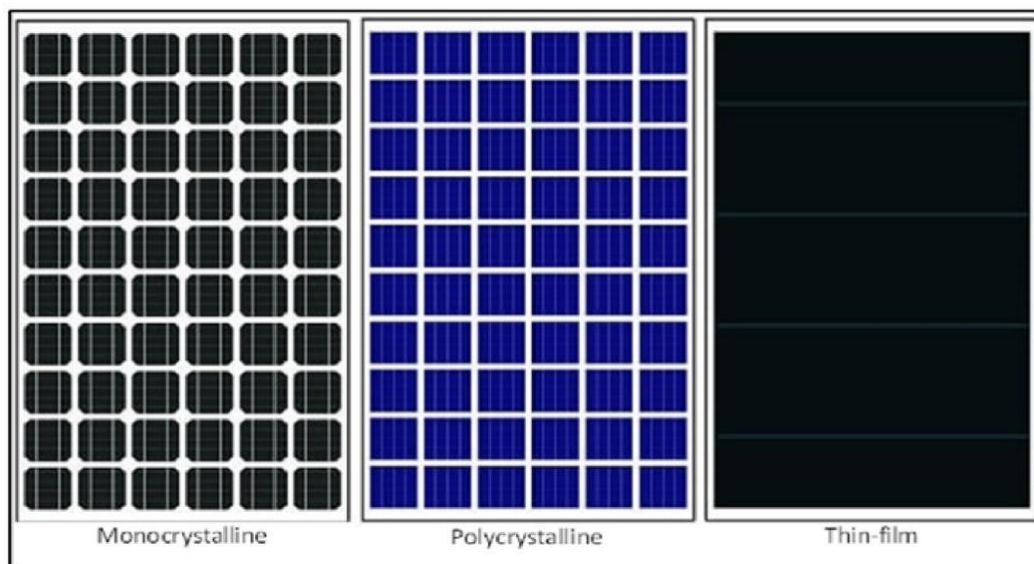


Figure 2-10: Types of Solar Panels (Northmore, 2015)

While monocrystalline panels offer the highest efficiency, they come at a higher cost. Polycrystalline panels provide a more cost-effective solution with slightly lower efficiency. Despite being the least efficient, thin-film panels are the most cost-effective and installation-friendly option. Emerging technologies such as PERC and bifacial panels offer higher efficiency

and the potential for greater energy output, though they are more expensive. The choice among these options depends on the specific needs of the installation site, budget constraints, and long-term energy goals.

2.13.1 Types of Solar Panels

Solar panels are available in various types to suit different applications and budgets. Among the most common types are:

1. **Rooftop Solar Panels:** Rooftop solar panels are the most widely recognised and commonly used type. They are installed on the roofs of homes and buildings, using otherwise unused space. This type is popular in residential and commercial sectors due to its efficiency and ability to reduce electricity bills (Office of Energy Efficiency & Renewable Energy, 2020).
2. **Canopy Solar Panels:** Canopy solar panels are installed on structures such as building front canopies, petrol stations and bus stops. These panels provide shade while generating electricity, making them a dual-purpose solution. Canopies are often used in parking lots or public spaces to create power and offer protection from the elements (Solar Energy Industries Association, 2022).



Figure 2-11: Types of Solar Panels on the Market (The Eco Experts, n.d.)

3. **Flat Roof Solar Panels:** These panels are installed on flat roofs, commonly found in commercial buildings. They can be mounted on racks that allow optimal tilt angles to maximise sun exposure throughout the year (International Renewable Energy Agency, 2021).

4. **Floor-Mounted Solar Panels:** Floor-mounted solar panels are typically used in large open spaces, such as solar farms or fields. These systems can be more easily adjusted for angle and orientation compared to rooftop panels, and they are often used for large-scale energy production (Sharma, 2019).

5. **Wall-Mounted Solar Panels:** Wall-mounted or façade solar panels are integrated into the sides of buildings. These panels are particularly useful in urban areas where roof space may be limited. They contribute to the building's energy efficiency by generating power and reducing the need for other materials on the building's exterior (Kalogirou, 2014). Figure 2-11 shows examples of various solar panel installations.

2.13.2 Benefits of Solar Panels

Solar panels offer numerous benefits, both for individual users and society as a whole:

1. **Reduction in Energy Bills:** Solar panels can significantly reduce or even eliminate electricity bills for homeowners and businesses by generating electricity on-site. This is particularly beneficial in areas with high electricity rates (Energy Saving Trust, 2023).

2. **Environmental Impact:** Solar energy is a clean and renewable source of power, producing no greenhouse gas emissions during operation. By reducing reliance on fossil fuels, solar panels help mitigate climate change and reduce environmental pollution (National Renewable Energy Laboratory, 2022).

3. **Increased Property Value:** Properties equipped with solar panels often see an increase in market value. Buyers are increasingly aware of the long-term savings and environmental benefits associated with solar energy, making solar-equipped homes more attractive (Zillow, 2019).

4. **Energy Independence:** Solar panels enable individuals and businesses to produce their own electricity, reducing dependency on the grid and providing a measure of energy security, particularly in areas prone to power outages (U.S. Department of Energy, 2021).

5. **Government Incentives:** Many governments offer incentives for installing solar panels, such as tax credits, rebates, or feed-in tariffs. These incentives can significantly reduce the initial cost of installation, making solar energy more accessible to a broader range of consumers (International Energy Agency, 2020).

2.14 Solar Pavements

In contrast to traditional pavements, solar walkable pavement slabs offer a transformative opportunity to align urban infrastructure with sustainability and net-zero goals. By integrating photovoltaic (PV) cells into the pavement surface, these slabs can generate renewable energy directly from sunlight, thereby contributing to the reduction of greenhouse gas emissions. Additionally, the use of recycled materials in the construction of solar pavements can further enhance their environmental benefits by reducing the reliance on virgin resources and minimising waste (Fthenakis & Kim, 2019).

In the context of growing environmental concerns and the need to reduce carbon emissions, transforming these conventional pavements into solar walkable pavement slabs presents a significant opportunity to contribute to renewable energy generation within urban environments. Solar walkable pavements integrate photovoltaic (PV) cells into the surface of the pavement, allowing these everyday structures to harness solar energy and convert it into electricity. Building upon the success of traditional solar panels, innovative applications such as solar pavements are emerging as promising solutions in the fight against global warming. Solar pavements integrate photovoltaic technology into walkways and roads, transforming ordinary surfaces into energy-generating platforms (Schoenenberger, 2019). This innovative approach maximises the utilisation of urban spaces, particularly in densely populated areas where available land is limited for conventional solar installations.

Implementations of solar pavements have demonstrated their potential effectiveness and practicality. For example, projects in countries like the Netherlands and France have successfully integrated solar cells into cycling paths and highways, generating clean energy while maintaining the functionality of the infrastructure (de Lima et al., 2020). These systems not only contribute to renewable energy production but also offer additional benefits such as powering streetlights, traffic systems, and even electric vehicle charging stations directly from the pavement itself.

Transitioning to renewable energy sources, with a strong emphasis on solar technologies, is essential for effectively tackling global warming (Ma et al., 2019). The continued development and distribution of solar panels and innovative solutions like solar pavements offer sustainable and efficient means to reduce greenhouse gas emissions and pave the way toward a greener and more resilient future. Embracing these technologies on a global scale will be critical in meeting

international climate goals and ensuring environmental sustainability for generations to come (Kern, 2020).

For years, most of the materials currently used on roads and highways have remained unchanged. However, a recent change has been made to make pavements more sustainable in various ways. More recycled materials, such as glass, asphalt shingles, recycled asphalt pavements, recycled rubber tyres, other additives in asphalt mixes, or recycled materials within the concrete, have been used in pavements. Researchers have developed these technologies in order to make pavements more sustainable (Northmore, 2014).

Solar pavement technology, which integrates photovoltaic (PV) technology into pavement surfaces, has emerged as a promising approach to enhancing sustainability in infrastructure. Various types of solar panels, including monocrystalline, polycrystalline, and thin-film technologies, have been explored for pavement applications. While monocrystalline solar cells provide higher efficiency, thin-film cells offer better flexibility and integration into concrete surfaces. The use of solar energy in civil engineering extends beyond pavement applications to include renewable energy solutions for urban environments, contributing to reduced dependence on traditional energy sources and improved energy efficiency in smart cities. However, several challenges must be addressed to facilitate the widespread adoption of sustainable materials and solar-integrated pavement technology. Issues such as durability, cost-effectiveness, and energy storage solutions require further research and development. The lack of standardised regulations and performance guidelines creates uncertainties in their application, necessitating more extensive material testing and performance monitoring. Additionally, concerns regarding long-term durability and material property variability highlight the need for ongoing innovation and industry collaboration to optimise material compositions and enhance mechanical properties.

2.15 Solar Pavement Structure

A solar slab panel with a three-layer composite structure consisting of transparent, optical, and base layers. The transparent layer handles direct vehicle interaction and allows solar radiation to pass through to the optical layer. Solar Road Panels are made of tempered glass, which is 4-5 times stronger than non-tempered glass. Further testing has revealed that the surface of the panel road is less slippery than a standard road and is easy to maintain. During winter, these panels can melt snow, making driving safe while also collecting sunlight. The optical layer transfers the load from the transparent layer to the base layer by directing it around the embedded solar cells within the

structural cut-outs. Lastly, the base layer supports the structure, transferring the load to the structured base beneath the panel, which could be made of a concrete housing base, according to Northmore & Tighe (2012b) and Kehagia, Mirabella & Psomopoulos (2019a).

The polycarbonate transparent layer samples are optical grade scratch-resistant polycarbonate, also known as hard-coated and scratch-resistant Lexan polycarbonate or safety glass, which is another suitable material for the solar tile's top layer. Polycarbonate is approximately 250 times more impact-resistant than standard glass, making it superior in terms of impact resistance. Additionally, the polycarbonate samples were given a scratch-resistant coating with nano SiO₂ sprayed on the surface to extend their lifespan and ensure efficient light transmission to the solar panel (Assessment, 2023b). See Figures 2-12a and b illustrate solar roadway structural layers.

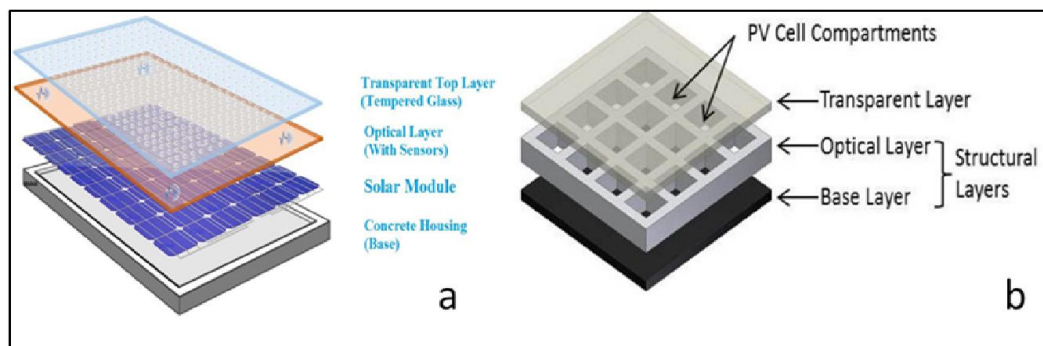


Figure 2-12: Layers of Solar Roadways (Rahman et al., 2017 & Northmore & Tighe, 2016)

2.16 Existing Research on Solar Pavements

In 2009, American electrical engineer Scott Brusaw introduced the concept of Solar Roadways, aiming to replace traditional asphalt and concrete pavements with energy-generating surfaces. His design features hexagonal solar panels functioning as paving tiles, each composed of multiple layers to ensure durability, functionality, and safety. The top layer consists of toughened, skid-resistant glass capable of supporting vehicles. In contrast, underlying layers include LED lighting for road markings, a circuitry layer for energy management, and a base layer for structural support. This innovative approach generates renewable energy and integrates features like illuminated road signals and potential heating elements to prevent snow and ice accumulation.

The production of these solar panels involves several critical steps to ensure they meet the required standards for durability, energy efficiency, and safety. The top layer is crafted from tempered, textured glass that is strong and transparent enough to allow sunlight to reach the photovoltaic

cells beneath. High-efficiency solar cells are embedded within the panels to capture solar energy and convert it into electricity. The LED lights and associated circuitry are installed to provide illumination and communication capabilities. The various layers are assembled into a cohesive unit, ensuring all components are securely integrated and protected from environmental factors. Each panel undergoes rigorous testing to assess its structural integrity, energy output, and safety features before deployment. The Solar Roadways project has garnered significant attention and support, including funding from the U.S. Department of Transportation for research and development. Pilot installations have been implemented in various locations to evaluate the panels' performance in real-world conditions. While challenges such as cost, durability, and energy efficiency remain, ongoing research and development efforts continue to refine the technology to create sustainable, energy-generating roadways in the future.

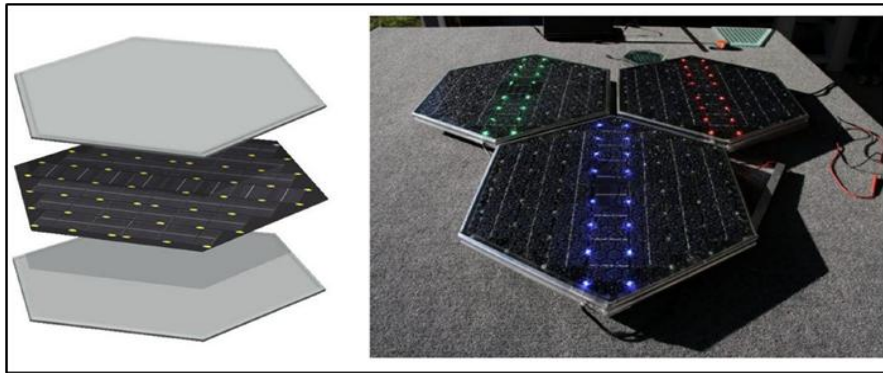


Figure 2-13: Solar Roadways (Scott Brusaw)

In 2016, Zha et al. proposed an innovative design for solar pavements, introducing a hollow-plate structure composed of three distinct layers. **Surface Transparent Protection Plate:** This top layer is made of polymethyl methacrylate (PMMA), a transparent material chosen for its durability and ability to protect the underlying components while allowing sunlight to reach the solar cells.

Middle Solar Panel Layer: Positioned beneath the protective plate, this layer contains the solar cells responsible for converting sunlight into electricity. **Prefabricated Concrete Hollow-Base Layer:** Serving as the foundation, this bottom layer is a hollow concrete slab designed to support structural loads and house the necessary electrical components.

The design aims to integrate energy generation into pavement structures without compromising their primary functions. The hollow base not only reduces the weight of the pavement but also provides space for housing electrical wiring and other necessary infrastructure. The PMMA

transparent layer ensures that the solar cells are protected from environmental factors while maintaining high light transmittance. This configuration allows the pavement to generate electricity while still serving as a functional roadway. To optimise the structural performance and economic feasibility of the design, Zha et al. conducted a series of analyses using the ANSYS software. They examined various parameters, including the panels' length and width, the sidewalls' thickness, and the PMMA layer's thickness. Based on their findings, they recommended an optimised structure with dimensions of 50 cm × 50 cm × 25 cm, featuring a 2 cm thick PMMA layer, 10 cm thick sidewalls, and a 10 cm thick baseplate. This configuration was determined to offer a balanced combination of mechanical strength, safety, and cost-effectiveness. This hollow-plate solar pavement design represents a significant advancement in the integration of renewable energy technologies into civil infrastructure, offering a promising approach to sustainable roadway development.

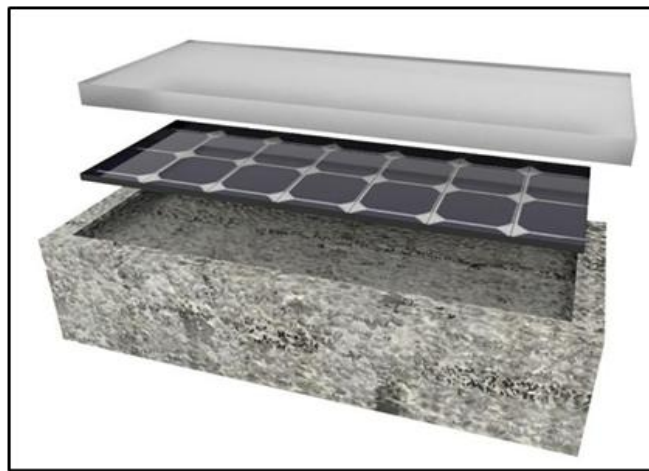


Figure 2-14: Hollow-Plate Solar Pavement Layers (Zha et al., 2016)

PLATIO Solar Paver: The PLATIO Solar Paver is an innovative, sustainable, and walkable building material designed to integrate solar energy harvesting into functional urban surfaces. It features high-performance solar cells embedded beneath heavy-duty, anti-slip, scratch-, and impact-resistant glass panels, ensuring both efficiency and durability in high-traffic areas. A sturdy, load-bearing frame structure supports the surface and protects internal cables, allowing it to withstand pedestrian and light vehicular loads. The frame is uniquely produced using recycled plastic waste, with no virgin plastic materials involved, promoting a circular economy approach and reducing plastic pollution. Each paver measures 353 mm x 353 mm x 41 mm and weighs 7.4 kg per unit, with a nominal peak power output of 21 Wp per paver (PLATIO Solar, n.d.). This

combination of renewable energy generation and waste reduction results in a durable and eco-friendly product capable of providing decades of reliable performance. PLATIO Solar Pavers are suitable for various applications, including public spaces, residential pathways, commercial developments, and smart cities, enabling urban environments to reduce their carbon footprint while producing clean energy. Figures 2-15 are sourced from the official website PLATIO Solar.



Figure 2-15: Platio Solar Pavement (PLATIO Solar Paver)

[\(https://www.smartpaverenewableenergy.com/platio-solar-pavers/\)](https://www.smartpaverenewableenergy.com/platio-solar-pavers/)

TNO Solar Road Panels: The Netherlands Organisation for Applied Scientific Research (TNO) is at the forefront of developing innovative, energy-efficient systems. One of its pioneering projects involves the development of Solar Road panels, a concept that integrates photovoltaic technology directly into road surfaces. This project aims to generate renewable energy and create a multifunctional infrastructure that contributes to broader sustainability goals (TNO, 2013).

The panels are designed as modular units, each measuring 1.5 by 2.5 meters. Their layered construction is a key feature, incorporating a glass top layer that protects the photovoltaic cells from weather-related damage while allowing sufficient sunlight to pass through. Beneath the glass, crystalline silicon solar cells convert sunlight into electrical energy, and a concrete slab base provides essential structural support, ensuring stability and durability under the varying loads and weather conditions typical of the Dutch climate (Northmore, 2014b).

TNO has collaborated with industry partners such as Ooms Avenhon Groep, a firm specialising in civil infrastructure, and Imtech, an electrical and mechanical engineering consultancy focused on refining the energy generation and distribution aspects of the project. This interdisciplinary approach allows the solar road panel concept to be specifically tailored for the Dutch environment

by initially targeting cycling paths. Using these paths as a controlled testing environment enables evaluation of performance, safety, and durability before the technology is considered for broader applications on busier vehicular roads (TNO, 2013).



Figure 2-16: Solar Roadways (TNO, 2013)

Despite the promising design, the project has experienced setbacks. The planned installation on a North Holland cycling path, initially scheduled for the summer of 2012, has been delayed. Such postponements are not uncommon in innovative infrastructure projects. They can result from technical challenges, such as ensuring the panels can withstand harsh weather and mechanical stresses over time, as well as the need to meet stringent regulatory and safety requirements and overcome logistical issues during integration. These challenges highlight the complexities of transitioning from a conceptual prototype to a fully operational system integrated into existing infrastructure (Northmore, 2014b).

Overall, TNO's Solar Road panels represent a significant step toward incorporating renewable energy solutions into everyday infrastructure, emphasising both the potential benefits and the practical challenges of pioneering such innovative technology.

The Netherlands: The Netherlands pioneered solar pavements by constructing a solar cycle path and a bike lane paved with glass-coated solar panels. Field testing over one year demonstrated that the installation could generate around 70 kWh/m²/year, an output sufficient to power a small household (Papadimitriou, Psomopoulos and Kehagia, 2019). This innovative approach converted

a common urban infrastructure into a renewable energy source, proving that everyday surfaces can contribute to sustainable energy generation.

Researchers conducted both field and laboratory evaluations to assess the system's performance. Continuous energy output monitoring in the field provided a realistic measure of the system's capacity under actual usage conditions. Laboratory tests complemented these findings by simulating environmental stressors, such as UV radiation, temperature fluctuations, and mechanical wear, to evaluate the durability and structural integrity of the solar panels.

Despite the promising energy results, significant challenges were identified. The solar panels employed in the project were considerably heavier than conventional pavement materials. This increased mass necessitated more robust mounting systems, complicating the installation process and raising concerns about the scalability of such technology in broader urban settings (Northmore, 2019). Moreover, the anti-slip coating, essential for ensuring safe cycling and pedestrian traffic, was found to deteriorate over time. Prolonged exposure to sunlight and fluctuating temperatures led to the peeling of this layer, thereby potentially compromising both the safety and the efficiency of light transmission to the photovoltaic cells (Shekhar et al., 2015b).



Figure 2-17: Netherlands Solar Cycle Path (SolaRoad, 2014)

These findings underscore the need for advancements in material science to improve the viability of solar pavements. Future research should focus on developing lighter composite materials that reduce installation challenges and enhancing the formulation of anti-slip coatings to withstand prolonged environmental exposure. By addressing these limitations, it will be possible to harness

the full potential of solar pavement technologies while ensuring long-term performance and safety. The Netherlands solar cycle path has provided invaluable insights into the feasibility of energy-generating pavements. Although the project achieved an impressive energy yield, the issues related to panel weight and coating durability highlight critical areas for future improvement. Addressing these challenges will be key to advancing solar pavement technology from experimental stages to widespread urban application, ultimately contributing to more sustainable and resilient infrastructure solutions.

George Washington University (GW) Campus in Ashburn, Virginia: The walkable solar photovoltaic pavement system at George Washington University’s Ashburn campus exemplifies an innovative approach to integrating renewable energy into urban design. Developed as a demonstration project, this system transforms a pedestrian pathway into an energy-generating asset, marking what is believed to be the world’s first walkable solar-panelled pathway (George Washington University). Engineered with safety and durability in mind, the pavement meets anti-slip standards and can withstand point loads of up to 400 kg. This robust design ensures that the pathway remains safe and functional under typical pedestrian use and light loads. At the same time, its maximum power output of 400 watts enables it to function as a mini power station powering 450-embedded LED lights for nighttime illumination (Engineering, Belnor).

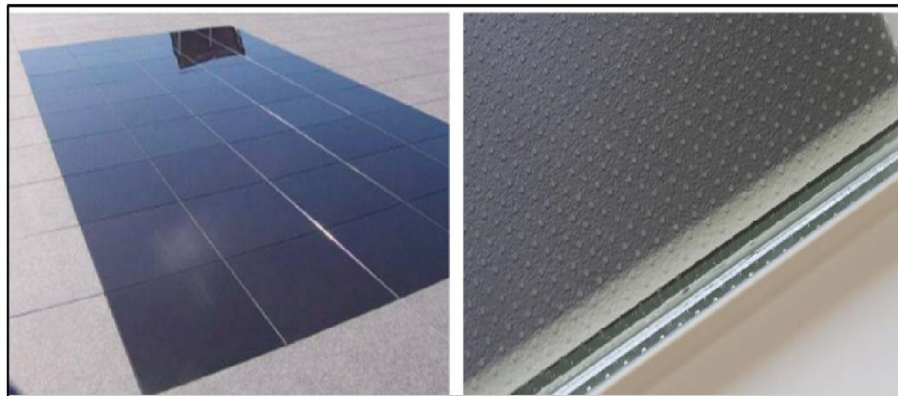


Figure 2-18: Walkable Solar Pavement System (Onyx Solar)

The system utilises amorphous silicon (a-Si) solar cells, which generally achieve an efficiency of 6–8%, lower than that of crystalline silicon cells, but are chosen here for their suitability in building-integrated photovoltaic (BIPV) applications. A key design element is the translucent front glass surface, which enhances the aesthetic appeal, ensures pedestrian safety and provides the

necessary protection for the solar cells. However, this glass cover reduces solar absorption, limiting the system's overall power output (Yang, 2016; George Washington University).

Despite these efficiency limitations, the project serves as a valuable proof-of-concept. It demonstrates the feasibility of embedding solar PV technology into urban surfaces and highlights the potential for further innovation in sustainable infrastructure. Future research may focus on improving cell efficiency and optimising the design balance between aesthetic appeal and energy capture, paving the way for broader adoption of BIPV solutions in diverse urban environments.

Jinan City, Shandong Province, China: Jinan City's solar highway project represents a pioneering step in integrating renewable energy directly into transportation infrastructure. Completed as a trial section in 2017 along the Jinan Expressway, the project spans approximately 5,875 square metres and is engineered to generate nearly one million kilowatt-hours of electricity annually—enough to power roughly 800 households (Hossain et al., 2021). The strategic placement along the city's ring road minimises transmission losses by supplying energy directly to nearby consumers, enhancing overall efficiency.

A robust three-layer structure underpins the highway's design. The top layer consists of a durable, transparent protective material that not only shields the embedded solar cells from environmental wear and tear but also reduces glare and improves safety. The middle layer houses the photovoltaic cells, while the bottom insulating layer provides structural stability and protection from mechanical stresses. This multilayer approach is critical in ensuring the road can withstand both passenger and heavy vehicle loads while maintaining its energy-generating capabilities (Kehagia, Mirabella and Psomopoulos, 2019a).

An innovative aspect of this project is its integrated snow-melting capability. By utilising a portion of the generated electricity to heat the road surface during winter, the system helps prevent the accumulation of snow and ice. This not only improves road safety but also reduces the reliance on traditional, labour-intensive snow removal methods. Such dual functionality underscores the potential for solar road projects to contribute to broader urban sustainability and operational efficiency goals.

Despite the promising outcomes, several challenges remain. The initial installation costs are notably high due to specialised materials and construction techniques. Additionally, concerns about long-term durability under extreme weather conditions and the relatively lower efficiency of solar cells compared to conventional rooftop installations continue to be areas of active

investigation (Hossain et al., 2021; Kehagia, Mirabella and Psomopoulos, 2019a). Nevertheless, the Jinan project serves as a valuable proof-of-concept, offering essential insights into how renewable energy solutions can be seamlessly integrated into everyday infrastructure and providing a basis for future improvements in design and cost-effectiveness.

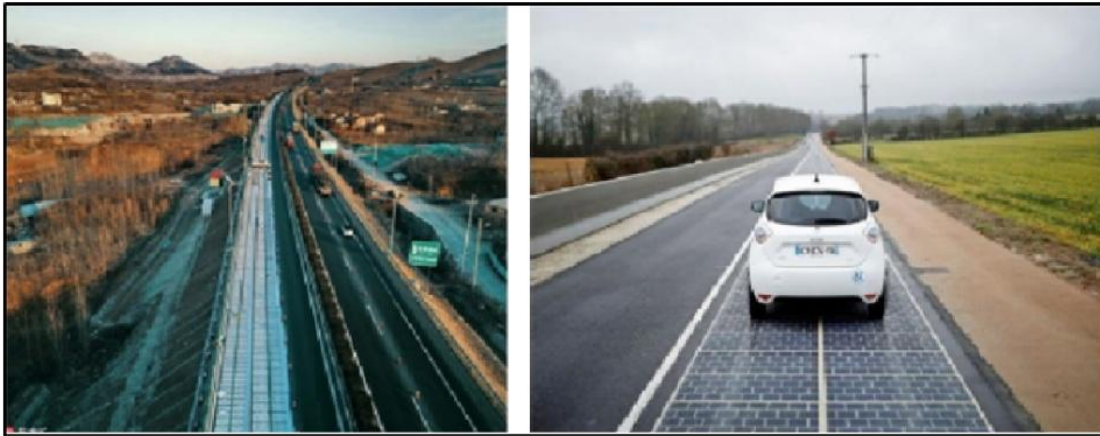


Figure 2-19: Solar Highway in China ((Hossain et al., 2021)

Tourouvre-au-Perche, France: The Wattway Solar Road, France pioneered the development of solar road technology with the installation of Wattway, a one-kilometre stretch of photovoltaic pavement in Tourouvre-au-Perche, Normandy. Constructed using Colas' Wattway technology, this 2,880 m² solar roadway was designed to integrate renewable energy production into road infrastructure by embedding thin photovoltaic panels capable of withstanding vehicular traffic (Kesari & Kumar, 2021). In addition to this large-scale project, a separate solar road trial was conducted at the Sense City experimental site in Marne-la-Vallée, near Paris, in 2016. This testbed simulated real urban conditions, including partially shaded areas from buildings, trees, and street fixtures, to evaluate solar road efficiency under diverse environmental factors. The system was accessible to pedestrians, cyclists, and light vehicles and was installed on a 195×85 cm² prefabricated concrete slab embedded with three 60 W photovoltaic panels. Each panel was coated with a 1 cm semi-transparent protective layer developed by IFSTTAR (French Institute of Science and Technology for Transport, Development, and Networks) to enhance durability and optimise solar absorption (Vizzari et al., 2021).

Development and Functionality of the Wattway Solar Road. The Tourouvre-au-Perche Wattway solar road was officially launched in December 2016, marking the first full-scale deployment of photovoltaic road technology. The project, spearheaded by Colas, aimed to replace conventional

asphalt surfaces with durable solar panels that could generate electricity while serving as a functional roadway. Unlike Solar Roadways in the United States, which utilised hexagonal interlocking modules, Wattway panels were ultra-thin and designed to be directly installed onto existing roads, allowing for a less invasive implementation process (The Guardian, 2016).

This photovoltaic road surface covered 2,800 square metres of resin-coated solar panels, generating electricity intended to power the village's street lighting system. The skid-resistant layer ensured that vehicles could safely traverse the surface, making it a potential sustainable alternative to conventional road construction (The Guardian, 2016).

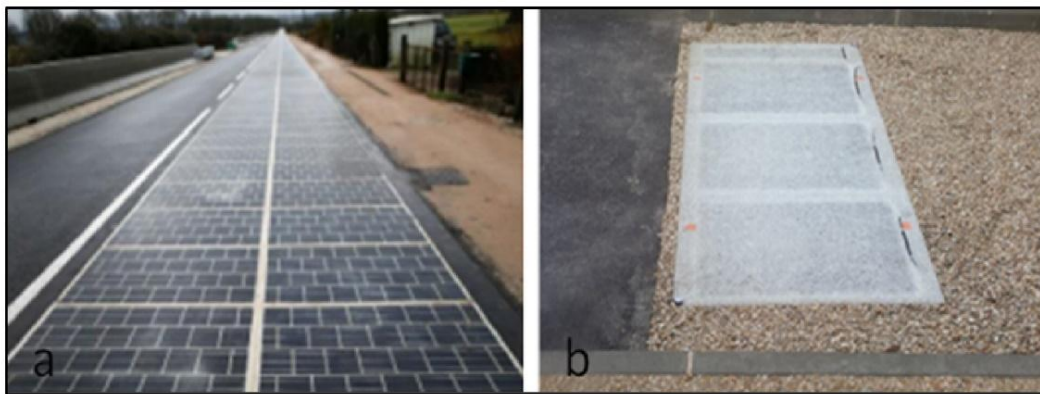


Figure 2-20: (a) Solar Roadway, (b) Solar Concrete Slab Prototype (IFSTTAR)

Despite the innovative approach, the project encountered major setbacks. The cost of generating electricity from Wattway Road was estimated at £14.50 per kilowatt-hour, far exceeding the £1.10 per kilowatt-hour produced by traditional solar panels (Popular Mechanics, 2019). This stark difference raised concerns about economic feasibility and long-term viability. Additionally, the road's actual energy production was significantly lower than expected, achieving only half of its projected output in the first year. Over time, the structural integrity of the panels deteriorated, with reports of delamination, surface cracking, and efficiency losses due to dirt accumulation and traffic load. The panels struggled to withstand heavy vehicles and harsh weather conditions, leading to further degradation (BBC, 2021). A solar road in France consists of approximately 2,880 m² of solar panels, built using Colas Watt way technology and runs for one kilometre in Tourouvre-au-Perche (Kesari & Kumar, 2021). In 2016, a large-scale experimental installation of a solar road was completed at the Sense City site, an experimental platform in Marne-la-Vallée near Paris. This installation mirrored authentic urban conditions, including areas partially shaded by neighbouring structures, trees, and masts, and was accessible to light vehicles, pedestrians, and bicycles. The

system was implemented onto a 195×85 cm² concrete slab comprising three parallel-connected 60 W PV panels, each covered by a 1 cm semi-transparent layer designed by IFSTTAR (Vizzari et al., 2021).

2.16.1 Benefits of Solar Walkable Pavements

1. **Energy Generation:** By integrating PV cells into the pavement, solar walkable slabs can generate electricity directly from sunlight. This energy can be used to power streetlights, traffic signals, or even nearby buildings, reducing the reliance on grid electricity generated from fossil fuels (Liu et al., 2017).
2. **Space Efficiency:** Solar pavements utilise existing infrastructure, such as sidewalks and pedestrian pathways, to generate renewable energy without requiring additional land (Kamel & Sadik, 2017).
3. **Aesthetic and Functional Integration:** Solar walkable pavements are designed to blend seamlessly with existing urban landscapes. They retain the aesthetic appeal and functionality of traditional pavements while adding the capability to produce renewable energy. This integration supports the creation of smart cities that prioritise sustainability and innovation (Zhang et al., 2020).
4. **Environmental Impact:** Replacing conventional pavements with solar walkable slabs contributes to reducing carbon emissions. The energy generated by solar pavements is clean and renewable, helping cities move closer to their net zero due to carbon emissions. Additionally, using recycled materials to construct these slabs can further reduce the environmental footprint of urban infrastructure projects (Fthenakis & Kim, 2019).
5. **Challenges and Considerations:** While solar walkable pavements are promising, several challenges need to be addressed. These include ensuring the durability of PV cells under constant foot traffic, maintaining efficiency in varying weather conditions, and the initial installation cost. However, ongoing advancements in material science and PV technology are gradually overcoming these challenges, making solar pavements a viable option for future urban development.

The transformation of existing walkable pavements into solar walkable pavement slabs represents a practical and innovative approach to urban sustainability. By converting everyday pedestrian pathways into energy-generating surfaces, cities can contribute to renewable energy production, reduce their carbon footprint, and move towards a more sustainable future. The integration of this

technology not only optimises space use but also aligns with global efforts to combat climate change.

2.16.2 Solar Paving Bricks

Solar brick lights have emerged as innovative solutions in urban illumination, combining aesthetic appeal with energy conservation. These modern lighting fixtures integrate photovoltaic cells, energy storage systems, and LED technology into a durable, transparent, and waterproof structure, offering reliable, sustainable, and cost-effective lighting solutions (Solar Centre, n.d.). The design of solar brick lights is particularly ingenious—the top surface contains solar cells that absorb sunlight during the day, storing the captured energy in an integrated battery, which powers the embedded LEDs when darkness falls. Their robust structure allows these units to be embedded into various surfaces, such as pavements, driveways, and public squares, providing ambient lighting and improving nighttime visibility (Brix, 2002). These lights operate on clean, renewable energy, producing zero emissions during use and reducing the dependence on grid electricity, thereby helping to mitigate climate change (Hu et al., 2021c).



Figure 2-21: Examples of Solar Paving Bricks

(<https://www.exteriorlights.co.uk/product/Paverlight-solar-brick-light>)

Compared to traditional lighting systems, solar brick lights eliminate electricity costs and require minimal maintenance, lowering their lifetime costs despite a potentially higher initial investment. Their durability and extended lifespan further reduce the need for frequent replacements and repairs, making them an economically attractive solution in the long run. Additionally, solar brick lights enhance safety through low-voltage operation, reducing wiring costs and electrical hazards.

A single day of solar charging can power a brick for up to eight hours to guide pedestrians at night. Figure 2-21 shows an example of a solar-powered ground lighting system designed to illuminate pavements and pathways, guiding people safely after dark. These solar paving bricks offer a long service life and represent an innovative, sustainable, and economical lighting solution for modern urban environments (Brix, 2002).

2.16.3 Current Application of Solar Bricks

Solar bricks are increasingly used in various urban and residential projects due to their dual functionality and aesthetic appeal. They are commonly installed along pathways, driveways, and sidewalks to provide necessary illumination for safety at night, enhancing both security and the visual appeal of outdoor spaces (Patel & Kumar, 2021b). In public parks and recreational areas, solar bricks light up walking trails and seating zones, promoting sustainability while reducing the need for extensive wiring and trenching. Additionally, they are popular in commercial and residential landscaping projects, where they create illuminated borders around gardens, patios, and courtyards. See Figure 2-22 for the solar brick light available online via the Solar Centre.

Their ability to function off-grid also makes them an attractive option for emergency lighting in municipalities, providing reliable illumination during power outages. Moreover, solar bricks are increasingly integrated into sustainable urban development projects, particularly in smart city initiatives prioritising energy efficiency and renewable energy sources (Smith & Lee, 2022a).



Figure 2-22 Solar Brick (Solar Centre)

Despite their advantages, solar bricks have several significant limitations. One of the main challenges is their high initial cost, typically around £30, which can be a deterrent for many

potential users. Additionally, their performance is highly dependent on sunlight, making them less reliable in regions with low solar exposure. The LED lights in solar bricks often produce insufficient brightness, particularly in areas where strong illumination is necessary for safety. Another critical issue is the limited battery life and energy storage capacity. Due to the compact design of solar bricks, the embedded batteries are small, restricting the amount of energy they can store. Consequently, the stored energy may only power the lights for a few hours at night (Patel & Kumar, 2021b).

Moreover, the materials used in the construction of solar bricks, often plastic, raise durability concerns. While plastic is lightweight and cost-effective, it may not be strong enough to endure heavy loads and continuous pressure from vehicles or frequent pedestrian traffic. This can lead to issues like cracking, deformation, or even failure, particularly in high-traffic areas. The compact size of the bricks further limits their energy storage and light output, which may necessitate the installation of additional units to achieve adequate lighting. This can increase costs and complicate installation processes (Smith & Lee, 2022).

2.17 Solar Garden Lights

Solar garden lights are outdoor lighting fixtures that utilise solar panels to absorb sunlight during the day and convert it into electrical energy stored in rechargeable batteries. This energy is then used to power LED lights during the night. Solar garden lights are used for decorative and security purposes in gardens, pathways, and driveways. Their popularity stems from their ease of installation, low maintenance, and the ability to operate independently of the electrical grid.

A study by Sharma et al. (2022b) highlights the advantages of solar garden lights, noting their contribution to reducing carbon footprints and electricity bills (Sharma et al., 2022b).

2.17.1 Current Application of Solar Garden Lights

Solar garden lights have become a popular choice for enhancing outdoor spaces in both residential and commercial environments. These lights are often placed along walkways, driveways, and garden perimeters to provide illumination that improves visibility and adds to the landscape's aesthetic appeal. In residential settings, they are commonly used to light up patios, decks, and gardens, creating inviting spaces for evening activities, as can be seen in Figures 2-23. Commercial properties, such as hotels, restaurants, and shopping centres, utilise solar garden lights to beautify outdoor areas while promoting energy efficiency. Moreover, in public parks and recreational

spaces, solar garden lights are installed to illuminate trails, playgrounds, and picnic areas, enhancing safety without the need for extensive electrical infrastructure. The growing trend of integrating solar garden lights into sustainable urban designs reflects their importance in modern landscape architecture (Johnson & Miller, 2022).



Figure 2-23: Solar Garden Lights Available in the UK (Solar Centre)

However, solar garden lights have their drawbacks. One notable issue is their relatively high cost, with prices often starting around £19.99 per unit, which can be considered expensive, especially when multiple units are required to illuminate a larger area adequately. Additionally, the illumination provided by these lights tends to be less bright, which can limit their effectiveness in situations where stronger lighting is needed. Another limitation is the battery capacity; many solar garden lights are equipped with batteries that provide less than 4 hours of light at night, particularly in conditions without sufficient sunlight during the day. This short battery life can result in the lights turning off before the night is over, which reduces their utility and may necessitate the purchase of additional lights or replacement batteries, further increasing the overall cost (Davis & Thompson, 2021).

2.18 Concrete

Over the years, concrete has been an essential building material that has progressed to fit the needs of contemporary engineering and architecture. It is the most utilised material in the world after

water, with an estimated 21 to 31 billion tonnes used globally in 2006. Concrete is a fundamental component of modern architecture (Jean Pierre Jacobs, 2009). It comprises coarse aggregates (gravel or crushed stone), fine aggregates (sand), water, cement, and other admixtures (Buenfeld & Okundi, 2018). These components are primarily sourced locally and available in large quantities, providing flexibility and accessibility for concrete manufacturing.

A critical element of concrete's adaptability is its ability to incorporate recycled materials. For example, aggregates derived from recycled concrete can sometimes replace raw resources, increasing the sustainability of the construction process (Fang, Hong & Zhang, 2018). Concrete can also incorporate by-products from other industries, such as waste foundry sand, fly ash from coal combustion, slag from steel manufacturing, and silica fume, which are used to create supplementary cementitious materials. These additions help reduce waste and improve concrete performance, such as durability and strength (Makul, 2020b) (Wang et al., 2021).

The use of recycled materials in concrete, such as crushed recycled concrete aggregate, has gained popularity. This strategy addresses waste management concerns and promotes environmentally friendly construction techniques. Recycled materials can alter the density, workability, and durability of concrete, making it suitable for various uses, including non-load-bearing structures, pavements, and barriers (Eastern, 1997).

Composite and other recycled materials represent further innovations in concrete technology. These materials combine conventional concrete with additives such as glass fibre, steel tyre fibre, carbon fibre, polystyrene, rubber tyre fibre, and plastics to improve the mechanical properties of concrete. Fibre-reinforced concrete, due to its enhanced tensile strength, ductility, and resistance to shrinking and cracking, is an excellent material choice for structures subjected to severe stress or dynamic loads (Amran, Farzadnia & Ali, 2015b).

2.19 The Use of Concrete in Pavements

Concrete pavements have been used for centuries, with early applications dating back to the Roman Empire. The Romans pioneered road construction using pozzolanic concrete, a blend of lime, volcanic ash, and aggregate, known for its impressive durability (Mehta & Monteiro, 2014). Modern concrete pavements emerged in the late 19th century, with the first Portland cement concrete pavement laid in 1891 in Bellefontaine, Ohio, USA (Tayabji & Lim, 2006). Since then, developments in reinforced concrete, jointed concrete pavements, and continuously reinforced concrete pavements (CRCP) have enhanced performance and extended service life.

The 20th century witnessed the expansion of concrete pavements due to the growing demand for robust transportation infrastructure. Innovations such as fibre reinforcement, high-performance concrete, and the use of supplementary cementitious materials (SCMs) have contributed to increased pavement longevity and reduced maintenance costs (ACI, 2010). More recently, sustainable practices, including the incorporation of recycled aggregates and industrial by-products, have gained prominence as the industry seeks to minimise environmental impact while maintaining performance standards.

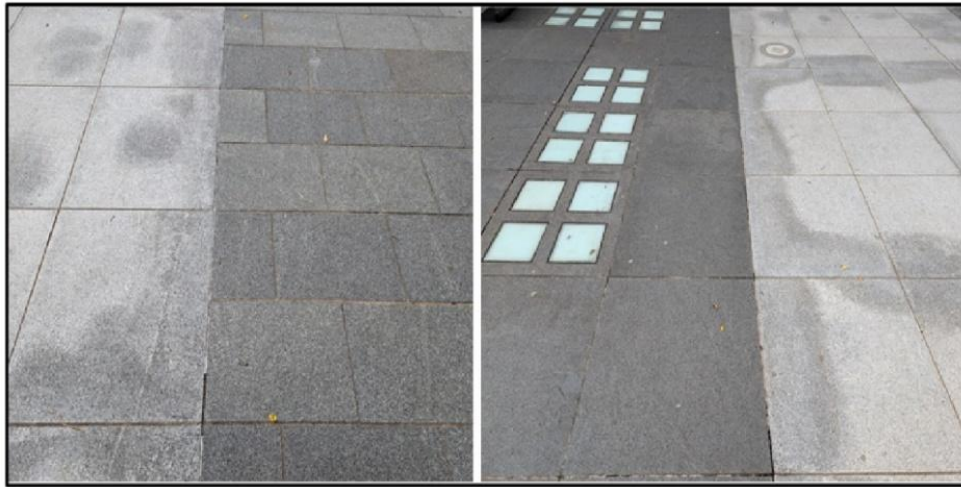


Figure 2-24: Walkable Pavement Slab, (University of Leicester, 2023)

2.19.1 Limitations of Traditional Pavements

1. **Heavy Materials:** Traditional pavement materials like concrete and asphalt are inherently heavy, which can impose significant loads on the underlying infrastructure. This is particularly relevant in urban areas where the weight of the pavement can contribute to subsidence and increased maintenance costs over time (Pacheco-Torgal & Jalali, 2011). The production and transportation of these heavy materials also contribute to substantial carbon emissions, further exacerbating their environmental impact.
2. **Non-Recycled, Resource-Intensive Materials:** Conventional pavements are often constructed using virgin materials, such as natural aggregates, Portland cement, and bitumen, which are extracted from the earth and processed through energy-intensive methods. This reliance on non-recycled materials not only depletes natural resources but also generates significant carbon emissions during extraction, processing, and transportation (Müller & Harnisch, 2008).

Additionally, the use of these materials does not contribute to the circular economy or sustainable resource management.

3. **Sustainability:** Traditional pavements, while functional, do not contribute to sustainability, particularly the aim of achieving carbon emissions. They do not generate renewable energy, reduce carbon footprints, or integrate recycled materials, making them passive components in the urban environment. As cities and governments around the world increasingly focus on reducing carbon emissions and promoting sustainability, these pavements offer little in terms of contributing to these broader environmental goals (UNEP, 2018). Figure 2-24 shows examples of using typical concrete pavement slabs.

2.19.2 Benefits and Challenges of Using Alternative Materials in Concrete Pavements

The use of innovative materials in pavement construction has become increasingly significant due to the need for more durable, sustainable, and cost-effective solutions. As infrastructure demands grow and environmental concerns rise, researchers and engineers continue to explore new materials that enhance pavement performance while addressing the limitations of conventional materials such as asphalt and Portland cement concrete. This discussion focuses on incorporating new materials into existing walkable pavement slabs, which provide pedestrian-friendly surfaces and are essential for urban infrastructure.

Integrating recycled and alternative materials into existing slabs presents numerous benefits, including increased longevity, reduced environmental impact, and improved structural performance. New materials such as recycled foundry sand, recycled steel tyre fibre, polystyrene, and superplasticisers offer innovative solutions that enhance the functionality and sustainability of walkable pavement slabs. However, there are also significant challenges related to cost, material availability, compatibility with existing infrastructure, and long-term performance reliability. This discussion explores the advantages and challenges of using these materials in walkable pavement slabs, ensuring that they meet the demands of durability, safety, and environmental sustainability.

2.19.3 Benefits of Using New Materials in Walkable Pavement Slabs

One of the most significant benefits of using new materials in pavement construction is enhanced durability and longevity. Traditional pavement materials, such as asphalt and concrete, often experience degradation over time due to environmental exposure, heavy traffic loads, and chemical reactions. Including recycled steel tyre fibre improves the toughness and tensile strength of

concrete, reducing cracking and extending pavement life (De Belie et al., 2018). Similarly, the incorporation of superplasticisers enhances the workability of concrete while maintaining its strength, allowing for more efficient construction and reduced material waste (Mehta & Monteiro, 2014).

Sustainability is another crucial advantage. Incorporating recycled foundry sand as a replacement for natural sand in concrete production reduces the environmental impact associated with sand mining and the disposal of industrial waste (Van Dam et al., 2015). Additionally, polystyrene-based lightweight concrete provides excellent thermal insulation, reducing energy demands for adjacent buildings and creating a more comfortable walking surface in extreme climates (Pomerantz, Akbari & Harvey, 2000). The use of these materials in walkable pavement slabs contributes to a circular economy, promoting resource conservation and waste reduction.

The use of alternative materials also improves pavement performance under various environmental conditions. For example, recycled steel tyre fibres enhance the impact resistance of pavement slabs, making them more resilient to mechanical loads and environmental stresses (Graybeal, 2014). Meanwhile, the inclusion of superplasticisers allows for a reduction in water content without compromising workability, resulting in high-strength, durable pavement surfaces. These advancements help extend the lifespan of pavements while reducing the frequency of repairs and maintenance.

In addition to mechanical and environmental benefits, the application of these materials contributes to cost savings. Recycled foundry sand and polystyrene are often more affordable than virgin aggregates, making them a cost-effective alternative in pavement construction (Buswell et al., 2018). The durability of fibre-reinforced concrete reduces long-term maintenance costs, while superplasticisers lower water consumption, reducing material costs without sacrificing performance. These factors collectively improve the economic feasibility of sustainable pavement solutions.

2.19.4 Challenges of Using New Materials in Walkable Pavement Slabs

Despite the numerous advantages, the adoption of new materials in pavement construction presents several challenges. One of the primary obstacles is the variability in material properties. Recycled foundry sand may contain residual contaminants that can affect the strength and durability of concrete, necessitating strict quality control measures (Van Dam et al., 2015). Similarly,

polystyrene can introduce air pockets within the concrete mix, potentially reducing compressive strength if not properly formulated (Mehta & Monteiro, 2014).

Material availability and supply chain constraints also pose significant challenges. The sourcing of high-quality recycled foundry sand and steel tyre fibres depends on the availability of industrial waste streams, which may not be consistent across different regions (Buswell et al., 2018). Furthermore, polystyrene recycling infrastructure varies globally, impacting its feasibility as a large-scale pavement material. Ensuring a stable and reliable supply of these materials requires careful planning and coordination among industries.

Compatibility with existing construction techniques is another important consideration. The integration of recycled materials into concrete formulations may require adjustments in mix design, curing methods, and finishing techniques (Tayabji & Lim, 2006). For instance, polystyrene-based lightweight concrete requires specialised handling during mixing and placement to prevent segregation and maintain uniformity. The need for modified construction practices can lead to increased labour costs and extended project timelines.

The long-term performance and durability of these materials remain areas of active research. While initial studies suggest that recycled steel tyre fibre and foundry sand enhance mechanical properties, their behaviour under prolonged exposure to freeze-thaw cycles, chemical attacks, and heavy pedestrian traffic requires further validation (De Belie et al., 2018). Extensive field testing and monitoring are essential to ensure that these materials meet the performance standards required for long-term infrastructure applications.

Regulatory acceptance and industry adoption also present barriers to the widespread use of these alternative materials. Existing pavement design codes and specifications are primarily based on traditional materials, and incorporating recycled or alternative components often requires rigorous testing and certification (Graybeal, 2014). Policymakers and industry stakeholders must work together to update standards and promote the safe and effective use of sustainable materials in pavement construction.

The use of recycled foundry sand, recycled steel tyre fibre, polystyrene, and superplasticisers as alternative materials for walkable pavement slabs presents numerous benefits, including enhanced durability, sustainability, cost-effectiveness, and improved mechanical performance. These materials contribute to resource conservation, reduce reliance on virgin aggregates, and offer innovative solutions for modern pavement engineering. However, challenges related to material

variability, supply chain limitations, construction compatibility, long-term performance, and regulatory acceptance must be addressed to facilitate broader adoption. Continued research, industry collaboration, and advancements in construction practices will be essential in ensuring the successful integration of these materials into mainstream pavement design, paving the way for more sustainable and resilient urban infrastructure.

However, the use of recycled materials in construction has become essential for reducing environmental impact and enhancing sustainability (Silva et al., 2017). Materials such as polystyrene, waste foundry sand, and recycled steel tyre fibres offer alternative solutions in civil engineering by improving material efficiency while reducing waste accumulation (Thomas and Gupta, 2020). Studies have shown that incorporating recycled materials in pavement structures enhances mechanical properties, reduces carbon footprint, and improves long-term sustainability (Tam et al., 2018).

In pavement engineering, the inclusion of recycled materials in foamed concrete can lead to lightweight, durable, and sustainable pavement solutions (Jones and McCarthy, 2005). Foamed concrete, which consists of a cementitious matrix with air voids, provides excellent thermal insulation and reduced material consumption (Rohith and Kumar, 2021). When combined with recycled components, it further improves the sustainability of pavement structures, making them more energy-efficient and environmentally friendly (Mohammed et al., 2020).

2.20 Reflection on the Literature Review

The necessity of this research is strongly justified in the context of existing literature, which highlights both the increasing demand for sustainable construction materials and the urgent need to improve the durability and efficiency of walkable pavement slabs. While previous studies have demonstrated the benefits of recycled materials such as foundry sand, steel tyre fibres, polystyrene, and superplasticisers, their specific application in modifying existing walkable slabs remains an area that requires further exploration. The literature confirms that these materials contribute significantly to reducing environmental impact, conserving natural resources, and enhancing mechanical properties (Mehta & Monteiro, 2014; Van Dam et al., 2015). However, challenges such as material variability, compatibility with traditional concrete, and regulatory acceptance persist, necessitating continued research and real-world validation.

Reflection on the literature review further underscores the necessity of this research. TNO, the Netherlands Organization for Applied Scientific Research, in collaboration with Ooms Avenhorn

Groep and Imtech, has explored innovative approaches to integrating solar energy into infrastructure. Their research focuses on the development of solar road panels designed for cycling paths, incorporating a glass top layer with crystalline silicon solar cells embedded in a concrete slab base. This initiative aligns with the broader goal of sustainable transportation by harnessing renewable energy while maintaining the structural integrity required for public pathways. The study contributes to the knowledge of energy-efficient infrastructure by demonstrating the feasibility of embedding solar cells within road surfaces while considering durability and climatic adaptability (TNO, 2013; Northmore, 2014b).

PLATIO has contributed to the field by introducing a solar paver system designed as a walkable and sustainable energy generator with a surface of 353 mm x 353 mm x 41mm. The research behind this product emphasises the use of high-performance solar cells protected by durable, anti-slip, scratch-resistant glass panels. A key innovation lies in the use of a frame structure made entirely from recycled plastic waste, reducing the environmental impact while ensuring long-term structural stability. By eliminating the need for new plastic materials, this study advances the understanding of circular economy applications in renewable energy systems. The findings from this research support the broader goal of integrating photovoltaic technology into urban landscapes, making clean energy more accessible for pedestrian-friendly environments (PLATIO Solar). The proposed solar pavement slab design builds on this concept by incorporating a lightweight foamed concrete base, integrating recycled materials such as foundry sand and steel tyre fibres, and offering improved mechanical properties while maintaining cost-effectiveness and sustainability.

Zha et al. (2016) have expanded the scope of solar pavement technology by proposing a hollow-plate structure composed of three functional layers. Their study explores the use of polymethyl methacrylate (PMMA) as a transparent protective layer, ensuring the longevity and efficiency of the underlying solar cells. The middle layer integrates photovoltaic technology, while the bottom prefabricated concrete hollow-base slab provides structural support and facilitates the integration of electrical components. A significant contribution of this research is the optimisation of pavement design using ANSYS simulations, assessing structural integrity, weight reduction, and economic feasibility. The findings from this study contribute to the knowledge of multi-functional pavement systems, demonstrating a method to integrate renewable energy while maintaining road usability (Zha et al., 2016). The proposed solar pavement slab expands upon this concept by

incorporating self-contained power storage, reducing installation complexity, and increasing the adaptability of the design for walkable pavements, ensuring higher durability and efficiency in urban environments.

The current solar pavement slab design demonstrates a distinct advantage in several key areas when compared with existing products such as solar brick lights and solar garden lights available online from Solar Centre, as well as the solar pavement slab from Solar Patio. This comparison focuses on the integration of self-contained devices, use of materials, product weight, cost, and overall functionality.

1. **Self-Contained Devices:** The proposed solar pavement slab is designed as a fully self-contained unit, integrating solar panels, cavities for electrical devices, and potentially LED lighting within a single, cohesive structure. This integration ensures efficient energy generation and reliable performance. In contrast, the solar brick and garden light, while also self-contained, are smaller and less powerful, providing lower light illumination compared to the current design. These products, available from Solar Centre, may be effective for decorative purposes but lack the robust energy generation capacity and brightness offered by the proposed solar pavement slab. Although made from recycled materials, the solar pavement slab from Solar Patio is not self-contained. It requires separate wired connections that are not included with the purchase, which adds complexity and potentially increases the overall cost.

2. **Material Use and Sustainability:** The current solar pavement slab is planned to be constructed from foamed concrete, which not only makes it lightweight but also incorporates recycled materials in order to minimise waste. This approach contrasts with the solar brick lights and solar garden lights, which are not made from recycled materials. While these products fulfil specific aesthetic purposes, their lack of sustainable materials and higher costs may detract from their appeal in environmentally-conscious markets. The Solar Patio slab, on the other hand, is made from recycled materials, which is a positive aspect. However, its lack of self-contained functionality and the need for additional wiring reduce its overall convenience and sustainability when compared to the current design.

3. **Weight and Ease of Installation:** The lightweight nature of the proposed solar pavement slab, due to its foamed concrete composition, offers significant advantages in terms of installation and handling. This makes it suitable for a wide range of applications, particularly in urban environments where ease of installation is crucial. The solar brick light and solar garden light are

naturally lightweight due to their smaller size, but this also limits their application to smaller-scale, less demanding uses. The Solar Patio slab, while likely more substantial due to its recycled material content, does not benefit from the same ease of installation as the current design, especially given the need for additional wiring.

4. **Cost and Value:** In terms of cost, the solar brick light and solar garden light from Solar Centre are noted to be relatively expensive, considering their limited functionality and smaller size. The current design, with its integrated devices and use of sustainable materials, offers a more cost-effective solution over the long term, especially when considering its superior light illumination and energy generation capabilities. The Solar Patio slab, being very expensive and requiring separate purchases for connections, further underscores the cost-effectiveness of the proposed design, which provides a more comprehensive solution in a single product.

5. **Overall Functionality:** The proposed solar pavement slab outperforms the existing products in terms of overall functionality. Its ability to combine multiple features—such as solar energy generation, LED lighting, and sustainability—into one cohesive, self-contained unit makes it a more attractive option for both consumers and developers. The solar brick light and solar garden light, while functional for specific decorative purposes, do not offer the same level of integrated performance or environmental benefits. The Solar Patio slab, despite being made from recycled materials, is less convenient and more costly due to its non-self-contained nature and the need for additional components.

When comparing the proposed solar pavement slab with existing products on the market, it is clear that the current design offers several advantages, particularly in terms of sustainability, cost-effectiveness, and integrated functionality. Its use of recycled materials, lightweight construction, and self-contained design make it a superior choice for sustainable infrastructure projects. While existing products like solar brick lights and solar garden lights may serve specific niches, they do not match the comprehensive benefits provided by the current solar pavement slab design. Similarly, the Solar Patio slab, although sustainable, falls short in terms of functionality and cost-efficiency, further highlighting the advantages of the proposed design.

By investigating the integration of these innovative materials into existing slabs, this study builds upon prior findings and addresses knowledge gaps related to long-term performance, cost-effectiveness, and implementation strategies. The distinct advantages of the proposed slab in terms of sustainability and self-contained functionality emphasise the practical significance of this study.

Unlike other solar pavement products currently available, the proposed design integrates innovative material usage, ensuring improved performance and environmental benefits while maintaining economic feasibility. The insights gained from this research can inform industry best practices, contribute to policy development, and support the transition towards more resilient and eco-friendly infrastructure. Ultimately, the adoption of these sustainable materials in walkable pavement slabs aligns with global efforts to create sustainable urban environments, reinforcing the importance of this research in advancing both theoretical knowledge and practical applications in pavement engineering.

Materials and the urgent need to improve the durability and efficiency of walkable pavement slabs. While previous studies have demonstrated the benefits of recycled materials such as foundry sand, steel tyre fibres, polystyrene, and superplasticisers, their specific application in modifying existing walkable slabs remains an area that requires further exploration. The literature confirms that these materials significantly reduce environmental impact, conserve natural resources, and enhance mechanical properties (Mehta & Monteiro, 2014; Van Dam et al., 2015). However, challenges such as material variability, compatibility with traditional concrete, and regulatory acceptance persist, necessitating continued research and real-world validation.

By investigating the integration of these innovative materials into existing slabs, this study builds upon prior findings and addresses knowledge gaps related to long-term performance, cost-effectiveness, and implementation strategies. The insights gained from this research can inform industry best practices, contribute to policy development, and support the transition towards more resilient and eco-friendly infrastructure. Ultimately, the adoption of these sustainable materials in walkable pavement slabs aligns with global efforts to create sustainable urban environments, reinforcing the importance of this research in advancing both theoretical knowledge and practical applications in pavement engineering.

The use of recycled foundry sand, recycled steel tyre fibre, polystyrene, and superplasticisers as alternative materials for walkable pavement slabs presents numerous benefits, including enhanced durability, sustainability, cost-effectiveness, and improved mechanical performance. These materials contribute to resource conservation, reduce reliance on virgin aggregates, and offer innovative solutions for modern pavement engineering. However, challenges related to material variability, supply chain limitations, construction compatibility, long-term performance, and regulatory acceptance must be addressed to facilitate broader adoption. Continued research,

industry collaboration, and advancements in construction practices will be essential in ensuring the successful integration of these materials into mainstream pavement design, paving the way for more sustainable and resilient urban infrastructure.

2.21 Summary

This chapter discusses the integration of photovoltaic cells into pavement slabs, known as solar pavement slab technology, contributing to urban sustainability by producing clean energy and reducing impervious surfaces. Additionally, the chapter covers the use of recycled and composite materials in concrete, which lowers the concrete's weight and improves its mechanical properties like compressive and tensile strength. Foamed concrete, characterised by its low density and good thermal and sound insulation properties, is highlighted for its suitability in weight-sensitive construction applications, with recent developments enhancing its strength and stability. Overall, the chapter emphasises the environmental and economic benefits of these innovative materials in reducing the construction industry's carbon footprint and managing waste more effectively.

Based on an extensive literature review and the findings of the researcher's studies that have been discussed in this chapter, the following summary can be reached:

1. Introduce the solar panel, the current application with regards to the type of solar panels available and the current application.
2. Solar pavement technology integrates photovoltaic cells into pavement slabs to generate electricity while serving typical paving functions. The primary benefits include producing clean energy and reducing impervious surface areas, thereby contributing to urban sustainability.
3. Recycled materials (such as carbon fibre, glass fibre, polystyrene, steel tyre fibre, rubber tyre fibre, plastic, and shredded carpet) are used within the concrete samples to enhance their physical and mechanical density.
4. Waste foundry sand has been used in the construction industry to replace normal sand, minimising waste and reducing the cost of the product while maintaining environmental sustainability.
5. Foamed concrete is a lightweight concrete made by incorporating air bubbles into the cement mix. This type of concrete is known for its low density, good thermal insulation, and sound

absorption properties. Recent developments have improved the strength and stability of foamed concrete, making it a viable option for a broader range of construction projects.

6. The current application of foamed concrete has been used in the construction industry in non/semi-structural applications such as void filling materials and thermal and sound insulation but not in structural applications when higher strength is required.
7. FC mechanical properties could be influenced by its density, cement/sand ratio, and additives that are added to FC mixes.

Chapter 3: Thesis Methodology

3.1 Introduction

This chapter presents the methodology adopted to achieve the research objectives of developing a sustainable solar walkable pavement slab. The methodology integrates material selection, experimental investigations, and numerical simulations to ensure that the final slab meets both structural and functional performance requirements. The research aims to develop a lightweight foamed concrete slab incorporating recycled materials and photovoltaic components capable of generating renewable energy while supporting pedestrian traffic.

The research approach began with an extensive literature review to understand the mechanical behaviour of foamed concrete, the potential use of recycled materials, and the requirements for integrating solar technology into pavement systems. Based on this review, suitable materials were selected, including waste foundry sand, recycled tyre fibres, polystyrene, and superplasticisers. These materials were incorporated into the foamed concrete mix to enhance its structural performance while promoting sustainability.

Subsequently, a series of experimental tests were conducted to optimise the foamed concrete mix and evaluate its properties, including compressive strength, flexural behaviour, density, and workability. The optimised mix was used to produce prototype slabs, which underwent load-deflection testing to assess their structural performance under pedestrian loading conditions. In parallel, finite element analysis (FEA) using ABAQUS software was employed to simulate the slab's structural response numerically.

Following the validation of the prototype, the final slab was constructed with integrated photovoltaic components. In-situ testing was carried out to monitor the slab's structural stability, surface durability, and energy generation performance under real-world conditions. Performance data were collected during both winter and summer seasons, allowing for a comparative assessment of energy efficiency across different environmental conditions.

This chapter provides a detailed account of the step-by-step methodology employed throughout the study, forming the basis for the practical and analytical work presented in the following phases.

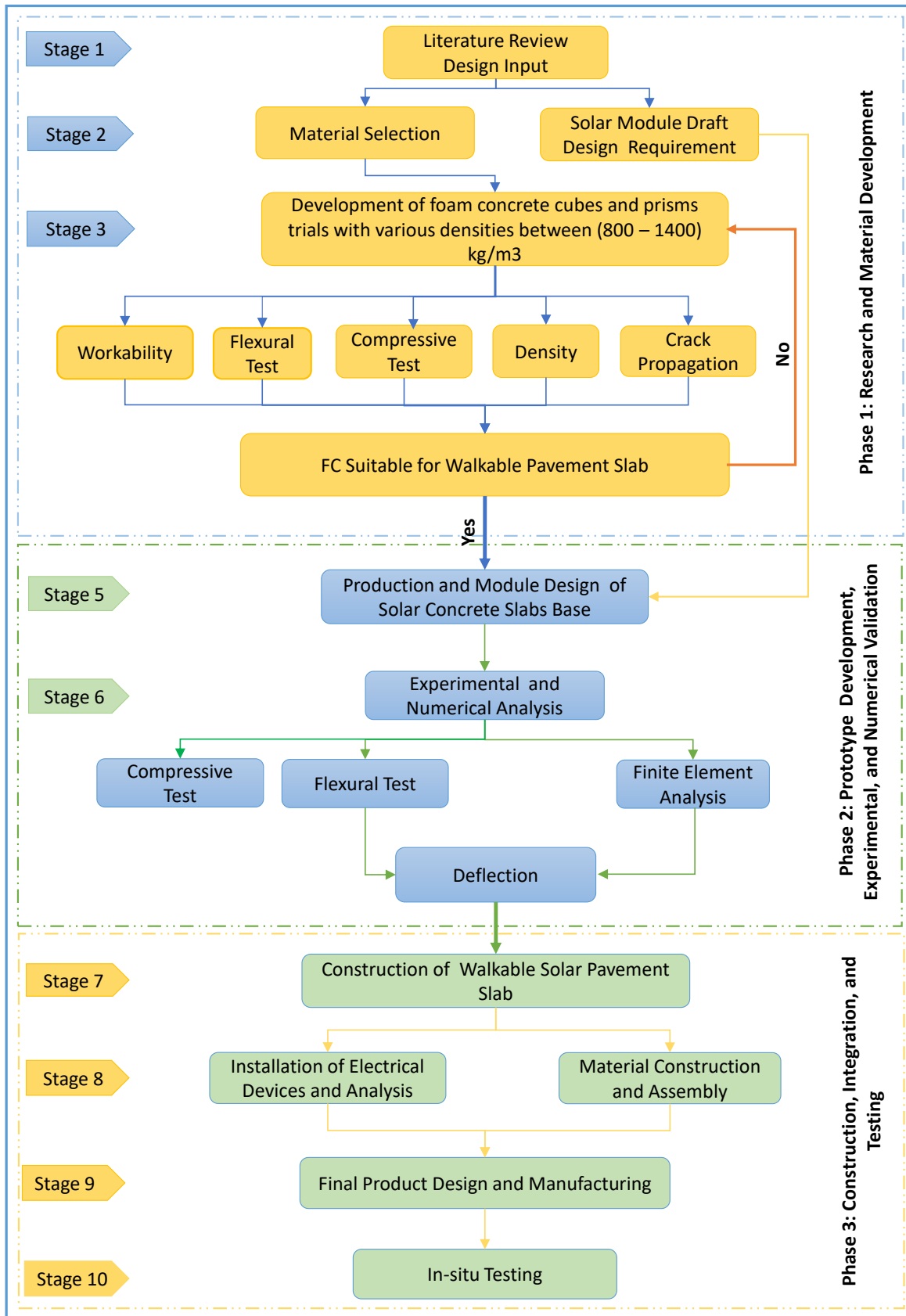


Figure 3-1: The Project’s Methodology and the Research Stages

3.2 Research Design and Rationale

The study adopts a mixed-methods approach, combining qualitative and quantitative research methods to understand the subject matter comprehensively. This approach allows for a holistic analysis, integrating numerical data with contextual insights. The research design is structured into distinct phases, each addressing specific aspects of the study:

3.2.1 Phase 1: Research and Material Development

This phase represents the initial research and development phase, focusing on establishing a fundamental understanding of the materials and design requirements necessary for developing the solar walkable pavement slab. This phase consists of a systematic approach divided into three key stages, beginning with a comprehensive literature review and culminating in the development and evaluation of foamed concrete mixes incorporating recycled materials.

Stage 1: Literature Review and Design Input

The first stage involved conducting an extensive literature review to gather knowledge regarding foamed concrete, solar pavement systems, and the utilisation of recycled materials in concrete applications. The review aimed to identify best practices, understand mechanical performance requirements and explore innovative material combinations. Key areas of focus included the mechanical behaviour of lightweight foamed concrete, its suitability for pedestrian pavement applications, and the structural challenges associated with integrating photovoltaic systems into concrete slabs.

The review also examined the impact of incorporating recycled materials into concrete, particularly waste foundry sand, polystyrene, and tyre fibres. Research indicated that these materials could enhance certain mechanical properties, such as reducing density and improving tensile strength, while contributing to sustainable construction practices. The findings from this review provided critical design input for the subsequent material selection and mix development stages, ensuring the proposed slab module would meet both structural and functional requirements.

Stage 2: Material Selection and Solar Module Draft Design

Based on the literature review, suitable materials were selected for the foamed concrete mix, emphasising sustainability and mechanical performance. The selected materials included waste foundry sand, polystyrene, recycled tyre fibres, and superplasticisers. These materials were chosen for their potential to enhance the strength, durability, and workability of the foamed concrete.

Waste foundry sand served as a partial replacement for fine aggregates, offering improved particle packing and reducing environmental waste. Polystyrene particles contributed to reducing the slab's weight and enhancing thermal insulation properties. Recycled tyre fibres were included to enhance tensile strength and crack resistance, while superplasticisers improved the workability and flow of the concrete mix, allowing for better compaction.

Concurrently, a draft design of the solar module was developed to ensure seamless integration of structural and photovoltaic components in the pavement slab. This conceptual design aimed to balance mechanical performance with energy-generating capabilities. Factors such as the positioning of solar cells, concrete cover thickness, and load-bearing capacity were considered to prevent compromising the slab's structural integrity.

Stage 3: Development of Foamed Concrete Mixes and Experimental Evaluation

The third stage focused on developing and testing various foamed concrete mixes with densities ranging between 800 kg/m³ and 1400 kg/m³. Experimental trials were conducted using concrete cubes and prisms to evaluate the concrete mixes' mechanical and physical properties.

The key tests performed included:

- **Workability Test:** Assessing the ease of handling and placing the foamed concrete and its flow behaviour and stability.
- **Flexural Test:** Evaluating the tensile strength and resistance to bending forces to ensure the slab could withstand pedestrian and light vehicular loads.
- **Compressive Test:** This measures the load-bearing capacity and overall compressive strength, which is critical for assessing the slab's ability to support structural loads.
- **Density Test:** This test determines the weight and lightweight characteristics of the concrete, ensuring the slab remains easy to transport and install.
- **Crack Propagation Test:** Observing the formation and growth of cracks under applied load, this test identifies potential weaknesses in the concrete matrix.

Multiple mix variations were prepared, adjusting the proportions of foaming agents, recycled aggregates, and fibre content. Each mix underwent rigorous testing to assess its suitability for the intended application. If a blend failed to meet the mechanical performance criteria, modifications

were made to the material composition, and the testing process was repeated until an optimal mix was achieved.

Phase 1 concluded with the successful development of a suitable foamed concrete mix with recycled materials. This mix demonstrated desirable mechanical properties, including sufficient compressive and flexural strength, reduced density, and improved crack resistance. It was deemed appropriate for use in the solar pavement slab, meeting both structural and sustainability goals.

The outcomes of Phase 1 provided a solid foundation for Phase 2, which involves prototype development, experimental testing, and numerical validation. The selected mix and draft design guided the fabrication of the prototype slab, ensuring it could undergo further evaluation in later phases to assess its long-term performance and energy-generating potential.

3.2.2 Phase 2: Prototype Development, Experimental, and Numerical Validation

This phase represents the transition from material research and mix development to the production and performance evaluation of a prototype solar slab base. This phase focuses on developing the physical module, subjecting it to experimental testing, and validating its performance through numerical analysis. structural requirements and the functional integration of solar components, ensuring that the slab would be capable of supporting pedestrian loads while serving as a platform for solar energy generation.

Stage 4: Production and Module Design

Building upon the outcomes of Phase 1, a prototype solar slab module was designed and produced. The foamed concrete mix incorporating recycled materials was used to cast the slab. The design process considered both the structural requirements and the functional integration of solar components, ensuring that the slab would be capable of supporting pedestrian loads while serving as a platform for solar energy generation.

The production of the slab involved careful mixing, pouring, and curing processes to achieve the desired density and mechanical properties. Particular attention was paid to ensuring uniform distribution of the recycled materials within the foamed concrete matrix. This process resulted in the fabrication of a full-scale prototype slab, which served as the basis for experimental evaluation and numerical modelling.

Stage 5: Experimental and Numerical Analysis

Following the production of the prototype, experimental and numerical analyses were conducted to evaluate its structural behaviour under load. The primary objective was to assess the slab's deflection performance and compressive strength.

1. Experimental Analysis:

Experimental testing was carried out to measure the deflection of the slab under loading conditions representative of pedestrian traffic. The slab was supported at its edges and subjected to a series of load increments, with deflection measurements recorded at key points using displacement measurement devices. The aim was to determine the load-deflection behaviour and assess the slab's stiffness and load-bearing capacity.

In addition to slab deflection testing, compressive strength tests were performed on concrete cubes produced alongside the slab. These tests provided a baseline assessment of the mechanical properties of the foamed concrete mix used in the slab's construction.

2. Numerical Analysis:

Finite element analysis (FEA) was employed using ABAQUS software to simulate the structural performance of the solar slab under load. A 3D numerical model was developed based on the actual dimensions and material properties of the prototype. The analysis included:

- **Meshing:** A detailed finite element mesh was generated to represent the slab accurately.
- **Boundary Conditions:** Supports were modelled to replicate the experimental setup.
- **Load Application:** Incremental vertical loads were applied to simulate pedestrian loading conditions.

The primary focus of the numerical analysis was to predict the deflection behaviour of the slab under load and identify stress distribution patterns. The results from the FEA model were compared with the experimental load-deflection data to assess the accuracy of the numerical predictions.

Stage 6: Experimental and Numerical Results and Discussion

The experimental deflection measurements and compressive strength results were analysed alongside the numerical FEA outputs. The comparison of experimental and numerical deflection

data provided insights into the slab's structural behaviour and the reliability of the computational model.

Key findings from this stage included:

- **Load-Deflection Behaviour:** The experimental and numerical load-deflection curves showed good agreement, validating the numerical model.
- **Structural Capacity:** The slab demonstrated sufficient stiffness and load-bearing capacity for pedestrian use.
- **Compressive Strength:** Cube testing confirmed that the foamed concrete mix achieved the desired compressive strength, meeting design expectations.

The integration of experimental and numerical results provided a comprehensive understanding of the prototype slab's performance. The validation of the numerical model ensured its reliability for future design optimisation and structural assessments.

Phase 2 successfully demonstrated the structural feasibility of the solar slab prototype. The combined experimental and numerical analysis validated the slab's load-bearing capacity and deflection performance, confirming that the foamed concrete mix with recycled materials was suitable for the intended application. These findings paved the way for Phase 3, which focuses on final product assembly, system integration, and in-situ testing.

3.2.3 Phase 3: Construction, Integration, and Testing

This phase represents the final and most critical phase in the development process, transitioning from validated prototypes to the walkable solar pavement slab's construction, assembly, and in-situ testing. This phase involves integrating structural and photovoltaic components, final product fabrication, and real-world performance evaluation to ensure the slab meets structural and functional requirements.

Stage 6: Construction of Walkable Solar Pavement Slab

The phase commenced with constructing the final walkable solar pavement slab based on the outcomes and validated design from Phase 2. The slab was cast using the optimal foamed concrete mix incorporating recycled materials, ensuring that the mechanical properties, density, and structural capacity identified in earlier testing were consistently achieved.

The slab was produced under controlled conditions to prevent inconsistencies in density and surface defects. Careful attention was given to ensuring uniform thickness across the entire slab, as deviations could compromise the structural performance and affect the integration of the solar components. Proper curing procedures were applied to enhance the mechanical strength and long-term durability of the slab. The surface was finished to achieve a smooth but slip-resistant texture, suitable for pedestrian use while allowing efficient placement of photovoltaic elements.

Stage 7: Installation of Electrical Devices and Material Assembly

Upon successful casting and curing, the next stage involved integrating the photovoltaic components into the slab. The solar modules were carefully embedded into pre-designated recesses on the slab surface. Electrical wiring and connections were installed to link the solar cells to the power management system, ensuring functional performance.

Material assembly also included securing the protective covering over the solar modules to safeguard against pedestrian traffic and environmental exposure. The assembly process aimed to ensure that the structural integrity of the slab was not compromised during the embedding of the photovoltaic components. Detailed checks were performed to verify electrical continuity and confirm that the solar module connections were secure and capable of efficient energy output.

Stage 8: Final Product Design and Manufacturing

After the structural and electrical integration, the slab was subjected to a final evaluation. Adjustments were made where necessary to optimise the product's robustness, functional efficiency, and surface quality. The final product design incorporated refinements in placing solar cells and surface finishing techniques to enhance slip resistance and ensure aesthetic appeal suitable for public environments.

The manufacturing phase ensured that the slab was a complete unit, combining structural strength with photovoltaic functionality. This marked the transition from laboratory-scale development to a product suitable for field installation and performance assessment.

Stage 9: In-Situ Testing

The last stage of Phase 3 involved placing the slab in a real-world environment to assess its performance under actual operational conditions. In-situ testing aimed to evaluate the structural behaviour, surface performance, and energy generation capability of the slab:

- **Structural Stability:** The slab was subjected to pedestrian loading to monitor for any signs of deformation, cracking, or surface degradation. Load-bearing performance was assessed under various weather conditions to ensure durability.
- **Surface Performance:** The wear resistance and slip resistance of the slab were examined to confirm its suitability for public foot traffic. Observations were made regarding its resilience to environmental factors such as rain, temperature variations, and dirt accumulation.
- **Energy Generation:** The photovoltaic system's energy output was monitored throughout different times of the day to evaluate its efficiency under natural sunlight conditions. Additionally, sensors were installed to monitor solar panel performance and battery storage during both winter and summer seasons. Energy absorption data was collected over these periods, and the performance of the system in winter was compared with that in summer.

This comparative analysis provided insights into seasonal variations in energy efficiency.

Observations and data from the in-situ testing provided valuable insights into the slab's operational performance. Any minor deficiencies observed during field testing were documented, and potential improvements were noted for future design iterations.

Phase 3 successfully demonstrated the transition from prototype validation to practical application. Integrating structural and photovoltaic components resulted in a functional, walkable solar pavement slab capable of withstanding pedestrian traffic while generating renewable energy. The in-situ testing phase confirmed the slab's ability to perform reliably in real-world conditions, validating its structural stability, durability, and energy generation capacity. Monitoring solar panel and battery performance across different seasons added further depth to the evaluation, enabling the identification of efficiency patterns under varying environmental conditions. These findings concluded the development process and paved the way for potential large-scale production and deployment in public spaces.

3.3 Ethical Considerations

Ethical considerations were carefully observed throughout the entire research and development process, spanning all phases from material selection and prototype development to final product testing and in-situ evaluation. The primary ethical focus was on ensuring environmental sustainability, user safety and data integrity.

Sustainability was a guiding principle across all phases. Recycled materials, including waste foundry sand and tyre fibres, were integrated into the foamed concrete mix to minimise the environmental impact of the pavement slab. This approach reduced waste and conserved natural resources, aligning with global efforts toward sustainable construction and renewable energy solutions.

Safety was prioritised at every stage. During Phase 1, material testing ensured that the selected components were structurally sound and suitable for public use. In Phase 2, prototype evaluation involved rigorous structural testing and deflection analysis to confirm the slab's load-bearing capacity and resilience. Phase 3 ensured that both structural integrity and slip resistance were maintained. Electrical safety was also critical when integrating solar modules, adhering to standard protocols to prevent hazards.

Data integrity and research transparency were upheld consistently. Results from laboratory experiments, finite element analysis, and in-situ testing were accurately recorded and reported. All performance evaluations were conducted impartially, ensuring the final assessment of the slab's mechanical and energy generation capabilities was reliable and bias-free. Across all phases, the research was guided by professional ethics, emphasising environmental responsibility, user safety, data accuracy, and the pursuit of sustainable innovation.

3.4 Summary

The development process of the walkable solar pavement slab was executed in three interconnected phases. Phase 1 involved material research and development, selecting recycled materials and optimising a foamed concrete mix with suitable mechanical properties. Phase 2 progressed to prototype production and performance validation through experimental deflection tests and numerical analysis using ABAQUS, ensuring the slab's structural reliability. Phase 3 finalised the slab's construction, integrating solar panels and electrical components, followed by in-situ testing under real-world conditions. Performance was monitored during winter and summer to evaluate structural stability, energy output, and surface durability. Ethical considerations throughout the research ensured sustainability, safety, data integrity, and social responsibility, resulting in a functional slab capable of supporting pedestrian traffic while generating renewable energy.

Chapter 4: Foamed Concrete Design and Experimental Study

4.1 Introduction

This chapter describes the first part of the experimental program in this study, which is concerned with creating and improving the mechanical characteristics and densities of concrete built with recycled materials. This phase involves design mix trials to make foamed concretes with densities ranging from 800 to 1400 kg/m³, both with and without additives, and with different percentages of recycled material ratios by volume. The work focuses on key mechanical qualities, such as compressive and flexural strength, to optimise these values for pavement applications.

This chapter aims to evaluate the mechanical properties and density of foamed concrete samples containing recycled materials, ultimately selecting the optimal formulation for the final product. The materials and additives employed in laboratory trials are outlined, while the investigation includes analysing key performance indicators such as compressive strength, tensile strength, hardness, and density. Achieving an appropriate balance between density and mechanical strength is crucial before any mixture can be deemed suitable for the intended application. Details of the production techniques involving both conventional and recycled materials are provided in the methodology chapter. Additionally, the inclusion of superplasticisers is introduced as a means to enhance workability and improve mechanical performance. This structured evaluation ensures that the chosen foamed concrete formulation meets both performance criteria and industry standards. The experimental phase involved the production of foamed concrete samples with densities ranging from 800 kg/m³ to 1400 kg/m³. Some samples incorporated additives, while others were prepared without them to assess the influence of supplementary materials on the concrete's characteristics. This process facilitated a detailed analysis of the mechanical and physical properties relevant to the proposed application.

Over 150 samples were produced, including 100 mm x 100 mm x 100 mm cubes and 100 mm x 100 mm x 50 mm prisms, ensuring compliance with established testing standards. The samples incorporated various recycled materials and density variations, enabling a comprehensive examination of how these factors affect mechanical performance, durability, and overall suitability for use in solar walkable pavement slabs.

4.2 Material Selection

In the initial phase, both conventional and recycled materials will be used. The following sections have identified and detailed the specific materials needed for this project. Below is a list of both recycled and standard materials:

4.2.1 Standard Material

The normal materials (standard) in the experiment are introduced, including sand, cement, water, and a foaming agent. These fundamental components are essential in creating the foam concrete mixture as a base for the material development, each contributing to the overall properties of the final product. Sand provides the necessary bulk and strength, cement acts as the primary binder, water facilitates the chemical reactions needed for setting, and the foaming agent introduces air bubbles to achieve the desired lightweight structure. The typical materials used to manufacture foam concrete are listed below:

4.2.2 Fine Aggregate (Sand)

Fine aggregate, such as sand, is essential in traditional concrete for adding bulk, strength, and stability. However, in foamed concrete, known for its lightweight and insulating qualities, the use of fine aggregate plays a different role. This type of concrete primarily depends on air voids instead of traditional aggregates for its structure, which alters the need for and impact of fine aggregate. When producing foamed concrete, selecting appropriate aggregates is essential for influencing the product's mechanical and physical properties. This experiment used a 1:2 ratio of one part cement and two parts sand with a particle size of up to 4 mm, which complies with BS EN 12620 and is commonly used for foam concrete.

To obtain finer sand particles around 0.2 mm or less from river-washed sand initially sized between 0.5 mm and 4 mm, a series of sieving steps using progressively finer sieves is required. Start with a sieve that retains particles larger than 5 mm to remove the coarser particles. Then, use intermediate sieves such as 2 mm (2000 μm), 1 mm (1000 μm), and 0.5 mm (500 μm) to narrow down the particle sizes progressively. To achieve particles around 0.2 mm or less, employ finer sieves of 0.25 mm (250 μm) and 0.2 mm (200 μm).

Begin by placing the river-washed sand sample on the largest sieve (5 mm) and shaking or vibrating the sieves to allow particles to pass through to the next smaller sieve. Collect the particles that pass through each sieve and transfer them to the subsequent finer sieve, continuing this process

until reaching the 0.2 mm (200 μm) sieve. For particles finer than 0.2 mm, use a sieve with a size of 0.15 mm (150 μm) to collect the finest particles.

By following this step-by-step sieving process, you can efficiently reduce the size of the river-washed sand to obtain finer particles around 0.2 mm or less, making them suitable for specific applications such as foam concrete. Figure 4-1 provides a visual representation of the washed river sand and cement materials utilised in this experimental work.



Figure 4-1: (a) River Washed Sand, (b) Ordinary Portland Cement

4.2.3 Ordinary Portland Cement (OPC)

In this investigation, Ordinary Portland Cement (OPC) 32.5N was employed, adhering to the British Standard BS EN 197: Part 1: 2000. This type of cement is commonly used in the production of foamed concrete due to its suitable mechanical properties. The OPC used in this experimental work facilitated the development of a stable and durable foamed concrete mix. A cement-to-sand ratio of 1:2 was adopted in accordance with relevant British Standards, ensuring proper workability and strength development within the produced slabs. This ratio was applied consistently across both the mortar and foamed concrete mixes used in the experiment.

The compatibility of OPC with foaming agents is vital for producing foamed concrete. Its reactive nature and fine particle size contribute to forming a stable cellular structure, which is crucial for achieving the desired density and strength. The effectiveness of OPC in foamed concrete is reflected in its positive impact on strength, workability, and durability—factors that are essential for applications ranging from substructure to structural use.

4.2.4 Water

The quantity of water required in concrete depends significantly on the components of the mix, including any added admixtures. Water plays a fundamental role in achieving concrete uniformity, consistency, and stability. It helps moisten aggregates, initiates chemical reactions with cement, and improves the mix's workability. The proportion of water added is determined by the water-to-cement ratio, guided by the BS: EN:1008:2002 standard. Insufficient water can make the concrete too rigid, potentially breaking bubbles during mixing and increasing density, as Nambiar & Ramamurthy (2006) noted. Conversely, excess water may result in a fluid slurry, causing bubble separation and increased density. Typically, the water-to-cement ratio ranges from 0.4 to 1.25, aligning with 6.5% to 14% of the target density.



Figure 4-2: Normal Water

Water quality is crucial, especially in the production of foamed concrete. Guidelines from ACI 523.3R-93 emphasise the need for water to be clean, fresh, and potable. Organic contaminants can degrade the effectiveness of protein-based foam agents and the integrity of foamed concrete mixes. Even non-potable water can be acceptable if it allows the concrete to achieve 90% of its strength within 7 to 28 days, similar to the performance observed with municipal water sources.

Valore (1954) highlighted the importance of adjusting the sand content relative to changes in the water/cement ratio. The British Cement Association recommends maintaining a water/cement ratio of about 0.5 to 0.6 for optimal results. The often-used water-to-cement ratio in this study is

constantly about 0.5%, and it is strategically recommended that this ratio enhance the concrete's performance and characteristics.

4.2.5 Foaming Agent

In this study, protein-based surfactants were chosen for their efficacy in producing high-quality foamed concrete. According to Ramamurthy and Nambiar (2009), protein surfactants are known for creating more stable and closed cells within the foam, significantly enhancing the strength of the resulting foamed concrete. Foamed concrete with protein surfactants exhibits a strength-to-density ratio of about 50-100% higher than concrete made using synthetic surfactants.

The foam was prepared using a 5% aqueous surfactant solution in a dry system generator, resulting in foam densities that ranged between 43 and 53 kg/m. Figure 4-3 depicts the foam-making process, including the foaming agent, machine, and foam itself.



Figure 4-3: Foaming Agent and Foam Generator

Propump designed the protein foaming agent Propump 26, which was utilised in this study and is appropriate for integration into mixture designs ranging from 200 kg/m³ to 1700 kg/m³. In this research, a specific commercially available protein-based surfactant, ProPump Protein 26, was used to generate preformed foam aimed at producing low-density foamed concretes with reasonable strength. The concentration of the surfactant solution used to create the foam was consistently 50 grams per litre of water, producing foam with a targeted density of 50 ± 5 kg/m³. The preformed foam was created using a 4% aqueous surfactant solution in a dry system generator, achieving a foam density ranging from 41 to 52 kg/m³.

Additionally, recycled materials such as waste foundry sand, polystyrene, and recycled steel tyre fibre are incorporated into the foam concrete to minimise density while maintaining mechanical strength, including compressive and flexural strength. The use of superplasticisers further enhances these properties by improving the workability and overall performance of the concrete. This combination of materials ensures an environmentally friendly approach without compromising on quality and strength.

4.2.6 Waste Foundry Sand

The use of waste foundry sand (WFS) as a replacement for natural sand in concrete production was critical to this experimental investigation. WFS is a byproduct generated during the metal casting process, where molten metal is poured into sand moulds and left to cool and harden before the casting is removed. This process results in used foundry sand, often discarded as waste. Integrating WFS into concrete mixes provides an environmentally beneficial alternative to traditional waste disposal methods.

This study used WFS to partially and fully replace natural sand in concrete at four replacement levels: 25%, 50%, 75%, and 100%. The goal was to assess the effects of different WFS proportions on the concrete's workability, compressive strength, and tensile strength. It was observed that increasing the WFS content reduced the workability of the concrete. This behaviour is attributed to the finer particle size and higher surface area of WFS, which increased water demand by approximately 15% compared to natural sand.

The particle size distribution of the WFS used in this experimental work typically ranged from 0.6 mm to 0.15 mm (No. 30 to No. 100 sieve), with a small fraction (5-12%) being finer than 0.075 mm (No. 200 sieve). This aligns with the general characteristics of foundry sand, as noted by FHWA.DOT.GOV. This uniform grain size contributed to the changes in workability and performance observed during mixing and casting.

The mechanical properties of concrete containing WFS were monitored closely. Previous research highlights mixed results concerning the influence of WFS on concrete strength. According to Siddique et al. (2011), incorporating WFS can slightly reduce compressive strength due to differences in physical characteristics compared to natural sand. Similarly, Etxeberria et al. (2007) noted that higher WFS content might lead to minor reductions in strength, though some studies have indicated comparable or improved strength at specific replacement levels. Tensile strength is

similarly affected, with Singh et al. (2013) suggesting that low to moderate WFS replacement levels generally maintain acceptable performance.

The WFS used in this experiment was sourced from William Lee Ltd, located at Callywhite Lane, Dronfield, Derbyshire, S18 2XU. This material was obtained through the Castings Development Centre, which can provide detailed specifications regarding the sand particle size and characteristics upon request.

4.2.7 Polystyrene

This experiment incorporated EPS beads into concrete mixes at volume-based additions of 10%, 20%, and 30%. These varying proportions aimed to minimise the concrete samples' overall self-weight while evaluating their mechanical properties. Particular attention was given to ensuring that the surface finish of the samples remained smooth, with no visible EPS particles exposed on the surface, to enhance both aesthetics and durability. The mixing procedure was also carefully controlled to achieve a uniform distribution of EPS beads throughout the concrete matrix. Proper compaction techniques were employed to prevent segregation and ensure consistent density across all samples. The curing process was closely monitored to ensure optimal hydration and strength development, as variations in the curing environment can significantly affect the performance of lightweight EPS concrete.

4.2.8 Recycled Steel Tyre Fibre

Another set of experimental mixes involved the incorporation of 1% recycled steel tyre fibre into the concrete by weight of cement. This addition was intended to enhance the mechanical properties of the concrete, particularly its tensile strength and crack resistance. The fibres were uniformly dispersed throughout the mix to ensure consistency and prevent clumping. Special attention was paid to the workability of the concrete during mixing, as introducing steel fibres can sometimes lead to difficulties in achieving a smooth and even mix. The surface finish of the samples was carefully assessed to ensure that the steel fibres were not protruding from the surface, thereby maintaining a clean appearance and ensuring that the samples met the required quality standards. The samples were also properly compacted to avoid voids and ensure uniform density, and the curing process was closely monitored to promote optimal strength development.

4.2.9 Superplasticisers

The superplasticiser was introduced into the concrete mix at a dosage of 1% by cement weight. The superplasticiser was added to enhance the workability and flowability of the fresh concrete, particularly in mixtures incorporating recycled materials or fibres, which tend to reduce the ease of mixing and placing. Including the superplasticiser facilitated better compaction and reduced the water-cement ratio without compromising workability, improving the concrete's strength and durability. Special attention was given to ensuring uniform dispersion of the admixture to prevent segregation or bleeding. The samples were monitored during casting and curing to evaluate the influence of the superplasticiser on the final surface quality and mechanical performance of the hardened concrete. Figures 4-4 illustrate the recycled and additives used in this experiment.



Figure 4-4: Waste Foundry Sand, (b) Polystyrene, (c) Recycle Steel Tyre Fibre, (d) Superplasticiser

4.3 Experimental Design

The mix design for M20 normal mortar involves a carefully proportioned mix of cement, sand, and water to achieve a target compressive strength of 20 MPa. For this mix, a typical ratio used According to BS EN 998-2, a prescribed mortar mix proportion for achieving an M20 strength class can be approximately 1:2 (cement to sand) by volume, with a water-cement ratio of 0.50, resulting in a mix that provides high strength suitable for structural applications. Approximately 576 kg of cement, 960 kg of sand, and 259 litres of water would be required to produce one cubic meter of M20 mortar. While British Standards such as BS 5628-1 and BS EN 998-2 provide guidelines for traditional mortar design. Table 4-1 design for three cubes and three prisms made of standard concrete mortar as (Control).

It is important to note that there are no specific British Standards (BS) for the design of foamed concrete. Foamed concrete mix design is typically determined through experimental testing and customisation based on the desired density and strength. It is different from traditional concrete due to the incorporation of foam and its lightweight nature. Tables 4-2 and 4-3 provide the design of foamed concrete mixes containing various recycled materials, with a specific target density of 1400 kg/m³. Each design includes three cubes and three prisms tested for their mechanical properties.

Table 4-1: Design Mix for Standard Concrete Mortar

SR Number	Description of Sample (Cube and Prism)	Building Number	Concrete Grade	Number of design mix	28 days testing date
Control	100 x 100 x 100 mm	1	M20	1	28
				2	
				3	
Control	100 x 100 x 500 mm	2	M20	1	28
				2	
				3	

Key Points:

Recycled Materials in the Mix Designs:

- NFC (Normal Foamed Concrete): This serves as the control without any recycled materials.
- WFS (Waste Foundry Sand): Normal sand was replaced with 25%, 50%, 75%, and 100% WFS in the mix. The WFS mixes aim to evaluate the effects of replacing fine aggregates with recycled sand.
- Polystyrene (PO): Using 10%, 20%, and 30% polystyrene in the mix reduces the concrete's density while enhancing its lightweight properties.
- Recycled Steel Tyre Fibre (RSTF): Adding 1% of RSTF acts as reinforcement, improving the tensile and flexural strength.
- Superplasticiser (SPs): A 1% superplasticiser is added to improve the workability and compressive strength by reducing the water-cement ratio.

Table 4-2: Foamed Concrete Mix Design for Cubes with a Target Density of 1400 kg/m³

SR Number	Description of Sample (Cubes)	Building Number	Target Density (kg/m ³)	Number of cubes	Curing Period
NFC	100 x100 x 100 mm	1	1400	1	28
				2	
				3	
WFS 25%	100 x100 x 100 mm	2	1400	1	28
				2	
				3	
WFS 50%	100 x100 x 100 mm	3	1400	1	28
				2	
				3	
WFS 75%	100 x100 x 100 mm	4	1400	1	28
				2	
				3	
WFS 100%	100 x100 x 100 mm	5	1400	1	28
				2	
				3	
PO 10%	100 x100 x 100 mm	6	1400	1	28
				2	
				3	
PO 20%	100 x100 x 100 mm	7	1400	1	28
				2	
				3	
PO 30%	100 x100 x 100 mm	8	1400	1	28
				2	
				3	
RSTF 1%	100 x100 x 100 mm	9	1400	1	28
				2	
				3	
SPs 1%	100 x100 x 100 mm	10	1400	1	28
				2	
				3	

Each design under evaluation involved fabricating three cubes and three prisms (see Tables 4-2 and 4-3). All cubes were cured for 28 days to ensure consistent strength development, and their average weights were recorded to evaluate density and uniformity. In total, 30 cubes and 30 prisms were produced across designs targeting a density of 1400 kg/m³, providing a robust dataset for assessing material performance.

Table 4-3: Foamed Concrete Design for Prisms with a Target Density of 1400 kg/m³

SR Number	Description of Sample (Prism)	Building Number	Target Density (kg/m ³)	Number of Prisms	Curing Period
NFC	100 x100 x 500 mm	1	1400	1	28
				2	
				3	
WFS 25%	100 x100 x 500 mm	2	1400	1	28
				2	
				3	
WFS 50%	100 x100 x 500 mm	3	1400	1	28
				2	
				3	
WFS 75%	100 x100 x 500 mm	4	1400	1	28
				2	
				3	
WFS 100%	100 x100 x 500 mm	5	1400	1	28
				2	
				3	
PO 10%	100 x100 x 500 mm	6	1400	1	28
				2	
				3	
PO 20%	100 x100 x 500 mm	7	1400	1	28
				2	
				3	
PO 30%	100 x100 x 500 mm	8	1400	1	28
				2	
				3	
RSTF 1%	100 x100 x 500 mm	9	1400	1	28
				2	
				3	
SPs 1%	100 x100 x 500 mm	10	1400	1	28
				2	
				3	

Additional foamed concrete mixes were designed for 800, 1000, and 1200 kg/m³ density, following the same procedure as in Table 4-2 for 1400 kg/m³ cubes. The same approach was used to prepare and test three cubes for each design to assess their compressive. Table 4-2 provides examples of designing foamed concrete with a desired density of (1400kg/m³).

Based on performance criteria, the best sample for the final product will be selected from all the recycled materials tested. The final decision regarding the optimal material will be determined and

discussed in the following chapters, where detailed analysis and results will guide the selection process.

The Experimental study has been practically carried out by the following procedures in order to fulfil the objectives fully, as indicated in the above design and development phases:

4.3.1 Foamed Concrete Mixing Design

There is no standard specification for foamed concrete mix design, encouraging the usage of the absolute volumes approach in their study—a method that has been used in various research projects (Gangatire and Suryawanshi (2016)). This approach includes critical initial procedures such as determining the water-to-cement (w/c) ratio, aiming for a specified plastic density, and calculating the cement amount, all of which are required for constructing foamed concrete mixes. As Ramamurthy and Nambiar (2009) note, this approach enables precise proportioning based on absolute volumes.

Lee et al. (2014) discovered that the optimal w/c ratio for foamed concrete is often between 0.4 and 0.6. However, adding a superplasticiser can decrease this ratio even further to around 0.25, improving the mix's properties by producing higher fluidity and increased strength. Nonetheless, because no superplasticiser was utilised for all the samples, a w/c ratio of 0.5 was used. This ratio provided acceptable consistency for the majority of the mixtures tested, efficiently accommodating a variety of densities and constituent materials. This method represents a reasonable compromise between achieving the specified mechanical properties and ensuring workable mix uniformity.

To illustrate the process, Figure 4:5 in the study displays various foam-making products, including the foaming agent, machine, and the foam itself, highlighting the equipment and materials involved in this method.

4.3.2 Foamed Concrete Calculation

To calculate the mix proportion, use the absolute volume method (ACI-523.3R-93,1993). According to Ruiwen (2004), the cement content in a conventional FC with or without sand must be between 250 and 500kg/m³, and the optimal water-cement ratio of foam concrete must be between 0.5 and 0.6. In this experiment, foam concrete was made with a 1:2 sand and cement mixture and a water ratio of 50%. The working example below explains how to calculate the design mix proportion for the control mix design with a 1600kg/ m³ wet density.

- Plastic density of foamed concrete required = 1600 kg/ m³

- $W/C = 0.5$
- Specific cement gravity= 3.15
- The specific gravity of sand = 2.35
- Unit weight of water= 1000 kg/m^3
- Unit weight of foam = 45 kg/m^3 .
- Total mass of raw materials $1 \text{ m}^3 \times 1600 \text{ kg/m}^3=1600 \text{ kg}$

Table 4-4: Experimental Calculations for Foamed Concrete

Material	Mass kg in m ³	Calcs	Volume
Cement	457.15	$457.15 \times \frac{1}{315 \times 1000}$	0.145
Sand	914.275	$914.275 \times \frac{1}{235 \times 1000}$	0.39
water	228.571	$228.575 \times \frac{1}{1 \times 1000}$	0.228
Total			0.736
Air Volume		$1 \text{ m}^3 - 0.736$	0.236

The air content in foam produced by Propump 26 foaming agent is about 95 %

Therefore $0.236/0.95 = 0.248 \text{ m}^3 \times 1000 = 248 \text{ L}$

The amount of foaming agent required to produce 248 L of foam is $0.8 \text{ mL} \times 248 \text{ L}/1 \text{ L}$
 $= 198.5 \text{ mL}/950 = 0.2 \text{ m}^3$

The amount of water required to produced 248L of foam is $45 \text{ g} \times 248 \text{ L}/ 1 \text{ L} = 11160 \text{ g}$
 $\Rightarrow 11.16 \text{ kg}$

Calculations for the samples in this experiment were carried out by using the same method above detailed in table 4-4.

4.3.3 Material Selection to Produce Foamed Concrete

The materials used to produce foam concrete include:

1. Cement: Ordinary Portland Cement (OPC) is commonly used, but the type can vary based on specific requirements.

2. **Fine Aggregate:** Natural siliceous sand with a particle size of up to 4 mm is typical. However, alternative materials like fly ash, crushed glass, and others can also be used to achieve specific properties or reduce density.
3. **Water:** Water quality should be compatible with concrete production and free from harmful quantities of salts, organic materials, etc.
4. **Foaming Agent:** A surfactant used to create stable air bubbles in the mix. The choice of foaming agent can significantly influence the density and strength of the foamed concrete.
5. **Admixtures:** Superplasticizers can be added to enhance workability and reduce water content, improving mechanical properties.

4.3.4 Mix Design

The desired final density and strength determine the mix design of foamed concrete. Unlike traditional concrete, the mix design for foamed concrete is often based on the volume of materials rather than weight, considering:

1. Desired plastic or dry density
2. Cement-to-water ratio (C/W)
3. Volume of foaming agent
4. Aggregate type and volume

4.3.4.1 Mixing Procedure

The following steps systematically explain the foamed concrete design procedure. See Figure 4-5 for the design procedure:

1. **Dry Mixing:** Mix the dry components (cement and any solids like fine aggregate or additives) in a mixer for a few minutes to ensure uniform distribution.
2. **Water Addition:** Add water (and any liquid admixtures) to the dry mix gradually, ensuring a homogenous mixture.
3. **Foam Generation:** The foaming agent is diluted with water and processed through a foam generator to produce stable foam.
4. **Incorporating Foam:** The generated foam is carefully mixed with the slurry, ensuring even distribution without collapsing the bubbles. This step is crucial for achieving the desired density.

5. 4. Moulding: Once mixed, the foamed concrete is poured into moulds or directly applied to the desired area. The mixture should be levelled and compacted slightly to ensure even filling and reduce the likelihood of air pockets.
6. Curing: To achieve its full strength, foam concrete requires curing, like traditional concrete. Curing methods can include covering with wet burlap, plastic sheeting, or applying a curing compound, and it typically needs to be kept moist for at least seven days.
7. Demoulding and Testing: After sufficient curing, the foamed concrete is removed from the moulds if applicable. It can then be subjected to various tests to determine its density, compressive strength, thermal conductivity, and other relevant properties.

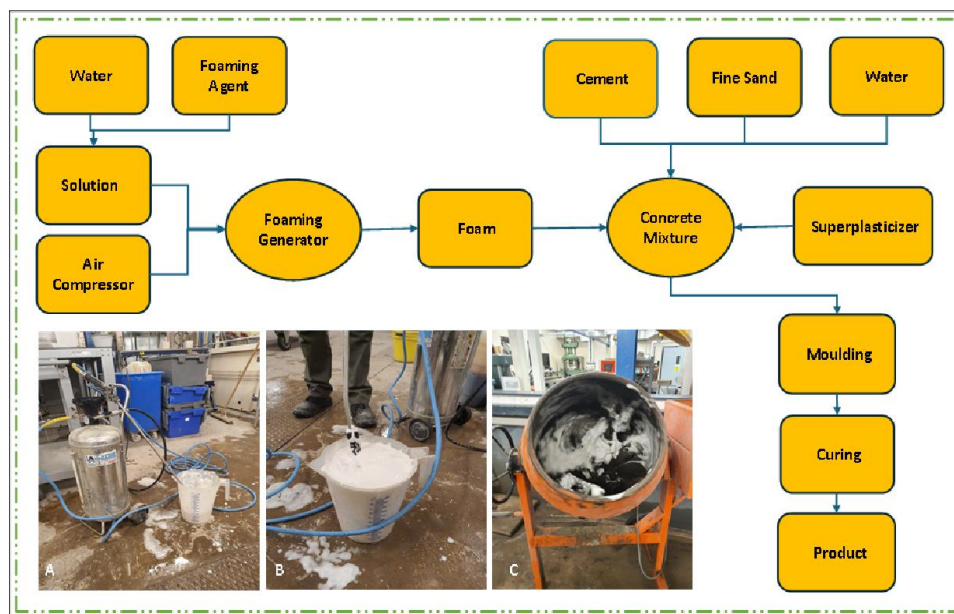


Figure 4-5: Foam Production Process for Foamed Concrete – (a) Foam Generator, (b) Foam, (c) Rotary Drum Mixer

4.3.5 Examine Flowability

In the fresh state, foamed concrete undergoes tests to determine its consistency and wet density. These tests are crucial for ensuring the mixture is workable and conforms to the required specifications for application:

1. Consistency Test: This test measures the flowability and spread of foamed concrete,

which indicates how easily it can be placed and compacted. The consistency is typically assessed using a flow table test or a slump test, depending on the desired accuracy and specific requirements of the project.

2. **Wet Density Test:** Wet density is measured immediately after mixing to verify that the concrete's density aligns with the design specifications. This test is essential for calculating the yield of the concrete and ensuring the correct proportion of foam has been added to achieve the targeted lightweight properties.

4.3.5.1 Examine Samples at Fresh State and Consistency

The workability of foamed concrete, precisely the flow behaviour, is typically evaluated using the modified Marsh cone method, which Dhir introduced in 1999 at Dundee University. This method has been widely adopted in subsequent research to assess the viscosity and fluidity of foamed concrete mixtures, as documented by various researchers, including Brady et al. (2001), Ozlutas (2015), Hilal (2015), Mohammad (2011), Hilal (2015), and Mehta (2017).

4.3.5.2 Foamed Concrete Flowability

1. A Marsh cone is attached to a stand. See Figure 4-6.
2. After closing the nozzle, the cone is filled with 1.5 litres of foamed concrete.
3. Determine how long it takes for 1 litre of foamed concrete to flow through the confined opening.

Table 4-5: Flow Time and Behaviour Classification (Jones et al., 2003)

Main Class	Flow Rate	Sub Class	Description of Flow
1	1 Letter in < 1 Minute	A	Constant flow
2	1 Letter in > 1 Minute	B	Interrupted flow
3	0.5 Letters < Efflux < 1 Letter	C	Completion of flow after gentle tamping
4	Efflux < 0.5 Letters	D	Low flow
5	No Flow	E	No flow

The modified Marsh cone setup, depicted in Figure 4-6, provides detailed dimensions and the arrangement necessary to carry out this test effectively. The modified Marsh cone is an adaptation of the traditional Marsh cone used in cement and mortar viscosity measurements. This specialised

cone is designed to allow foamed concrete, which is typically more viscous than standard cement mixtures, to flow through under gravity, measuring the time it takes to discharge a set volume. The flow time is indicative of the mixture's workability; shorter times suggest higher fluidity and better workability, which is crucial for ensuring the foamed concrete can be easily placed and uniformly compacted without segregation.

This method provides a reliable measure of the foamed concrete's consistency, helping to adjust the water content or the amount of foaming agent to achieve the desired flow characteristics. By utilising the modified Marsh cone method, researchers and engineers can more accurately control the quality of foamed concrete, ensuring it meets the specific needs of various construction applications.

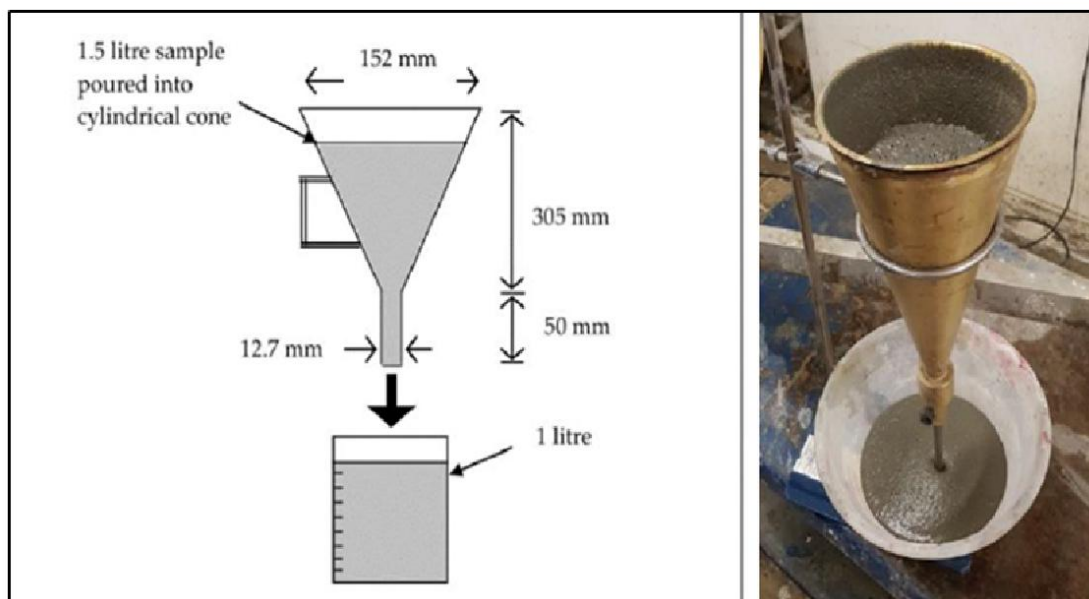


Figure 4-6: Dimensions of Modified Marsh Cone

4.3.6 Density

The plastic density of foamed concrete is measured following the guidelines in BS EN 12350-6 (2000), ensuring that the density falls within a precise tolerance of $\pm 50 \text{ kg/m}^3$ of the targeted density. This measurement is crucial for verifying that the produced foamed concrete meets specific design requirements. The process involves several steps represented in Figure 3-5 and executed as follows:

1. Filling the Container: A container of known volume and mass is filled with foamed concrete to ensure measurement accuracy.
2. Levelling the Surface: Any excess concrete is carefully removed from the top of the container to create a flat surface. This is done without compacting the mix to avoid altering its natural settling and density.
3. Weighing: After levelling, the container is weighed. The mass obtained is used to calculate the plastic density of the foamed concrete.
4. Calculating Plastic Density: The calculation of plastic density for foamed concrete follows a defined formula as per Equation 4-1:

$$\rho_m = \frac{(M_2 - M_1)}{V} \quad \text{Equation 4-1}$$

Where:

ρ_m - is the target plastic density in kg/m³,

M_2 - is the combined mass of the container and the foamed concrete sample in kilograms,

M_1 - is the mass of the empty container in kilograms,

V - is the volume of the container in cubic meters.

This equation facilitates the determination of the density by subtracting the mass of the empty container from the total mass when filled with foamed concrete and then dividing it by the volume of the container. By adhering to this standardised method, consistency and reliability in the density measurements of foamed concrete are ensured, supporting the quality control process in the production of this lightweight construction material.

This precise measurement is fundamental in achieving the desired properties of foamed concrete, particularly in terms of its structural integrity and insulating capabilities. Further enhancing the understanding of density relationships in foamed concrete, Jones, Ozlutas, and Zheng (2016) developed a linear equation to correlate the plastic density of foamed concrete with its dry density, particularly within a density range of 1200 kg/m³ to 1800 kg/m³. As per Equation 4-2:

$$\rho_{dry} = \frac{\rho_{wet} - 105}{1.05}$$

Equation 4-2

Where:

ρ_{dry} - is the combined mass of the container and the foamed concrete sample in kilograms,

ρ_{wet} - is the measured wet density in kg/m³.

This equation suggests that to achieve the desired dry density, the plastic design density should be at least 105 kg/m³ greater than the required dry density.

Table 4-6 presents comparative data on plastic (wet) and target densities for cube samples. Each design consists of three cubes, and the average density was recorded. The data apply to 1:1.5 cement-to-sand ratio mixes for waste foundry sand (WFS) and normal sand (Control) with densities ranging from 800 kg/m³ to 1400 kg/m³. These values represent the mean average of three 100 x 100 x 100 mm cubes. Figure 4-7 visually summarises the designed wet, measured wet, and fully dried densities, illustrating the change across different stages of the mixing design process.

Table 4-6: Wet Plastic Density and Corresponding Dried Density

Mix	Design Wet Density (kg/m ³)	Average Measured Wet Density (kg/m ³)	Average Measured Dry Density (kg/m ³)	Flow Rate Class
8Co	800	805	666	A
8WFS	800	780	642	A
10Co	1000	990	842	A
10WFS	1000	910	766	B
12Co	1200	1212	1054	A
12WFS	1200	1190	1033	B
14Co	1400	1500	1328	A
14WFS	1400	1480	1309	B

Note: *8Co is the control FC with a target plastic density of 800 - 1400 kg/ m³

*8WFS is waste foundry sand with a target plastic density of 800 – 1400 kg/ m³

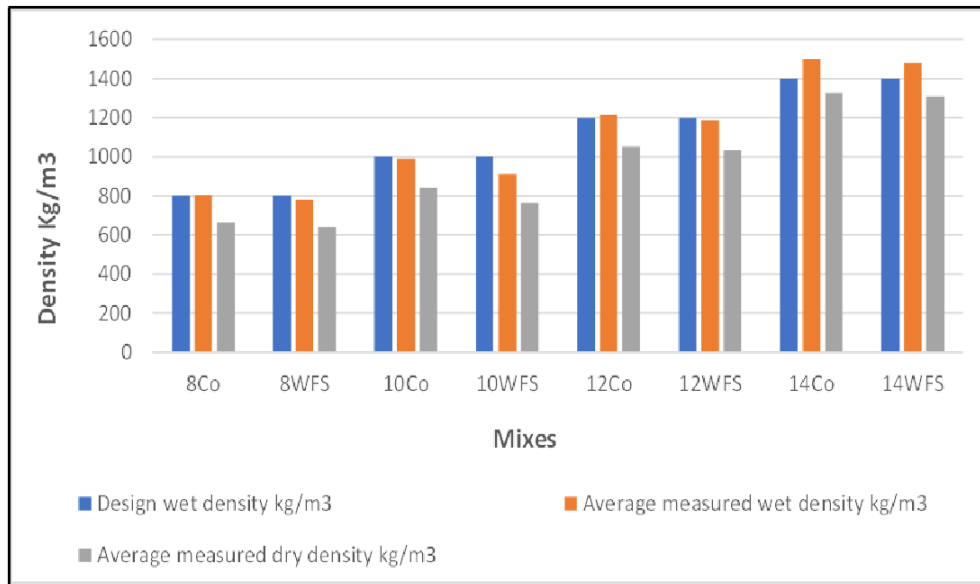


Figure 4-7: Designed Wet, Measured Wet, and Fully Dried Densities of Foamed Concrete

4.3.7 Foamed Concrete Samples Production

There is no set standard for producing foamed concrete. As a result, the strategy given by Jones et al. (2005), which researchers widely use, was used in this investigation, as represented in Figure 4:8. The dry components like cement, fine aggregate, and additives are initially combined in a rotating drum mixer for about one minute. The complete amount of water is then added, and the mixture is mixed for another 2 to 4 minutes to ensure a lump-free, homogeneous solution.

Concurrently, pre-formed foam is created with a foam generator and quickly absorbed into the base mixture. This mixture is then swirled for about one minute or until the foam is evenly distributed throughout it. Following that, the plastic density of the mix is quickly determined to ensure compliance with BS EN 12350-6 (2009).

A sample is weighed in a pre-weighed container with a known volume to determine if the plastic density of foamed concrete reaches the allowable tolerance limit of $\pm 50 \text{ kg/m}^3$.

If the detected plastic density exceeds this tolerance, more foam is created and added to the mixture on the spot to achieve the required density. Mixes with plastic densities lower than the allowed limit, on the other hand, are discarded. The production process, which is mostly carried out in a rotating drum mixer, as shown in Figure 4-8, ensures that the foamed concrete satisfies the specified standards and quality requirements.



Figure 4-8: (a) Cube Moulds, (b) Prism Mould

4.3.7.1 Samples Preparation

Before mixing, various forms, such as cubes, prisms, and slabs, are cautiously prepared to shape the foamed concrete. To facilitate the removal of these shaped samples after setting, mould-release oil is carefully applied to all internal surfaces of the forms using a brush. This preparation ensures that the concrete does not adhere to the moulds, thus easing the demoulding process without damaging the concrete structures. See Figure 4-9 for material preparation for the experimental work.



Figure 4-9: Foamed Concrete Production and Moulds, (b) Rotary Drum Mixer

After pouring the concrete into the prepared moulds, the samples must be handled carefully, as shown in Figure 4-10. Following these preparation stages, the samples are allowed to set and harden in controlled environments for 24 hours. However, the initial setting time varies according to the composition of the foamed concrete and the ambient circumstances.



Figure 4-10: Experimental Samples in Moulds and During Curing

After setting, the samples are removed from their moulds. The application of mould-release oil facilitates demoulding, resulting in smooth and unbroken surfaces suitable for future testing and analysis. Each form is wrapped with cling film to prevent moisture loss during the early curing time. This covering helps to maintain a consistent humidity level surrounding the concrete, which is critical for attaining optimal curing conditions and maintaining uniform hydration of the cement. It is critical to closely monitor the setting process to ensure the concrete achieves the necessary mechanical properties and structural integrity.



Figure 4-11: Examples of Weighing Samples – (a) Cube, (b) Prism

To summarise, precise mould preparation and cautious handling of foamed concrete samples are critical processes that substantially impact the quality and accuracy of experimental results in concrete research. These stages, from mould preparation to sample curing and demoulding, are critical for creating repeatable and uniform concrete samples for testing and use in this project.

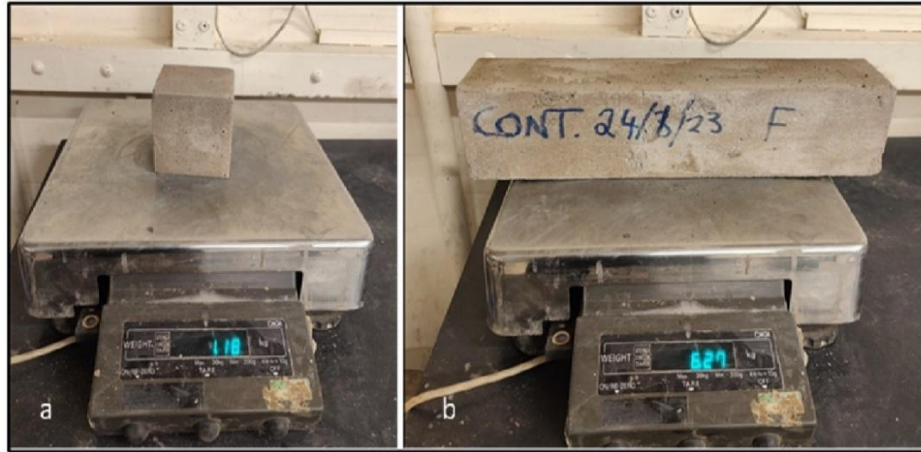


Figure 4-12: Examples of Weighing Cubes and Prisms

After weighing then the samples are subjected to a variety of tests to determine characteristics such as compressive strength, tensile strength, and elasticity, which provide useful information for evaluating the foamed concrete's performance.

4.3.8 Mechanical Analysis

Compared to normal concrete, foam concrete is primarily designed to reach a specified density rather than flexural and compressive strength, which is a common benchmark for regular concrete. The density and sand/cement ratio are the most important factors influencing the flexural and compressive strength of foamed concrete, with the water/cement ratio having a minor impact. The thorough testing process for foamed concrete indicated above ensures reliable and consistent findings, which are critical for confirming the material's structural and functional properties.

4.3.8.1 Compressive Strength

To investigate the compressive strength of the samples, a variety of procedures have been implemented, including:

1. **Sealed Curing:** Sealing the cubic specimens (100 x 100 x 100 mm) during curing minimises moisture loss, a critical factor in achieving the correct hydration process and, thus, the expected mechanical properties of foamed concrete. Sealed curing replicates realistic conditions under which the concrete will function, maintaining the integrity of the internal structure and moisture content. For accurate measurement, cured cubes of 100 x 100 x 100 mm are subjected to

compressive strength tests after 28 days in accordance with the criteria established in BS EN 12390-3 (2009).

2. **Calibrated Equipment:** The precision in the calibration of the testing equipment ensures that the loading conditions are controlled accurately, reflecting the lightweight nature of foamed concrete. This precision avoids the application of excessive force that could result in premature failure of the specimen or inaccurate readings of its strength capabilities. During testing, the specimens are carefully positioned and centred beneath the loading plate to achieve homogeneous contact with the plates, as shown in Figure 4-13.

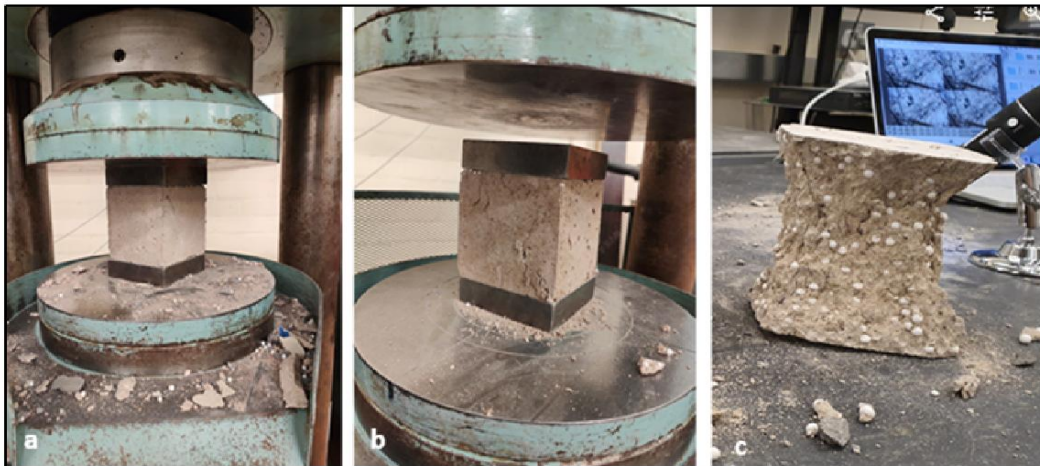


Figure 4-13: Cube Compression Test Using Hydraulic Compression Machine

3. **Load Application Rate:** Applying load from (10-50 N/sec) is suitable for the properties of foamed concrete. This slower rate of load delivery aids in precisely defining the point of failure, which is critical for materials such as foamed concrete, which may have lower compressive strength and different failure modes than typical concrete

4. **Documenting failure loads:** Documenting the results helps researchers and engineers better understand the behaviour of foamed concrete under stress. This data can be used to improve mixed designs and performance characteristics. Equation 4-3 calculates compressive strength to the nearest 0.1 N/mm², allowing for precise analysis and comparison with theoretical strength models or requirements for specific construction applications.

The equation supplied is a fundamental formula for calculating the compressive strength of concrete objects, such as cubes or cylinders. The calculation determines how much stress a

concrete substance can withstand before failure. The compressive strength for cubes is calculated as follows: equation 4-3.

$$f'_c = \frac{F}{A_c}$$

Equation 4-3

Where:

f'_c - represents the concrete's compressive strength. It is expressed in Newtons per square millimetre (N/mm²), a unit of pressure.

F - This is the maximum load applied to the specimen at the time of failure, measured in Newtons. This is the peak load capacity recorded during the compressive strength test.

A_c - This is the cross-sectional area of the specimen where the load is applied. For cubes, this is typically the area of one face (length x width), and for cylinders, it is the area of the circle (πr^2 , where r is the radius of the cylinder). This area is measured in square millimetres (mm²).

Adhering to testing standards like ASTM or BS EN ensures consistency in how tests are conducted, which is critical for comparing results accurately across different tests or materials. This method provides a clear and direct measure of the material's ability to resist compressive loads, which is crucial for structural applications of concrete, including foamed concrete.

4.3.8.2 Flexural Test

The Four-point flexural test is a critical method for assessing the flexural strength, or modulus of rupture, of concrete prisms and slabs. This test provides valuable data about the material's behaviour under bending stresses, which is crucial for structural applications where bending loads are common. Here's a deeper look into the test procedure and its implications:

1. Specimen Preparation: The samples include 33 prisms (100 mm x 100 mm x 500 mm)

These measurements are chosen to ensure that the specimens reflect the concrete's performance in practical pictures, as shown in Figures 4-14 below.

2. Test Step up: The prisms and beams are placed centrally on two supports within a three-point. This setup involves two load application points, creating a uniformly distributed load over the central section of the specimen. Care is taken to ensure the surfaces in contact with the loading plates are even to distribute the load uniformly.

3. Loading Rate: A constant loading rate of 500 N/min is used for low-density specimens, while high-density specimens are subjected to a loading rate of 1000 N/min. This differentiation in loading rates helps in understanding the behaviour of different densities under similar stress conditions.

4. Data Recording: Digital tools are used to record the load and the corresponding deflection at the moment of failure. This automatic data collection enhances the accuracy and repeatability of the results.

The modulus of rupture (f_r) is calculated using a specific formula designated in the BS EN 12390-5 standard. The location of the fracture significantly influences this calculation, as it provides insights into the stress distribution and the weakest point of the specimen. According to Wahyuni (2012), the values of tensile strength obtained from the flexural test are typically higher than those from the cylinder splitting test, which in turn are higher than those obtained from direct uniaxial tension tests. Flexural tests induce bending stresses that might allow the material to exhibit higher tensile strengths due to the distribution of stresses over a larger area.

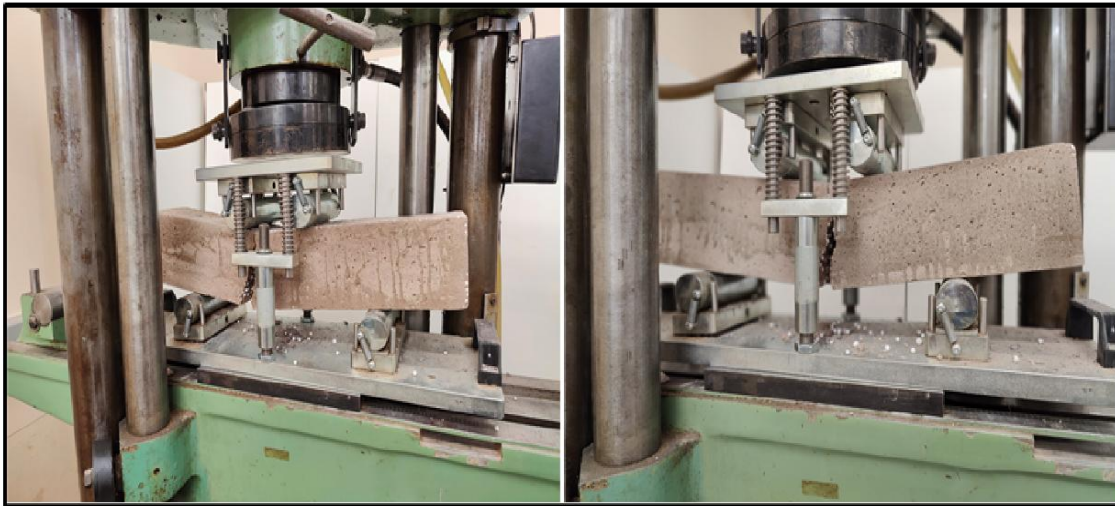


Figure 4-14: Prisms Flexural Test Using Hydraulic Flexural Testing Machine

This stepped testing approach enables engineers and researchers to gain a full understanding of material properties under different circumstances and load types, assisting in the design and application of concrete structures in a variety of construction scenarios. Understanding these variations is critical for correctly interpreting test results and applying them to structural design and analysis.

The equation you provided for calculating the modulus of rupture, f_r , is a standard method for assessing the flexural strength of a concrete specimen in accordance with BS EN 12390-5. This test method and the associated equation are critical for evaluating the performance of concrete in conditions that simulate real-world scenarios where the material is subjected to bending stresses. Equations 4-4 show the breakdown of the flexural calculation of beams and prisms.

$$f_r = \frac{3PL}{2bd^2}$$

Equations 4-4

Where:

f_r - Flexural strength measured in Newtons per square millimetre (N/mm²).

P - Maximum load at the time of failure, measured in Newtons (N).

L - Beam span, the distance between the supports, measured in millimetres (mm).

b - Average specimen width, measured in millimetres (mm).

d - Average specimen depth, as oriented during testing, measured in millimetres (mm).

The formula calculates the maximum stress experienced by the specimen at the moment of failure under a bending load. It assumes a linear elastic behaviour up to the point of failure, which is generally acceptable for conventional concrete testing. See Table 4-7 for the BS standard concerning compressive and flexural tests.

Table 4-7: Compressive and Flexural Test According to British Standard (BS)

Testing Types	Actual Test	BS, Code	No, of Group	No, of Sample	Sample size (mm)	Images
Compressive Test	Determine the compressive strength of concrete	BS EN 12390-3, (2009)	20	60	100 x 100 x 100	
Flexural Test	Determined the flexural strength of concrete	BS EN 12390-5, (2009)	16	48	100 x 100 x 500	

In practical application, the value of f_r compares different concrete mixes or techniques and their capacity to resist bending, which is especially relevant in applications like beams and slabs. For

structure design, the flexural strength assists in the design of concrete elements, ensuring that they can handle expected loads without excessive bending or failure. Regular testing utilising these methods can help to maintain the quality of concrete production by ensuring that the concrete used in construction satisfies the required strength standards. Overall, the modulus of rupture is an important metric for determining the bending strength of concrete, which is necessary for safe and efficient structural construction.

4.3.9 Summary

The experimental program aimed to enhance the mechanical properties of foamed concrete (FC) for broader applications, including structural uses, by addressing its inherent low compressive strength. The research involved over 150 specimens, categorised into four density groups (800, 1000, 1200, and 1400 kg/m³), with mixes incorporating recycled materials and additives such as waste foundry sand, polystyrene, recycled steel fibre, and superplasticiser. Key tests assessed density, workability, compressive strength, and flexural strength.

1. Experimental Design:

More than 150 specimens were prepared and divided into four density categories. Each category included control samples and variations with waste foundry sand, polystyrene, recycled steel fibre, and superplasticiser to enhance mechanical properties.

2. Testing Procedures:

Density and workability tests were critical for ensuring mix consistency, suitability for different applications. Compressive strength tests assess the maximum load that foamed concrete can withstand. Flexural strength tests evaluated the material's behaviour under bending and tension, which is crucial for structural applications.

3. Expected Outcomes:

The addition of various materials aimed to address specific weaknesses of foamed concrete. Enhanced compressive strength was critical for structural applications and was potentially achieved by optimising the cement matrix and including fibres. Improved flexural strength was anticipated, with steel fibres significantly enhancing this property, making foamed concrete viable for elements like panels and lintels. Better bond behaviour was expected through the strategic use of additives and fibres, improving the bond between the concrete matrix and embedded material

Chapter 5: Foamed Concrete – Results and Discussion

5.1 Introduction

This chapter describes the results and data analysis for concrete cubes, prisms, and slabs created at the NTU laboratory. The results will be presented in the form of tables, graphs, element images, and discussions. In this experiment, two types of concrete were created: foamed concrete containing recycled components and conventional concrete. The objectives of making these concrete forms are to investigate the properties, strength, and flexural behaviour of both foamed and conventional concrete and explain the findings.

This chapter will also analyse and discuss the traditional concrete components such as cement, sand, and aggregates and the specific additives and recycled materials used to enhance the concrete's performance. Key materials like waste foundry sand, polystyrene, recycled steel fibres, and superplasticisers will be examined for their impact on the mechanical properties, including compressive and flexural strength, of the foamed concrete.

Foamed concrete (FC) is a lightweight concrete variant distinguished by its unique composition and structure. Primarily made of cement, sand, water, and air introduced through a foaming agent, it features a homogeneous pore structure that significantly reduces its density compared to traditional concrete, Hamad (2014b). The inherent properties of FC, such as its reduced weight, also result in lower compressive, flexural, and tensile strengths, which are critical factors to consider when evaluating its suitability for various applications.

The 28-day compressive strength of foamed concrete mixes, varying in density from 800 to 1400 kg/m³, was examined with and without additives. This study was part of a broader experimental program aimed at enhancing and understanding the mechanical properties of foamed concrete by manipulating various mix components such as cement/sand ratios and integrating different types of recycled materials and additives.

5.2 Experimental Design

The following numbers are analysed after the experimental work carried out, including:

1. Sand Ratios: Different ratios were tested to determine the optimal mix for achieving the best compressive strength.
2. Additives and Recycled Materials: The use of superplasticisers and other additives was

explored as partial replacements for sand to enhance the concrete's performance, as recycled materials, such as waste foundry sand and polystyrene, were incorporated at various volumes to assess their impact on the mix's properties.

3. **Steel Tire Fiber:** Steel tire fibres were also included in some mixes to investigate potential improvements in compressive and flexural strength.
4. **Density Variations:** The concrete mixes were prepared at varying densities ranging from 1400 kg/m³ to explore the density's effect on mechanical properties. Different densities, achieved through varying the aggregate types and quantities, show distinct patterns in strength characteristics. Typically, higher densities correlate with higher compressive strength, attributed to the greater mass of material available to resist loading.
5. **Compressive Strength Testing:** Each mix experienced standard compressive strength testing after 28 days of curing to evaluate the effectiveness of the different mix configurations.
6. **Flexural Strength Assessment:** The impact of additives like steel tyre fibres on flexural strength was also a key focus, with tests conducted to determine enhancements in this area.

5.3 Result Analysis

This experimental approach has allowed for a comprehensive understanding of how different variables affect the mechanical properties of foamed concrete. By systematically varying the cement/sand ratio and incorporating different recycled materials and additives, it was possible to identify effective strategies for enhancing the structural capabilities of foamed concrete, catering to diverse construction needs. The findings highlight the potential for using a variety of waste materials and innovative additives to improve the sustainability and performance of construction materials.

5.3.1 Compressive Strength

Table 5-1 summarises the various outcomes, covering specific data points relating to the compressive strengths attained with each combination. Table 5-1 presents the analysis of how the strength outcomes are impacted by each variable, including density, additives, recycled materials, and sand ratio. According to the experimental findings, certain additives and recycled materials significantly impact the compressive and flexural strengths of foamed concrete, especially when combined with particular cement/sand ratios. The information in this table is structured in an

approach that facilitates a deeper understanding of how each element affects the mechanical properties of the concrete.

Table 5-1: Compressive Strength of Foamed Concrete vs. Normal Concrete Cubes

Concrete Cube Design	Compressive Strength (MPa)			Average Compressive Strength (MPa)	Density (kg/m ³)	Note
Control	30.7	31.2	31.5	31.1	2160	Normal Mortar Concrete Cube Density 2160 kg/m ³
NFC	15.5	15.8	15.9	15.7	1400	Normal Foamed Concrete Cube Density 1400 kg/m ³

Table 5-2: Compressive Strength of Concrete Cubes with Varying Densities and Sand Ratios

Foamed Concrete Design Mix	Material Replacement or Addition (%)	Average Compressive Strength (MPa)				Note
		Density 800, (kg/m ³)	Density 1000, (kg/m ³)	Density 1200, (kg/m ³)	Density 1400, (kg/m ³)	
NFC	0%	3.97	6.1	10.83	15.7	No replacement or additives
WSF	25%	3.9	6	9.42	15.11	Replaced with normal sand (Mass)
WFS	50%	3.43	5.1	8	13.91	Replaced with normal sand (Mass)
WFS	75%	3	4.8	7.93	11.15	Replaced with normal sand (Mass)
WFS	100%	1.97	3.21	4.71	6.1	Replaced with normal sand (Mass)
PO	10%	3.31	5.3	7.88	10.33	Replaced to the mortar cube by (Volume)
PO	20%	2.69	5	7.54	9.83	Replaced with the mortar cube by (Volume)
PO	30%	1.02	2.22	3.8	5.61	Replaced to the mortar cube by (Volume)
RSTF	1%	4.44	6.21	11	16.12	1.2% of the cement amount added (Mass)
SPs	1%	4.71	7.6	13.6	19.4	1% of the cement amount added (Mass)

According to Table 5-2, the average compressive strength of those cubes substituted with 100%, 75%, 50%, and 25% in (weight) waste sand dropped by approximately 16 MPa, 15 MPa, 13 MPa, and 10 MPa, respectively, compared to the regular mortar cube. However, the self-weight of the cubes that replaced waste foundry sand completely with normal sand is 0.30 kg lighter than the standard concrete mortar. During the cube testing technique, the cubes constructed from recycled sand absorbed more water, causing the samples to collapse faster under the compressive testing equipment as stress was applied.

5.3.2 Effect of Replaced Recycled Materials on Compressive Strength

Typically, the strength of concrete cubes is assessed through compression testing, which determines the material's resistance to the load imparted by the compression testing apparatus. Figure 5-1 illustrates the distinctions in outcomes between conventional foamed concrete with additives and recycled materials. As predicted, the load-bearing capacity of normal foamed concrete cubes is greater than that of foamed concrete. Foamed concrete cubes from this experiment have carried a maximum applied load of 15.7 MPa. The results of this experiment are consistent with the research conducted by Kearsley and Moster (2005) and Hilal et al. (2015).

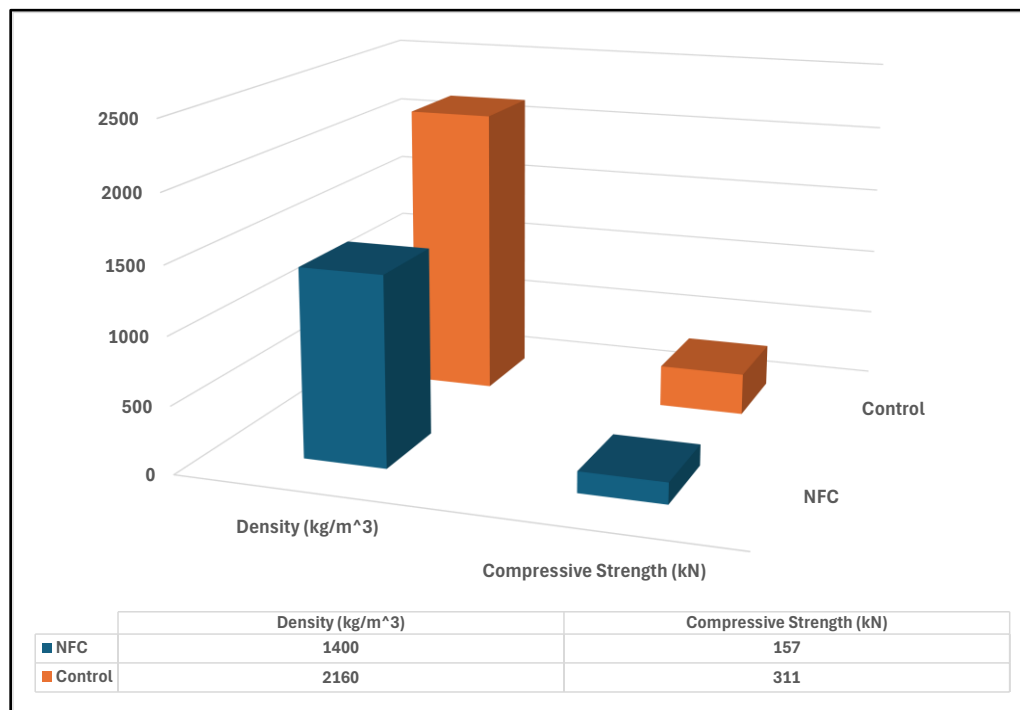


Figure 5-1: Compressive Strength vs. Density of Mortar Concrete and Foamed Concrete

The results presented in Figure 5-2 demonstrate the correlation between the percentage of recycled materials, specifically Waste Foundry Sand (WFS), and the compressive strength of the aggregate design. According to the data, mixtures comprising recycled material in lower proportions (e.g., 25% and 10%) demonstrate enhanced compressive strength compared to mixtures containing higher percentages of Waste Foundry Sand (WFS) and Polystyrene (PO). The results show that replacing 25% of WFS increases the mechanical strength of the combination by 100% compared to samples made completely of WFS.

The results show that polystyrene can be used as a replacement material in mortar mixtures. When 10% of the mortar volume is replaced with polystyrene, the compressive strength increases by 110% compared to using a larger fraction, such as 30%. This significant increase in strength can be mainly due to the increased presence of sand in the mix with only a 10% replacement of polystyrene. The sand contributes to stronger bonding among the particles of the foamed concrete (FC), thus enhancing the overall compressive strength.

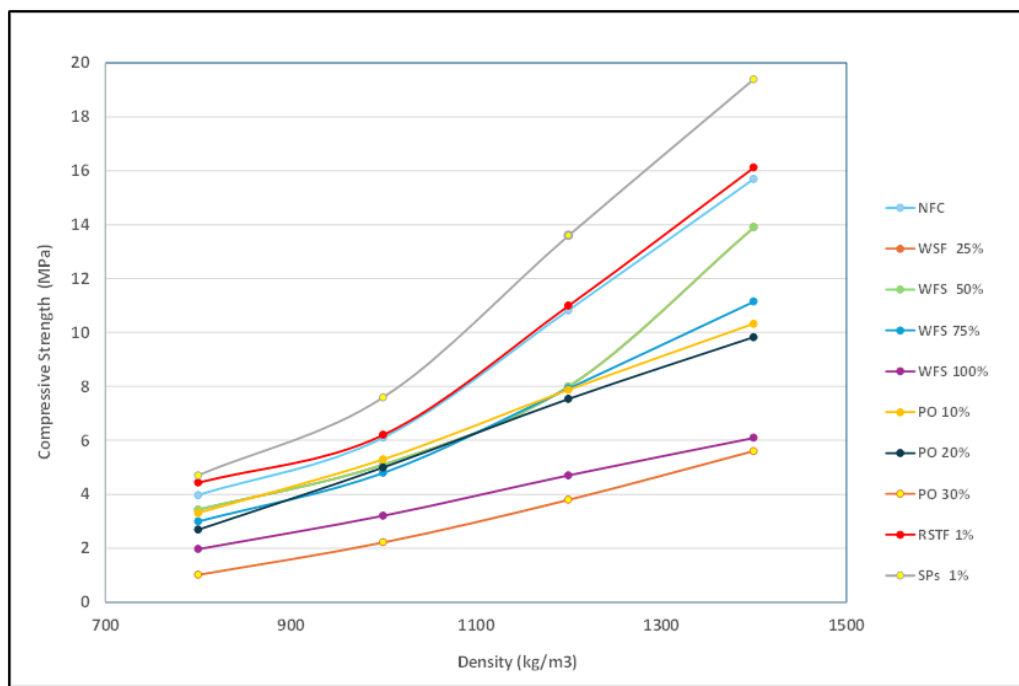


Figure 5-2: Compressive Strength of Concrete Mixes with Varying Densities and Sand Ratios

In an experiment, a concrete mixture with a density of 1400 kg/m³ was used to analyse the effects of substituting traditional materials with waste foundry sand and polystyrene. The results showed that incorporating 20% waste foundry sand into the foamed concrete mix decreased its

compressive strength by about 3% when compared to the normal foamed concrete. This modest reduction in strength suggests that waste foundry sand can be used as a partial replacement for sand with a relatively small impact on the structural integrity of the concrete. Conversely, the introduction of 10% polystyrene led to a much more significant reduction in compressive strength, nearly 52%.

The relationship between the compressive strength of the mortar and its sand content is nonlinear rather than linear. This indicates that while increasing the amount of sand generally leads to higher compressive strength, the increase does not happen constantly. The nonlinear pattern indicates that adding additional sand may have a decreasing benefit in terms of its ability to increase strength. This understanding points to the necessity of finding an optimal balance in material composition to maximise the structural benefits while incorporating sustainable materials like polystyrene, which can reduce weight and potentially enhance other desirable properties of the mortar.

The drastic decrease in compressive strength with the introduction of polystyrene is attributed primarily to the poor bonding between the polystyrene aggregates and the cement paste. Furthermore, the chemical interactions between the cement paste and the polystyrene may also contribute to weaker bonds, as these interactions can affect the curing process and the microstructure of the cement matrix.

The decrease in compressive strength can primarily be linked to several factors. For instance, recycled materials often do not bond as effectively with the cement paste as traditional materials do. This can be due to differences in porosity or chemical composition. For instance, non-absorptive materials like some polystyrene might not adhere well to the cement matrix, leading to weaker overall structural integrity. Recycled materials may inherently possess lower mechanical strength compared to conventional materials. When these weaker materials replace stronger traditional materials in a concrete mix, they naturally lead to a reduction in overall compressive strength. Some recycled materials can react chemically with the cement paste in ways that may alter the hydration process or produce deleterious compounds, further weakening the concrete.

5.3.3 Effect of Density on Compressive Strength

The analysis of the compressive strength results for foamed concrete (FC) involves examining the relationship between the density of the mix and its compressive strength. The data from the compressive strength testing of FC cubes, conducted as per the BS EN 12390-3 (2009) standard, reveals a clear and positive correlation between the density of FC mixes and their compressive

strength. This relationship is illustrated by the increasing compressive strength as the density of the mix increases, which is evident from the provided results at various densities.

The results show that as the density increases from 800 kg/m³ to 1400 kg/m³, the compressive strength also rises, with recorded values at select density points being 3.97 MPa, 6.1 MPa, 10.83 MPa, and 15.7 MPa, respectively. See Figure 5-3 for foamed concrete made of different densities. These results specifically highlight the progressive increase in strength with increasing density, demonstrating the critical role that density plays in the structural behaviour of FC. This dramatic increase suggests that denser mixes contain fewer air voids or micro-pores, leading to higher mechanical integrity and resistance to compression. The results show that each 200 kg/m³ increase in density leads to an average 290% increase in compressive strength. This exponential rise in strength with relatively small increases in density highlights the efficiency of densification in enhancing the structural properties of foamed concrete.

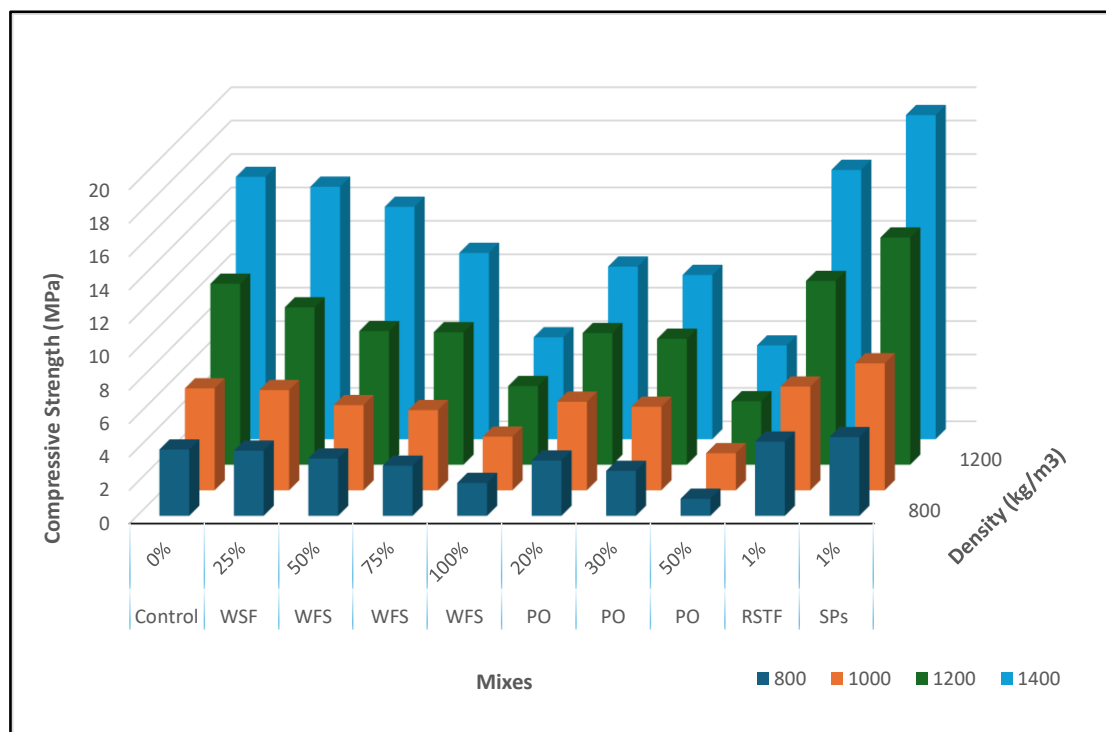


Figure 5-3: Compressive Strength versus Density of Cubes with Recycled Materials

The 1:2 cement to sand (c/s) ratio used in the control mixes might be optimal for achieving a balance between material cost and mechanical properties. This ratio ensures adequate paste to fill the voids between sand-recycled particles, leading to higher compressive strength.

However, the findings are consistent with expectations from earlier research by Gangatire and Suryawanshi (2016) and Mydin (2010), which also noted the sharp decrease in compressive strength with reduced density. The current results not only align with these studies but also present higher strength-to-density ratios compared to findings from Jones and McCarthy (2005), Nambiar and Ramamurthy (2006), and Ameer (2015). This suggests an improvement in material formulation or processing techniques over time or possibly a different concrete mix composition that yields better performance.

5.3.4 Effect of Additives on Compressive Strength

The findings regarding the effects of additives on foamed concrete (FC) offer valuable insights into optimising its mechanical properties through mixed design modifications. The addition of superplasticisers is shown to enhance the compressive strength of foamed concrete significantly. By including 1% of superplasticiser relative to the cement weight, compressive strength is an average increase of 20%. This improvement is attributable to the superplasticiser's ability to reduce the water-cement ratio while maintaining the mix's workability. This lower water-cement ratio results in a denser, more compact microstructure, enhancing strength. In the study, a 1% superplasticizer-to-cement ratio was used to optimise the mechanical characteristics and workability of the experimental samples.

However, a noted drawback is the accelerated destabilisation of the foam bubbles by the chemical reaction induced by the superplasticiser, leading to an unintended increase in density (6-10%). While potentially beneficial to strength, this density increase could alter other desired properties of the FC, such as thermal insulation and weight.

Adding 1% recycled steel tyre fibre to the mix leads to an increase in compressive strength of about 3-5%. This improvement, though less pronounced than that from superplasticisers, is still significant. The steel fibres help to bridge cracks that form during loading, distributing stress more evenly throughout the material and thus increasing both compressive and flexural strength. The fibres essentially act as reinforcement within the matrix, improving the toughness and ductility of the foamed concrete. For the standard foamed concrete (control) with a density of 1400 kg/m³, the compressive strength increases from 15.7 MPa to 16.12 MPa with the addition of steel fibres. This modest increase highlights the potential of using fibres to enhance structural performance without substantially altering the material's density.

These findings suggest that careful selection and proportioning of additives can be a powerful strategy in tailoring the mechanical properties of foamed concrete to specific applications. For instance, structures requiring high strength could benefit from mixes enhanced with superplasticisers and steel fibres, while applications, where weight is a critical factor, might use a carefully measured amount of superplasticiser to balance strength and density.

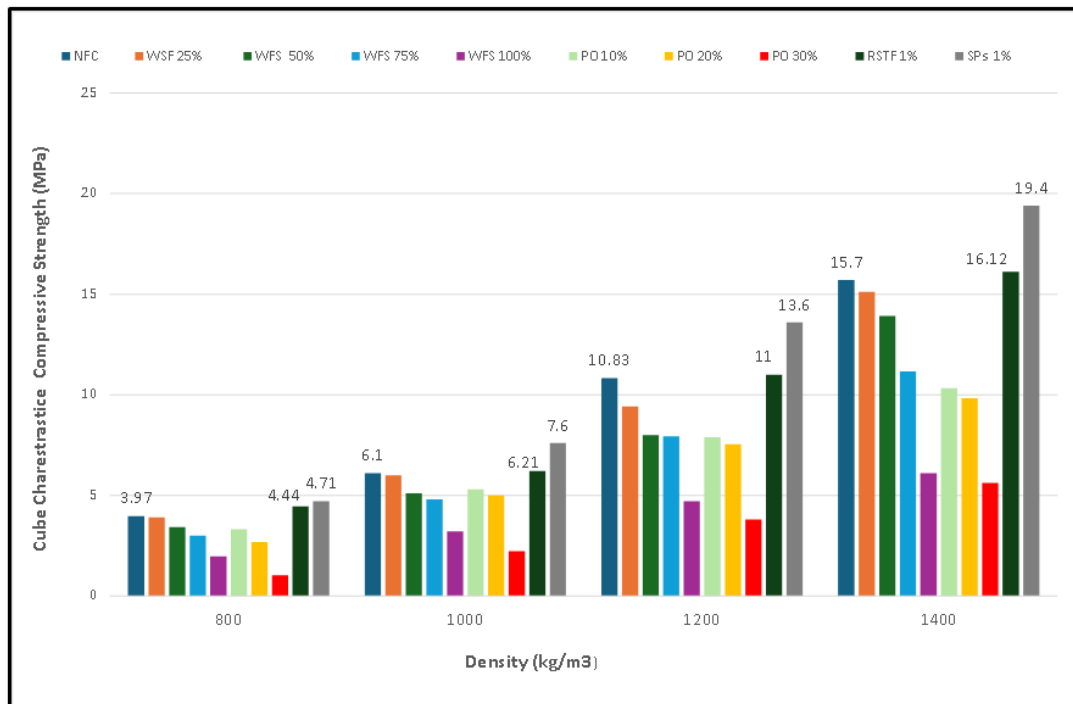


Figure 5-4: The Impact of Additives on Compressive Strength

Nwoye (2020) discusses the benefits of adding superplasticisers to concrete in amounts ranging from 0.5% to 1.5% of the cement ratio. This addition improves the mechanical properties of concrete by dispersing the cement particles and reducing the need for additional water, thus maintaining optimal workability. Further studies have investigated the potential of using specialised cement types, such as high-strength and quick-setting Portland cement, in accordance with BS 915:1983 standards, to improve the performance of foamed concrete.

5.3.5 Effect of Density with Various Recycled Materials on Compressive Strength

The effect of density on the compressive strength of various recycled materials is an important factor in sustainable construction and material science. Recycled materials, including waste foundry sand (WFS), recycled steel tyre fibre (RSTF), recycled polystyrene (PO), and other

admixtures like superplasticisers, can improve the mechanical strength and density of concrete mixtures.

Table 5-3 represents the changes in density for different design mixtures that incorporate recycled materials. This table provides an understanding of how changing the quantity of recycled materials in a mix influences the ultimate density of the samples after curing. The data allows investigators to compare these densities to a specified target density. The primary purpose of altering these proportions is to create a finished product with a lower density, making it easier to handle and potentially removing the need for bulky machinery during installation or transportation.

The examination of the differences in density documented in Table 5-3 determines the most useful quantity of recycled material to incorporate into the mixture to attain the required properties.

By integrating recycled materials into the mix, the density of the samples has been notably reduced, particularly with the inclusion of polystyrene. Data indicates a dramatic decrease in density, ranging from 5% to 8%, compared to standard foamed concrete, as noted in the control samples.

Table 5-3: Comparison of Measured Density Against Target Density of Sample

Foamed Concrete Design Mix	Samples Average Density				Note
	Density 800, (kg/m ³)	Density 1000, (kg/m ³)	Density 1200, (kg/m ³)	Density 1400, (kg/m ³)	Description
NFC	812	1029	1237	1441	No replacement or additives
WSF 25%	800	1005	1197	1395	Replaced with normal sand (Mass)
WFS 50%	790	995	1195	1388	Replaced with normal sand (Mass)
WFS 75%	780	977	1197	1380	Replaced with normal sand (Mass)
WFS 100%	780	983	1181	1379	Replaced with normal sand (Mass)
PO 10%	769	951	1157	1361	Replaced the mortar cube by (Volume)
PO 20%	760	942	1147	1350	Replaced the mortar cube by (Volume)
PO 30%	740	911	1100	1299	Replaced the mortar cube by (Volume)
RSTF 1%	817	1041	1250	1460	Added to the mass of the cube, (Mass)
SPs 1%	807	1030	1243	1452	1% of the cement amount added (Mass)

Figure 5-5 illustrates how the gradual incorporation of polystyrene leads to a corresponding reduction in the weight of the samples. For example, the samples that contained 30% polystyrene were almost 8% lighter than the normal foamed concrete (NFC) and even lighter than the rest of the samples tested. According to the findings, replacing foundry sand also contributed to a minor reduction in density. The samples where 100% of the normal sand was replaced with foundry sand showed a decrease in density by approximately 2%. The use of waste foundry sand also contributes to a minor reduction in the total weight of the cube, as it is naturally lighter than standard sand. While polystyrene presents challenges during the mixing process due to its lack of workability, waste foundry sand offers a smoother and more manageable alternative during both the mixing and casting stages. For example, incorporating a higher proportion of specific lightweight recycled materials can be beneficial in reducing overall density, which is useful for lightweight structural applications such as wall panels, foundations, and pavements.

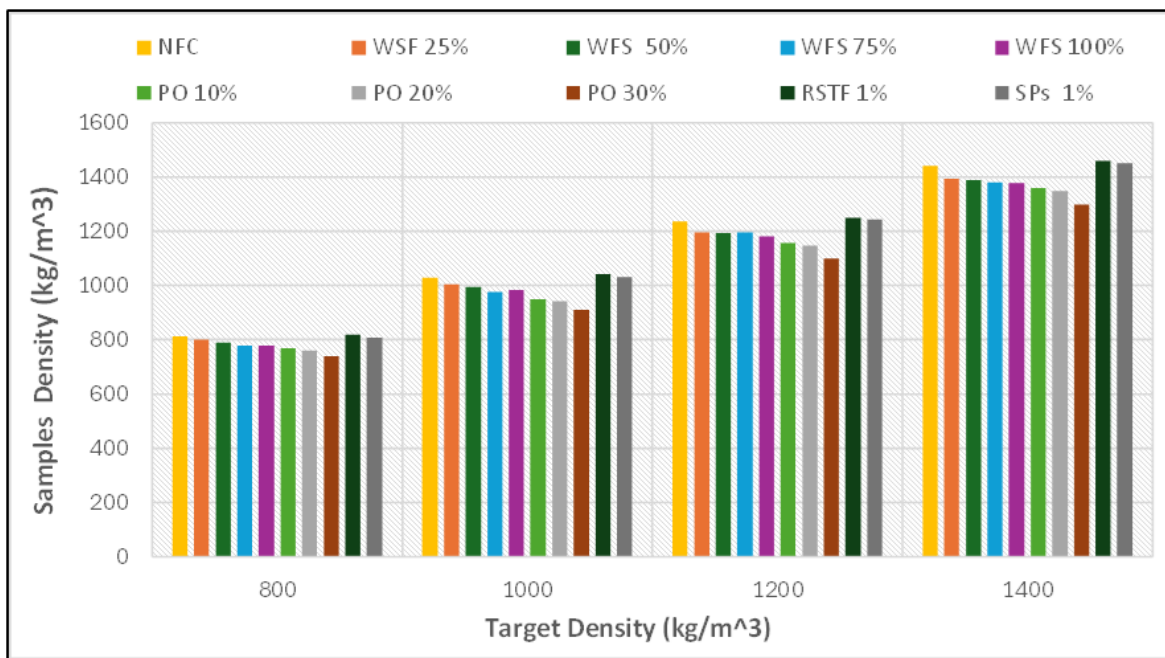


Figure 5-5: Average Density of Samples with Lightweight Recycled Materials Replacement

5.3.6 Flexural Strength

The flexural strength of a concrete sample measures its ability to resist bending moments under an applied load. Different additives and materials used in concrete mixtures can significantly affect this strength characteristic. Comparing foamed concrete, waste foundry sand, polystyrene, recycled tyre steel fibre, and standard concrete mortar samples reveals a range of flexural strengths

due to their varying densities and compositions. The maximum load and deflection measurements for modified prisms with dimensions of 100 x 100 x 500 mm, including a range of recycled materials and admixtures, are displayed in Table 5-4

Table 5-4: Maximum Load and Deflection for Prisms with Various Recycled Materials

Foamed Concrete Design Mix	Material Replacement or Addition	Maximum Applied Load (kN)	Maximum Deflection	Note
Material type	(%)	Density 1400, (kg/m³)	(mm)	Description
Control	0	47	8.1	Normal Mortar Density, 2160 (kg/m ³)
NFC	0	38	6.72	No replacement or additives
WSF	25	37	7.5	Replaced with normal sand (Mass)
WFS	50	36	6.13	Replaced with normal sand (Mass)
WFS	75	31.6	4.5	Replaced with normal sand (Mass)
WFS	100	28.7	3.4	Replaced with normal sand (Mass)
PO	10	31	8.9	Replaced to the mortar cube by (Volume)
PO	20	26.7	9.3	Replaced to the mortar cube by (Volume)
PO	30	22.3	10	Replaced to the mortar cube by (Volume)
RSTF	1	42.1	11	1% of the cement amount added (Mass)
SPs	1	40	8.7	1% of the cement amount added (Mass)

Flexural strength testing, specifically the four-point loading method, was carried out when the concrete samples reached 28 days of age to measure the modulus of rupture (f_r). This testing process was performed in strict compliance with the standards outlined in BS EN 12390-5 (2009). This standard procedure ensures that the measured strength reflects the material's capacity to resist failure under bending stresses, providing essential data for evaluating the structural integrity of the concrete.

5.3.7 Flexural Strength of Normal and Foamed Concrete

Figure 5-6 compares the applied load and deflections of two materials: a normal mortar prism (control) and a normal foamed concrete (NFC) prism. The greatest load that a normal mortar prism can withstand is 47 kN, while a normal foamed concrete prism can sustain a maximum load of 38 kN. The standard mortar prism can withstand a greater load before failing than the NFC prism,

specifically withstanding a 9 kN higher load than the NFC prism. This signifies that the typical mortar has a higher load-bearing capacity.

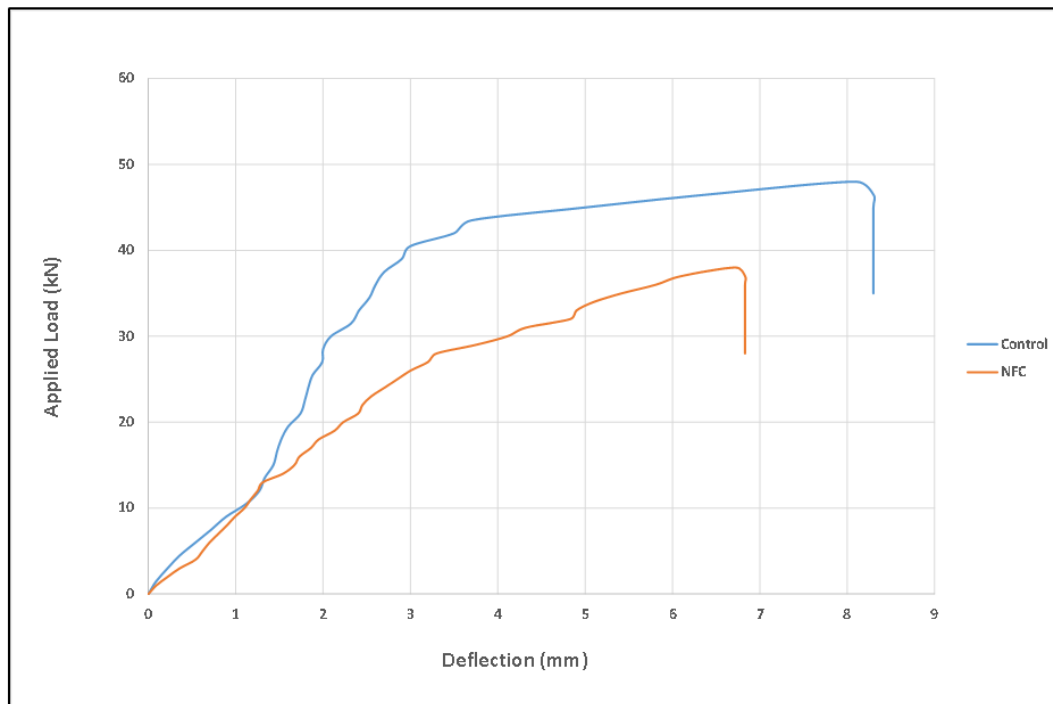


Figure 5-6: Applied Load versus Deflection for Control (Normal Mortar) and NFC Prisms

The normal mortar prism withstands a maximum load of 47 kN, which is 8.11% more than the NFC prism, which withstands a maximum load of 38 kN. This percentage indicates that the flexural strength of the normal mortar is superior to that of the NFC. The deflection recorded for the normal mortar prism under the maximum applied load is 8.1 mm. For the NFC prism, the deflection is 6.72 mm at the maximum applied load. Deflection measures how much the material bends or deforms under load. The control mortar prism shows a higher deflection compared to the NFC prism, suggesting that the normal mortar, while stronger in terms of load-bearing capacity, is also less stiff compared to the foamed concrete. Flexural strength is the material's ability to resist tension; the higher the tensile strength, the better the material can withstand applied load. Figure 5-6 detailed normal concrete mortar (control) and normal Foamed concrete (NFC).

According to the findings, the NFC prism displays lower stiffness compared to normal concrete mortar due to its lower density and the presence of numerous air bubbles. These air voids reduce the material's resistance to deformation, making foamed concrete less stiff. In contrast, normal

concrete mortar, with its higher density and fewer air voids, shows greater stiffness, meaning it resists deformation more effectively and will not bend or compress as much as foamed concrete. Foamed concrete tends to be less brittle than normal concrete mortar because the air voids within it provide some degree of cushioning, allowing the material to absorb and dissipate energy before breaking. This characteristic makes foamed concrete more ductile, enabling it to deform more before failure. In contrast, normal concrete mortar is generally more brittle; it can withstand high compressive loads, but when it fails, it does so suddenly and with little deformation, which is typical of brittle material.

5.3.8 Effect of Waste Foundry Sand (WFS)

The study examined the structural performance of foamed concrete samples with varying percentages of waste foundry sand (WFS) replacing normal sand, specifically at 25%, 50%, 75%, and 100%. According to Figure 5-7, the applied loads for these samples were recorded as 37 kN, 36 kN, 31.5 kN, and 28.7 kN, respectively, while the corresponding deflections were 7.5 mm, 6.13 mm, 4.5 mm, and 3.4 mm. These results are compared with both normal foamed concrete (NFC), which had an applied load of 38 kN and a deflection of 6.75 mm, and normal concrete mortar discussed earlier.

The sample with 100% waste foundry sand presented the highest brittleness, as it had the lowest load-bearing capacity (28.7 kN) and the smallest deflection (3.4 mm). This indicates that the material failed more suddenly compared to other samples, suggesting that a higher replacement of normal sand with WFS increases brittleness. Conversely, the sample with 25% WFS replacement was the least brittle, with the highest deflection (7.5 mm) and a load-bearing capacity close to that of NFC (37 kN vs. 38 kN). This implies that lower WFS content results in a more ductile material, which can deform more before failure.

The sample with 100% WFS replacement showed the greatest stiffness, as it exposed the smallest deflection (3.4 mm) under a load of 28.7 kN. Although this sample had a lower load-bearing capacity, its high stiffness indicates it deformed less under the applied load, meaning it is less flexible. In contrast, the 25% WFS replacement sample had the lowest stiffness, as indicated by the largest deflection (7.5 mm) under a similar load. This lower stiffness suggests a higher capacity to absorb energy before failure, making it more bent in the elastic zone compared to the samples with higher WFS content.

In terms of bending behaviour, the 25% WFS replacement sample demonstrated better performance, with a higher load-bearing capacity (37 kN) and greater deflection (7.5 mm) compared to the other WFS samples. This indicates a more favourable bending behaviour, where the sample could sustain a higher load while still undergoing significant deformation, which is beneficial for structures requiring some degree of plasticity under load. As the WFS content increased to 50%, 75%, and 100%, both the load-bearing capacity and deflection decreased, indicating a trend towards more brittle and stiffer behaviour with less favourable bending characteristics.

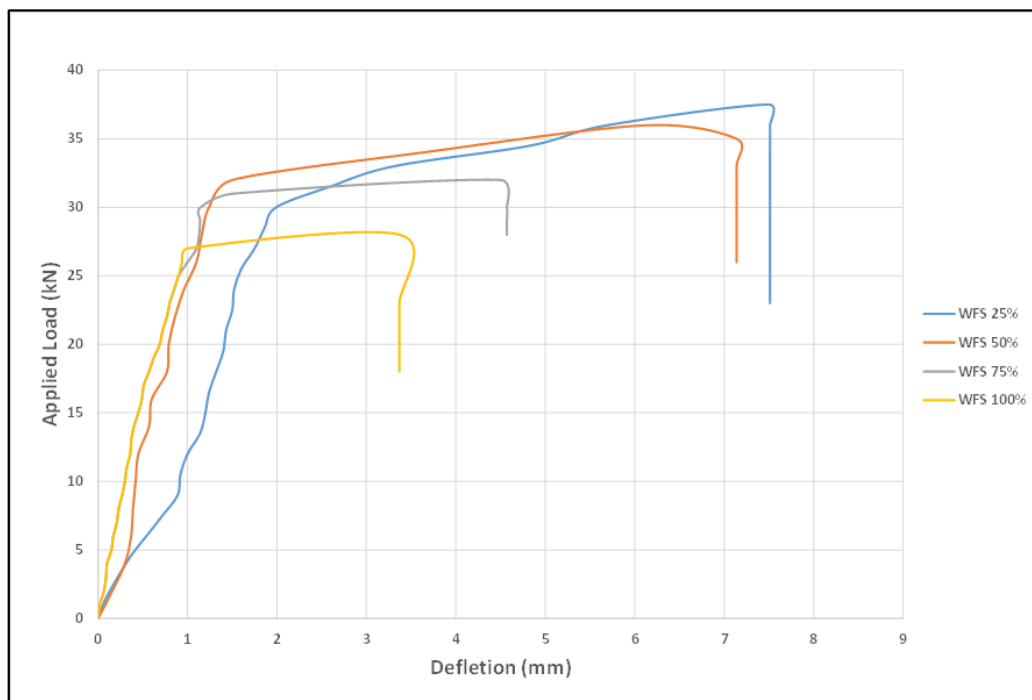


Figure 5-7: Maximum Applied Load versus Deflection for WFS Prisms

When compared to normal foamed concrete (NFC), which exhibited a load-bearing capacity of 38 kN and a deflection of 6.75 mm, the 25% WFS replacement sample performed similarly in load-bearing capacity (37 kN) but showed a higher deflection (7.5 mm), this suggests that the 25% WFS replacement offers a slightly more elastic alternative to NFC, even if with comparable strength.

In contrast to normal concrete mortar, which is stiffer and more brittle, all foamed concrete samples (including those with WFS) displayed greater elasticity and less stiffness, as indicated by their higher deflection values. The normal mortar would likely have a much lower deflection under similar loads but would also fail more suddenly due to its brittle nature. This comparison highlights

that even with increased WFS content, foamed concrete maintains a more favourable ductility than traditional mortar, though its stiffness and brittleness can be tuned by adjusting the WFS content. Additionally, the mixing process for concrete containing WFS presented some challenges. Samples with WFS cured more rapidly than normal foamed concrete and required an approximately 15% increase in water content.

5.3.9 Effect of Polystyrene

The structural performance of foamed concrete with varying polystyrene content, replacing the mortar mix by volume at levels of 10%, 20%, and 30%, reveals individual differences in mechanical properties. According to the finding in Figure 5-8, when subjected to applied loads of 31 kN, 26.7 kN, and 22.3 kN, respectively, the samples showed corresponding deflections of 8.9 mm, 9.3 mm, and 10 mm. These results offer insights into how the amount of polystyrene incorporated influences the material's brittleness, stiffness, and bending behaviour.

According to the findings, the foamed concrete becomes less brittle when the polystyrene content increases. The 30% polystyrene sample, despite having the lowest load-bearing capacity at 22.3 kN, displays the highest deflection of 10 mm. This indicates a more ductile nature, allowing more significant deformation before breaking, in contrast to the 10% polystyrene sample, which, with a higher load capacity of 31 kN and a deflection of 8.9 mm, is comparatively less ductile.

The increasing deflection from 8.9 mm at 10% to 10 mm at 30% polystyrene replacement suggests that the material becomes less stiff with higher polystyrene content. Although this increased elasticity can be advantageous in specific applications, it corresponds with a reduced ability to bear loads. The sample with 30% polystyrene content bends more under load, as evidenced by its highest deflection and lowest load-bearing capacity.

In contrast, the 10% polystyrene sample, with its higher load capacity and lower deflection, demonstrates a more balanced bending response, indicating it might be better suited for applications requiring a combination of strength and plasticity. For example, a concrete sample with 10% polystyrene by volume might sustain a load of 31 kN, but as the polystyrene content increases to 20% or 30%, the load it can support decreases, and the amount of deflection increases. This behaviour indicates that while polystyrene reduces the load-bearing capacity, it increases the material's ability to deform more under stress, which could be utilised to absorb impacts or vibrations in specific engineering applications.

Compared to normal foamed concrete (NFC), which had a load-bearing capacity of 38 kN and a deflection of 6.75 mm, the introduction of polystyrene clearly reduces both stiffness and strength. Even at 10% polystyrene replacement, there is a noticeable decrease in load capacity, though the material retains more flexibility. As polystyrene content increases to 30%, these effects become more pronounced, with a significant reduction in load-bearing capacity and a marked increase in deflection. The investigation into foamed concrete modified with 1% steel fibre (RSTF) and 1% superplasticiser (SPs) revealed notable differences in mechanical performance

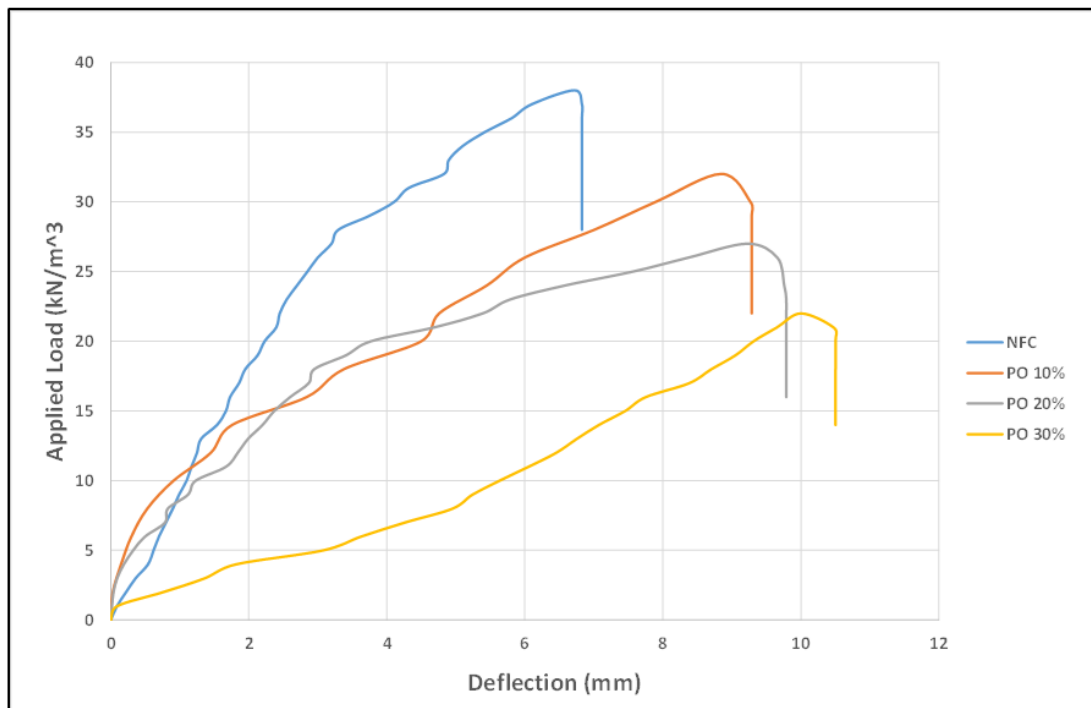


Figure 5-8: Maximum Load and Deflection of Prisms with Different Polystyrene Ratios

As figure 5-9 revealed the samples demonstrated applied loads of 42.1 kN and 40 kN for the superplasticizer and steel fibre respectively, while the deflections were recorded as 11 mm and 8.7 mm. These results were compared against normal foamed concrete (NFC), normal mortar (control), as well as findings from studies incorporating waste foundry sand (WFS) and polystyrene.

The inclusion of superplasticizer resulted in a less brittle material, demonstrated by its higher deflection and greater load-bearing capacity (42.1 kN and 11 mm). The concrete became more ductile, allowing for greater deformation before failure. In contrast, the steel fibre modification, while still reducing brittleness compared to NFC, showed a lower deflection (8.7 mm) and slightly

lower load-bearing capacity (40 kN), indicating increased stiffness and a reduction in elasticity compared to the superplasticizer-modified concrete.

Regarding bending behaviour, the superplasticizer-modified sample presented better plasticity, bending more under load while maintaining a high load-bearing capacity. The addition of steel fibre, on the other hand, provided enhanced stiffness, making it ideal for applications where resistance to deformation is critical. However, it was slightly less elastic than the superplasticizer-enhanced mix. When compared to normal foamed concrete, both superplasticiser and steel fibre additives improved performance, with the superplasticiser offering the best balance of strength and plasticity.

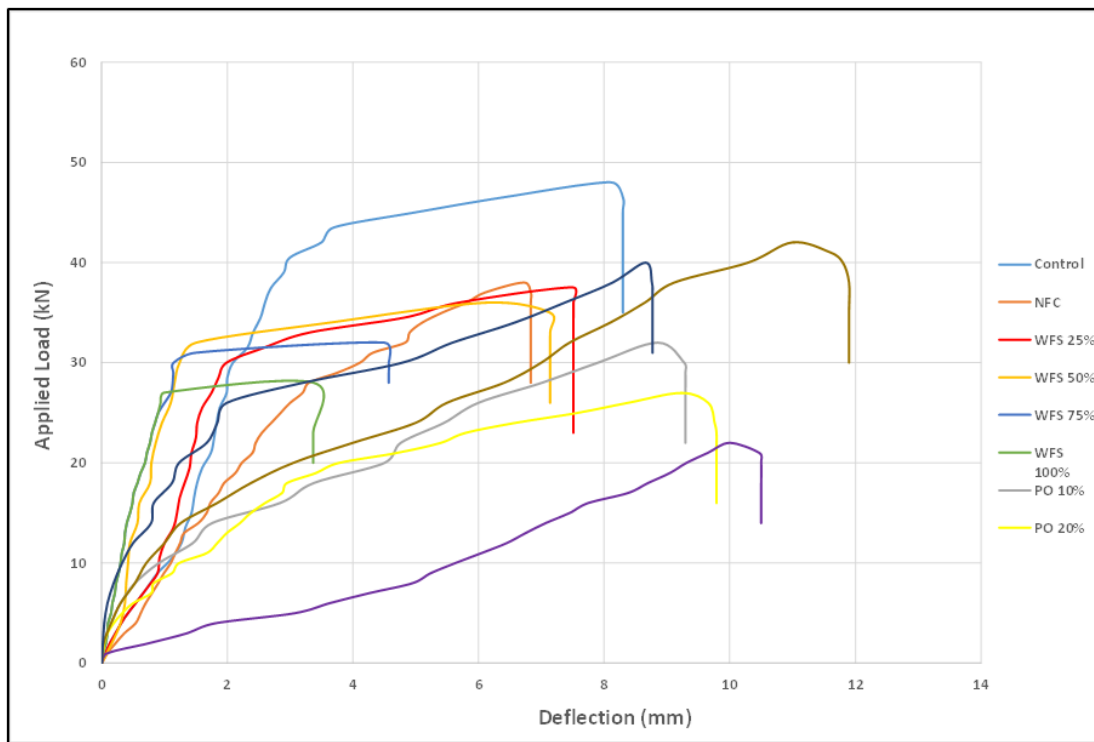


Figure 5-9: Applied Load versus Deflection for All Prisms

5.3.10 Relationship Between Compressive and Flexural Strength

The comparison between the flexural and compressive strengths of foamed concrete cubes (100x100x100 mm) and prisms (100x100x500 mm) provides valuable insights into the mechanical performance of different material compositions. The samples include foamed concrete with varying percentages of polystyrene replacement, waste foundry sand (WFS) replacement, recycled steel tyre fibre addition, and superplasticiser enhancement. The compressive and flexural strengths

of these various samples offer a clear perspective on how each modification impacts the overall strength characteristics of the foamed concrete. Tables 5-5 explain the relationship between compressive strength and flexural strength for all the materials tested in the current experiment.

Table 5-5: Compressive and Flexural Strength Calculations for Cubes and Prisms

Concrete Design	Material Replacement or Addition	Average Compressive Strength (MPa)	Average Flexural Strength (MPa)	Note
Concrete type	(%)	Density 1400, (kg/m ³)	Density 1400, (kg/m ³)	Description
Control	0	31.1	3.91	Normal mortar density = 2160, (kg/m ³)
NFC	0	15.7	1.98	Normal Foamed concrete
WSF	25	15.11	1.95	Replaced with normal sand (Mass)
WFS	50	13.91	1.87	Replaced with normal sand (Mass)
WFS	75	11.15	1.67	Replaced with normal sand (Mass)
WFS	100	6.1	1.24	Replaced with normal sand (Mass)
PO	10	10.33	1.61	Replaced with the mortar cube by (Volume)
PO	20	9.83	1.57	Replaced with the mortar cube by (Volume)
PO	30	5.61	1.19	Replaced the mortar cube by (Volume)
RSTF	1	16.12	2	1% of the cement amount added (Mass)
SPs	1	19.4	2.21	1% of the cement amount added (Mass)

For foamed concrete containing 10%, 20%, and 30% polystyrene by volume, the compressive strengths were recorded as 10.33 MPa, 9.83 MPa, and 5.61 MPa, respectively. Correspondingly, the flexural strengths were 1.61 MPa, 1.57 MPa, and 1.19 MPa. As the percentage of polystyrene increases, both compressive and flexural strengths decrease. The reduction in compressive strength is more pronounced, with the 30% polystyrene sample showing a nearly 45% decrease in strength compared to the 10% sample. The decrease in strength with increased polystyrene is likely due to the lower density and higher air content within the matrix, which reduces the material's ability to resist both compressive and tensile stresses.

In the case of waste foundry sand replacing normal sand at 25%, 50%, 75%, and 100%, the compressive strengths observed were 15.11 MPa, 13.91 MPa, 11.15 MPa, and 6.1 MPa, respectively. These values indicate in Figure 5-10 a steady decline in compressive strength as the

percentage of WFS increases, similar to the curve seen with polystyrene replacement. However, the compressive strength of the sample with 25% WFS replacement (15.11 MPa) is significantly higher than that of any polystyrene-replaced sample, indicating that partial replacement of normal sand with WFS may still produce a relatively firm material, though the strength decreases substantially as WFS content increases. This suggests that WFS has a less detrimental effect on compressive strength compared to polystyrene but still leads to weaker materials at higher replacement levels.

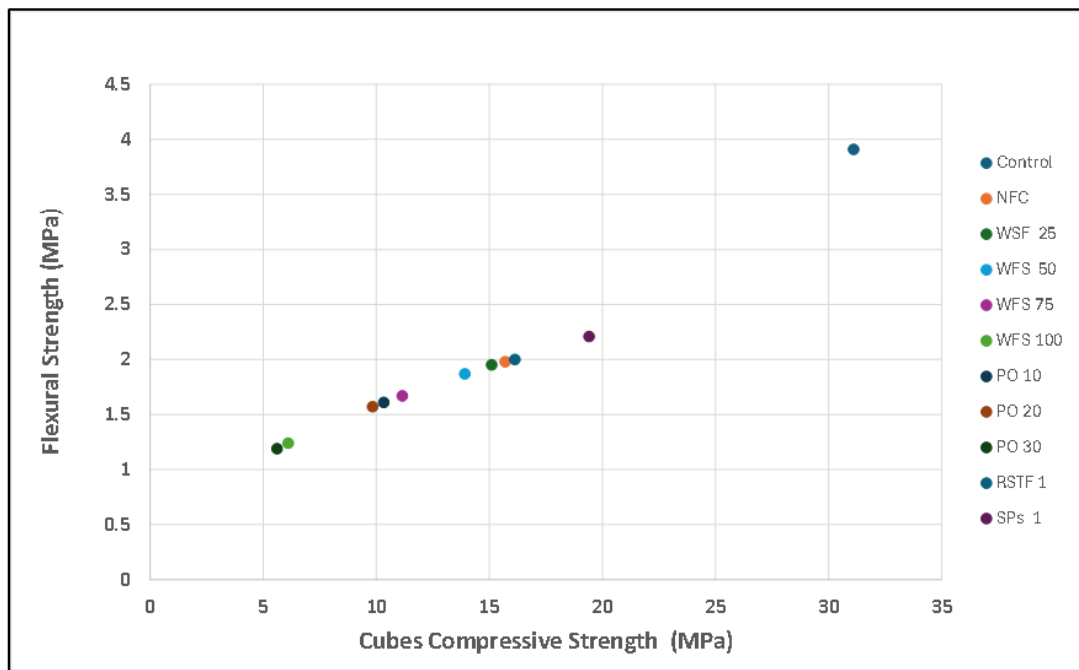


Figure 5-10: Relationship Between Compressive Strength and Flexural Strength

For samples containing 1% recycled steel tyre fibre by weight of cement, the compressive strength was measured at 16.12 MPa, and the flexural strength at 2 MPa. Including steel fibres significantly enhances the flexural strength compared to the polystyrene and WFS samples, highlighting the fiber's ability to improve the material's resistance to tensile stresses and cracking. The compressive strength is also improved, indicating that the fibres help maintain the matrix's integrity under compressive loads, likely by bridging micro-cracks and preventing their propagation. This combination of high compressive and flexural strength makes steel fibre-reinforced foamed concrete a promising option for applications where both types of strength are critical.

Using a superplasticiser (1% by weight of cement) resulted in the highest recorded compressive strength of 19.4 MPa and flexural strength of 2.21 MPa, as seen in Figure 5-10. The superplasticiser enhances the workability and compaction of the foamed concrete mix, resulting in a denser and more homogeneous material. This improvement in density likely contributes to the superior compressive strength observed. Additionally, the increased flexural strength indicates that the superplasticiser not only aids in compressive load-bearing capacity but also enhances the material's tensile strength, making it more resilient under bending loads.

When comparing these results, it is evident that the type of material modification significantly influences both compressive and flexural strengths. Polystyrene replacement leads to the most substantial reduction in both types of strength, particularly at higher replacement levels. Waste foundry sand replacement also reduces strength but less drastically than polystyrene, especially at lower replacement levels. In contrast, the addition of recycled steel tyre fibres and superplasticisers significantly enhances both compressive and flexural strengths, with the superplasticiser showing the most evident improvement.

5.3.11 Cracks Propagation

This section examines the crack propagation characteristics of concrete samples containing recycled materials, specifically focusing on those with 20% to 100% waste foundry sand (WFS). The similarity in crack patterns across these samples is recognised as poor bonding between the foundry sand aggregates and the cement paste. This weak bond, possibly due to the physical properties of the waste foundry sand, such as its grain texture and shape, critically undermines the structural integrity of the concrete.

During preparation, these mixtures waste foundry sand and require about 15% more water than standard mixes. This increased water content worsens bonding issues by increasing porosity and reducing the density of the cement paste, leading to enhanced susceptibility to cracking. The additional water also promoted higher shrinkage rates during drying and curing, contributing further to cracking and debonding. These challenges suggest a systemic issue related to material compatibility and mix proportioning that necessitates comprehensive investigation.

Microscopic examinations post-testing revealed interfacial debonding and microcracks, particularly around aggregates, acknowledging the bonding difficulties. The increased water content required by the mixtures not only heightened porosity but also decreased the cement paste

density, thus weakening the overall structure. The higher shrinkage rates during drying and curing, encouraged by the additional water, further worsened the propensity for cracking and debonding. Adjustments such as modifying particle size distribution or improving adhesion through additives might mitigate these problems.

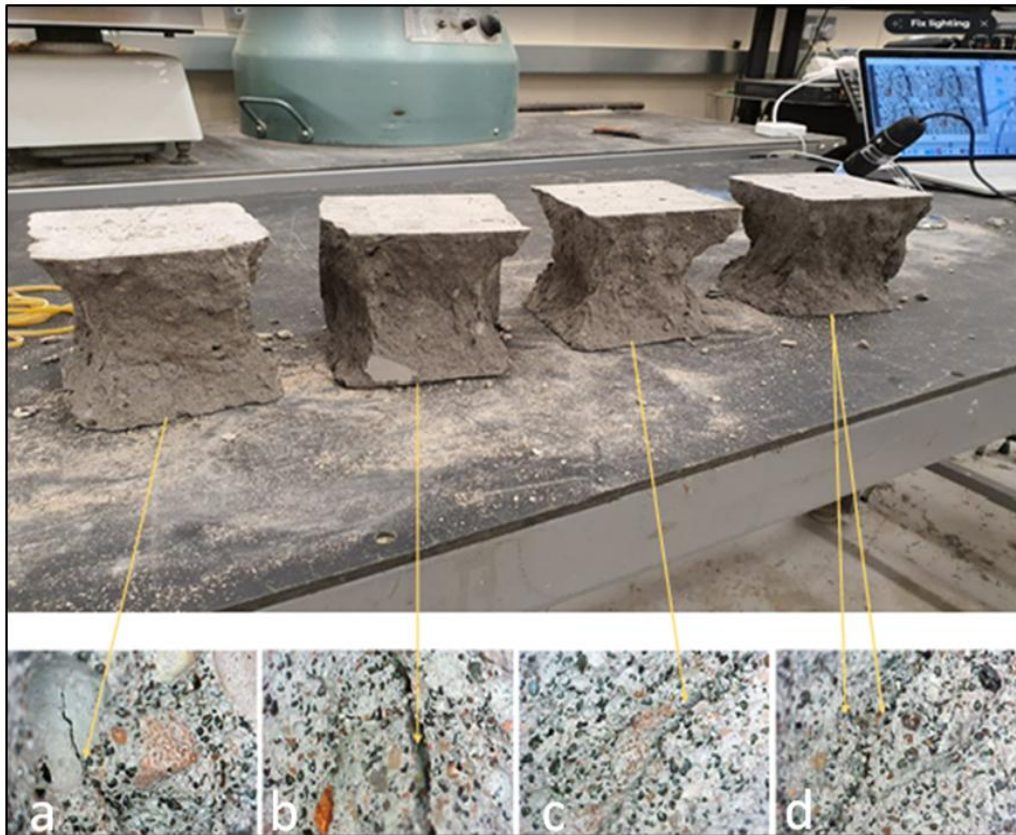


Figure 5-11: Mixture Components with Foundry Waste Sand – (a) 25%, (b) 50%, (c) 75%, (d) 100%

For instance, using finer particles or incorporating bonding agents could enhance the compatibility between the WFS aggregates and the cement paste, thereby reducing the formation of microcracks and improving the overall durability of the concrete.

Although water infiltration is identified as a potential factor weakening the concrete, the direct link between the use of recycled materials and observed failures remains unconfirmed. The presence of water can lead to increased internal stresses and further cracking, but the specific role of WFS in this process requires more detailed analysis. Understanding the interaction between water and recycled aggregates is crucial for developing more resilient concrete mixtures.

The microscopic examination of the samples, as illustrated in Figure 5-11, highlights significant issues with the use of polystyrene in concrete. The images reveal interfacial debonding at the points where recycled materials meet the mortar paste, characterised by micro-cracks and voids. These defects are particularly exacerbated by direct axial forces during testing, compromising the structural integrity of the concrete. The presence of voids and cracks around the polystyrene particles highlights the challenges of incorporating such materials into concrete, especially without adequate surface treatment or bonding agents.

In contrast, samples containing 1% recycled steel tyre fibre (RSTF) displayed superior crack resistance, as seen in Figure 5-12.



Figure 5-12: The Components of the Mixture: (e) Recycled Steel Tyre Fibre, (f) Polystyrene

The steel fibres serve as effective reinforcement, preventing the progression of cracks within the concrete matrix. This reinforcement mechanism significantly enhances the ductility of the samples under both compressive and flexural stresses. The RSTF aids in evenly distributing the load throughout the concrete, thereby reducing the formation of stress concentrations that typically lead to cracking.

On the other hand, concrete samples containing polystyrene show different behaviour. These samples tend to form cracks at the sites where polystyrene particles are embedded, primarily due to the weak interfacial bonding between the polystyrene and the cement paste. This weak bond fails to effectively transfer stress across the composite material, causing the polystyrene particles to act as stress concentrators rather than load distributors, which in turn initiates and propagates cracks. Incorporating recycled steel and rubber tyre fibres can lead to complex behaviour in flexural strength. Steel fibres improve tensile strength and toughness, allowing the concrete to sustain more considerable deflections before failure. Rubber fibres can improve impact resistance and energy absorption, resulting in concrete that has high flexural strength and ductility (Pilakoutas, Neocleous, and Tlemat, 2004).

Lightweight materials, including waste foundry sand, foamed concrete, and polystyrene-containing concrete, are designed to minimise the weight of the slabs. Adding air bubbles to foamed concrete makes it much less dense but also more brittle and weaker in tension due to the lack of aggregate to fill the gaps. Polystyrene beads, lacking the same load-bearing network as regular aggregates, produce a material that cannot handle tensile stresses and is more likely to break, although they make the structure lighter (Shi et al., 2016).

5.4 Proposed Sample Selection for Further Investigation

Chapter 5 identifies a range of material combinations that demonstrate both desirable mechanical properties and reduced density, making them ideal candidates for the development of solar walkable slab bases. These materials have been selected not only for their performance but also for their environmental and economic advantages, as outlined below:

1. 50% Waste Foundry Sand (WFS):

The replacement of normal sand with 50% waste foundry sand offers a sustainable alternative that maintains adequate compressive and flexural strength. Waste foundry sand, a byproduct of industrial processes, contributes to environmental sustainability by diverting waste from landfills. From an economic perspective, it provides a cost-efficient substitute for conventional aggregates, reducing material costs while maintaining mechanical performance.

2. 10% Polystyrene (PO):

Polystyrene, incorporated at a 10% replacement level, effectively reduces the density of the concrete mix while maintaining sufficient compressive strength. As a lightweight material,

polystyrene enhances ease of handling and installation. Environmentally, the use of recycled polystyrene contributes to reducing plastic waste. Its integration also lowers the demand for traditional, high-density aggregates, thereby providing an economical solution for lightweight concrete production.

3. 1% Recycled Steel Tyre Fibre (RSTF):

The addition of 1% recycled steel tyre fibre significantly improves both the compressive and flexural strength of the concrete. This reinforcement enhances the slab's toughness and durability while utilizing a recycled material, which aids in reducing waste from discarded tyres. The economic benefit of this material lies in its low cost relative to traditional reinforcing fibres, providing a sustainable and financially viable reinforcement option.

4. 1% Superplasticiser (SP):

Superplasticisers play a critical role in improving the concrete mix's workability while increasing compressive and flexural strength. By reducing the water-cement ratio, superplasticisers create a denser, more compact concrete without compromising its lightweight characteristics. This additive optimises material use and enhances durability, contributing to both environmental sustainability and cost-effectiveness by reducing the overall amount of cement required.

These proposed material combinations will undergo further investigation to assess their suitability for the solar walkable slab base. Each combination offers a unique balance of mechanical strength, reduced density, and environmental and economic advantages. The final material selection will prioritise not only the structural integrity and lightweight properties of the slab but also its contribution to sustainable construction practices and overall cost-efficiency.

5.5 Summary

This analysis evaluates concrete cubes with various additives and recycled materials for their flexural and compressive strengths. The impact of density, additives, and recycled materials on foamed concrete's mechanical properties. Key findings are:

1. **Compressive Strength Analysis of Foamed Concrete:** Normal foamed concrete has a higher load-bearing capacity than lightweight ones. Concrete with additives like Waste Foundry Sand (WFS) and Polystyrene (PO) shows varying compressive strengths, with lower recycled material percentages demonstrating stronger compressive strengths.

2. **Influence of Recycled Materials on Compressive Strength:** Adding recycled materials impacts mechanical properties. Lower WFS percentages improve strength, but higher percentages reduce it. Small polystyrene inclusion boosts strength, while higher levels decrease it due to poor bonding and increased air voids.
3. **Density and Strength Correlation in Foamed Concrete:** Higher densities yield stronger concrete, indicating density is crucial for determining foamed concrete's mechanical properties.
4. **Effects of Additives on Foamed Concrete:** Superplasticisers and recycled steel tyre fibres enhance compressive and flexural strengths. Superplasticisers improve strength by reducing the water-cement ratio, and steel fibres distribute stresses evenly.
5. **Impact of Recycled Materials on Concrete's Structural Integrity:** Recycled materials reduce concrete's density and strength due to poor bonding and increased porosity, but moderate replacements can maintain acceptable strength and support sustainable construction practices.
6. **Flexural Strength:** Flexural strength tests show normal mortar prisms outperform foamed concrete prisms. Lower WFS content improves ductility, while higher content leads to brittleness. Polystyrene reduces flexural strength but increases ductility.
7. **Crack Propagation:** Recycled materials impact crack propagation. Poor WFS bonding increases cracking, steel fibres enhance ductility, and polystyrene increases crack formation

Chapter 6: Design and Development of Solar Slab Prototype

6.1 Introduction

The design and building of the solar pavement slab involve a detailed and methodical process of material selection, precise cutting, and careful assembly to ensure a functional and durable product. Prior to using the actual material to build the prototype, testing of the design ideas has been done using a mock-up from foam that product designers commonly use to experiment with design features and dimensions. The CAD drawing, shown in Figure 6-1, serves as the blueprint for the solar slab base, with dimensions set at 400x400x50 mm. This CAD model guides the creation of the trial prototype, which is made from grey foam rather than concrete, allowing for initial testing and evaluation of the design before manufacturing final products. The dimensions and the selection of features came following a product design evaluation of the solar area and space needed for the electronics, as well as the matching process to standard products in the market.

Acrylic glass and grey foam as a slab base are key materials used in this trial model. Acrylic glass is selected for the top layer due to its high mechanical strength, UV resistance, and transparency, which ensures both protection and functionality. Solar cells, typically made from monocrystalline silicon for their high efficiency and good temperature tolerance, are integrated into the slab design. The trial model construction process begins with the preparation and laser-cutting of acrylic glass panels to precise dimensions, as specified in the CAD drawing, ensuring accurate assembly.

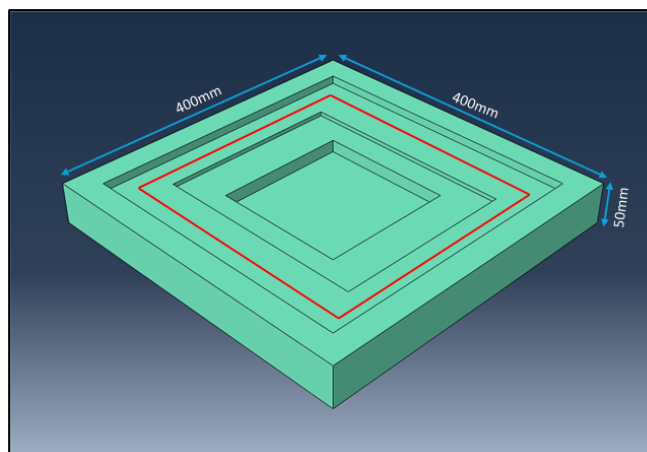


Figure 6-1: Base Design of the Prototype Solar Slab

In this design, grey foam is used to replicate the solar slab base, with specific elements cut out to house the electrical components. Solar cells and other electrical components, including LED lights, batteries, light sensors and controllers, are then carefully positioned within cavities created in the foam base. The prototype's performance will be assessed based on this trial model, and if successful, the process will proceed with a concrete-based final design. Otherwise, design modifications will be made until the final solution is optimised.

6.2 Solar Pavement Slab Trial Assembly Diagram

The provided solar walkable pavement trial sample made with a grey foam base diagram represents an integrated system combining a solar-powered lighting and monitoring setup embedded within a grey foam base. The schematic outlines the connections and components used to ensure the system's functionality, along with images showcasing the fabrication, testing, and performance of the solar walkable pavement trial sample made with a grey foam base.

1. **Solar Panel and Power Supply:** At the core of the system is a solar panel responsible for harnessing solar energy to power the entire setup. This solar panel is connected to a charging regulator, which controls the flow of energy and prevents overcharging of the battery. The battery acts as an energy storage unit, ensuring that the system remains operational during periods of low sunlight or at night.
2. **Microcontroller and Sensors:** A microcontroller is incorporated into the system to manage various electronic components and automate processes. It serves as the control hub, processing inputs from sensors and managing the output to devices like LED lights. The LED sensor depicted in the diagram monitors environmental conditions, such as light levels, ensuring that the lighting system operates efficiently and conserves power.
3. **LED Lighting System:** The LED strip light is embedded around the solar walkable pavement trial sample made with a grey foam base, providing illumination when needed. This component is particularly useful in enhancing the visibility of pedestrian pathways or solar pavements during low-light conditions. The wiring connections illustrated in the diagram demonstrate how the components work together, with red lines representing the power supply and blue lines representing data or sensor connections.
4. **Assembly and Testing:** The images below the schematic provide a practical context for the solar walkable pavement trial sample made with a grey foam base. The first image shows a researcher

assembling and configuring the electronic components within the foam base. The second image displays the completed solar walkable pavement trial sample made with a grey foam base and illuminated LED strip lights, indicating a successful assembly and operational system. The third image captures the solar walkable pavement trial sample made with a grey foam base installed outdoors during nighttime, with the LED lights activated, demonstrating its functionality in real-world conditions. Figure 6-2 illustrates a schematic diagram of devices installed within the solar slab.



Figure 6-2: Schematic Diagram of Devices Installed Within the Trial Sample Made with Grey Foam Base

5. Trial Sample Evaluation and Future Steps: This solar walkable pavement trial sample made with a grey foam base is primarily an experimental prototype designed to demonstrate the functionality of the system. It serves as an example of how the integrated components work together. The trial aims to assess the performance in terms of energy efficiency, battery level sustainability, solar radiation absorption, LED light brightness, and sensor functionality. If the performance proves satisfactory during this phase, the next step would involve manufacturing a final prototype using a lightweight concrete base, which will then be installed for practical application.

Overall, this solar walkable pavement trial sample made with a grey foam base diagram illustrates an innovative approach to integrating renewable energy, lighting, and monitoring systems within a concrete or foam-based slab. It highlights the potential for enhancing the functionality and sustainability of construction materials, particularly for pedestrian pavements and solar walkways.

The system's design emphasises energy efficiency, automation, and safety, showcasing the future of smart and sustainable construction technologies. to integrating renewable energy, lighting, and monitoring systems within a concrete or foam-based slab. It highlights the potential for enhancing the functionality and sustainability of construction materials, particularly for pedestrian pavements and solar walkways. The system's design emphasises energy efficiency, automation, and safety, showcasing the future of smart and sustainable construction technologies.

6.3 Trail Prototype Design and Fabrication

The solar slab design began with a grey foam trail model produced to demonstrate the slab's structural framework, monitor the integration of electrical components, and evaluate aesthetic considerations. This model served as a foundation for refining the overall system before transitioning to a fully functional prototype. The two key phases of this design process—developing design requirements and creating the component system—ensured that the final design would meet both practical and visual expectations.

6.3.1 Component System Design

The grey foam model provided insight into the key design features, including structural integrity and material selection. It facilitated an understanding of the slab's mechanical load capacity, durability, and aesthetic fit for urban environments. This phase also allowed us to test the integration of photovoltaic technology, ensuring that energy efficiency and material performance align with the slab's design requirements. The next chapter will involve creating an actual prototype that mirrors these design principles with real materials.

6.3.2 Electrical Requirements

In the grey foam model, the placement and configuration of the electrical components were simulated, including LED strip lights, batteries, converters, and sensors. This allowed the researcher to ensure proper spacing, protection, and integration of these components within the slab's cavities, testing their interaction without yet incorporating real materials. Key challenges such as waterproofing and acrylic plastic cover to stand pedestrians were addressed in the model to guide future prototype development. The next phase will involve transferring these electrical configurations to a fully operational system in the actual prototype using the concrete-based material.

6.3.3 Electrical System Design

The grey foam model allowed for testing the basic layout of the electrical connections, ensuring that the internal hardware could be arranged effectively. This stage confirmed the compatibility of the photovoltaic cells, LED lights, and other components, although no real electrical functionality was tested at this stage. The upcoming chapter will focus on translating these designs into a working prototype with operational photovoltaic cells, real connections, and fully functioning components.

6.3.3.1 Photovoltaic Cell Selection

As the focus of this thesis is on the structural design of the panel, it was decided that the electrical system would use conventional high-efficiency components and allow for future testing of additional solar technologies in solar road panel applications. Monocrystalline silicon photovoltaic cells are chosen and are available in a variety of sizes to meet various needs in custom OEM products. The typical size used in utility power generation applications is 150-mm square solar cells, as these can be produced efficiently with relatively high energy conversion rates.

The Colossal 6V 9W Solar Panel has been used in this research, and it is designed to deliver efficient power generation for various applications. With a power output of 9 watts and an operating voltage of 6 volts, it provides a current of 1.5 amps, making it suitable for charging small devices and supporting portable electronics. Typically constructed from monocrystalline or polycrystalline silicon, the panel boasts an efficiency range of 15% to 20%. It is compact and lightweight, with dimensions of approximately 10 x 8.8 inches (254 x 223.5mm), making it easy to transport and install. Figure 6-3 is an example of the solar panel used in this project. It is built to endure diverse environmental conditions, often featuring an aluminium frame for durability and ease of mounting. The panel can operate in temperatures ranging from -40°C to +85°C, ensuring functionality in various climates. Equipped with junction boxes and standard connectors like MC4, it integrates seamlessly with other solar components.

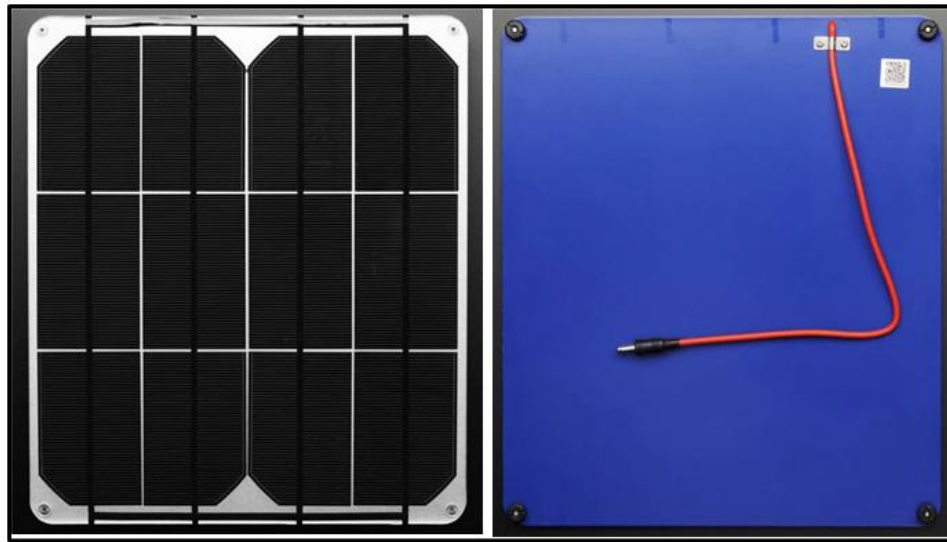


Figure 6-3: Selected Solar Panel for the Prototype

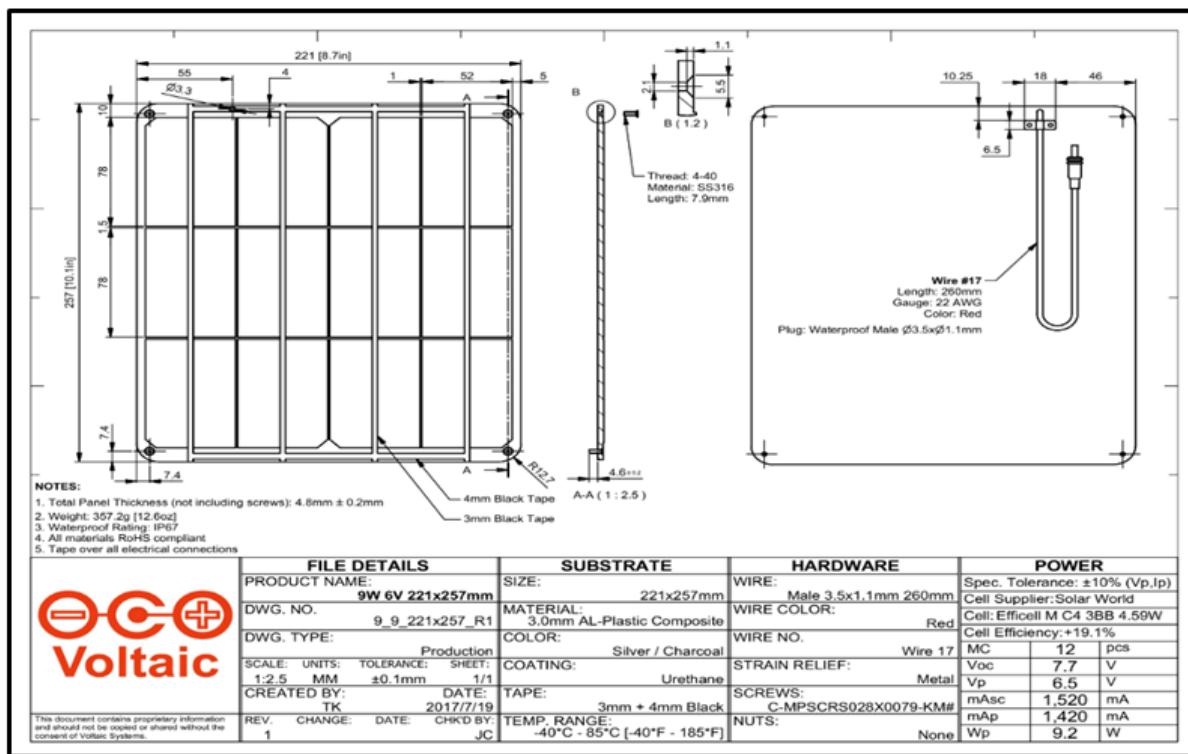


Figure 6-4: Solar Panel and Its Specifications, Voltaic Systems (2017)

The panel is ideal for outdoor activities, remote monitoring systems, and educational projects. Its warranty period can vary, reflecting the manufacturer's confidence in its longevity and performance. Consulting the manufacturer's datasheet is recommended for precise performance

metrics under different conditions. Figure 6-4 details the dimensions of the solar cell selected for this project, illustrated with all of the specified details.

6.3.3.2 Internal Hardware

The solar pavement slab is being developed as a self-contained, energy-efficient lighting solution integrated with several advanced devices. Beneath the slab, an Adafruit Universal USB / DC / Solar Lithium Ion/Polymer Charger (bq24074) manages solar energy harvested by the Colossal 6V 9W Solar Panel. This energy is stored in an RS PRO 3.7V Lithium-Ion Rechargeable Battery Pack (7.8Ah) for nighttime use. The system is controlled by an Adafruit Trinket 3.3V MCU Development Board, which monitors the battery and manages power distribution. A mini PIR sensor detects motion in the dark, triggering a 3V Bright White LED Strip (30 cm x 4) to illuminate the area. At dawn, the sensor turns off the LEDs to conserve power. This innovative integration ensures the pavement slab operates autonomously, providing reliable, eco-friendly lighting. Detailed explanations and images of each component will be provided in the following section, showcasing the innovative design and functionality of this self-contained solar pavement slab.

6.3.3.3 RS PRO 3.7V Lithium-Ion Rechargeable Battery Pack, 7.8Ah

The RS PRO 3.7V Lithium-Ion Rechargeable Battery Pack (7.8Ah) plays a crucial role in solar power assembly by serving as the primary energy storage component. It stores the electrical energy generated by the Colossal 6V 9W Solar Panel during the day, providing a stable 3.7V output to power devices like the 3V Bright White LED strip at night or during periods without sunlight. With a capacity of 7.8Ah, it ensures sufficient energy availability, supporting prolonged usage of connected devices. The battery pack features built-in protection circuits to prevent overcharging, over-discharging, and short circuits, ensuring safe and reliable operation. Its compatibility with the Adafruit bq24074 charger allows efficient and regulated charging. Additionally, the high energy density, long cycle life, and low self-discharge rate of lithium-ion technology ensure the battery's effectiveness and longevity, making it an essential component for maintaining continuous and reliable power in the solar power system.

6.3.3.4 Solar Lithium Charger

The Adafruit Universal USB / DC / Solar Lithium Ion/Polymer Charger (bq24074) plays a critical role in managing the power flow within the solar pavement slab system. Its primary function is to efficiently convert and regulate the energy harvested from various input sources, including USB,

DC, and solar panels, to charge lithium-ion or lithium-polymer batteries. The charger can accept input from multiple sources, making it versatile and adaptable. Its Maximum Power Point Tracking (MPPT) technology optimises the power output from the solar panel by continuously adjusting the load to ensure it operates at its maximum efficiency. This ensures the solar panel provides the highest possible power output under varying sunlight conditions.

In the context of the solar pavement slab, the bq24074 charger ensures that energy harvested from the solar panel is efficiently converted and stored in the RS PRO 3.7V Lithium-Ion Rechargeable Battery Pack (7.8Ah). It maintains optimal battery health and performance through its advanced charging and protection features. The charger includes various safety features such as over-voltage protection, under-voltage protection, over-current protection, and thermal regulation, preventing damage to the battery and connected devices. Managing power paths ensures that the battery is charged while simultaneously powering the LED strip and other components, thereby supporting the autonomous and efficient operation of the solar pavement slab system. The status indicator LEDs provide visual feedback on the charging process and operational state, aiding in monitoring and troubleshooting. Figure 6-5 illustrates the Solar Lithium Charger and Lithium-Ion Rechargeable Battery.

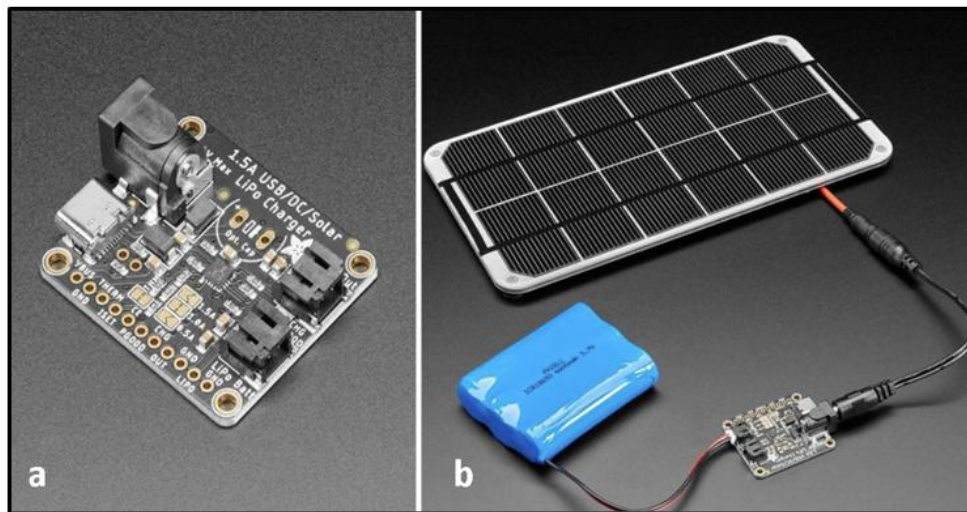


Figure 6-5: (a) Solar Lithium Charger, (b) Lithium-Ion Rechargeable Battery (RS Components Ltd., 2023)

6.3.3.5 Adafruit Trinket 3.3V

The Adafruit Trinket 3.3V MCU Development Board (product ID: 1500) is a compact, low-cost microcontroller designed to add programmable control to various electronic projects. Powered by the ATtiny85 microcontroller, it operates at 8 MHz and features 8 KB of flash memory, 512 bytes of SRAM, and 512 bytes of EEPROM. With five general-purpose I/O pins for digital input/output, analogue input, and PWM output, the Trinket can interface with a wide range of sensors and components. It runs on 3.3V, making it suitable for low-power projects, and can be powered via USB or an external battery. The built-in USB bootloader allows for easy programming directly from a computer using the Arduino IDE, making it accessible for beginners. In the context of a solar power system, the Trinket can monitor battery voltage, track charging status, manage power distribution, log data, and automate tasks, enhancing the system's efficiency and functionality by ensuring optimal power usage and reliable operation. See Figure 6-6 indicates Adafruit Trinket 3.3V MCU.

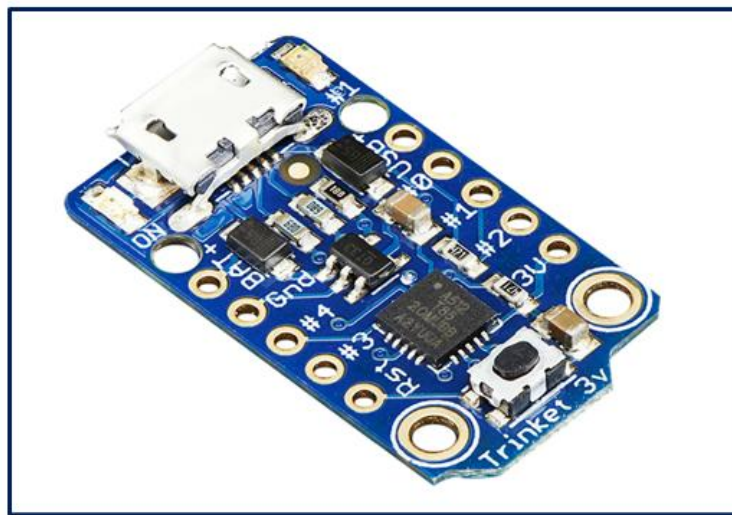


Figure 6-6: Adafruit Trinket 3.3V MCU (RS Components Ltd., 2023)

The Adafruit Trinket 3.3V MCU Development Board is suitable for the solar power assembly involving the Colossal 6V 9W Solar Panel, Adafruit bq24074 charger, and the RS PRO 3.7V Lithium-Ion Rechargeable Battery Pack. The Trinket can perform several critical functions to ensure the system operates efficiently and effectively. It can monitor the battery voltage using its analogue input, track the charging status through the bq24074 charger's status indicators, and manage power distribution to the LED strip and other connected devices. Additionally, it can log

data such as solar panel output and battery charge cycles, which can be used to optimise the system's performance. The Trinket can also automate tasks, such as turning the LED strip on at dusk and off at dawn, based on the battery's state of charge and solar power availability. Its compact size, low power consumption, and compatibility with the Arduino IDE make it an ideal choice for integrating programmable control into this solar power assembly.

6.3.3.6 LED Strip Light

The 3 Volt Bright White LED Strip, comprising four 30cm pieces from Layouts4u, serves as the primary lighting source for the solar pavement slab system. Located at 38 Elwyndene Road, March, PE15 9BL, these LED strips provide bright, energy-efficient illumination, enhancing visibility and safety during nighttime or low-light conditions. Operating at 3 volts, they are highly efficient and consume significantly less power compared to traditional lighting solutions, making them ideal for a solar-powered system where energy conservation is crucial.

Each LED strip's modular design allows for flexible installation, providing uniform lighting over a larger area or concentrated lighting in specific sections of the pavement slab. Their durability ensures they can withstand various environmental conditions, making them suitable for outdoor installations and reducing the need for frequent replacements. These LED strips are easy to integrate into the solar power system, connecting seamlessly with the Adafruit Trinket 3.3V MCU Development Board, which controls their operation based on input from a mini-PIR sensor and the available power from the battery pack. Automated to turn on when motion is detected in darkness and off when daylight appears, these LED strips maximise energy efficiency and ensure lighting is available only when needed, enhancing both the functionality and aesthetic appeal of the solar pavement slab.

6.3.3.7 Mini PIR Sensor

The Mini PIR (Passive Infrared) Sensor plays an essential role in the solar pavement slab assembly, offering both motion detection and intelligent control of the LED lighting system. Its primary functions are designed to ensure that the lights are used efficiently, which not only conserves energy but also enhances the safety of the illuminated area. By detecting movement within its range, the sensor triggers the LED lights to turn on only when there is activity nearby, ensuring that illumination is provided precisely when needed.

Integrated with the system's light level detection capabilities, the Mini PIR Sensor also helps differentiate between day and night. As daylight fades, the sensor readies the LED lights for activation. When motion is detected in darkness, it sends a signal to the Adafruit Trinket 3.3V MCU Development Board, which then turns on the LED lights. These lights remain on as long as motion is detected and ambient light levels are low. This intelligent automation ensures that the lights operate only during necessary periods, thereby conserving the stored energy in the RS PRO 3.7V Lithium-Ion Rechargeable Battery Pack for use throughout the night. See Figure 6-7 for the LED Strip light and Mini PIR Sensor.

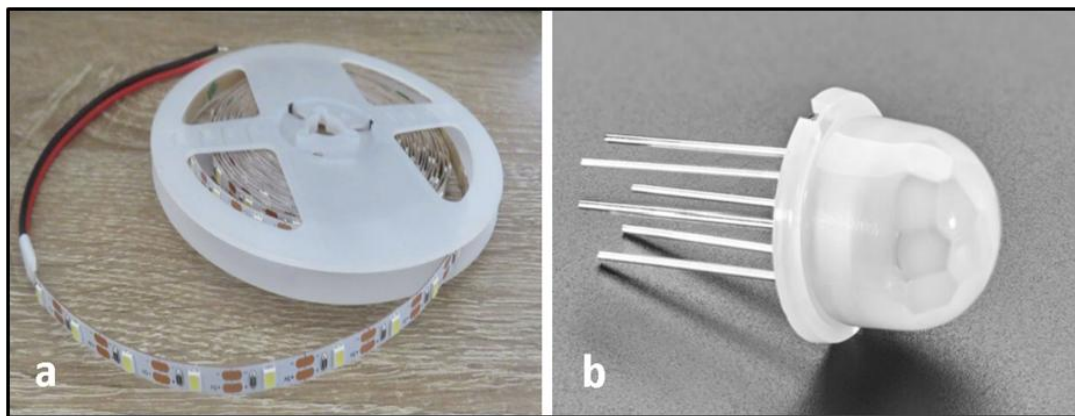


Figure 6-7: (a) LED Strip Light, (b) Mini PIR Sensor (RS Components Ltd., 2023)

Moreover, the Mini PIR Sensor's functionality is further enhanced by its customisable settings. The sensor's sensitivity can be adjusted to control the detection range, and the delay settings can be fine-tuned to determine how long the lights stay on after motion is no longer detected. This level of control prevents the lights from staying on unnecessarily, optimising energy usage.

In essence, the Mini PIR Sensor is a vital component of the solar pavement slab system, providing smart, automated control of the LED lighting. It ensures that the lights are activated only when needed during the night and turn off at dawn, conserving energy for the next cycle. This seamless integration of motion detection and light level sensing creates a reliable, energy-efficient lighting solution that enhances both functionality and safety.

6.3.3.8 Acrylic Top Layer Design

The design of the 340x340x10mm acrylic plastic (Acrylic PMMA) top layer for solar pavement has been utilised in this design phase. This acrylic service, as the top layer of the solar pavement slab design, incorporates key characteristics that make it ideal for this application. Acrylic PMMA

(Polymethyl Methacrylate) is a transparent thermoplastic known for its lightweight and shatter-resistant properties, making it a superior alternative to glass. With dimensions of 340mm by 340mm and a thickness of 10mm, the top layer provides ample coverage for the underlying solar components while offering sufficient strength to withstand pedestrian traffic and environmental stresses. Its high transparency allows maximum sunlight to pass through to the solar cells beneath, ensuring efficient energy harvesting.

Acrylic PMMA's excellent impact resistance and weathering properties make it durable enough to endure foot traffic and various environmental conditions. It is also lightweight, facilitating easier handling and installation compared to glass, which reduces the overall weight of the solar pavement slab. Furthermore, its resistance to UV radiation and weathering ensures the top layer remains clear and functional over time without significant degradation or yellowing, maintaining both efficiency and aesthetics.

Overall, the 400x400x10mm acrylic plastic (Acrylic PMMA) top layer is designed to provide a robust, transparent, and durable covering for solar pavements. Its combination of strength, lightweight, and resistance to environmental factors make it an ideal material for protecting solar panels while allowing efficient energy harvesting. This thoughtful design ensures the solar pavement system remains reliable, efficient, and safe, enhancing both functionality and aesthetics in public spaces.

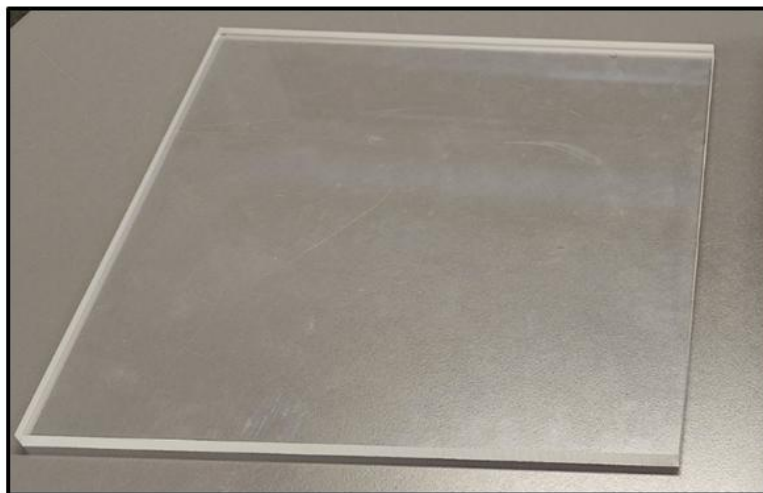


Figure 6-8: Solar Slab with Transparent Top Layer

The safety features of acrylic PMMA, including its tendency to break into larger, less dangerous pieces upon impact, enhance pedestrian safety. Additionally, the material can be easily cut, drilled,

and shaped to meet specific design requirements, allowing for precise customisation and seamless integration with the solar pavement's structural and aesthetic design. The surface of the acrylic sheet can be treated with anti-slip coatings to ensure pedestrian safety even when the surface is wet.

6.3.4 Trial Design of the Structural and Electrical Prototype

The trial design of the structural and electrical prototype aimed to create a 400x400x50mm solar pavement slab. To initiate this process, an initial prototype module made entirely of grey foam was manufactured to conduct experimental work before constructing the actual product. This approach allowed for precise testing and adjustments to ensure optimal performance of the final slab. Grey foam, measuring 600x600x100 mm, was purchased for this purpose. The foam was used to create the module profile for the solar pavement panel, shaping the cavity for electronic components such as the battery, charger, and control systems.

In addition to the primary cavity, the foam was meticulously designed to include a square 4-sided slot for the recessed LED strip light, ensuring that the lighting component could be securely and effectively integrated. See Figure 6-9 for the trial model prototype slab assembly made out of grey foam. Figures 6-9 illustrate the detailed setup of the foam module, showcasing the precise placement and testing of the electronic components.

Advanced design tools such as CAD drawings and SolidWorks were employed to achieve the precise dimensions and features required for this prototype. These tools allowed for accurate shaping of the entire module, ensuring that all components would fit perfectly and function as intended. Once the foam module was shaped, it was used to install and test the electronic devices. This step was crucial to verify the integration and functionality of the battery, charger, control systems, and LED strip within the designated cavities. The experimental work conducted with this foam prototype provided valuable insights and data, enabling refinements and ensuring that the final product would meet all design and performance criteria. Lab technician Mathew Garlic meticulously handled the connections, ensuring that all electronic components were correctly wired and integrated. This step was crucial for validating the design and ensuring that the system could operate as intended. At the laboratory, various simulation electric tests were conducted to verify that all devices were working perfectly and fit for purpose. These simulations ensured that all components were accurately suited to each other and functioned harmoniously within the

module. This thorough preparatory phase was essential in developing a reliable and efficient solar pavement slab, ensuring the final product's success in real-world applications.

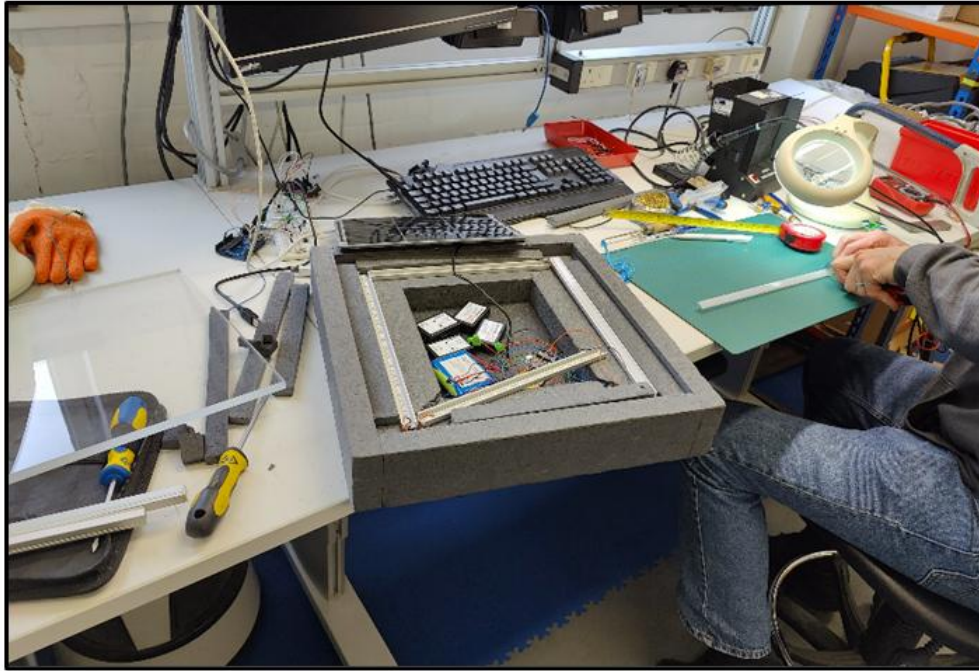


Figure 6-9: Assembly of Electronics and Data Loggers in Solar Slab Prototype Base

6.3.5 Walkable Solar Pavement Slab Trial Prototype

A complete trial prototype was created with all the electronic devices built in, forming a fully self-contained product prepared for initial testing. As can be seen in Figure 6-10, the self-contained solar pavement slab trial sample is made out of grey foam, providing a precise and functional prototype. The design and fabrication of the module took place at the Nottingham Trent University laboratory, where advanced CAD drawings and SolidWorks models were utilised to ensure accurate shaping and placement of the electronic components.

The grey foam structure includes cavities designed explicitly for housing the battery, charger, control systems, and a recessed slot for the LED strip light. This careful design ensures that each component fits securely and operates effectively within the module. Including these elements within a cohesive unit allows for comprehensive testing of the system's functionality and integration before proceeding to the final construction phase.

The initial testing phase involves verifying each component's performance, assessing the module's overall functionality, and making any necessary adjustments based on the test results. The grey foam prototype serves as a practical and scalable model for the eventual production of the solar

pavement slab, allowing for iterative improvements and refinements. This approach demonstrates the feasibility of the design and provides valuable insights into potential enhancements, ensuring that the final product will be both reliable and efficient in real-world applications.

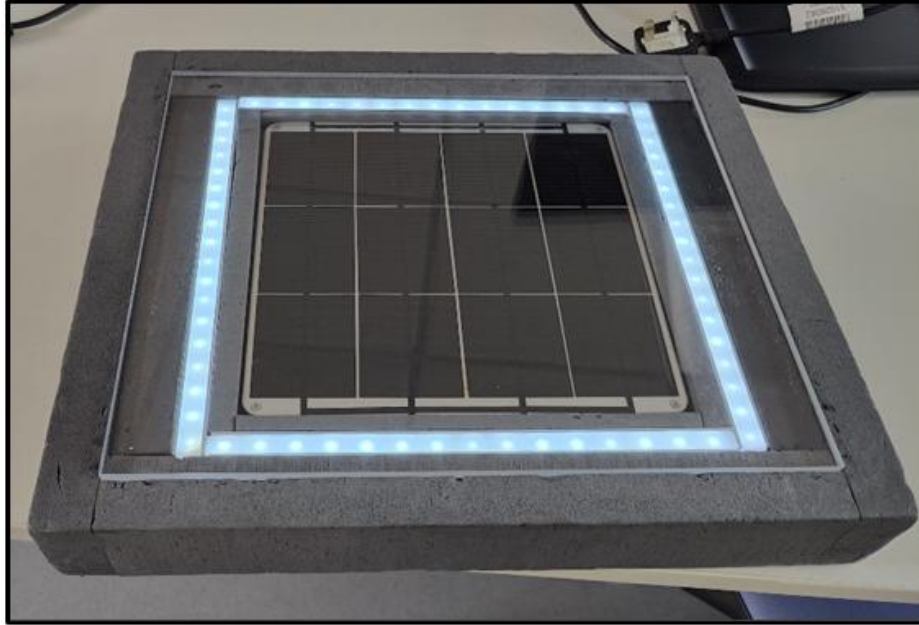


Figure 6-10: Solar walkable Pavement Slab Prototype

6.4 Summary

The solar pavement slab design process is centred on creating a functional solar product through meticulous design features, cutting, and assembly using foam to create a mock-up of the final product. A CAD model was used to guide the fabrication of a trial mock-up prototype made from grey foam, intended to test the overall functionality before producing the final slab with concrete-based recycled materials. The design integrates solar cells and essential electrical components for efficient energy generation and durability.

1. The design starts with a CAD model (figure 6-1) that outlines the dimensions of the solar slab, set at 400 x 400 x 50 mm, ensuring precise specifications for the prototype construction.
2. The prototype is made from grey foam rather than concrete to allow for easy modification and testing of functionality before moving to the final product.
3. Key materials include acrylic glass for the top layer due to its UV resistance, high mechanical strength, and transparency, along with grey foam for the base.

4. Monocrystalline silicon solar cells integrated into the foam base are chosen for their high efficiency and good temperature tolerance.
5. The design incorporates LED lights, batteries, light sensors, and controllers, all positioned within cavities in the grey foam base for easy access and functionality.
6. The prototype aims to evaluate the overall functionality and performance of the design. If successful, the final slab will be constructed using concrete; otherwise, design modifications will be implemented until optimal results are achieved.

Chapter 7: Experimental and Numerical Design of Solar Slab Base

7.1 Introduction

This chapter covers the development of an actual solar walkable slab base made from lightweight foamed concrete containing recycled materials. The process is divided into two phases: the experimental phase, which focuses on manufacturing the slab, and the numerical phase, where the slab is prepared for meshing in finite element analysis (FEA) using ABAQUS. However, only the meshing process is performed at this stage, with the analysis and results deferred to a later chapter. The slab dimensions remain 400mm x 400mm x 50mm, and CAD-generated images have been created to assist in the design and module creation.

The experimental design phase involves the detailed development and production of a solar slab base prototype made from lightweight foamed concrete mixed with recycled materials. The manufacturing process is illustrated in the flowchart, and images provided in Figure 7.1 demonstrate the critical steps undertaken. The initial step involves the profile fabrication and solar slab base design. CAD modelling software produces a 3D design with dimensions 400mm x 400mm x 50mm. The CAD-generated diagram serves as a reference for mould preparation and production. The mould assembly is developed using timber and grey foam layers, cut precisely to match the slab profile. These materials are combined to form a stepped mould structure, ensuring accurate cavity shaping during the casting process. The concrete mixture comprises cement, fine sand, water, and recycled materials. A foaming generator produces foam, which is subsequently blended into the concrete mix to reduce density and achieve the desired lightweight properties. The target density is approximately 1400 kg/m³. The prepared foamed concrete is poured into the mould, covering the layered grey foam pattern, and levelled to ensure uniform thickness. Once moulded, the slab undergoes a curing process to develop its mechanical properties and strength. Upon completion, the slab is extracted from the mould as a finished product and is ready for additional electrical integration. The final slab prototype is visually inspected, and minor surface corrections are made. The images provided depict the mould preparation phase, concrete pouring, and the completed slab base.

The numerical design phase focuses on developing a finite element model of the slab base using ABAQUS software. A CAD-generated representation is imported into ABAQUS, and the meshing

process is performed to discretise the slab for future mechanical analysis. The meshing phase is crucial as it ensures accurate stress distribution and load-bearing analysis in later stages.

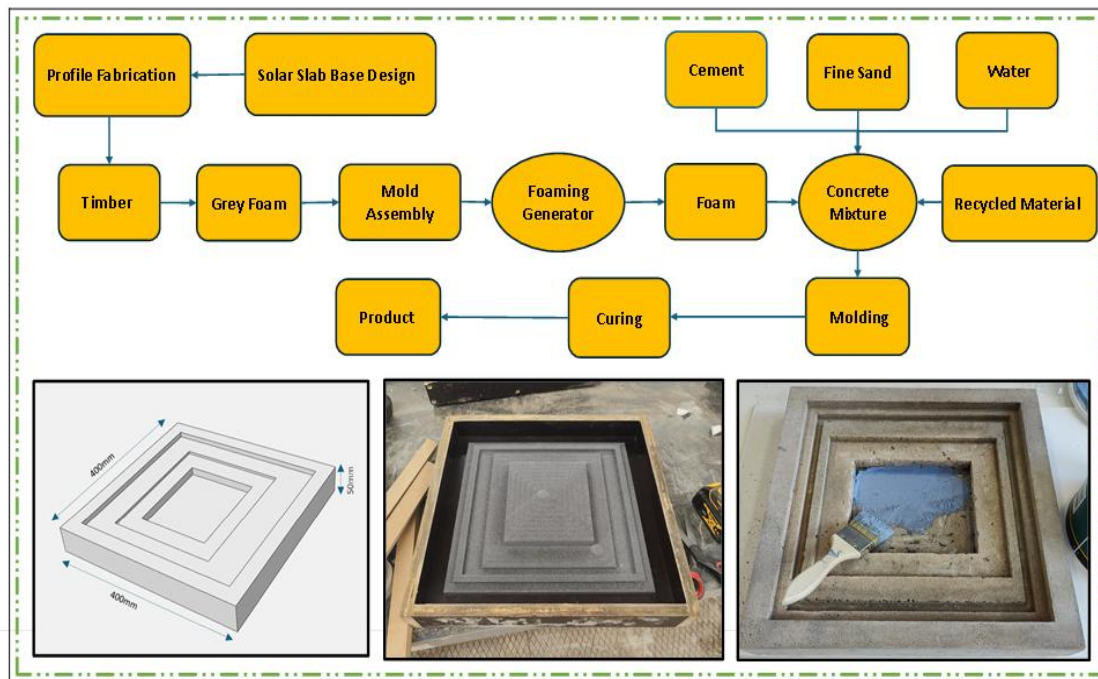


Figure 7-1: Solar Slab Production – (a) Slab Geometry, (b) Mold Fabrication, (c) Solar Slab Structure

7.2 Stage 1: Experimental Design

In this phase, the focus is on producing the actual solar slab base. The slab is made from foamed concrete, incorporating recycled materials to ensure sustainability and lightweight characteristics while maintaining the standard dimensions of 400mm x 400mm x 50mm.

Timber is used to create the base mould due to its strength and ease of use, while grey foam provides internal profiles and insulation. The slab's design allows for the integration of solar components, ensuring it can endure outdoor conditions while maintaining its energy-generating functionality. The CAD images guide the construction process, ensuring precision and accuracy during manufacturing. The experimental phase focuses on fabricating the solar slab base, utilising foamed concrete with recycled materials to ensure sustainability and lightness. The slab's dimensions remain at 400mm x 400mm x 50mm to align with the original prototype design. During this phase, key tasks include preparing the base mould using timber for structural support and incorporating grey foam for insulation and profiles. Precise material cutting and assembly,

followed by the curing process, ensure that the slab is both functional and durable. CAD-generated images guide each step of the fabrication process, ensuring accurate construction.

7.2.1 Stage 1: Production and Fabrication

The first stage involves the design and production of foam concrete samples, along with the analysis of the prototypes after construction. This design process includes constructing foam concrete moulds containing various materials, which incorporate both normal materials such as sand, cement, water, and foaming agents and recycled materials like waste foundry sand, polystyrene, and recycled steel tyre fibre. Superplasticisers are also introduced to enhance mechanical properties and workability. The foam concrete samples are then produced, and their mechanical behaviour, such as compressive and flexural strength, is investigated to determine the maximum applied load and deflection.

7.2.2 Solar Slab Construction

The solar pavement slab prototypes were constructed at Nottingham Trent University, adhering strictly to health and safety procedures, with all personnel wearing appropriate Personal Protective Equipment (PPE). The process involved several systematic stages using materials such as grey foam, wood, screws, and double-sided tape. Initially, the workspace was prepared and materials organised, with grey foam cut to the required dimensions to create a mould for the foamed concrete. A sturdy frame was constructed around the foam using wood and screws to hold it in place during the pouring and curing of the concrete, which included a cavity for future electrical components. The prepared foamed concrete mix, containing waste foundry sand, steel tyre fibre, and superplasticiser, was then poured into the mould, with vibrating tools used to eliminate air bubbles and ensure a uniform mix.

After the concrete had been set and cured, a 10mm thick acrylic plastic top layer was installed and secured with weather-resistant clear silicone chosen for its transparency and durability. The tanking coating was applied to the interface of the cavity in order to be weather-ried. The final stage involved a thorough quality inspection to ensure the slab met all required specifications, including checking dimensions, structural integrity, and surface finish. This systematic construction approach and the use of specific materials ensured the successful creation of the prototypes, focusing on structural performance with provisions for future electrical component

integration. Material details and instructions for each construction stage are explained in the following sections.

7.2.3 Profile Fabrication

The fabrication of the solar pavement slab involves the use of several materials to create a robust foamed concrete base panel. The primary materials used in this process are plywood and grey foam. Plywood is utilised to construct the outer frame of the mould, providing the necessary support and structure to contain the foamed concrete during the pouring and curing process.

7.2.4 Plywood

The brown film-faced plywood, with a thickness of 20mm, has been used to construct a base frame and reused multiple times. The plywood was purchased in 1200x2400mm sheets, cut into the required size, and assembled by screwing the edges to create a 400x400x50mm tray. Specifically, the 1200 x 2400mm sheets are cut into smaller pieces to achieve the final tray dimensions. Each sheet can be cut into six 400 x 400mm pieces per row, yielding three rows per sheet, which provides a total of 18 pieces of 400x400mm from one sheet. For each tray, one piece of 400x400mm is used as the base, and four pieces of 400 x 70mm and 440 x 70mm are used for the sides, assembled into a tray with dimensions of 400 x 400 x 50mm by screwing the edges together. The thickness of the plywood, being 20mm, ensures the sturdiness and durability of the tray. The images illustrating this process can be seen in Figures 7-2.



Figure 7-2: Solar Pavement Slab with Profiled Base

The assembly process involves cutting the plywood into the required sizes, forming the base and sides with one piece as the base and four 70mm wide strips as the sides, and then screwing the strips to the base. The edges are sanded to remove splinters and optionally sealed for moisture protection. This construction method provides a sturdy, reusable tray that is ideal for various construction applications.

7.2.5 Grey Foam

A grey foam piece, measuring 600 x 600 x 50 mm, was purchased and used to create the inner profile for the solar base, shaping the cavity for the electronic components such as the battery, charger, and control systems. Additionally, the foam was designed to include a square 4-sided slot for the recessed LED strip light. To achieve this, CAD drawings and SolidWorks were utilised to shape the inner sections required for the electronic devices accurately. The grey foam was carefully placed in the middle of the tray at an equal distance and secured with double-sided tape to hold it firmly while pouring the foamed concrete into the profile base. Before pouring the concrete, oil grease was applied to the inner section of the profile to facilitate easy de-moulding and avoid damaging the product. After the foamed concrete was poured, the structure was left to cure for 24 hours. Following this curing period, the grey foam was meticulously removed to reveal the cavity. This process ensured that the cavity was precisely formed and ready for the integration of the electronic components. Figure 7-3 illustrates the placement of the grey foam within the tray, demonstrating its positioning and how it was held in place during the pouring process.

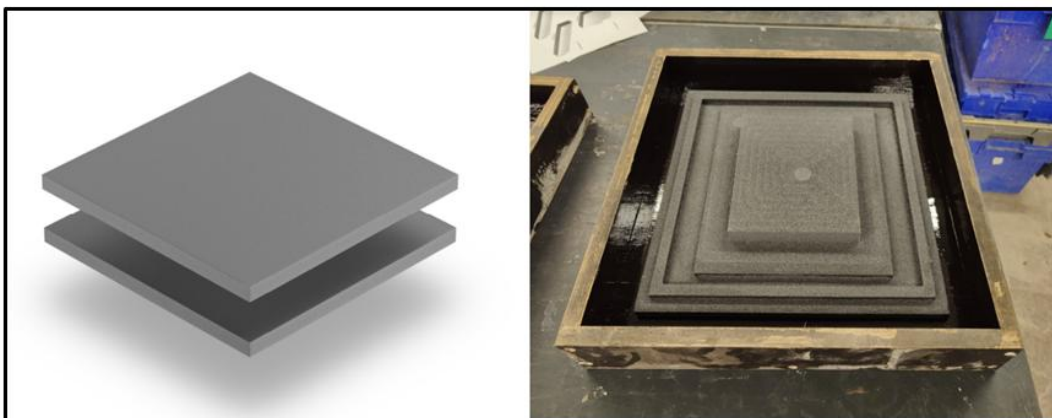


Figure 7-3: Grey Foam Profile

7.3 Foamed Concrete Slab Manufacture

The process for producing foamed concrete samples for the solar slab follows a structured approach designed to ensure consistency and reliability. Using a method similar to that employed by Jones et al. (2005), dry components such as cement, fine aggregate, and additives are mixed in a rotating drum mixer for one minute. After achieving uniform distribution of the dry materials, water is added to the mixture, and the blending continues for an additional 2 to 4 minutes to create a lump-free, homogeneous solution. Simultaneously, pre-formed foam is generated and incorporated into the mixture. This foam is essential to achieve the required lightweight properties and is stirred into the base mixture until it is evenly distributed. The plastic density of the concrete mix is monitored carefully, ensuring that it complies with standards such as BS EN 12350-6 (2009). If the density exceeds or falls below the acceptable range, adjustments are made to maintain the integrity of the mixture. This step is critical to producing foamed concrete slabs with consistent density and quality.

7.3.1 Experimental Work Preparation

The production process for the solar slab involved six distinct design mixes, each of which was used to create three slabs, resulting in a total of 18 slabs. Table 7-1 illustrates the mixing design of the solar slab base. These designs incorporate different recycled materials to assess their impact on the mechanical properties of the foamed concrete. The materials selected for these mixes were based on the results of previous tests on cubes and prisms, and they were identified as having the best properties for this specific application. The design mixes are detailed in the following numbers:

1. Normal concrete mortar was used as a baseline for comparison.
2. A foamed concrete mixture was utilised to achieve lightweight characteristics.
3. To explore the use of industrial by-products, 50% recycled waste foundry sand was used as a replacement for normal sand.
4. 10% polystyrene was added to the foamed concrete mix to utilise recycled materials and reduce weight.
5. 1% recycled steel tyre fibre was added to the sand-to-cement ratio, introducing elasticity and increased tensile strength to the mixture.

6. 1% superplasticiser was incorporated into the cement ratio to improve the concrete's workability and overall performance.

Table 7-1: Slab Design Incorporating Different Percentages of Recycled Materials and Additives

Sample Types	Description of Sample (Slabs)	Building Number	Target Density (kg/m ³)	Number of Slabs	Curing Period
Control	400 x400 x 50 mm	1	1400	1	28
				2	
				3	
FC	400 x400 x 50 mm	2	1400	1	28
				2	
				3	
WFS 50%	400 x400 x 50 mm	3	1400	1	28
				2	
				3	
PO 10%	400 x400 x 50 mm	4	1400	1	28
				2	
				3	
RSTF 1%	400 x400 x 50 mm	5	1400	1	28
				2	
				3	
SPs 1%	400 x400 x 50 mm	6	1400	1	28
				2	
				3	

These design mixes were selected based on their ability to provide an optimal balance of mechanical strength and density in the foamed concrete, making them well-suited for the solar slab. Using these materials is key to enhancing sustainability by incorporating recycled content while also meeting the slab's structural requirements.

Each of the six design mixes was poured into prepared plywood moulds with dimensions of 400mm x 400mm x 50mm. To facilitate easy demoulding after curing, mould-release oil was applied to the interior surfaces of the moulds. This ensured that the slabs could be removed without surface damage after the curing process. Once poured, the slabs were allowed to cure for 24 hours in a controlled environment. During this curing period, a cavity was created within each slab using a frame, allowing for the future installation of electrical components and an acrylic cover. The curing process ensures the slabs develop the necessary strength and durability for subsequent testing and analysis. The procedure follows the same method as in Chapter Four for cubes and prisms, which is to produce foamed concrete slab base samples during laboratory work. During

the production of each slab, the plastic density of the foamed concrete was closely monitored. Samples from each design mix were weighed using pre-weighed containers to determine whether the mixture met the required density standards. If necessary, adjustments were made by adding more foam or modifying the mixture to ensure compliance with the desired tolerance.



Figure 7-4: (a) Preparation of Materials, (b) Concrete Mixture Drum

This monitoring step is critical to maintaining consistent quality across all 18 slabs, ensuring that each design variation meets the mechanical and structural demands of the project.

Once poured, the slabs were allowed to cure for 24 hours in a controlled environment. During this curing period, a cavity was created within each slab using a frame, allowing for the future installation of electrical components and an acrylic cover. The curing process ensures the slabs develop the necessary strength and durability for subsequent testing and analysis.



Figure 7-5: Casting of Slab Samples

Additionally, to integrate electrical components and the acrylic cover, a cavity is formed within the slab by inserting a frame into the concrete before curing. This cavity will house the solar panel components, making the slab functional for energy generation.



Figure 7-6: De-moulding of the Slabs

After the 24-hour curing period, the slabs were carefully de-moulded, with particular attention given to avoiding any structural damage or surface imperfections. This step required precision, as the slabs were still relatively fragile. Improper handling during demoulding could compromise the quality and durability of the slabs. Special care was taken to loosen and remove the slabs from the moulds evenly without introducing cracks or weakening the edges.



Figure 7-7: Curing of Slabs in a Water Container

Once the samples were de-moulded, the slabs were immediately placed into a curing tank for an extended curing period. This process allows the slabs to hydrate and strengthen fully, ensuring

they meet the necessary mechanical performance standards. The controlled moisture in the tank promotes consistent curing throughout the slab, which is essential for achieving uniform strength and long-term durability. See Figure 7-7 for the slabs during the curing period.

The grey foam is carefully removed before the testing process. Images in Figures 7-8 illustrate the concrete preparation. This thorough curing and preparation process ensures the durability and functionality of the solar pavement slab. The slab's design includes a cavity with dimensions of 200mm by 150mm, which is intended to house the electrical components necessary for the solar pavement system. This thoughtful design makes the slab self-contained, simplifying the installation process and ensuring all components are protected and integrated efficiently. This cavity allows for the continuous incorporation of the solar panel, battery, and other electronic controls, creating a compact and durable solar pavement solution.

The mechanical properties and the self-weight of the slab will be thoroughly analysed in Chapter 8, highlighting its structural integrity and lightweight nature, which facilitates easier handling and installation. The use of foamed concrete reduces the weight and enhances the slab's thermal insulation properties, making it a superior choice for sustainable construction projects. This figure provides a visual representation of the slab, highlighting the integration of the cavity for electrical components and demonstrating the slab's readiness for installation in a solar pavement project

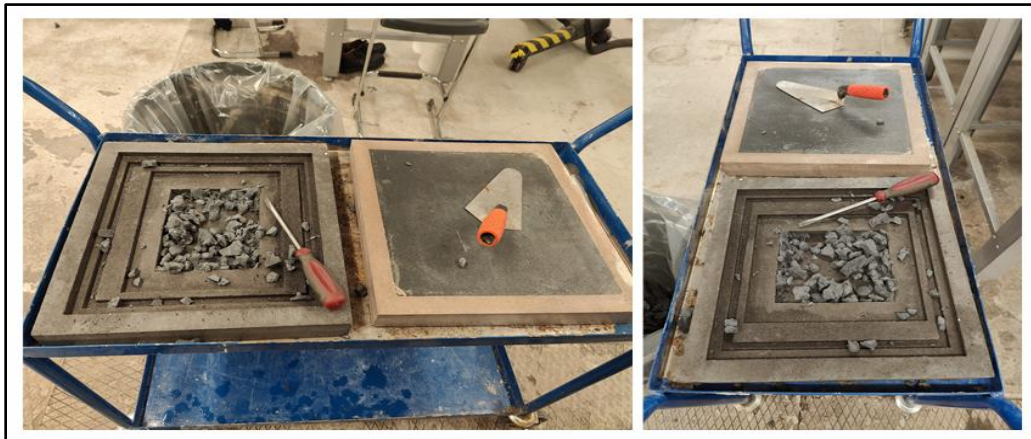


Figure 7-8: Removal of Grey Foam from Slab Cavity

7.3.2 Flexural Analysis

The three-point flexural test is a critical method for assessing the flexural strength, or modulus of rupture, of concrete prisms and slabs. This test provides valuable data about the material's behaviour under bending stresses, which is crucial for structural applications where bending loads

are common. The test procedure involves several detailed steps. Firstly, specimen preparation includes 12 slabs (400 mm x 400 mm x 50 mm) chosen to reflect the concrete's performance in practical applications. The test setup places the prisms and beams centrally on two supports with a single load application point at the centre, creating a bending moment over the span of the specimen and focusing the maximum stress at the midpoint. Care is taken to ensure the surfaces in contact with the loading plates are even to distribute the load uniformly. A constant loading rate of 300 N/sec is used for low-density specimens, while high-density specimens are subjected to a loading rate of 500 N/sec, aiding in understanding the behaviour of different densities under similar stress conditions. See Figure 7-9 for the slab under the hydraulic machine.



Figure 7-9: Solar Slab Under Hydraulic Testing Machine

Digital tools record the load and the corresponding deflection at the moment of failure, enhancing the accuracy and repeatability of the results. The modulus of rupture (f_r) is calculated using a specific formula designated in the BS EN 12390-5 standard, with the location of the fracture providing insights into the stress distribution and the weakest point of the specimen. According to Wahyuni (2012), tensile strength values from the flexural test are typically higher than those from the cylinder splitting test and direct uniaxial tension tests due to the distribution of stresses over a larger area. This stepped testing approach enables engineers and researchers to gain a comprehensive understanding of material properties under different circumstances and load types, assisting in the design and application of concrete structures in various construction scenarios.

Understanding these variations is critical for correctly interpreting test results and applying them to structural design and analysis.

7.4 Stage 2: Numerical Modelling

This stage focuses on developing a finite element model for the foam concrete slab module to enable future computational analysis. The primary objective is to prepare the slab model for finite element analysis (FEA) using ABAQUS software. The numerical phase involves creating a digital representation of the slab and discretising it into more minor elements through meshing. Meshing is a crucial step in finite element modelling as it divides the slab into small interconnected elements, allowing for detailed stress, deflection, and strain analysis in later stages. This phase ensures the model is geometrically accurate and structurally ready for subsequent analysis. However, this chapter does not cover the analysis or results; these will be addressed in a later chapter. At this point, the focus is solely on model preparation and meshing to ensure the module is appropriately set up for future computational evaluation.

7.4.1 ABAQUS Overview

Various finite element analysis (FEA) software packages are widely utilised in concrete structural analysis, each offering distinct capabilities tailored to different analytical needs. ABAQUS, part of the SIMULIA product suite from Dassault Systèmes, is notably recognised for its robust nonlinear and linear static and dynamic analysis capabilities, making it a popular choice for complex structural simulations (Dassault Systèmes, 2014). The ABAQUS product suite consists of three main components: ABAQUS/CAE, ABAQUS/Standard, and ABAQUS/Explicit. Each component is designed to address specific aspects of structural analysis. For instance, ABAQUS/CAE (Complete ABAQUS Environment) was employed in this study to simulate concrete slabs, utilising its capabilities in linear analysis. ABAQUS/CAE provides an integrated platform where users can create, analyse, and visualise models within a single interface. This highly customisable environment features a graphical user interface (GUI) that can be adapted to meet specific user requirements.

A significant aspect of ABAQUS/CAE is its flexibility in handling geometry creation and importation. Users can design models directly within the GUI or import complex CAD models, which are then meshed and prepared for analysis. This capability is particularly advantageous for structural engineers working with detailed designs. Once the geometry is defined and meshed,

ABAQUS/CAE supports comprehensive analysis, including linear and nonlinear behaviours, static and dynamic loads, and other complex interactions within the structure. Linear analysis was a key focus in this research, as it provides valuable insights into the elastic behaviour of concrete structures under various loading conditions without the computational complexity of nonlinear analysis.

Furthermore, ABAQUS/CAE is equipped with sophisticated visualization tools that enable users to effectively interpret and communicate analysis results. These tools offer a wide range of data display options, from basic displacement plots to advanced stress-strain visualisations, essential for understanding the performance of concrete structures under various conditions. Presenting results clearly and intuitively enhances decision-making and improves overall comprehension of structural behaviour, making ABAQUS/CAE a vital tool for structural analysis in academic and professional contexts.

The Finite Element Method (FEM) itself is a computational technique used to analyse the behaviour of entire structures and materials by breaking them down into smaller, more manageable components. FEM is widely employed in engineering and scientific fields to optimise designs, predict performance, and simulate physical processes (Zienkiewicz, 1971). The core concept of FEM involves discretising a continuous system, such as a structure or material, into finite elements to model its behaviour. A mesh is formed by connecting these elements at specific nodes. By applying appropriate mathematical models and boundary conditions, the behaviour of each element and its interaction with neighbouring elements can be analysed numerically.

7.4.2 Linear Finite Element Method (FEM).

The Linear Finite Element Method (FEM) is a fundamental approach in structural analysis that operates under the assumption that material properties, such as Young's modulus and Poisson's ratio, remain constant and that deformations are small and within the elastic range. This method is particularly useful for analysing problems with a direct, proportional relationship between the applied loads and the resulting displacements, meaning that the structure's response can be predicted with a high degree of accuracy without considering complex nonlinearities.

In linear FEM, the governing equations are simplified because the relationship between stress and strain is linear, which implies that the superposition principle can be applied. This allows for the straightforward combination of different loading scenarios to predict the overall response of the structure. For instance, in linear static analysis, which is one of the most common applications of

linear FEM, the focus is on determining the structural response under steady-state loads. This type of analysis ignores time-dependent effects such as those caused by transient or dynamic loads, making it ideal for scenarios where the loads are applied gradually and the material remains within its elastic limit (Crisfield, 1997).

One of the key advantages of linear analysis is its computational efficiency. Because the assumptions of linearity reduce the complexity of the equations involved, linear FEM models can be solved more quickly and with less computational power compared to nonlinear models. This makes it an attractive option for preliminary design and analysis phases, where rapid iteration and assessment of different design scenarios are required. Moreover, linear FEM is widely applicable across various fields of engineering, from civil and mechanical engineering to aerospace and materials science, wherever the behaviour of materials under load needs to be understood within the elastic regime.

Linear FEM also provides a reliable baseline for more advanced analyses; in cases where initial results indicate that the material may undergo large deformations or enter a plastic range, a linear analysis can serve as a preliminary step before moving on to more complex nonlinear analysis. This stepwise approach allows engineers to first understand the basic response of the structure under simplified conditions before delving into more detailed and computationally intensive simulations (Wriggers, 2008a).

7.4.3 Modelling Concrete Elastic Behaviour

Accurately modelling the elastic behaviour of concrete in finite element analysis (FEA) requires precise characterisation of its mechanical properties. Linear elasticity, characterised by a constant modulus of elasticity and Poisson's ratio, is a common assumption in these models. The modulus of elasticity (E) quantifies the material's stiffness, calculated as the stress-to-strain ratio within the elastic deformation range (Mindess, Young, & Darwin, 2003). This parameter is crucial for predicting concrete deformation under load and ensuring the structural model's accuracy.

The modulus of elasticity for foamed and normal concrete varies significantly, influenced by the material's density and composition. Jhatial et al. (2018) reported that the foamed concrete with a density of 1400 kg/m^3 has a modulus of elasticity of 6 GPa, indicating moderate stiffness compared to higher-density concretes. Raj, Sathyan, and Mini (2019) provide a broader range, stating that the modulus of elasticity for foamed concrete typically falls between 1 and 12 GPa, reflecting the varying densities and compositions of foamed concrete mixtures.

Beng (2021) further notes that foamed concrete with a density of 1800 kg/m^3 has a modulus of elasticity of 16 GPa, demonstrating that higher density results in increased stiffness, closer to that of normal concrete. However, the modulus of elasticity for foamed concrete is generally about 25% less than that of normal concrete, highlighting its reduced rigidity due to its cellular structure and higher air content.

In contrast, normal concrete exhibits significantly higher stiffness. Abdelgader (2014) reports that the modulus of elasticity for normal concrete ranges from 29 to 35 GPa, influenced by the type of aggregates and concrete mix. Similarly, Beng (2021) states that the modulus of elasticity for normal concrete is around 28 GPa. These values illustrate the much higher stiffness of normal concrete compared to foamed concrete, making it more suitable for applications requiring high load-bearing capacity and minimal deformation.

The differences in the modulus of elasticity between foamed and normal concrete underscore the impact of material composition and density on mechanical properties. Foamed concrete, with its lower density and higher air content, offers benefits such as reduced weight and improved thermal insulation, making it ideal for non-structural applications. In contrast, normal concrete, with its higher modulus of elasticity, is preferred for structural applications where high stiffness and load-bearing capacity are crucial. See Table 7-2 for the normal concrete modulus of elasticity and Poisson ratio.

Table 7-2: Modulus of Elasticity of Normal and Foamed Concrete (Beng, 2021)

Property	Normal Concrete	Foamed Concrete
Modulus of elasticity (MPa)	28000	16000
Poisson Ratio	0.2	0.25

Concrete's quasi-brittle nature means it responds differently to compressive and tensile stresses, typically being much stronger in compression than in tension. This requires careful consideration in modelling to capture these differences accurately. Using C3D8 elements, which are 8-node linear brick elements, is appropriate for capturing the three-dimensional stress state in concrete structures (Bathe, 1996). These elements effectively represent the material's response to loading conditions, accounting for the non-uniform stress distributions that typically occur in concrete. Developing a finite element model to study the behaviour of concrete is inherently challenging due to its heterogeneous nature and complex fracture mechanics. However, employing appropriate

material models and element types, such as the linear elastic model with C3D8 elements, facilitates a more accurate simulation of concrete behaviour under different loading scenarios. This approach allows for a detailed analysis of stress distributions and deformation patterns, which are critical for assessing the structural integrity and performance of concrete elements (Neville, 1995).

7.4.4 Load Stepping Using (ABAQUS)

In the analysis of a 400x400x50 mm concrete mortar slab using ABAQUS, proper load stepping is essential to ensure accurate results, especially when dealing with material behaviour. Linear analysis was used in this study; the application of load increments still plays a crucial role in achieving a stable and reliable solution. In ABAQUS, automatic time stepping controls the size of load increments throughout the analysis. The initial increment size in this study was set to 0.001, providing a balanced starting point that helps capture the slab's initial response to the applied load. As the analysis progresses, if the solution behaviour remains stable, ABAQUS increases the load increment size up to a maximum of 0.01. This increment increase allows the analysis to proceed more quickly when the response is smooth and linear, thereby improving computational effectiveness. The minimum increment size was set to 1E-015, ensuring that even the smallest necessary steps can be taken to maintain accuracy.

The overall period for the analysis was defined as 0.1, with a maximum of 100,000 increments allowed. This setup ensures that the simulation has sufficient capacity to handle the load application. By carefully managing load increments, ABAQUS helps ensure that the linear analysis of the concrete mortar slab remains accurate and efficient, capturing the essential structural response of the slab under the applied loads.

7.4.5 Method for Linear Analysis Solution

In ABAQUS, linear analysis involves evaluating the structural response of a model under the assumption that the stress-strain relationship is linear, meaning the material behaves elastically and displacements are sufficiently small to disregard geometric nonlinearity. This type of analysis is beneficial in preliminary design stages or when assessing structures under loads that do not exceed the material's elastic limit. Two slabs, each measuring 400x400x50 mm, were examined for this specific analysis. One slab was constructed from normal concrete mortar, known for its high stiffness and density, typically around 2100 kg/m³. The other slab was made of foamed concrete, which has a lower density of 1400 kg/m³ and is often used in applications where reduced

weight is advantageous. However, it typically has lower stiffness than normal concrete. The process begins by creating a 3D part in ABAQUS representing each slab as a simple rectangular brick with the specified dimensions. ABAQUS, a widely used software for finite element analysis, provides an extensive library of elements suitable for various structural analyses. For this linear analysis, the slabs are discretised into finite elements using 3D solid elements like C3D8R, which are 8-node linear elements with reduced integration. The C3D8R element is particularly effective for linear analysis because it balances computational efficiency with accuracy by reducing numerical integration to minimise the number of calculations required while still capturing the essential behaviour of the material.

Using these elements accurately assesses how the slabs respond under load, including the distribution of stress and strain throughout the material. The choice of element type and the linear assumption is critical for ensuring that the model accurately reflects the behaviour of the actual structure under the applied loads; this approach is widely validated in structural engineering practices, making it a reliable method for the initial design and analysis phases, mainly when working with homogeneous materials like concrete.

7.4.6 Element Types in ABAQUS

ABAQUS offers a broad, versatile element library to address various engineering problems. Each element in ABAQUS is designated by a unique name that reflects its characteristics, such as dimensionality, node configuration, and specific features. For instance, elements like C3D8R, S4R, T2D2, or C3D8I are commonly used, each serving different modelling needs. The naming convention typically indicates whether the element is a continuum (C), a shell (S), a truss (T), and so on, followed by details about the number of nodes, integration scheme, and any additional special attributes (like reduced integration, indicated by "R").

7.4.7 Concrete Modelling

Depending on whether the model is 2D or 3D, different element types are utilised when modelling foamed concrete slabs in ABAQUS.

1. **2D Models:** For 2D simulations, a four-node element is typically employed. This element type has two degrees of freedom at each node, corresponding to translations in the x and y directions. These elements can capture complex behaviours such as plastic deformation, cracking, and crushing, which are essential for accurately modelling the behaviour of concrete under various

loading conditions. This element type's geometry and node locations are crucial for ensuring that the simulation can effectively predict the structural response. These 2D elements are beneficial in scenarios where out-of-plane stresses and displacements are negligible or where a simplified analysis is sufficient. The node positions and geometry for this element type are depicted in Figure 7-10a.

2. 3D Models: In 3D simulations, an eight-node linear brick element is commonly used. This type of the element, such as C3D8 in ABAQUS, has three degrees of freedom at each node, corresponding to translations in the x, y, and z directions. These elements are more robust and versatile, capable of simulating the full three-dimensional behaviour of concrete structures, including complex phenomena like plastic deformation, cracking, and crushing. The ability to model these behaviours in 3D is crucial for more accurate and realistic simulations, particularly when dealing with complex geometries or loading conditions that induce stresses and deformations in all three spatial dimensions. The node positions and geometry for this 3D element type are shown in Figure 7-10b.

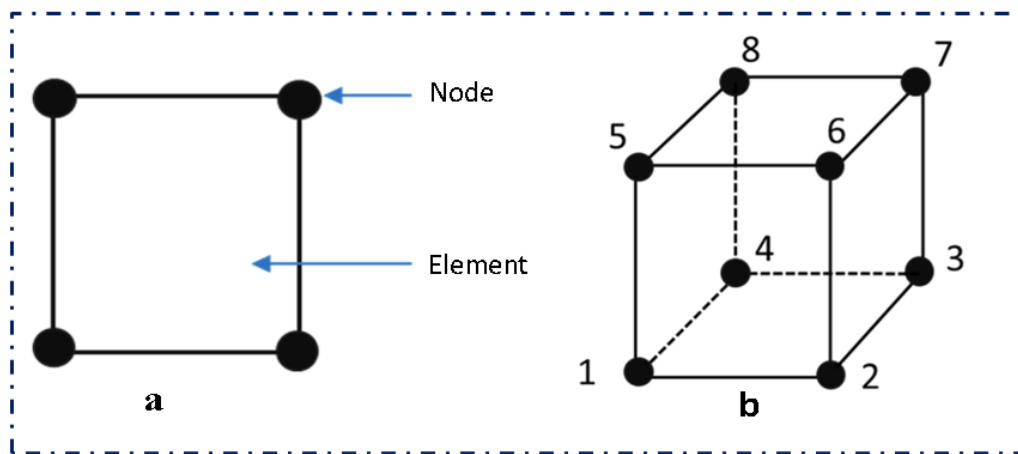


Figure 7-10: ((a) Plane Stress Quadrilateral Four-Node Element, (b) Eight-Node Linear Brick Element

The choice between 2D and 3D elements depends on the specific requirements of the analysis, including the level of detail needed and the computational resources available. While 2D models can provide valuable insights with lower computational cost, 3D models offer a more comprehensive understanding of the structural behaviour, particularly for complex or highly loaded concrete structures like foamed concrete beams.

7.4.8 Embedded Model

Embedded Model for a Concrete Mortar Slab Without Reinforcement in ABAQUS. In the context of finite element analysis (FEA) using ABAQUS, the concept of an "embedded model" typically refers to situations where reinforcement (such as rebar) is embedded within a host material like concrete. However, the term "embedded model" does not apply directly to a concrete mortar slab with no reinforcement involved. Instead, the analysis models the slab as a homogeneous, solid body.

When using the ABAQUS student version, it's essential to be aware of the limitations imposed by the software, particularly the maximum number of nodes allowed in a model. The student version of ABAQUS restricts models to a maximum of 1,000 nodes. This limitation affects the complexity and size of the models that can be created, and careful consideration is required when setting up finite element analyses, especially for detailed 3D models. See Figure 7-11 for how this model would be set up and analysed in ABAQUS.

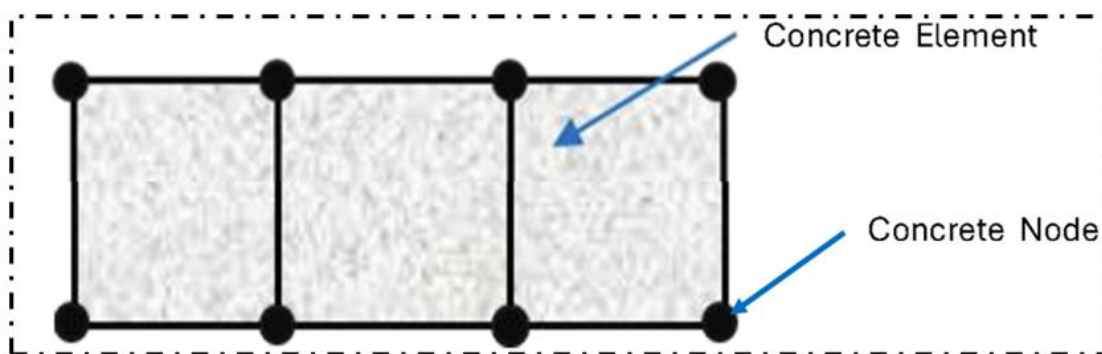


Figure 7-11: Embedded Formulations for Concrete Mortar

Next, the material properties of the slabs are defined. For the normal concrete mortar slab, properties include Young's Modulus, which represents the stiffness of the concrete, typically ranging between 15,000 MPa to 30,000 MPa, and Poisson's Ratio, typically between 0.2 and 0.3 for concrete, representing the ratio of lateral strain to axial strain. The normal mortar concrete slab's density is 2100 kg/m³. For the foamed concrete slab, the density is defined as 1400 kg/m³, with appropriate adjustments to Young's Modulus to reflect the reduced stiffness of foamed concrete compared to normal concrete. The initial components of Finite Element Modelling are geometry definition, material properties assignment, mesh generation, boundary conditions,

analysis setup, solution, and post-processing. Figure 7:12 represents a step-by-step method for performing such an analysis.

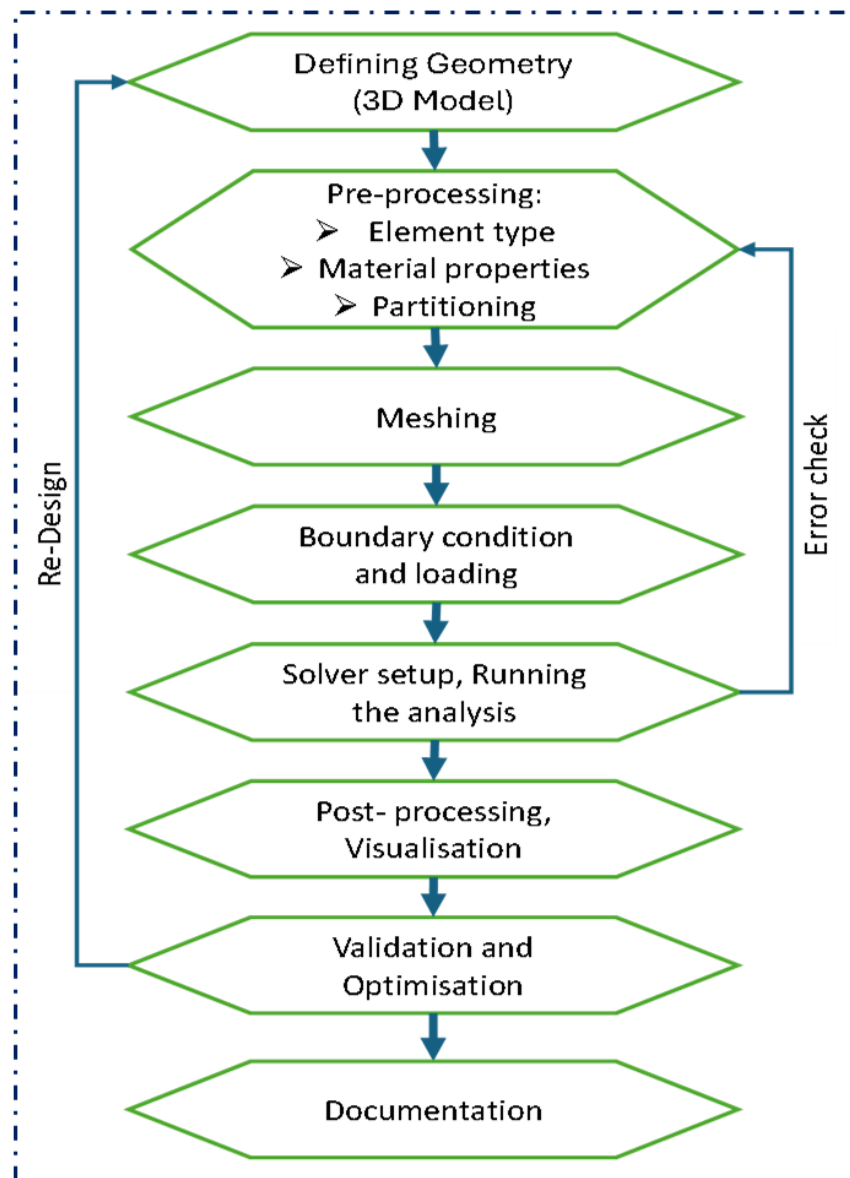


Figure 7-12: Step-by-Step Process in ABAQUS Simulation

Boundary conditions and loading are then applied to each slab model. Loading conditions might include a uniform pressure or a concentrated force at specific points, such as mid-span for bending analysis. The load magnitude must remain within the material's elastic limit to ensure the analysis remains valid under linear behaviour. A linear static analysis step is then defined in ABAQUS, where the loading is assumed to be applied gradually, and the structure responds immediately

without time-dependent effects. Load stepping in linear analysis is straightforward, with ABAQUS applying the load incrementally. However, the increments are typically more prominent than in nonlinear analysis due to easier convergence in linear systems.

The solver for linear static analysis in ABAQUS is direct, solving the matrix equations, which is feasible given the manageable problem size. Once all the steps are defined, the analysis is submitted as a job in ABAQUS, where the software processes the input data and solves the equilibrium equations to calculate the stress, strain, and displacement fields within each slab. Outputs such as displacements, reaction forces, and stress distributions can be requested to evaluate the slabs' performance under the applied load.

7.4.9 Geometry

In the beginning, the geometry of the slab is defined within ABAQUS as a 3D solid part with dimensions 400x400x50 mm. This rectangular block represents the entire slab of concrete mortar. The next step involves defining the material properties of the concrete mortar. Key properties include Young's Modulus, which reflects the stiffness of the material, typically ranging between 6,000 MPa to 30,000 MPa for mortar concrete, and Poisson's Ratio, usually between 0.2 and 0.3. See Figure 7-13 for the geometry of the slab using FEM.

The density of the material is also crucial, with normal mortar concrete typically having a density of 2100 kg/m³ and foamed concrete having a density of 1400 kg/m³. Through meshing, the geometry is divided into more minor elements, resulting in the formation of a finite element mesh. The mesh density is selected to represent the system's behaviour accurately.

To start, open Abaqus and navigate to the 'Part' module to create a new part. Set the part type to 3D, the geometric shape to 'Deformable', and the base feature to 'Solid'. In the 'Create Part' dialogue box, set the approximate size to 500 mm to comfortably fit the slab dimensions. Proceed to the sketcher, select the rectangular tool, and draw a rectangle with precise dimensions of 400 mm x 400 mm using the dimension tool. Once the sketch is complete, click 'Done'. In the 'Create Part: Extrude' dialogue box, set the extrusion depth to 50 mm and confirm to create the 3D solid part representing the slab. Ensuring the geometry is clean and free from defects such as small edges, faces, or slivers is crucial to avoid complications during meshing.

Next, the geometry is visualised by rotating and zooming in to confirm that the dimensions are precisely 400 mm x 400 mm x 50 mm using the measure tool. For linear analysis, it's essential to have finer mesh control in critical areas. Consider partitioning the geometry using the 'Partition'

tool to divide the slab into smaller sections, which can help manage mesh density more effectively. This step is critical in nonlinear analysis where higher stress and strain distribution accuracy is required. Regularly save your model to prevent data loss. Ensuring the geometry is accurately created, cleaned, and adequately partitioned establishes a robust foundation for the meshing process, reducing potential errors and enhancing the quality and accuracy of your nonlinear finite element analysis.

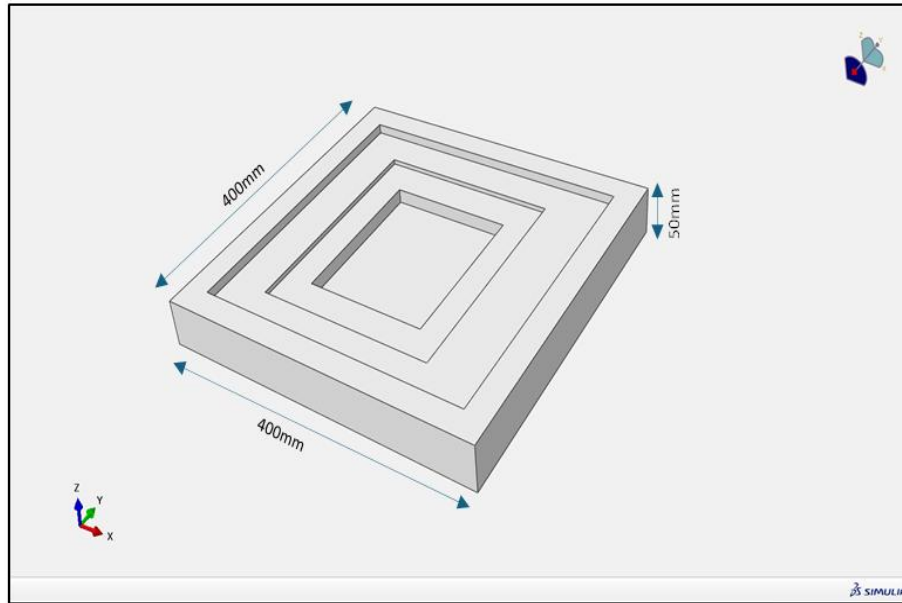


Figure 7-13: Solar Prototype Geometry

7.4.10 Loading and Boundary Conditions

The beams were subjected to a three-point bending test to evaluate their performance under load. For the finite element model (FEM) setup, the conditions were designed to replicate the experimental testing of the slab. Two supports were pinned, and a roller support was placed 50 mm from each end of the slab. The system's constraints and loading are defined by boundary conditions, which include boundary conditions, applied forces, and fixed supports. The type of boundary conditions and constraints applied to the geometry are illustrated in Figure 7-13.

1. Boundary Conditions

Once the slab is meshed, boundary conditions must be applied to simulate how the slab is supported in reality. For example, if the slab is supported on its edges, you would apply constraints that prevent vertical displacement (translation in the Z direction) while allowing rotation.

Alternatively, if the slab is fixed, all degrees of freedom at the support points would be constrained. The next step involves applying the load. This could be a uniform pressure across the slab's top surface to simulate a distributed load or a point load applied at the centre to simulate a concentrated load, such as a column or a heavy object.

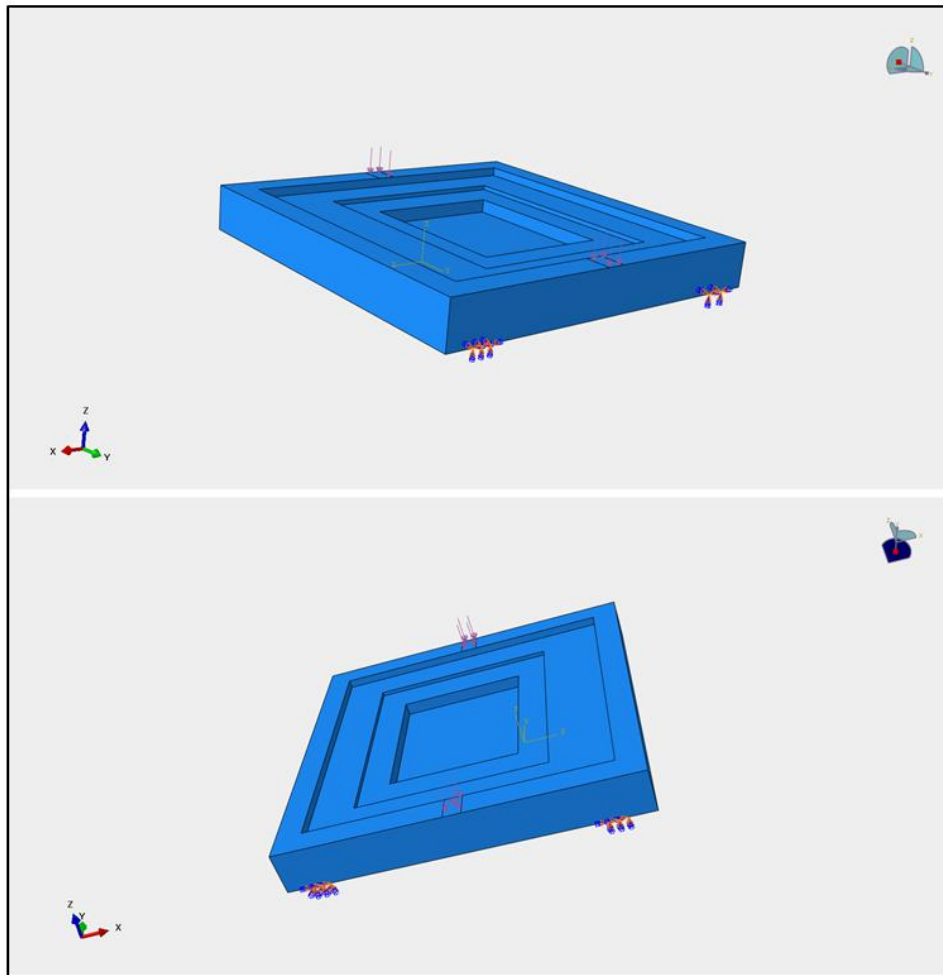


Figure 7-14: Boundary Conditions of the Solar Slab

After preparing the geometry, the next crucial step in finite element analysis (FEA) is accurately defining the boundary conditions. This step ensures that the model's constraints and supports mimic real-world conditions. Two supports were modelled as pinned supports, allowing rotation but resisting translational movements in all directions. These supports were positioned 50 mm from both ends of the slab. Additionally, roller support was applied at specific points on the slab, constraining vertical movement while permitting horizontal displacement. If symmetry conditions are applicable, they can be used to reduce the model size and computational effort by constraining

displacement and rotation along the plane of symmetry. Other constraints and interactions, such as tying different parts of the model together, ensure that the slab behaves as a single unit under loading conditions.

2. Loading Application

Regarding loading, forces were applied at the midpoint of the span length between the supports, as depicted in Figure 7-14. This setup ensures that the loading conditions in the FEM closely mimic those used in the experimental tests. To simulate the experimental loading conditions, a loading rate of 300 N/sec was applied, reflecting the actual rate used during the tests. This consistent approach helps accurately capture the slab's behaviour under load, providing reliable data for analysis and comparison.

By carefully defining the boundary conditions and applying the loads in a controlled manner, the finite element model can accurately simulate the real-world behaviour of the slab under three-point bending. This precise setup is crucial for obtaining meaningful and reliable results from the FEA, allowing for a thorough analysis and validation against experimental data. The same applied load rate of 300 N/sec was implemented for both the experimental and numerical simulations to ensure consistency and comparability between the two methods. In the experimental setup, a load of 300 N was applied to the slab every second. This identical loading rate was precisely replicated in the ABAQUS numerical simulation. By maintaining the same loading rate in both scenarios, the numerical results accurately reflect the experimental test conditions, allowing for a direct and reliable comparison of the slab's behaviour under load.

7.4.11 Meshing

After defining the geometry and material properties, the slab must be discretised into finite elements. In ABAQUS, 3D solid elements such as C3D8R (an 8-node linear brick element with reduced integration) are commonly used for this purpose. The meshing process involves dividing the slab into smaller components, which will be used to calculate the stress, strain, and displacement fields during the analysis. The mesh size should be chosen based on the desired accuracy, with a finer mesh providing more detailed results at the cost of increased computational resources.

After defining the geometry and boundary conditions, the next critical step is meshing the model. Meshing divides the geometry into smaller elements that can be analysed. In Abaqus, this process

begins with selecting an appropriate mesh type and element size to balance accuracy and computational efficiency. For the slab with dimensions 400 x 400 x 50 mm, a structured mesh is ideal due to its regularity and control over element quality. The element size should be fine enough to capture stress gradients accurately, especially around supports and load application points.

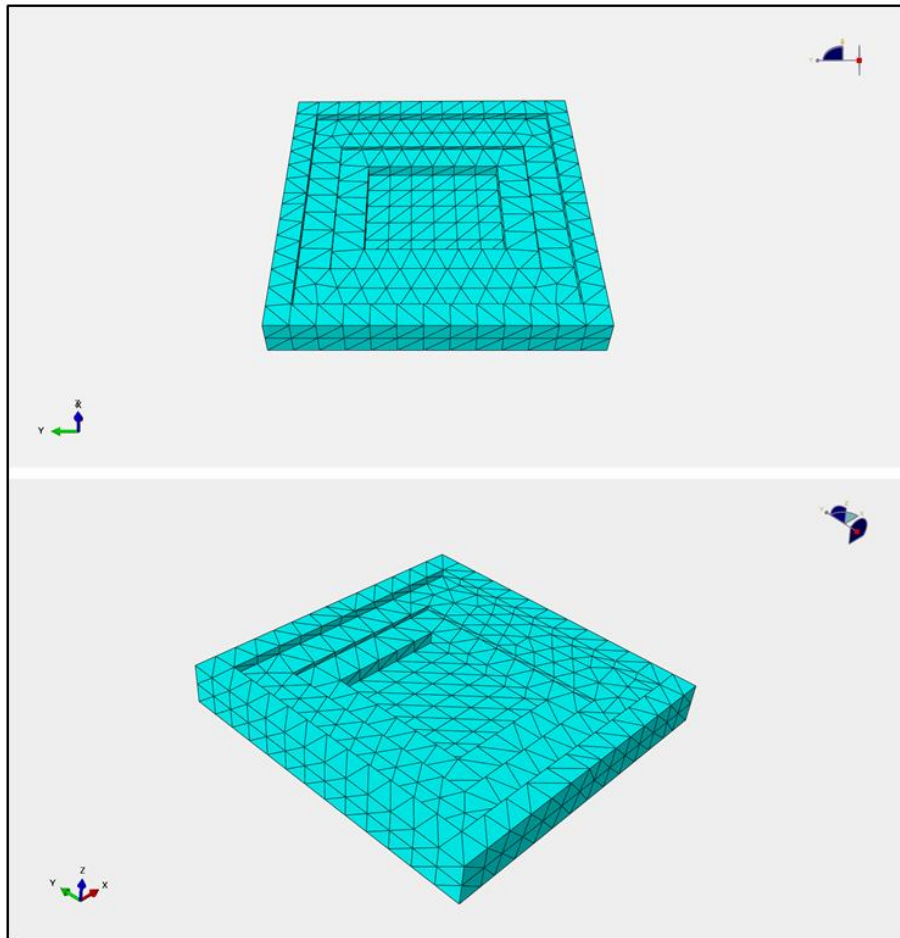


Figure 7-15: Meshing of the Slab Base Model

Mesh controls are applied to ensure uniformity and quality, focusing on critical areas where high stress or strain is expected. For nonlinear analysis, a finer mesh is particularly important to capture the detailed behaviour of the material under load. Abaqus provides tools to check mesh quality, such as aspect ratio and skewness, to ensure that elements meet the required standards. Poor-quality elements can lead to inaccurate results and convergence issues, so it's essential to refine the mesh iteratively. Once the mesh is generated, it should be visually inspected and adjusted if necessary, ensuring it meets the criteria for a successful analysis. This meticulous approach to

meshing is vital for obtaining reliable and precise results in finite element analysis. See Figure 7-15 for meshing the slab.

7.5 Summary

The solar walkable slab base was produced using six design mixes, incorporating various recycled materials, including foundry sand, polystyrene, recycled tyre fibres, and superplasticiser. A total of 18 slabs were created (three slabs per mix) using foamed concrete-based material, with dimensions of 400mm x 400mm x 50mm. The slabs were cast in plywood moulds, cured for 24 hours, carefully de-moulded to prevent damage, and placed in a curing tank for extended curing. Mechanical testing will follow, assessing flexural strength to evaluate their performance in real-world conditions.

In the numerical design phase, the slab's geometry was defined, and its material properties were assigned in ABAQUS. After setting up boundary and loading conditions, the slab was meshed using linear elements, breaking the model into smaller parts for detailed analysis. A linear static analysis was prepared to study the slab's response under various loads, ensuring the mesh was fine-tuned for accuracy. The analysis results, along with experimental testing, will be presented and assessed in Chapter 8.

Chapter 8: Experimental and Numerical Results and Discussion

8.1 Introduction

This chapter focuses on the comprehensive mechanical evaluation of solar walkable pavement slabs, combining experimental testing and numerical modelling to assess their performance. The chapter is structured into two phases: the Experimental Prototype Analysis and the Numerical Prototype Analysis using ABAQUS. The primary goal is to compare the load-deflection behaviour of the slabs across different design prototypes, highlighting their structural performance and identifying key trends.

In the first phase, experimental results from physical testing are presented, demonstrating the slabs' behaviour under various loading conditions. The second phase involves a detailed numerical analysis using finite element modelling in ABAQUS, focusing on simulating the load-deflection behaviour of the slabs. While the deflection results are directly compared between experimental and numerical findings, a separate stress-strain analysis is also conducted numerically. This provides additional insights into the slabs' mechanical properties, although no direct experimental comparison is made for stress analysis.

The close alignment of the experimental and numerical deflection results validates the accuracy of the numerical model, offering valuable insights into the overall structural integrity of the slabs. By combining both methods, this chapter provides a detailed understanding of the performance, durability, and practicality of integrating solar technology into walkable pavement slabs.

8.2 Experimental Results and Discussion

Following the experimental design, the experimental results provided valuable insights into the behaviour of the solar walkable slabs. The results focus on load-deflection curves, mechanical properties, and the overall performance of the different design prototypes. The discussion compares the flexural strength of the slabs, highlighting the impact of the recycled materials used in each design mix. Further analysis reveals the relative performance of foamed concrete versus traditional concrete mortar mixes. Table 8-1 presents the experimental outcomes for solid slab bases fabricated from various recycled materials as part of this study. The table indicates the flexural result of the slabs as each recycled material brings its unique characteristics to the solid slab.

Figure 8-1 provides a graphical representation of the behaviour of these materials under test conditions. The graph plots critical performance indicators like flexural strength against each type of recycled material used. According to the finding, and can be seen in Figure 8-1, the control slab with normal foamed concrete mortar demonstrated a maximum applied load of 5.48 kN with a corresponding deflection of 1.7 mm. This result is a baseline for comparison with the modified foamed concrete slabs. The control sample's relatively high load-bearing capacity and moderate deflection indicate a balanced stiffness and ductility, making it suitable for general structural applications.

The NFC slab, which represents standard foamed concrete without any special modifications, displayed a slightly lower maximum applied load of 4.2 kN and a deflection of 1.39 mm. Compared to the control slab, the NFC slab reduces load capacity and deflection, reflecting its slightly lower stiffness and strength. The decrease in performance could be recognised by the inherent properties of NFC, which typically have a lower density and strength than normal foamed concrete mortar.

Table 8-1: Flexural Strength and Deflections of Slabs

Foamed Concrete Design Mix	Material Replacement or Addition	Maximum Applied Load (kN)	Maximum Deflection	Note
Material type	(%)	Density 1400, (kg/m³)	(mm)	Description
Control	0	5.48	1.7	Normal mortar density = 2160, (kg/m ³)
NFC	0	4.2	1.39	Normal Foamed concrete
WSF	50	4.1	1.35	Replaced with normal sand (Mass)
PO	10	3.9	1.3	Replaced to the mortar cube by (Volume)
RSTF	1	4.58	1.69	1% of the cement amount added (Mass)
SPs	1	4.56	1.46	1% of the cement amount added (Mass)

The slab with 50% waste foundry sand (WFS) replacing normal sand showed a maximum applied load of 4.1 kN and a deflection of 1.35 mm. These results are very close to those of the NFC slab, indicating that replacing half of the normal sand with WFS does not significantly degrade the mechanical performance of the slab. The deflection is slightly less than that of the NFC slab,

suggesting a marginal increase in stiffness, likely due to the different particle characteristics of WFS compared to normal sand. However, the slight reduction in load capacity indicates that the WFS replacement still impacts the overall strength of the slab.

The slab containing 10% polystyrene replacement by volume showed a maximum applied load of 3.9 kN with a deflection of 1.3 mm. This slab demonstrated the lowest load-bearing capacity among the tested samples, indicating that the inclusion of polystyrene significantly reduces the slab's strength. The lower deflection, however, suggests that the slab is relatively stiff, possibly due to the polystyrene's influence on the matrix structure, which reduces its ability to deform under load. This increased stiffness, combined with reduced strength, points to a more brittle behaviour, where the slab can withstand less load before failing.

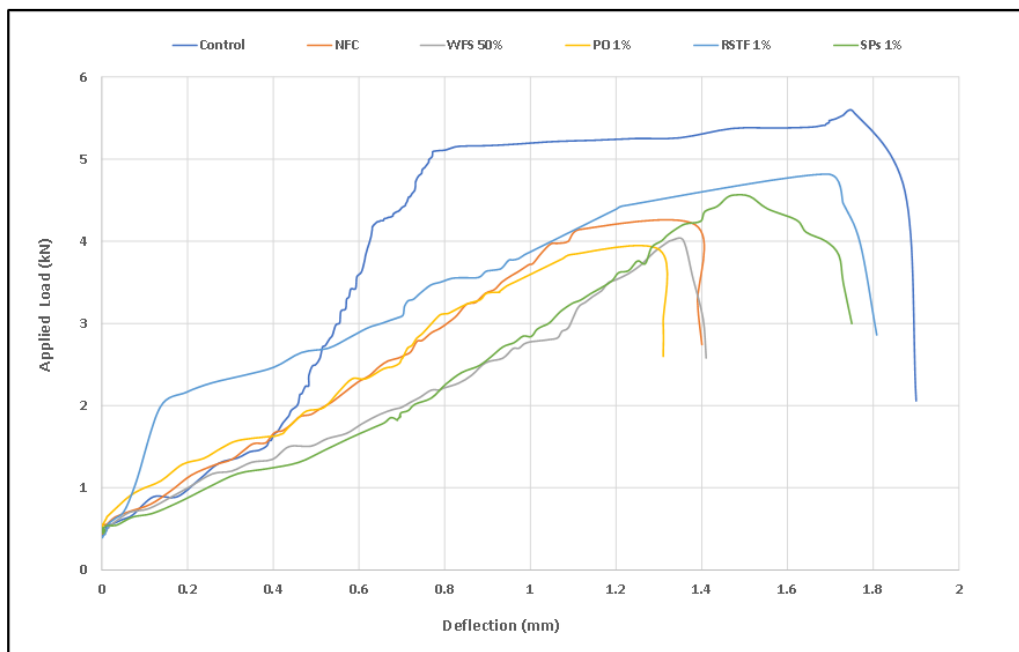


Figure 8-1: Experimental Results for Concrete Slab

Adding 1% recycled steel tyre fibre to the cement ratio resulted in a slab with a maximum applied load of 4.58 kN and a deflection of 1.69 mm. This slab demonstrated enhanced performance compared to the NFC and WFS-replaced slabs, with an increased load-bearing capacity close to that of the control sample. The deflection was also close to the control's, suggesting that the steel fibres contribute significantly to both strength and ductility. The fibres likely help bridge micro-cracks and distribute stress more evenly across the slab, which enhances both stiffness and load-

bearing capacity without compromising flexibility. Figure 8-2 displays the slabs under applied load through the hydraulic machine.

The slab with 1% superplasticiser added to the cement mix showed a maximum applied load of 4.56 kN and a deflection of 1.46 mm. The performance of this slab is similar to that of the slab with steel fibres, indicating that the superplasticizer enhances the slab's workability and density, leading to improved strength and stiffness. The slightly lower deflection compared to the control suggests that the superplasticiser increases the material's resistance to deformation under load, contributing to a more rigid slab that can still bear a substantial load before failure.

Comparing these slabs, the control slab made with normal foamed concrete mortar displayed the highest load-bearing capacity, indicating that the unmodified material performs best under load. The NFC slab, with slightly lower performance, still serves as a strong baseline but is outperformed by the slabs incorporating recycled steel tyre fibres and superplasticiser, which approach the control slab's load capacity and deflection performance.



Figure 8-2: Flexural Test Under Universal Testing Machine (UTM)

The slabs with waste foundry sand and polystyrene replacements show reduced performance, with the polystyrene slab being the weakest in load capacity. However, both replacements lead to stiffer slabs with lower deflections, indicating a compromise between strength and stiffness that must be considered depending on the intended application. The WFS replacement, while reducing strength

slightly, maintains a good balance of stiffness and load capacity, making it a viable alternative where cost or sustainability considerations are vital.

According to Amran, Farzadnia, and Ali, (2015), the brittleness of foamed concrete can be somewhat controlled by adjusting the mix's density and composition. Adding fibres or other reinforcing materials can improve ductility to some extent, allowing the foamed concrete to absorb and dissipate energy more effectively before failure.

8.3 Numerical Validation

This phase is dedicated to analysing the flexural behaviour of both regular and foamed concrete slabs, focusing on their deflection and failure modes under various loading conditions. The experimental work conducted in the lab provided essential data on load-deflection characteristics, which were subsequently compared with results from finite element analysis (FEA) simulations using ABAQUS. This comparison is a critical step in validating the accuracy of the numerical model, ensuring that it can reliably predict the real-world behaviour of concrete slabs under load. The study highlights the significance of understanding the load-deflection relationship in concrete slabs, which is crucial from a serviceability standpoint. By examining how these slabs respond to bending stresses, the research provides valuable insights into the performance and safety of concrete structures under different loading scenarios. The slabs were subjected to a three-point load test, and the deflections observed in these tests were meticulously compared with those predicted by the FEA model.

The chapter presents and analyses the deflection data and includes graphical representations of load-deflection curves for various types of concrete mixes. It also discusses the finite element analysis model used in the simulations, detailing the software, assumptions, and parameters employed. The comparative analysis between experimental deflection data and numerical simulation results demonstrates the accuracy and reliability of the FEA model, reinforcing its value in structural engineering research and practical applications.

8.3.1 Linear Analysis Method

Linear analysis for a concrete slab, such as the 400x400x50 mm mortar concrete slab and foamed concrete, refers to a finite element analysis (FEA) method where the material behaviour is assumed to be linear elastic. This means that the relationship between stress and strain in the material is directly proportional, following Hooke's Law. In this analysis, the slab is subjected to loads, and

the resulting stresses, strains, and displacements are computed under the assumption that the material will return to its original shape once the loads are removed without any permanent deformation. This type of analysis is typically used for developments where the applied loads are relatively small, and the material does not experience significant cracking, plastic deformation, or other nonlinear behaviours. Figure 8:3 brief steps of the leaner methods for the provided slabs details.

In the context of ABAQUS, a linear analysis involves creating a model of the slab with defined material properties like Young's modulus and Poisson's ratio, which are constants that describe the stiffness and compressibility of the mortar concrete.

The slab is then meshed into smaller finite elements, and boundary conditions, such as fixed supports, are applied to simulate how the slab is held in place. Loads are applied to the model, and the software solves the equations governing the material's response to these loads. The results provide insight into the slab's behaviour, including the distribution of stress and strain, the displacement of the slab under load, and the reaction forces at supports. This analysis is crucial in understanding how the slab will perform under service loads, ensuring it can safely support the applied forces without excessive deformation or failure.

8.3.2 Load Deflection Analysis

The ultimate load for the normal concrete slab was 5.6 kN, while the foamed concrete contained 50% of the waste foundry sand of the slab could withstand 4.1 kN. These loads were used in ABAQUS simulations to analyse the deflection of the slabs under the applied loads. The numerical results from the ABAQUS simulations indicated that the normal concrete slab experienced a deflection of 1.55 mm, while the foamed concrete slab showed a deflection of 1.2 mm under the same loading conditions, see Figure 8-3. These numerical deflection results will now be compared with the deflection results obtained from experimental tests conducted under the same loading conditions. This comparison is crucial for validating the accuracy and reliability of the numerical model used in the ABAQUS simulations, ensuring that the model accurately represents the real-world behaviour of both types of concrete slabs.

The deflection results from the ABAQUS simulations indicate that the normal concrete slab demonstrated slightly more deflection than the foamed concrete slab. This outcome is somewhat expected, as normal concrete generally has higher stiffness compared to foamed concrete. The difference in deflection (1.55 mm vs. 1.2 mm) suggests that while foamed concrete is less stiff

than normal concrete, the difference in their deflections under similar loading conditions is relatively small. This might imply that the foamed concrete slab, despite its lower density and stiffness, still performs comparably well in terms of deflection when subjected to the same load.

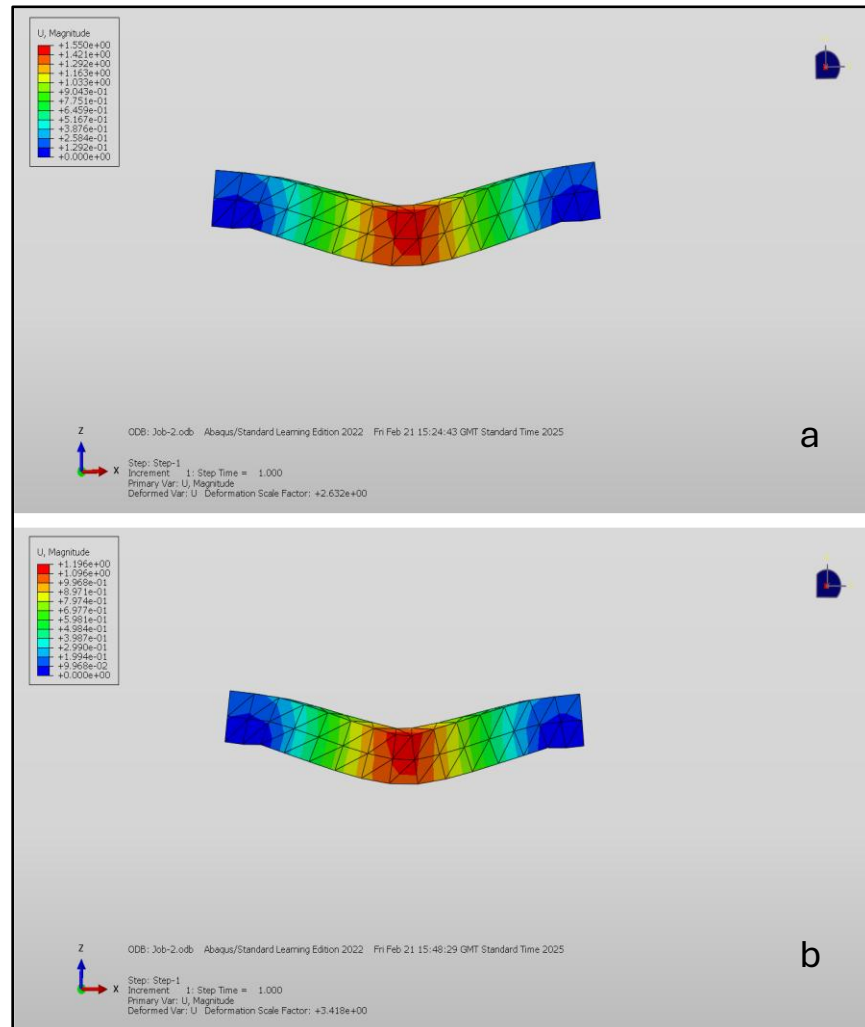


Figure 8-3: Solar Slab Deflection Analysis – (a) Normal Concrete Mortar, (b) Foamed Concrete

The ultimate load capacities of 5.6 kN for the normal concrete and 4.1 kN for the foamed concrete also reflect the inherent differences in material properties between the two types of concrete. Normal concrete, being denser and more robust, can carry a slightly higher load before failure. However, the foamed concrete, while lighter, still demonstrates a significant load-bearing capacity, making it a potentially viable option in applications where weight reduction is crucial. Figures 8-4a and 8-4b only present the deflection of the slab from a different angle with the same applied load.

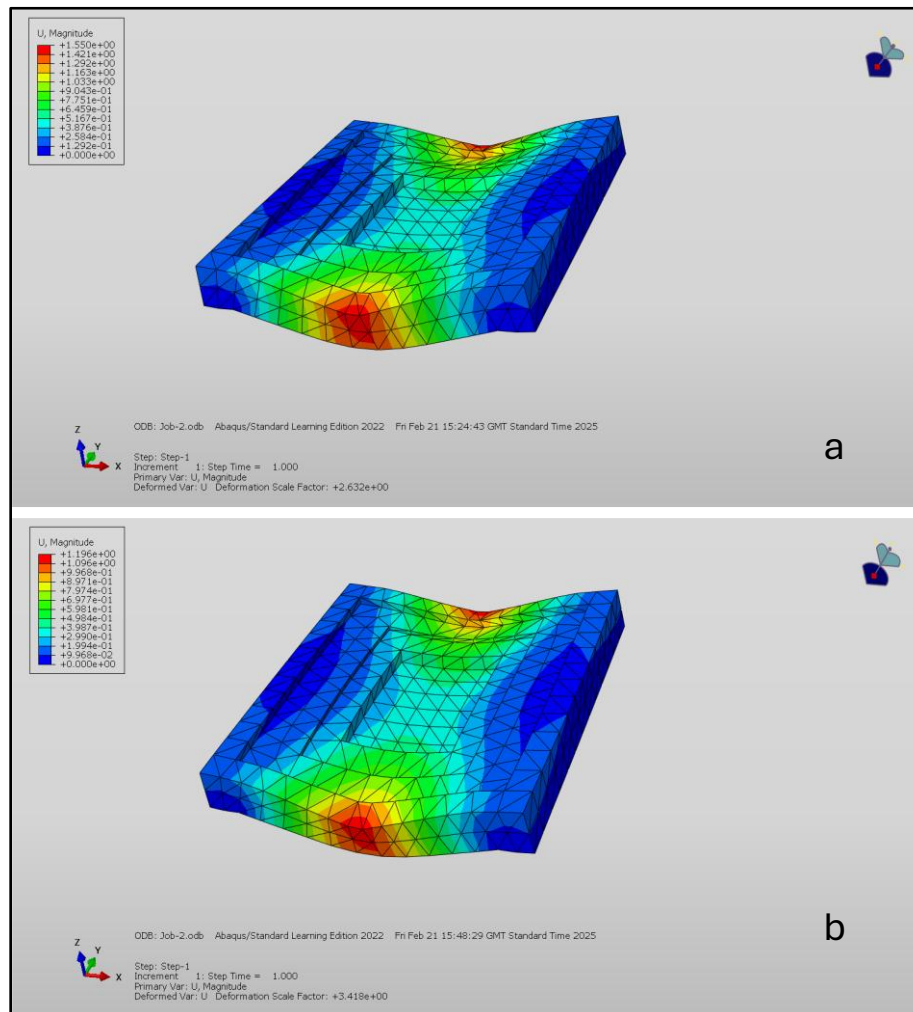


Figure 8-4: Solar Slab Deflection Analysis Presented from Different Angles

8.3.3 Deflection Comparison

The analysis and comparison of the numerical and experimental results for the two concrete slabs, one constructed from normal concrete (NC) and the other from foamed concrete containing 50% waste foundry sand (wfs), revealed interesting findings see Figures 8-5 and 8-6. According to the ABAQUS simulation, the deflections under load were calculated as 1.55 mm for the normal concrete slab and 1.2 mm for the foamed concrete slab. On the other hand, experimental data indicated slightly higher deflections, measuring 1.74 mm for the normal concrete and 1.36 mm for the foamed concrete made with 50% waste foundry sand.

The experimental results highlight a closer deflection response between the two materials, with only a 0.38 mm difference between the NC slab's deflection (1.74 mm) and the FC with the waste foundry sand slab's deflection (1.36 mm). This further supports the idea that using foamed concrete

with 50% WFS as a sustainable alternative to normal concrete does not drastically compromise the slab's structural performance in terms of deflection.

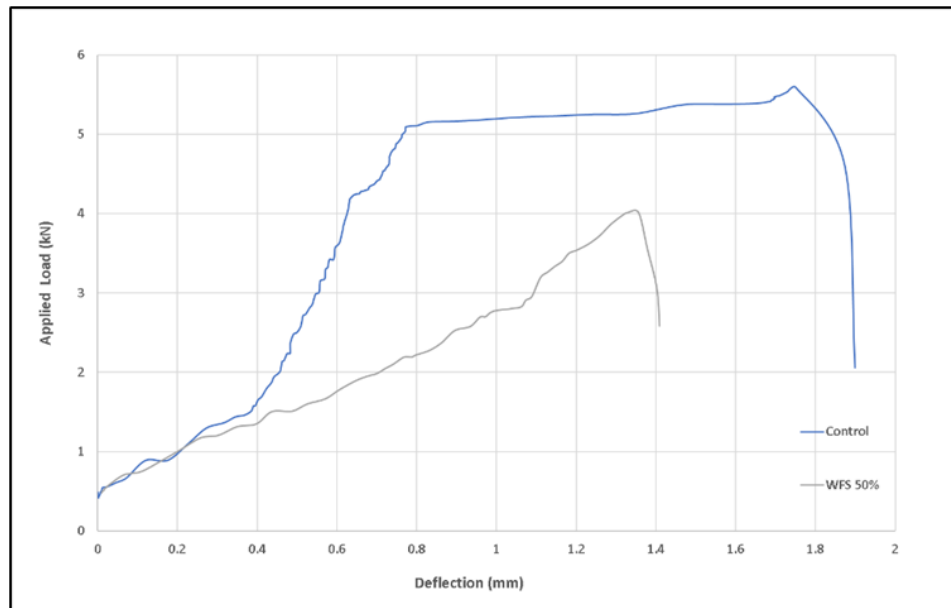


Figure 8-5: Experimental Comparison of the Control Slab and the Slab with 50% WFS

When comparing numerical and experimental results, the experimental deflections were slightly higher than the numerical predictions. For the NC slab, the experimental deflection was 1.74 mm compared to the simulated 1.55 mm, resulting in a difference of 0.19 mm. Similarly, the FC slab contained 50% of (wfs) experimental deflection at 1.36 mm, slightly exceeding the numerical result of 1.2 mm by 0.16 mm. These differences, although minor, indicate that the numerical model provides a reasonably accurate approximation of real-world behaviour, though factors such as material imperfections or boundary conditions in the experimental setup may contribute to the higher deflections observed in practice. See Figures 8-6 and 8-7 for the comparison between experimental and numerical definitions.

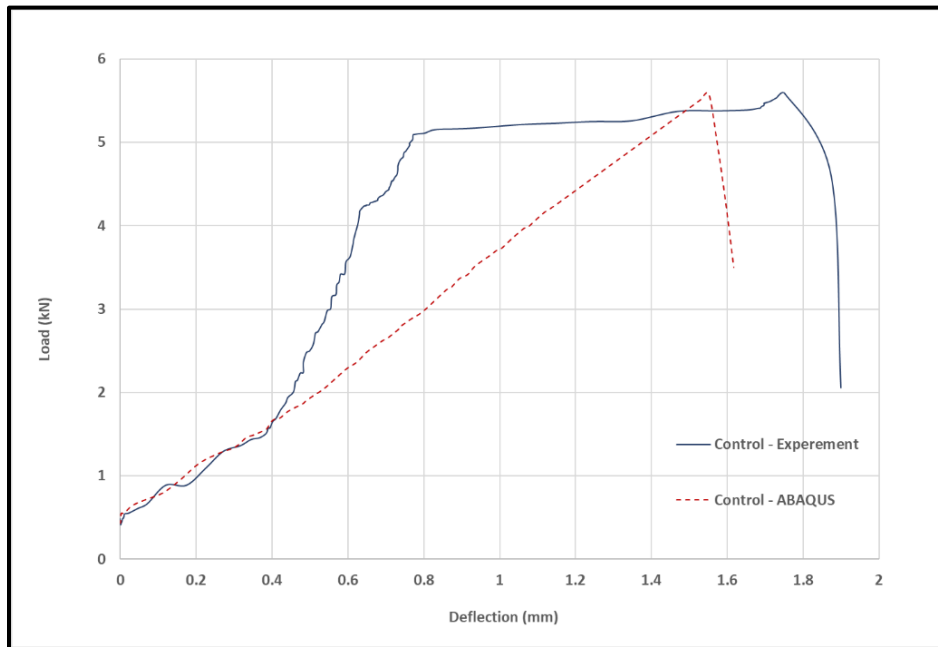


Figure 8-6: ABAQUS vs Experimental Analysis for Control Sample

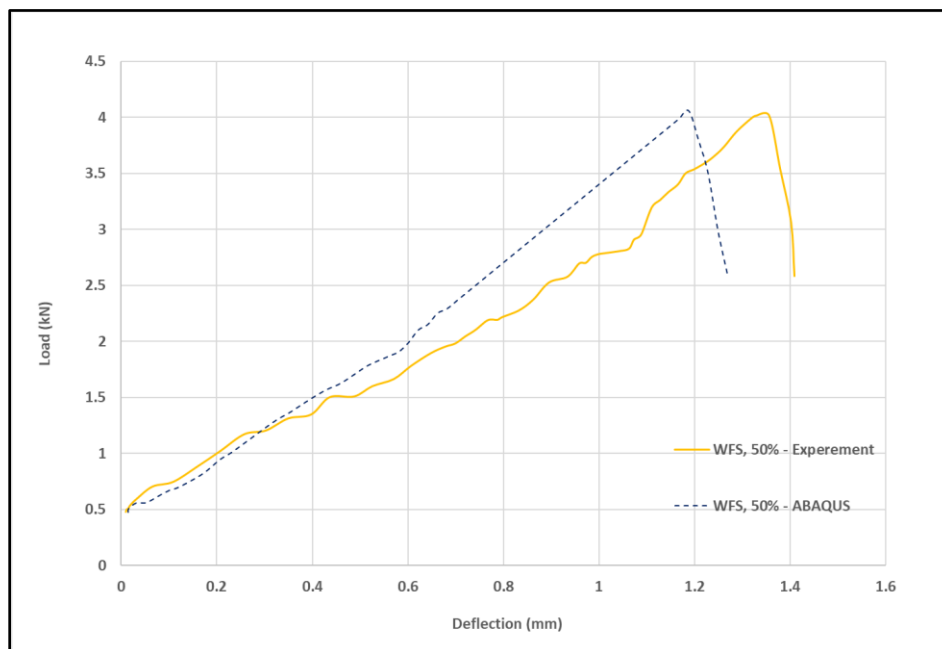


Figure 8-7: ABAQUS vs Experimental Analysis for Sample Made with WFS

The comparison between experimental and numerical results validates the ABAQUS model as a reasonably accurate tool for predicting NC and FC slab deflection. The minor discrepancies between the two suggest that the model could be fine-tuned with further refinement to account for the minor experimental variations. Ultimately, the findings indicate that foamed concrete, despite

its lower stiffness, is a viable alternative to normal concrete. It offers similar structural performance while contributing to sustainability by incorporating recycled materials.

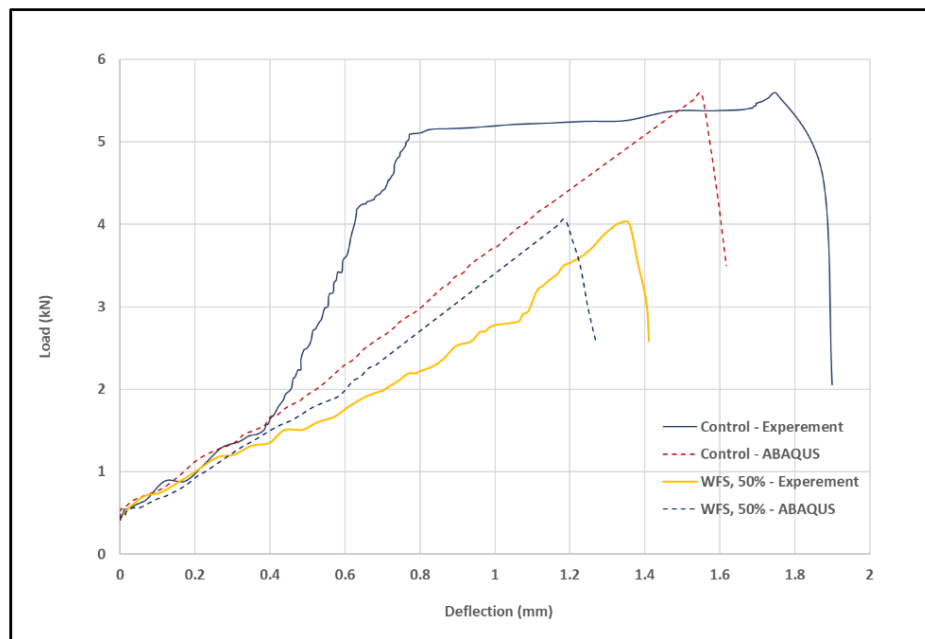


Figure 8-8: ABAQUS vs Experimental Analysis Comparison

8.3.4 Stress and Strain of Concrete Slabs

Understanding the stress and strain responses of concrete slabs under various loading conditions is pivotal in structural engineering. This analysis aims to provide an overview of the stress-strain behaviour of normal concrete (NC) and foamed concrete (FC) slabs, particularly focusing on their flexural performance.

8.3.4.1 Stress

Stress analysis involves determining the internal forces that develop within a material in response to external loading. The bending stresses occur due to the applied loads for the concrete slabs studied. For a normal concrete slab, the applied load of 5.6 kN demonstrated bending stresses concentrated at the mid-span, where the load was applied. The stress distribution across the cross-section of the slab showed that the maximum tensile stress occurred at the bottom fibre, while the maximum compressive stress was observed at the top fibre. Similar stress distribution patterns for the foamed concrete slab were observed under an applied load of 4.1 kN. However, due to the lower modulus of elasticity of the foamed concrete, the stresses were less compared to a normal concrete slab.

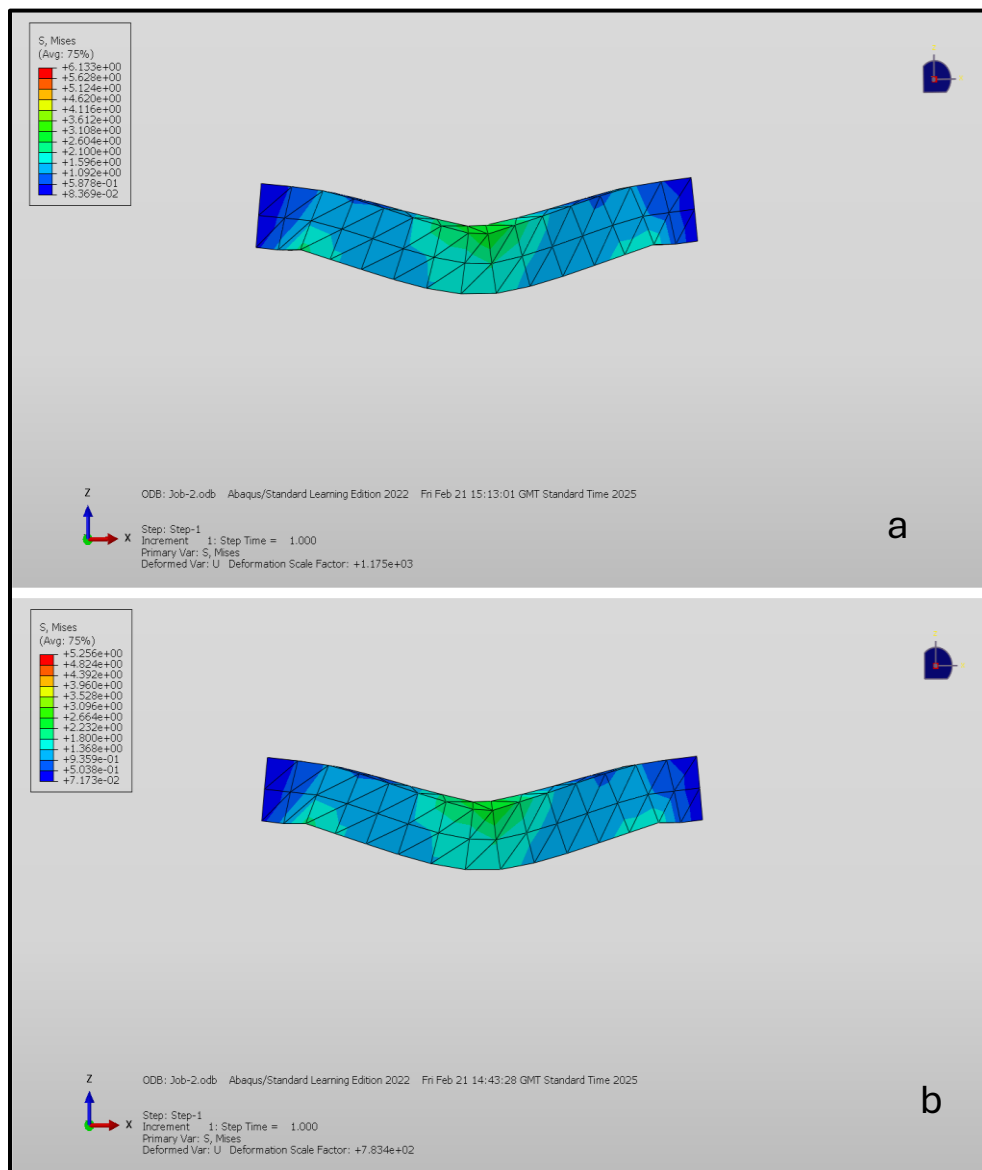


Figure 8-9: Numerical Stress Value, (a) Normal Concrete Slab, (b) Foamed Concrete Slab

The bending stresses observed in both the normal concrete slab and the foamed concrete slab, despite being different in magnitude (6.13 MPa for the normal concrete slab and 5.25 MPa for the foamed concrete slab), could be considered negligible due to the overall setting of the load conditions. Given the relatively low applied loads of 5.6 kN for the normal concrete and 4.1 kN for the foamed concrete, the resulting bending stresses, though measurable, are not significant enough to cause substantial deformation or failure in either slab.

In structural applications where the bending stresses are well below the material's yield strength, these stresses are often considered negligible because they do not compromise the structural

integrity or performance of the slabs. Therefore, the minor bending stresses in both slabs under these specific loading conditions suggest that both materials can safely support the applied loads without experiencing significant bending-related issues. See Figure 8-9 for the bending stees of both slabs made with normal concrete mortar (NC) and foamed concrete (FC).

8.3.4.2 Strain

Strain analysis provides insight into the deformation characteristics of the material under loading. Strains were measured at various points along the slab's length to capture flexural behaviour accurately. The strain distribution for the normal concrete slab showed higher values at the mid-span, corresponding to the regions of maximum deflection. The strain values indicated the extent of deformation the slab underwent, validating the slab's flexural rigidity. The foamed concrete slab displayed a more uniform strain distribution along its length. The lower modulus of elasticity resulted in higher strains for a given load than normal concrete, reflecting the material's increased flexibility and lower stiffness. See Figure 8-9a and 8-9b for both slab's strain values.

The strain values recorded from the ABAQUS simulation for the concrete slabs under different applied load levels were 0.043 and 0.033. Since strain is a dimensionless quantity, these values represent the deformation ratio to the material's original length. A strain value of 0.043 indicates that the material has undergone a deformation of 4.3% of its original length, while 0.033 indicates a 3.3% deformation. Both values suggest minor strain, which is likely negligible in the overall structural performance. However, as shown in Figure 8-10b, slight stress caused by the pressure applied was observed at the bottom of the middle span in both slabs made with normal mortar and foamed concrete. This minor stress reflects localised areas of strain, but given the overall low strain values, this effect is not expected to affect the structural integrity of the slab significantly.

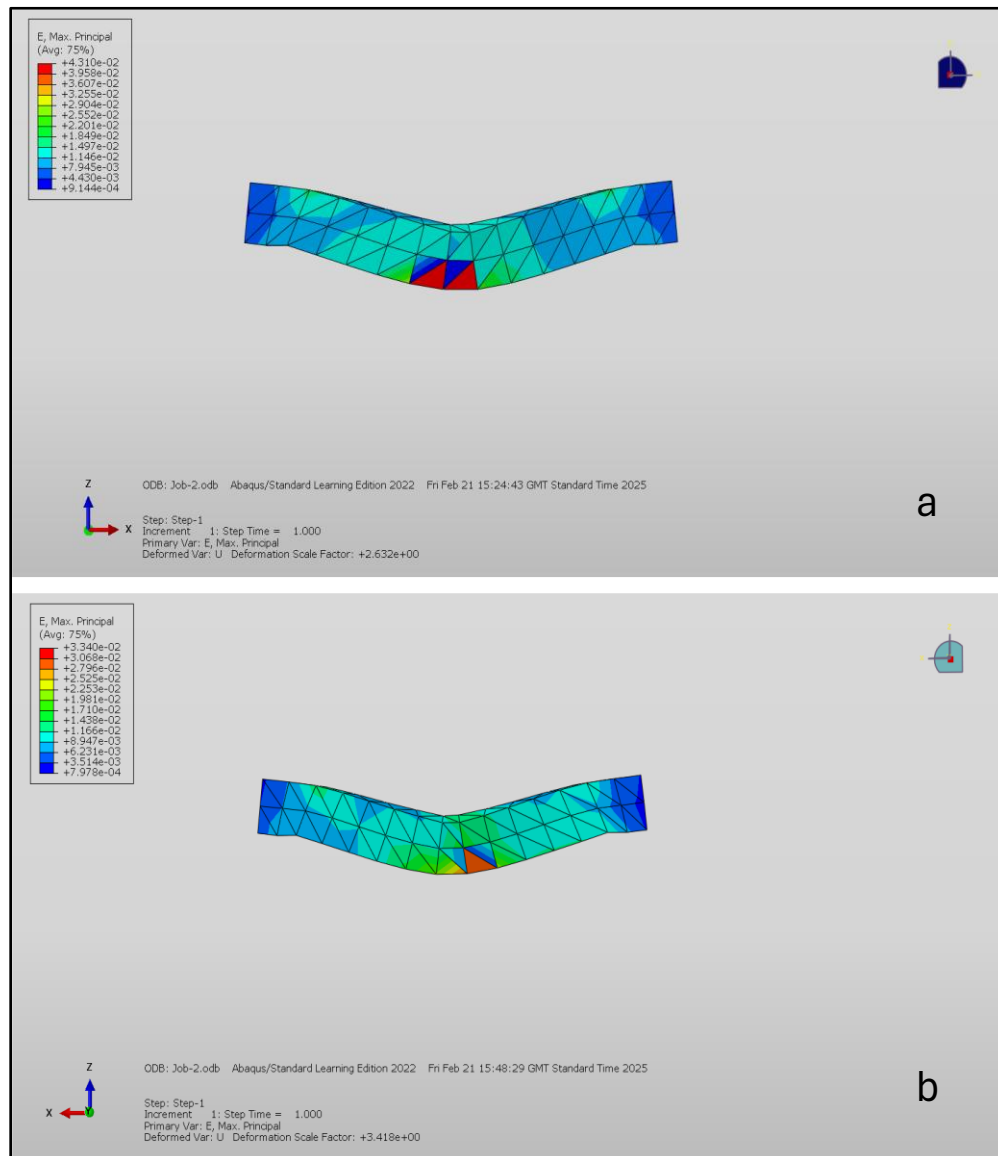


Figure 8-10: Numerical Strain Value, (a) Normal Concrete Mortar, (b) Foamed Concrete

8.4 Rationale for Selecting a Slab with 50% Waste Foundry Sand

The decision to select the slab made from 50% waste foundry sand for the final product is based on several compelling reasons that align with both academic research and sustainability purposes. First and foremost, waste foundry sand (WFS) provides an economically viable and environmentally friendly alternative to traditional sand. Foundry sand is a by-product of the metal casting industry, and its use in concrete significantly reduces the demand for natural sand, thereby addressing the growing issue of sand depletion in construction. Reusing industrial waste

contributes to sustainable construction practices and minimises the environmental footprint of the final product.

From a mechanical performance perspective, the experimental results demonstrated that the slab incorporating 50% WFS maintained a suitable balance between strength and stiffness. Although the load-bearing capacity was slightly lower than the control slab, it still provided sufficient strength for practical applications, with minimal reduction in performance. The slightly increased stiffness due to the particle characteristics of WFS contributed to a lower deflection than other designs, making the slab ideal for use in applications where reduced deformation is critical.

Moreover, the choice of 50% WFS aligns with cost efficiency and material availability, as waste foundry sand is readily accessible and often considered a waste product by industries. Utilising WFS in solar walkable slabs not only reduces material costs but also promotes circular economy principles by converting waste into valuable construction material.

Finally, the use of WFS addresses a key research gap in the field of sustainable construction. Incorporating recycled industrial materials such as WFS into concrete mixes has been studied, but large-scale applications in solar pavement slabs remain relatively unexplored. This thesis not only demonstrates the technical feasibility of using WFS but also contributes to the growing body of knowledge on sustainable material integration in civil engineering, making the research both novel and impactful in addressing contemporary environmental challenges.

In conclusion, the 50% WFS slab offers a robust, cost-effective, and sustainable solution for solar walkable pavement slabs, combining mechanical performance, environmental benefits, and sustainability goals. It stands out as the optimal choice for the final product in this research, with significant implications for the future of green construction.

8.5 Summary

This chapter focused on the experimental and numerical analysis of solar walkable pavement slabs incorporating various recycled materials. A total of 18 slabs, produced from six different design mixes, were tested to assess their mechanical properties under different loading conditions. The design mixes included combinations of waste foundry sand, polystyrene, recycled steel tyre fibres, and superplasticizers, each contributing to the flexural, compressive, and tensile strength of the slabs.

Through experimental testing, the slabs' load-deflection behaviour was evaluated, with the control slab made of normal concrete mortar serving as a baseline for performance comparison. The

numerical analysis using finite element analysis (FEA) in ABAQUS simulated the deflection behaviour, with results closely matching the experimental data. The chapter concluded with a comparative analysis of both experimental and numerical findings, confirming the validity of the numerical model and providing insights into the structural integrity of the slabs.

Chapter 9: Final Design and Evaluation of Solar Walkable Slab

9.1 Introduction

This chapter focuses on the final design of the solar walkable slab with concrete-based material, incorporating both structural development and electrical analysis. The optimised slab design, featuring 50% waste foundry sand (WFS), is now ready for installation and testing. The primary goal is to assess the slab's performance in terms of energy generation, structural integrity, and overall user experience. Following the rigorous experimental and numerical analysis conducted in previous chapters, this chapter presents the practical aspects of integrating the solar slab into real-world conditions. The chapter also examines how the slab handles pedestrian loading, environmental stresses, and power generation, paving the way for future applications of sustainable, energy-generating pavements.

The final slab design represents the culmination of experimental investigations and material testing aimed at developing a lightweight, durable, and energy-efficient walkable pavement solution. Special attention was given to selecting the optimal mix design and ensuring compatibility between structural and electrical components. The slab is designed to withstand not only pedestrian traffic but also environmental factors such as moisture, temperature variations, and mechanical wear. This final stage integrates structural performance with functional energy generation, creating a product capable of supporting both load-bearing and power-generating functions.

The structural development process ensured that the slab could endure pedestrian traffic and weather conditions while maintaining energy production efficiency. The electrical analysis examines the slab's solar power generation and the performance of the integrated electrical components, such as photovoltaic cells, batteries, and LED lighting. The system's operational efficiency is evaluated under varying environmental conditions, including summer and winter, providing insights into the slab's reliability and energy output. See Figure 9-1 for the complete design of the solar table slab. Figure 9.1: Complete Final Product Made from Concrete-Based Material – Solar Slab Design



Figure 9-1: Final Product Solar Slab Design Made from Concrete-Based Material

9.2 Structural Development

The integration of solar technology into walkable pavement slabs presents a dual challenge. creating a pedestrian-friendly surface while ensuring efficient energy generation. Structurally, the slabs must withstand pedestrian loads, resist static and repeated stresses, and provide a safe surface with adequate friction. Simultaneously, the surface must allow sunlight to penetrate the embedded photovoltaic cells for energy conversion.

Achieving the right balance between surface texture for safety and transparency for solar efficiency is key. The design employs a transparent protective layer cantilevered above the solar cells, ensuring the layer is robust enough to prevent deflection and damage to the cells beneath. This protective layer is also designed to be weatherproof, shielding the system from moisture and contaminants while maintaining structural integrity.

On the electrical side, the slab integrates photovoltaic cells configured to convert solar energy into electricity, which is stored in batteries and used to power LED lighting and other devices. The development process involved iterative testing to ensure optimal integration of structural and electrical components, with an emphasis on maximising energy transfer efficiency while maintaining durability.

The second phase of the project focused on the electrical analysis, assessing the slab's performance in various environmental conditions, particularly during summer and winter. The analysis

measured the current generated by the photovoltaic cells, battery performance, LED lighting efficiency, and environmental factors such as temperature and humidity. The data collected from these tests provided insights into the slab's power generation capabilities and highlighted areas for potential improvement.

The final assembly involved sealing the solar panel with a transparent top layer, followed by thorough testing of the electrical connections to ensure functionality. After testing, the slab was prepared for installation, including site preparation and drainage system installation, to ensure long-term performance. This comprehensive approach ensured the final product met both structural and electrical requirements, providing a viable and sustainable solution for solar walkable pavement slabs. This chapter integrates both structural and electrical analyses, offering a complete understanding of the slab's capabilities, durability, and energy generation potential. The findings provide valuable insights into the slab's load-deflection behaviour and electrical performance, serving as a foundation for future developments in the field of solar-powered infrastructure.

9.2.1 Material Analysis

In the material analysis phase, different materials were comprehensively evaluated to identify those best suited for the solar pavement slab panel. Key considerations included mechanical strength, elasticity, density, durability, slip resistance and resistance to environmental factors such as UV radiation and temperature fluctuations. The analysis focused on several materials:

9.2.2 Traditional Slab Analysis

A traditional pavement slab measuring 400x400x50mm typically weighs around 19-22 kg and is made from a concrete mix comprising cement, sand, gravel, and water, sometimes with additives to enhance durability according to Gurjar, A. & Chandak, R. (2013). These slabs generally have a compressive strength ranging from 30 to 40 MPa, a flexural strength of 5 to 10 MPa, and a modulus of elasticity typically around 15 to 20 GPa, with a density of approximately 2100 kg/m³. They are designed to withstand freeze-thaw cycles, varying weather conditions, and pedestrian and vehicle traffic, with good abrasion resistance and moderate chemical resistance. The surface finish can vary, offering smooth, textured, and patterned options for aesthetic appeal and slip resistance. These slabs are relatively easy to install and require minimal maintenance, making them suitable for pedestrian pathways, patios, and areas with light vehicle loads such as bicycles and small carts,

according to Neville, A.M. (2011). Table 9-1 details the compressive and flexural strength of normal mortar concrete.

Table 9-1: Mechanical Properties of Traditional Slab Material (Neville, 2011)

Materials	Compressive Strength of Cube (MPa)	Flexural Strength of Slab (MPa)	Young's Modulus (GPa)	Density (kg/cm³)
Normal Concrete Mortar	30 - 40	5 -10	25 - 35	2180

9.2.3 Mechanical and Functionality

Solar pavement slabs, particularly those measuring 400x400x50 mm, are designed to incorporate both structural integrity and functionality. These slabs usually feature a base made of foamed concrete and a top layer of acrylic plastic (Acrylic PPMA), with each material contributing to the overall mechanical properties, including slip resistance—a critical factor for ensuring safety in pedestrian areas. Foamed concrete provides a stable and durable foundation for the solar pavement slab. Key mechanical properties include:

1. **Density and Compressive Strength:** Foamed concrete has a density of 1400 kg/m³ and a compressive strength of a cube of 15.7 MPa; the flexural strength is 0.42 MPa for the current manufactured slab, depending on the mixing ratio. This ensures the slab can support pedestrian and light vehicular loads effectively (Jones & McCarthy, 2005).
2. **Durability:** Its resistance to freeze-thaw cycles and chemical attacks enhances the longevity of the slabs, making them suitable for outdoor applications (Hilal et al., 2015).
3. **Acrylic Top Layer:** Acrylic plastic (Acrylic PPMA), derived from polymethyl methacrylate (PMMA), serves as the protective top layer for the solar cells. This material is selected for its mechanical properties, including:
 4. **Tensile Strength and Impact Resistance:** Acrylic has a high tensile strength (around 70 MPa) and good impact resistance, which protects solar cells from mechanical damage (Strong, 2006).
 5. **Transparency and UV Resistance:** Acrylic's high transparency allows maximum light transmission, while its UV resistance prevents degradation from sunlight exposure, maintaining efficiency and longevity (Domininghaus, 2012).

6. **Scratch Resistance:** Acrylic is resistant to scratches and abrasion, preserving the clarity and functionality of the solar cells (Smith, 2003).
7. **Slip Resistance:** The slip resistance of the acrylic layer is crucial for safety. Acrylic can be textured or treated with anti-slip coatings to improve traction, reducing the risk of slips and falls, especially in wet conditions. Proper texturing and surface treatments can achieve high slip resistance ratings, ensuring safe pedestrian use (Yildirim, 2016).
8. **Impact Resistance:** Acrylic is known for its excellent impact resistance, being about 17 times more impact-resistant than glass of the same thickness.

The mechanical properties of solar pavement slabs, particularly with a foamed concrete base and an acrylic top layer, are designed to ensure structural stability, durability, and safety. The foamed concrete base provides a lightweight yet strong foundation with excellent thermal insulation, while the acrylic top layer ensures protection for the solar cells with high transparency, UV resistance, and enhanced slip resistance through texturing or coatings. These properties make solar pavement slabs a practical and safe solution for integrating solar technology into pedestrian and light vehicular pavements. Tables 9-2 and 9-3 indicated the compressive, flexural and impact resistance of the foamed concrete and the top layer (acrylic plastic) materials.

Table 9-2: Mechanical Properties of the Current Solar Pavement Slab

Materials	Compressive Strength of Cube (MPa)	Flexural Strength of Slab (MPa)	Young's Modulus (GPa)	Density (kg/cm³)	Transparency (%)
Normal Concrete Mortar	31.1	2.52	25 - 35	2160	
Foamed Concrete Mortar	15.7	2.41	1 -12	1400	
Acrylic Plastic	70 - 110	70	2.7 – 3.3	1180	
Optical Clarity					92

Table 9-3: Acrylic Plastic Technical Data (PPMA, Technical Datasheet)

Mechanical Properties		
Tensile Strength	(psi)	8,000 - 11,000
Tensile Modulus	(psi)	350,000 - 500,000
Tensile Elongation at break	(%)	2
Flexural Strength	(psi)	12,000 - 17,000
Flexural Modulus	(psi)	350,000 - 500,000
Compressive Strength	(psi)	11,000 - 19,000
Compressive Modulus	(psi)	-
Hardness	Rockwell	M80 - M100
IZOD Notched Impact	(ft-lb/in)	0.3
Thermal Properties		
Coefficient of Thermal Expansion	(x 10 ⁻⁵ in./in./°F)	5 - 9
Flammability Rating	UL94	-
Heat Deflection Temperature @264	(psi)	150-210 / 65-100
Melting Temp	(°F / °C)	265-285 / 130-140
Max Operating Temp	(°F / °C)	150-200 / 65-93

9.2.4 Solar Pavement Slab Structural Design

The solar pavement slab design aims to innovate by utilising recycled materials to reduce product cost and optimise self-weight while maintaining high performance. The slab fits seamlessly over the structural base, ensuring pedestrian safety with adequate protection and an aesthetically pleasing finish. This integration results in a robust, efficient, and sustainable product that leverages advanced materials and intelligent design, providing reliable performance in diverse environmental conditions. The structural design of the solar pavement slab comprises two primary components: the structural model and the top layer. The structural model is engineered to provide strength and durability, utilising recycled materials that offer both environmental benefits and cost savings.

This model ensures that the slab can withstand various loads and impacts, making it suitable for pedestrian traffic and other stresses. Together, these components form a solar pavement slab that is not only structurally sound but also environmentally friendly. The use of recycled materials minimises the carbon footprint, and the acrylic top layer provides long-lasting protection and efficiency. This innovative design ensures that the solar pavement slab is a sustainable solution for modern infrastructure, combining functionality, safety, and environmental consciousness.

9.2.5 Actual Prototype Design

The construction of the prototype was completed, and the electrical devices were prepared for integration. Lab technician Mathew Garlic meticulously handled the connections, ensuring that all electronic components were correctly wired and integrated. This step was crucial for validating

the design and ensuring that the system could operate as intended. At the laboratory, various simulation electric tests were conducted to verify that all devices were working perfectly and fit for purpose. These tests confirmed that the components were accurately suited to each other and functioned harmoniously within the prototype, ensuring the reliability and efficiency of the final solar pavement slab. See Figure 9-2 for the electrical dives that are installed within the solar pavement slab sample.



Figure 9-2: Installation of Electrical Devices onto the Concrete Base

The simulation tests included checking the performance of the battery, charger, control systems, and LED strip light under various conditions to mimic real-world scenarios. An essential part of these tests involved the built-in sensor that monitors daylight and darkness. This sensor is designed to automatically turn on the LED lights when it gets dark and turn them off the next morning when daylight appears. The tests verified that the sensor responded accurately to changes in light levels, ensuring the LED lights were activated correctly in low light conditions and deactivated during daylight, thereby optimising energy usage and ensuring consistent operation.

Additionally, detailed inspections were carried out to ensure that all connections were secure and that there was no risk of short circuits or other electrical failures. This meticulous process not only validated the design but also ensured that the prototype met all safety standards and performance criteria. The successful completion of these tests and inspections demonstrated the robustness and functionality of the solar pavement slab, paving the way for its application in real-world settings.

9.2.5.1 OMEGA Data Logger Loggers

The OM-CP-VOLT101A is a versatile voltage data logger designed for precise monitoring and recording of voltage levels over time. This device is particularly valuable in various industries where accurate voltage measurements are crucial, such as in electrical systems, manufacturing processes, and environmental monitoring. It can measure a wide range of voltages, making it suitable for different applications. The OM-CP-VOLT101A is capable of recording voltages from -2 V to 30 V, providing flexibility in monitoring various electrical systems. With an accuracy of $\pm 0.1\%$ of the reading and a resolution of 0.01 V, the data logger ensures precise and reliable voltage measurements, which is essential for critical applications where even small deviations can be significant.

The OM-CP-VOLT101A features a substantial memory capacity, capable of storing up to 2,064,384 readings. This extensive storage allows for long-term monitoring without the need for frequent data retrieval. The device is equipped with an easy-to-use software interface, enabling users to configure the device, download data, and analyse the recorded voltage levels. The software provides graphical and tabular data representations, facilitating a comprehensive analysis. Powered by a long-life lithium battery, the data logger can operate for extended periods, reducing the need for frequent maintenance. Its rugged construction ensures durability and reliable performance even in harsh environments.

The OM-CRHTEMP101A is a compact and reliable data logger designed for monitoring and recording humidity and temperature levels. This device is essential in environments where maintaining specific climate conditions is critical, such as in laboratories, storage facilities, and HVAC systems. The OM-CRHTEMP101A can simultaneously measure and record both humidity and temperature, providing a comprehensive overview of the environmental conditions. This dual functionality is crucial for applications where both parameters are interdependent. The data logger ensures precise environmental monitoring with an accuracy of $\pm 3\%$ RH for humidity and $\pm 0.5^\circ\text{C}$ for temperature. Accurate data is vital for maintaining optimal conditions in sensitive environments.

The OM-CRHTEMP101A can store up to 1,000,000 readings, allowing for prolonged monitoring periods without data loss. This feature is particularly useful for long-term studies and monitoring projects. The device includes intuitive software for configuration, data retrieval, and analysis. Users can easily view and analyse the recorded data, generating reports and graphs to assess

environmental conditions. The data logger operates on a long-life lithium battery, ensuring continuous operation for extended periods. Its compact and portable design makes it convenient for deployment in various locations, providing flexibility in monitoring different environments. Built to withstand challenging conditions, the OM-CRHTEMP101A is designed for durability and consistent performance, ensuring reliable data collection even in demanding environments.

Both the OM-CP-VOLT101A voltage data logger and the OM-CRHTEMP101A humidity and temperature data logger play crucial roles in monitoring and recording essential parameters in various industrial and environmental applications. Their high accuracy, extensive data storage, and user-friendly interfaces make them invaluable tools for ensuring optimal operation conditions and maintaining the integrity of sensitive environments. Four OMEGA data loggers have been strategically placed within a solar slab cavity to monitor various parameters in the setup. These loggers are crucial for capturing the performance and environmental conditions inside the solar slab, ensuring efficient operation and maintenance. See Figure 9-3 for the data logger devices.

1. Recording Solar Panel Voltages

The first OM-CP-VOLT101A data logger is used to monitor the voltage generated by the solar panels from the sun during the day. This data logger captures the voltage output fluctuations as the sunlight intensity varies throughout the day. By recording these voltage levels, it is possible to assess the efficiency of the solar panels, identify peak performance periods, and detect any anomalies or drops in performance which could indicate issues such as shading or panel degradation.

2. Recording Charging Battery Voltages

The second OM-CP-VOLT101A data logger is dedicated to monitoring the voltages of the charging batteries within the solar slab. This logger tracks the voltage levels as the batteries charge and discharge. By analysing this data, one can determine the charging efficiency and the state of charge (SOC) of the batteries and identify any potential problems with the charging system, such as overcharging or undercharging, which could affect the overall lifespan and performance of the batteries.

3. Recording LED Strip Light Voltages

The third OM-CP-VOLT101A data logger is set to record the voltage levels of the LED strip lights embedded in the solar slab. This monitoring ensures that the LED lights receive the correct voltage,

which is crucial for optimal performance and longevity. Fluctuations or deviations in the recorded voltage can help diagnose issues such as wiring problems, power supply inconsistencies, or LED strip failures. Figure 9-3 illustrates four data loggers installed within the solar panel cavity to monitor the device's voltages and temperature & humidity



Figure 9-3: Data Loggers for Voltage and Temperature/Humidity Monitoring

4. Recording Humidity and Temperature

The OM-CRHTEMP101A data logger is employed to monitor the humidity and temperature within the cavity of the solar slab. This logger provides valuable data on how the environmental conditions fluctuate within the slab. Understanding these fluctuations is essential for several reasons:

- **Performance Analysis:** Temperature changes can affect the efficiency of the solar panels and the batteries. Higher temperatures might reduce efficiency, while extreme conditions could damage components.
- **Moisture Control:** Monitoring humidity is critical to preventing moisture buildup, which could lead to corrosion or other damage to the electrical components.
- **Thermal Management:** By understanding temperature trends, better thermal management systems can be designed to maintain optimal operating conditions for all components within the solar slab.

9.2.6 Solar Walkable Slabs Assembly

The diagram illustrates the final assembly of the solar walkable pavement design, showcasing how various solar and electrical components are integrated into the system. The primary component is the solar panel, which harvests solar energy during daylight hours and converts it into electrical power. A charging regulator regulates this energy to ensure the battery is not overcharged. The battery stores the electrical energy and provides power to the system during periods of low sunlight, such as at night.

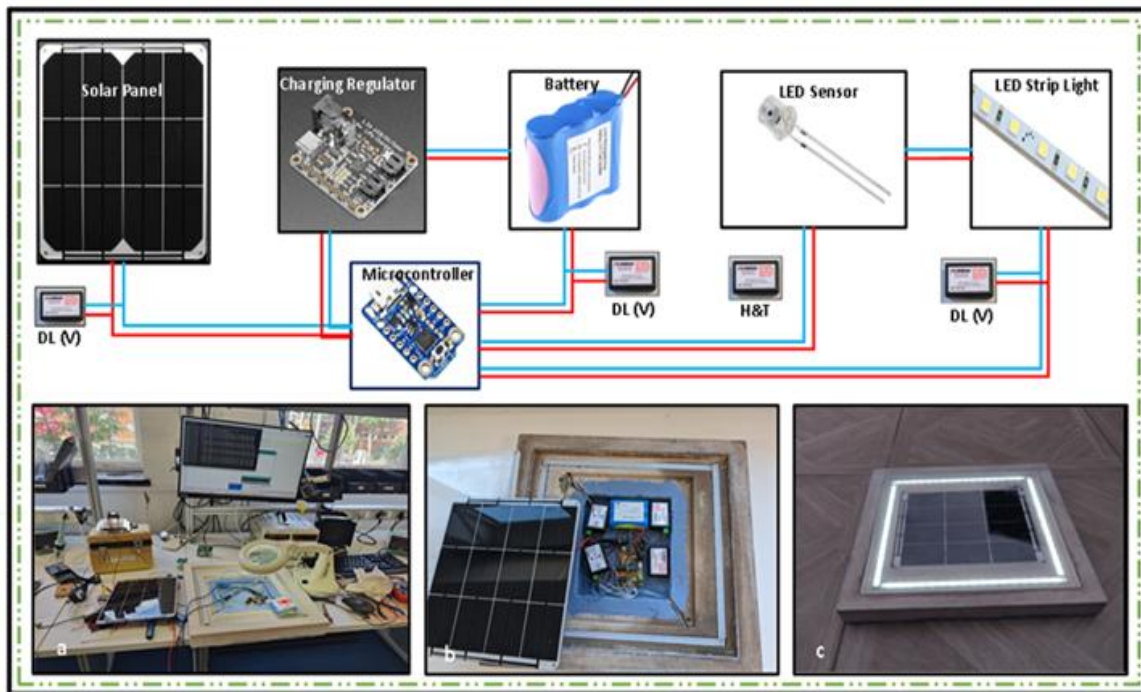


Figure 9-4: Schematic Diagram Showing the Installation of Electrical Devices for Performance Monitoring

A microcontroller is included in the system to manage the overall operations, including input from the sensors and the control of the lighting system. The LED sensor detects environmental conditions like temperature and humidity, providing data to the microcontroller for efficient system management. The system also includes an LED strip light, which illuminates the pavement slab at night or in low-light conditions, powered by the battery. Additionally, digital displays (DL) are placed throughout the system to provide real-time voltage readings, allowing for easy monitoring of the system's performance.

The lower section of the diagram shows images of the assembly process. Image (a) depicts the testing of individual components, including the solar panel, battery, and microcontroller, ensuring proper functionality before integration. Image (b) shows the prototype, where the components are enclosed in the slab base for protection. Image (c) illustrates the final product, a fully integrated solar pavement slab with LED lighting surrounding the solar panel. This design enables the pavement slab to operate efficiently, using renewable solar energy to power the lights and manage energy use sustainably. See Figure 9-4 for the solar walkable pavement slab assembly diagram.

9.2.7 Final Design of Solar Walkable Pavement Slab

The prototype construction of the product showcased in Figures 9-5 represents a fully developed, self-contained solar pavement slab. It integrates advanced materials and smart design to harvest and utilise solar energy efficiently. This innovative slab incorporates a range of integrated devices into a cohesive unit, combining structural integrity with advanced energy management capabilities. The construction involved meticulous planning to ensure seamless integration of all components. The structural base includes a cavity designed to house the electronic components, such as the battery, charger, control systems, and LED strip light, ensuring protection and efficient operation. A key feature of the prototype is the anti-slip surface treatment, ensuring pedestrian safety even in wet conditions. The top layer is made from durable, weather-resistant acrylic plastic, allowing maximum sunlight to reach the solar cells for efficient energy harvesting while protecting the underlying components.



Figure 9-5: Final Prototype Prepared for Testing

The lab technician handled connections and integrations, ensuring all electronic components were correctly wired. Various simulation electric tests were conducted in the laboratory to verify the functionality and compatibility of all devices, including the sensor that automatically controls the LED lights based on ambient light levels. The prototype is now entirely manufactured and ready for user experience trials. The anti-slip solar pavement slab is designed to provide reliable and efficient performance in real-world conditions. This thorough development and testing process ensures that the final product is practical and innovative, ready to meet modern infrastructure needs.



Figure 9-6: Solar Pavement Slab Placed for Testing in Leicester, UK

Figure 9-6 shows the solar pavement slab prototype installed for outdoor testing in Leicester, UK, highlighting its performance across diverse environmental conditions. The top-left image depicts the slab during the daytime, showcasing the integration of a photovoltaic panel with perimeter LED lighting designed to harness solar energy and illuminate the slab during low-light conditions. The top-right image demonstrates the slab's functionality at night, with the LED lights activated using energy stored from the solar panel, enhancing visibility and improving pedestrian safety. The bottom-left image presents the slab embedded in an outdoor paved walkway, indicating its compatibility with urban surfaces and its ability to withstand pedestrian loading. The bottom-right image captures the slab partially covered in snow, emphasising its weather resistance and

durability under winter conditions. These images collectively illustrate the slab's year-round functionality, structural resilience, and ability to generate and utilise renewable energy in real-world applications. The testing phase validates the slab's practical viability, demonstrating that it can maintain both structural and electrical performance across varying environmental conditions, supporting its potential adoption for sustainable pavement systems in urban and public spaces.

9.3 Phase 2: Electrical Analysis and Discussion

This phase explores the comprehensive electric analysis of the solar panel system on two separate occasions, namely summer and winter. This analysis mainly focuses on the maximum current obtained from solar radiation and the data logged by four specific instruments associated with the system: the solar panel, battery, LED light, and an environmental data logger placed on the panel to record temperature and humidity. The subsequent section explained the performance of the devices that were installed within the solar panel over the summer to generate power.

9.3.1 Performance of the Solar Slab in Summer

The experimental setup involved attaching data loggers to various components of a solar panel system to monitor and record critical performance and environmental parameters. Specifically, data loggers were connected to the solar panel to measure voltage and current output, to the battery to track its charging and discharging cycles, and to the LED light to record power consumption and light output. Additionally, two data loggers were placed inside the panel cavity to measure ambient humidity and temperature. The subsequent analysis of the recorded data focused on evaluating the solar panel's efficiency, assessing battery performance, examining the LED light's operational parameters, and understanding the impact of environmental conditions on the overall system. This comprehensive analysis aimed to provide insights into the system's operational efficiency, reliability, and potential areas for improvement.

9.3.2 Solar Panel Performance

The solar panel installed in the user's garden from August 26 to September 10 demonstrated significant performance, as detailed in Figure 9-7. The panel specifications, rated at 9 watts and 6 volts, revealed an overcharge condition during the sunny days of this period, with the panel consistently reaching a maximum voltage of 7.2 volts. This overcharging indicates that the solar panel was highly efficient in converting sunlight into electrical energy, surpassing its nominal voltage rating due to the intense solar exposure.

In August 2023, the UK experienced approximately 13 hours of daylight and 11 hours of night. The panel managed to fully charge during these long sunny days, with the data showing that the maximum current was achieved around midday. From the morning, the current picked up, reaching its peak by mid-afternoon, and gradually decreased towards the evening as sunlight disappeared. Naturally, no current was recorded during the night. This consistent performance pattern underscores the panel's effectiveness in utilising solar energy.

The orientation and placement of the panel significantly influenced its performance. Positioned upright like a typical solar pavement slab, the panel did not benefit from an angled southeast-facing orientation like rooftop installations, which typically maximise sunlight exposure throughout the day. Consequently, the panel was subject to shading from surrounding buildings after 3 pm, reducing its direct sunlight exposure. Despite this, the panel received direct sunlight from 10 am to 3 pm, during which it captured the bulk of its energy. For the remaining daylight hours, the energy was absorbed from ambient daylight rather than direct sunlight. This configuration indicates that even in sub-optimal conditions, the solar panel performed admirably, ensuring sufficient current generation during the prime sunlight hours.

9.3.3 Performance of LED Strip Lights

The solar slab system was equipped with four LED strip lights, each 30 cm in length, arranged in a square around the solar panel. These lights, designed to provide bright illumination at 3 volts, were intended to enhance pedestrian safety by lighting the pathway during the night. The activation and deactivation of the LED lights were controlled by an Adafruit Trinket 3.3V MCU Development Board (product ID: 1500). This microcontroller, equipped with a light sensor, signalled the LED strip lights to turn on when daylight faded in the evening and to turn off when daylight reappeared in the morning.

According to the data logger results shown in Figure 9-7, the LED strip lights functioned effectively throughout most of the monitoring period, providing consistent brightness without significant reduction during the night. This indicates that the system design, including the solar panel and the battery pack, could maintain an adequate power supply to the LED lights throughout the night hours. The LED lights were powered by an RS PRO 3.7V Lithium-Ion Rechargeable Battery Pack of three with a capacity of 7.8Ah, which proved sufficient for nightly operations.

However, disruptions were noted between September 7 and 9. These days, the LED lights have experienced operational issues, likely due to external reflections impacting the sensor. Possible

sources of these reflections include car headlights or nearby streetlights. Since the solar panel and sensor were installed in the back garden where cars typically park, and streetlights are present, these reflections could cause the sensor to misinterpret the ambient light levels, leading to incorrect signalling of the LED lights. Another potential cause of the disruptions could be electrical faults within the solar panel or the sensor system itself. Faulty wiring or connections might have led to irregular signals being sent to the microcontroller, thereby affecting the LED lights' operation.

9.3.4 Battery Performance

The RS PRO 3.7V Lithium-Ion Rechargeable Battery Pack, comprising three units with a total capacity of 7.8Ah, has been integrated into the solar pavement slab system. This battery pack is crucial for storing the energy generated by the solar panel and providing a reliable power source for the LED strip lights during the night. The battery pack demonstrated notable performance throughout the charging and discharging cycles, as illustrated in Figure 9-7.

The battery pack was fully charged on most days during the observation period from August 26 to September 10. The data shows that the battery reached a maximum voltage of 4.19 volts, just shy of its maximum safe charging limit of 4.2 volts. This indicates that the solar panel effectively generated sufficient energy to charge the battery pack daily. The only exception was on August 26, when the voltage fell below 4 volts, possibly due to less sunlight exposure or initial charging conditions.

At night, when the LED strip lights were operational for approximately 11 hours, the battery voltage decreased by only about 0.1 to 0.15 volts. This minimal reduction in voltage signifies that the battery pack had ample capacity to power the lights throughout the night without significant reduction. The steady voltage levels during the night underscore the efficiency of the battery pack in maintaining consistent power output.

The Adafruit Universal USB / DC / Solar Lithium Ion/Polymer Charger (bq24074) plays a critical role in this system by managing the power flow to and from the battery pack. This charger ensures that the battery is charged safely and efficiently, preventing overcharging by regulating the maximum voltage to 4.2 volts. The charger's functionality is vital for protecting the battery pack and prolonging its lifespan, ensuring that it operates within safe voltage limits.

The performance of the RS PRO 3.7V Lithium-Ion Rechargeable Battery Pack within the solar pavement slab system indicates that it is well-suited for the application, providing reliable power storage and output. However, there are several considerations and potential improvements to

optimise the system further. The current battery capacity of 7.8Ah appears sufficient, given the minor voltage drop observed during nighttime use.

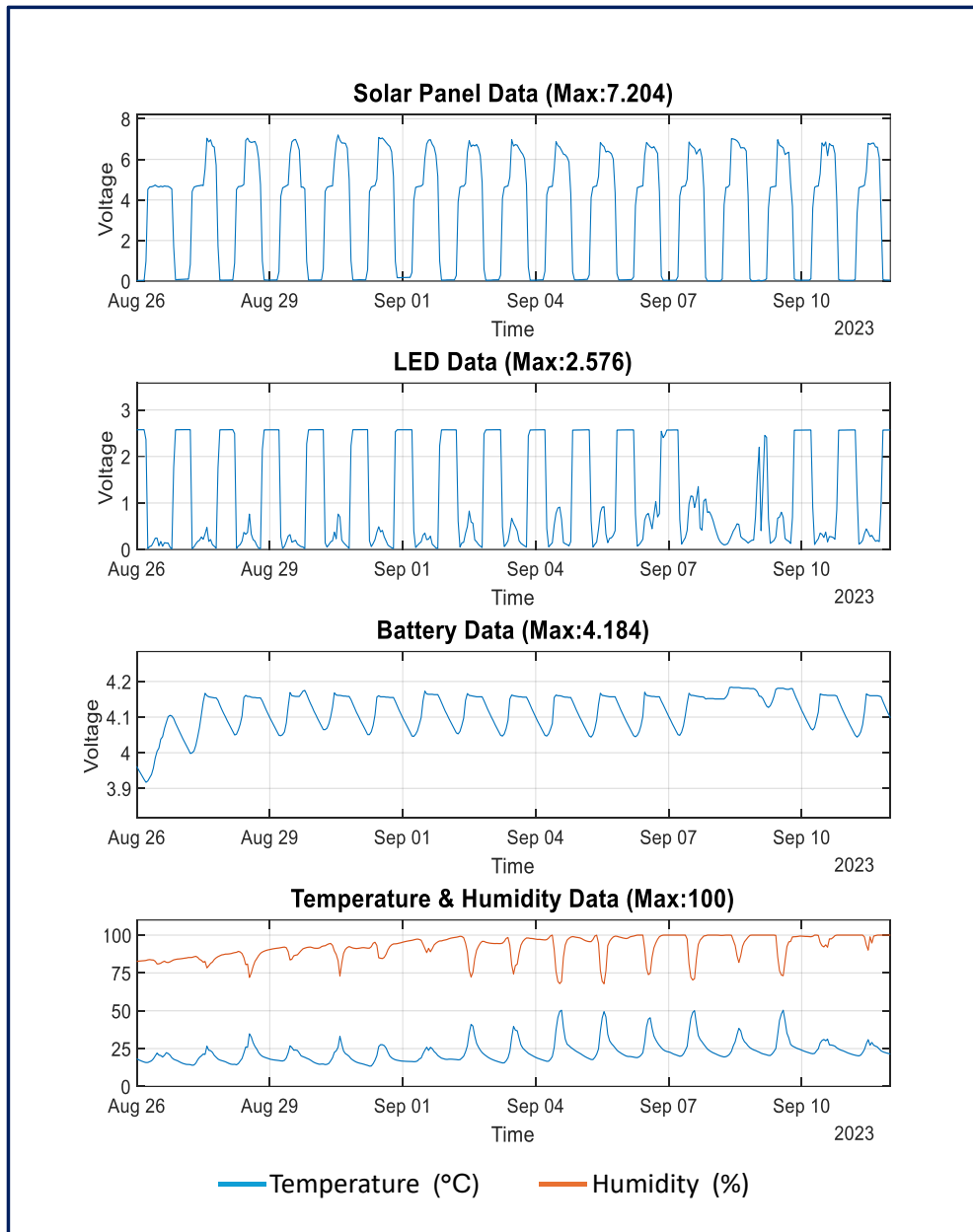


Figure 9-7: Solar Panel Device Analyzed in August 2023 (Leicester, UK)

9.3.5 Humidity and Temperature

The humidity and temperature data logger installed within the solar pavement slab provided crucial insights into the solar panel system's environmental conditions. Figures 9-7 show that the maximum humidity levels reached 100%, particularly noticeable after September 6, predominantly

at night. A decrease in temperature often accompanied this increase in humidity. Conversely, during the day, as temperatures rose, humidity levels decreased. From August 26 to September 4, temperatures ranged from 25 to 35 degrees Celsius, while humidity levels were 75 to 80%.

The data indicated an inverse relationship between temperature and humidity within the panel: high temperatures corresponded with low humidity and vice versa. According to the data logger, the minimum temperature recorded was 25 degrees Celsius during the day for most days, including the period from August 28 to 30. From September 2 onward, temperatures escalated, reaching approximately 50 degrees Celsius. This significant increase in temperature within the solar panel could be caused by the heat generated by the electrical devices housed within the slab.

9.4 Performance of the Solar Slab in Winter

This section analyses the functionality of electrical devices integrated into the concrete slab during testing in the winter. The following sections discuss and compare the results for the solar panels, battery performance, LED strip light, and the temperature and humidity inside the solar slab cavity. This analysis evaluates the overall efficiency, reliability, and performance of the solar pavement slab. By examining these key factors, the study shows how each part contributes to the system and identifies ways to improve the solar pavement slab.

9.4.1 Solar Panel Performance

The solar pavement panel, installed in the user's garden, remained in the same location throughout both the summer and winter periods. During the summer period from August 26 to September 10, the panel demonstrated remarkable performance. Rated at 9 watts and 6 volts, it frequently achieved voltages as high as 7.2 volts on sunny days, indicating overcharging. With approximately 13 hours of daylight and 11 hours of night, the panel managed to fully charge each day, showing maximum voltage readings of 4.19 volts, except for August 26, when it dipped slightly below 4 volts.

In contrast, the winter period from November 22 to December 1 presented more challenging conditions for the solar panel, which remained in the same location. During this cold spell, the maximum voltage obtained from daylight radiation was only 4.97 volts, significantly lower than the summer peak. With no direct sunlight due to overcast skies and the shading effect of surrounding buildings, the panel relied solely on daylight. Despite the shorter daylight hours, only

9 hours compared to 14 hours of the night, the solar panel still managed to provide adequate power. See Figure 9-8 for solar panel performance during winter.

The comparison between the summer and winter performance of the solar panel reveals several key insights. During the summer, the panel benefited from longer daylight hours and direct sunlight, resulting in higher voltage outputs and frequent overcharging. The summer conditions, with approximately 13 hours of daylight, allowed the panel to achieve maximum voltage readings of up to 7.2 volts on sunny days. This consistent overcharging indicates the panel's high efficiency in converting sunlight into electrical energy during optimal conditions.

Conversely, in the winter, the panel's voltage output was significantly reduced due to shorter daylight hours and reliance on daylight rather than direct sunlight and the winter period, characterised by only 9 hours of daylight and overcast skies, led to a maximum voltage of 4.97 volts, which is lower than the summer peak. The shading effect of surrounding buildings further compounded this reduction in performance. Despite these challenges, the panel's ability to maintain performance under adverse conditions highlights its resilience and efficiency.

In the summer, favourable conditions with ample daylight and direct sunlight exposure allowed for optimal performance. However, in the winter, overcast skies, shorter daylight periods, and building shadows posed significant challenges. The system's ability to maintain adequate power output during winter underscores its robustness.

9.4.2 LED Strip Light Performance

During the monitoring period, the data logger indicated that the LED strip lights maintained consistent brightness throughout the long winter nights without noticeable reduction. The voltage supplied to the LED lights remained steady at around 2.58 volts, similar to the voltage levels observed in the summer. This consistent performance, as illustrated in Figure 8-9, underscores the system's reliability and efficiency across both seasons.

From August 26 to September 10, the solar panel benefited from approximately 13 hours of daylight, frequently achieving voltages as high as 7.2 volts. This ample sunlight allowed the RS PRO 3.7V Lithium-Ion Rechargeable Battery Pack to be consistently fully charged. The LED strip lights, powered by this battery, maintained steady brightness throughout the night. Despite minor disruptions from external light reflections, the LED lights showed no significant reduction in brightness, with a stable voltage of around 2.58 volts.

In the winter period from November 22 to December 1, the solar panel faced more challenging conditions with only 9 hours of daylight and no direct sunlight, leading to a maximum voltage of 4.97 volts from diffuse daylight. Despite these less favourable conditions, the LED strip lights continued to perform well, maintaining steady brightness during the longer winter nights. The voltage supplied to the LED lights remained consistent at 2.58 volts, comparable to the summer period.

The summer months they provided ample sunlight, enabling the solar panel to capture and convert a significant amount of solar energy, often resulting in overcharging. This abundance of energy ensured that the LED lights operated at optimal brightness without voltage drops. In winter, although the solar panel's energy capture was reduced due to shorter daylight hours and lack of direct sunlight, the system still managed to store enough energy to power the LED lights effectively.

The battery demonstrated excellent efficiency in storing and delivering power in both seasons. During summer, the battery quickly reached full charge, providing a stable voltage of 2.58 volts to the LED lights. Despite lower energy input in winter, the battery maintained sufficient charge to ensure consistent LED brightness throughout the extended night hours. This indicates robust battery performance and effective energy management within the system.

The LED lights' consistent performance across both seasons highlights the resilience and adaptability of the solar panel system. In summer, the system capitalised on abundant sunlight, while in winter, it adapted to less favourable conditions by efficiently utilising the available diffuse daylight. The steady voltage and brightness of the LED lights in both scenarios demonstrate the system's ability to maintain reliable operation regardless of seasonal variations.

9.4.3 Battery Performance

According to the data logger results in Figure 9-8, the battery performance during the winter monitoring period, starting on November 22, showed a gradual decline in voltage. Initially, the battery level was just under 4 volts. Throughout the monitoring process, the voltage consistently decreased, reaching approximately 3.6 volts or slightly below on November 29 and 30. This steady decline reflects the limited daylight hours and absence of direct sunlight, which hindered the solar panel's ability to recharge the battery each day fully.

In contrast, the battery demonstrated a different performance pattern during the summer period from August 26 to September 10. The longer daylight hours, averaging around 13 hours, and

frequent direct sunlight allowed the solar panel to consistently achieve high voltage outputs consistently, often reaching up to 7.2 volts. This ample energy generation enabled the battery to remain fully charged, maintaining a voltage of around 4.19 volts. The battery effectively powered the LED lights throughout the night, with only minor voltage drops of 0.1 to 0.15 volts, indicating robust energy storage and management.

The contrast between the battery performance in summer and winter highlights the impact of seasonal variations on solar energy systems. In summer, the abundance of sunlight ensured the battery was consistently charged to near maximum capacity. The solar panel's high voltage outputs contributed to a stable battery voltage of around 4.19 volts, supporting the continuous operation of the LED lights with minimal voltage reduction.

In winter, the situation was markedly different. The limited daylight hours, coupled with overcast skies and the absence of direct sunlight, have resulted in reduced energy capture by solar panels. Consequently, the battery voltage began just under 4 volts and steadily declined to around 3.6 volts by the end of November. Despite this decline, the system managed to provide adequate power for the LED lights, albeit with a noticeable reduction in overall battery voltage.

9.4.4 Humidity and Temperature

On November 25, the temperature dropped below 10 degrees Celsius and continued to fall, reaching -5 degrees Celsius during the nights of November 29 and 30, as seen in Figures 9-8. Throughout this period, humidity levels fluctuated between 73% and a maximum of 83%. However, on November 30, the daytime temperature rose slightly, and humidity levels fell below 75%, although they increased again at night. Compared to the summer period, these winter conditions were notably harsher. During the summer period from August 26 to September 10, the temperature and humidity levels were considerably different. Summer temperatures were consistently higher, typically ranging between 15 and 25 degrees Celsius. Humidity levels during the summer were more stable and lower, generally fluctuating between 50% and 65%. These favourable conditions in the summer supported optimal performance for the solar panel system, allowing for efficient energy capture and storage.

The comparison between winter and summer reveals significant variations in environmental conditions. In winter, the lower temperatures and higher humidity levels posed challenges for the solar panel system. The cold temperatures likely reduced the efficiency of the battery and the solar panel, as lower temperatures can increase internal resistance in batteries and reduce the efficiency

of photovoltaic cells. Higher humidity levels can also contribute to condensation and potential moisture-related issues in the electrical components, further affecting performance.

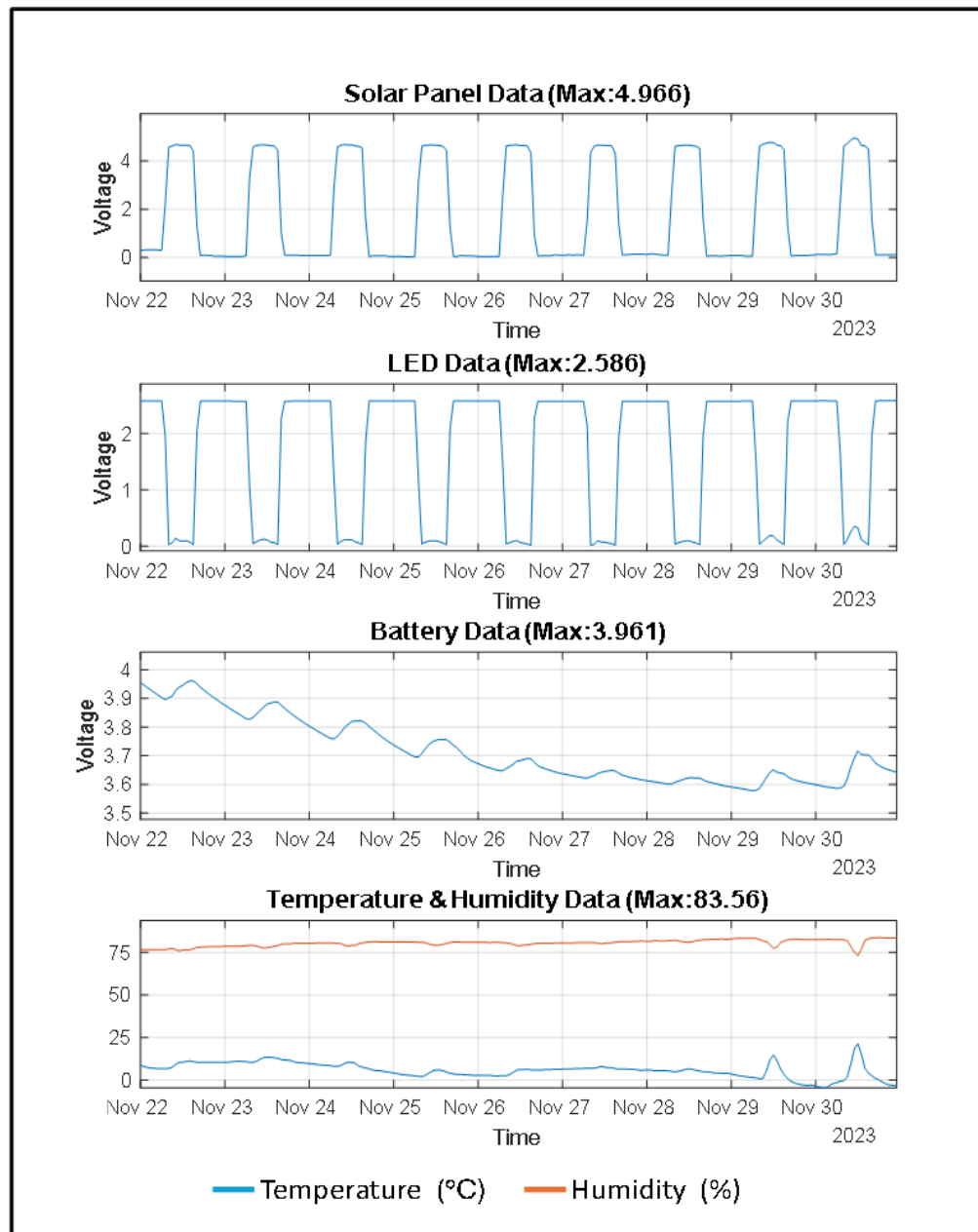


Figure 9-8: Devices Analyzed in December 2023 (Leicester, UK)

Conversely, the summer conditions with higher temperatures and lower humidity provided an ideal environment for the solar panel system. The warmer temperatures improved battery efficiency, and the lower humidity levels reduced the risk of moisture-related issues. These conditions enabled

the solar panel to consistently achieve high voltage outputs, ensuring the battery remained fully charged and the LED lights maintained steady brightness.

The environmental conditions during winter, characterised by lower temperatures and higher humidity, presented significant challenges for the solar panel system, impacting its efficiency and performance. In winter, the lower temperatures caused a decrease in the solar panel's efficiency in converting sunlight into electrical energy, and the battery's internal resistance increased, leading to less efficient energy storage and delivery. The higher humidity levels increased the risk of condensation, which could damage electrical components and further reduce system performance. In contrast, summer conditions with higher temperatures and lower humidity were more conducive to optimal operation. The higher temperatures improved the efficiency of both the solar panel and the battery, allowing for more effective energy capture and storage. The lower humidity levels during summer reduced the risk of moisture-related issues, ensuring the longevity and reliability of the electrical components.

9.5 Comparison of Solar Pavement Design with Existing Market Products

As detailed in Table 9-4, the solar walkable slab is a self-contained product made from foamed concrete that includes recycled materials. This innovative design provides several key advantages over existing products available from the Solar Centre and Solar Patio websites. One of the standout features of the current solar walkable slab is its ability to deliver consistent illumination for more than 16 hours after a relatively short charging period of 3 to 4 hours under direct sun rays. This extended lighting capability is better than that of the solar brick lights and solar garden lights from Solar Centre, which, while also self-contained, do not match the current product in terms of brightness or duration of illumination.

The solar walkable slab is not only functionally superior but also environmentally conscious. The use of foamed concrete with recycled content ensures that the product is lightweight and sustainable. In contrast, the solar brick and solar garden lights from Solar Centre are not made from recycled materials, representing a missed opportunity for environmental sustainability. Furthermore, these products, despite being smaller in size compared to the current design, are relatively costly, offering less value for their price in terms of both material sustainability and performance.

Table 9-4: Comparison of Market Products with the Developed Solar Slab

Design	Product Examples	Product information	Product size	Application
1		Solar garden made with 100% plastic	72mm diameter by 320mm height	Lighting, garden (No cost of installation required)
2		Solar Brick, made with plastic and steel	200 x100 x 55mm	Walkway lighting, surface illumination Installation cost required
3		Solar pavement made with recycled plastic	330 x330 x 6cm	Driveways, pathways (Installation cost required)
4		Current product: Solar walkable pavement slab made with lightweight concrete and recycled materials	400 x 400 x 50 mm	Driveways, pathways, garden features, surface illumination (Installation cost required)

On the other hand, the solar pavement slab available from Solar Patio also incorporates recycled materials, which is a positive aspect. However, it differs significantly from the current solar walkable slab because it is not self-contained. The Solar Patio product requires separate wired connections, which are not included in the purchase, adding to the overall expense and complexity of installation. Despite its recycled content, the Solar Patio slab is very expensive and does not offer the same ease of use or integration as the current product. The current solar walkable slab design is best suited to several critical areas, including self-contained functionality, sustainability through the use of recycled materials, superior lighting capabilities, and cost-effectiveness. These features position it as a more practical and environmentally friendly option than the solar brick and garden lights from Solar Centre and the solar pavement slab from Solar Patio. 353 mm x 353 mm x 41.

9.6 Summary

This chapter detailed the final assembly, electrical analysis, and structural development of the solar walkable slab prototype, incorporating the optimised design with 50% waste foundry sand (WFS).

The slab was prepared for installation, focusing on both structural integrity and electrical performance to ensure it meets real-world application requirements.

The structural development emphasised the slab's ability to withstand pedestrian loads and environmental factors while maintaining transparency for efficient solar energy conversion. The surface was designed to balance safety and durability while allowing sunlight to reach the embedded photovoltaic cells. The electrical analysis evaluated the slab's performance in various conditions, particularly the energy generated by the solar cells and the functioning of batteries and LED lighting. The system's ability to perform in summer and winter environments was also examined, providing insights into its efficiency and reliability.

The final prototype featured an anti-slip surface and a durable, weather-resistant acrylic top layer, ready for user trials. The solar pavement slab installed in a user's garden in Leicester received positive reviews for its aesthetic appeal and practicality. The slab provided consistent lighting, with up to 18 hours of light during the summer and about 14 hours in the winter. It operated reliably in both cold and hot climates, demonstrating robustness and adaptability. Sensor functionality automatically turned the LED lights on at dusk and off at dawn, though occasional disruptions from car headlights and debris required regular maintenance.

Overall, the solar pavement slab system proved to be a worthwhile investment, offering consistent performance, aesthetic benefits, and ease of installation. Addressing minor sensor issues through regular maintenance ensures its reliable operation throughout the year.

The final product was successfully tested and prepared for installation through careful integration of electrical and structural components, demonstrating its potential as a sustainable solution for solar walkable pavement slabs. The chapter concluded with a comprehensive overview of the slab's load-bearing capacity, deflection behaviour, and energy generation capabilities, establishing its viability for real-world applications.

Chapter 10: Conclusions

10.1 Overview

The aim of this study is to develop self-contained, walkable solar pavement slabs made from foamed concrete incorporating recycled materials. This innovative approach generates renewable energy and enhances environmental protection by decreasing reliance on virgin construction materials and effectively repurposing waste materials, hence reducing embodied carbon. This study offers a thorough analysis of the mechanical properties, strength, and flexural behaviour of foamed and conventional concrete. The objective was to evaluate how different mix components, such as sand ratios, superplasticisers, and recycled materials, such as waste foundry sand and polystyrene, affect these properties. This approach would optimise mix proportions to enhance compressive and flexural strengths. The normal concrete mortar and foamed concrete containing recycled components were utilised in this study. Various densities, sand ratios, and additives were assessed to understand their impact on mechanical properties. Standard compressive strength tests and flexural strength evaluations, particularly the impact of steel tyre fibres and other additives, were performed after 28 days of curing. The numerical validation using ABAQUS was analysed to compare the results with the experimental analyses, aiming to understand the normal and foamed concrete slab's deflection behaviour under the applied load.

Moreover, the study also assessed a solar panel system's efficiency across the summer and winter seasons. It evaluated the system's ability to capture and store solar energy, powering LED strip lights consistently throughout the year. Temperature and humidity significantly impacted the system's performance, underscoring the need for optimised design and placement to enhance reliability and efficiency.

10.2 Conclusions

From the results and discussions of the experimental, numerical, and electrical performance analysis conducted in this research on developing solar walkable pavement slabs incorporating foamed concrete with recycled materials, the following key conclusions have been drawn from the research:

1. Increasing foamed concrete density demonstrated a positive correlation with compressive strength. Density values ranging from 800 kg/m³ to 1400 kg/m³ resulted in a 290% increase in compressive strength, confirming that denser mixes offer superior mechanical performance.
2. Partial replacement of normal sand with WFS led to a reduction in compressive and flexural strength; however, replacement levels between 25% and 50% maintained acceptable structural performance. A 50% WFS mix achieved a balance between sustainability and strength, with a maximum applied load of 4.1 kN and deflection of 1.35 mm, demonstrating stiffness comparable to Normal foamed concrete (NFC). Water demand increased by approximately 15% when incorporating WFS, leading to higher porosity and microcracking at replacement levels exceeding 50%.
3. Incorporating polystyrene as a lightweight aggregate replacement reduced both density and compressive strength. Higher replacement levels (20% and 30%) resulted in significant strength reductions, while a 10% replacement achieved a favourable balance, increasing compressive strength by 110% compared to mixes with higher polystyrene content.
4. The 10% PO slab displayed the lowest load capacity (3.9 kN) and deflection (1.3 mm), demonstrating brittle behaviour and increased stiffness, which could limit performance under dynamic loading. Mixing challenges were identified, with void formation and weak interfacial bonding contributing to reduced structural capacity, particularly when polystyrene content exceeded 10%.
5. The addition of 1% recycled steel tyre fibre enhanced both compressive and flexural strength, contributing to ductility improvements and crack resistance. Load capacity increased to 4.58 kN, with a deflection of 1.69 mm, indicating improved stress distribution. Minimal issues were encountered with fibre distribution, but uniform distribution is critical for large-scale applications to ensure consistent performance.
6. Incorporating 1% superplasticiser increased compressive strength by approximately 20%, improved workability, and enhanced microstructural density. Load capacity increased to 4.56 kN, with a deflection of 1.46 mm, confirming improved mechanical properties. Foam destabilisation was observed, leading to a slight increase in density.
7. Samples containing WFS and polystyrene presented microcracks and interfacial debonding, particularly at higher replacement levels, indicating weaker bonding between aggregates and cement paste. In contrast, RSTF-modified slabs demonstrated reduced crack formation and

improved toughness, with fibres effectively bridging microcracks and enhancing stress distribution.

8. Normal concrete mortar exhibited the highest flexural strength, outperforming foamed concrete mixes. RSTF and SP-enhanced foamed concrete samples displayed improved flexural capacity, offering a suitable alternative where lightweight yet elastic materials are required.
9. Numerical ABAQUS simulations closely aligned with experimental deflections, showing minor discrepancies of 0.21 mm for normal concrete and 0.06 mm for foamed concrete. This validates the reliability of numerical modelling in predicting slab performance, demonstrating its applicability to further structural optimisation.
10. The normal concrete slab exhibited a maximum stress of 57.1 MPa and strain of 0.045, while the foamed concrete slab exhibited a stress of 47.5 MPa and strain of 0.036. These stress and strain levels were considered negligible under the applied loads, indicating that both slab types can withstand expected pedestrian loads without deformation concerns.
11. In summer, the 9W panel consistently overperformed, reaching 7.2V under direct sunlight during peak hours, ensuring full daily battery charging. In winter, output reduced to a peak of 4.97V due to shorter daylight hours, cloud cover, and shading, though sufficient power was still generated for LED operation.
12. LED strip lights performed consistently across both summer and winter, maintaining a steady voltage of 2.58V during night-time operation. Minor disruptions in lighting control were noted, caused by external reflections affecting the light sensor, suggesting the need for improved shielding or sensor recalibration.
13. The 3.7V Lithium-Ion battery pack (7.8Ah) proved effective, with daily full charging observed in summer (4.19V). In winter, battery voltage gradually declined to 3.6V but continued to support LED operation, indicating adequate capacity under typical conditions.
14. Summer cavity temperatures ranged from 25°C to 35°C, while humidity reached 100% after September 6, indicating moisture accumulation overnight. Winter temperatures dropped to -5°C, with humidity levels fluctuating between 73% and 83%, suggesting condensation risks that may affect electrical components. Additional sealing and ventilation measures may be necessary to mitigate humidity-related degradation.

10.3 Contribution to the Knowledge

This research has made several original contributions to the field of sustainable construction materials and the development of solar-integrated pavement systems. It advances the understanding of how recycled materials and renewable energy can be integrated into walkable slab systems, offering practical solutions for urban infrastructure. The key contributions are detailed as follows:

1. A new design approach was developed, integrating sustainable lightweight pavement slab construction with embedded solar technology. This work advances the understanding of combining structural functionality with energy efficiency, guiding future developments in multi-functional construction products.
2. A 400 mm x 400 mm x 50 mm solar walkable slab was successfully designed, produced, and tested, demonstrating the practical feasibility of integrating energy generation and pedestrian loading capacity into a single pavement unit. This represents a significant advancement in developing dual-function surface solutions for urban spaces.
3. The slab's lightweight composition allows for easy handling and installation without requiring heavy machinery, addressing a key challenge in traditional paving systems. This development reduces installation costs and labour demands while supporting material efficiency.
4. The slab's combination of pedestrian functionality with embedded solar-powered lighting offers an innovative solution for enhancing both safety and aesthetics in public and private spaces. It demonstrates the potential for smart pavements that contribute to energy self-sufficiency while serving traditional infrastructure roles.
5. The research systematically developed and tested different mix designs, resulting in an optimised foamed concrete containing 50% waste foundry sand (WFS), achieving a balance between structural performance and environmental sustainability. This validated the suitability of waste materials in enhancing lightweight pavement systems.

This research supports the broader implementation of multi-functional construction products, offering innovative solutions for modern infrastructure.

10.4 Recommendations for Future Work

The essential findings from this research have demonstrated the potential of integrating lightweight concrete containing recycled materials with solar technology to develop a sustainable solar walkable pavement slab. While the experimental and numerical analyses provided valuable insights, further research and improvements are necessary to enhance both the structural and electrical performance of the slab system. The following recommendations are proposed to advance the development and practical implementation of solar pavement slabs:

1. The replacement ratio of WFS should be optimised, particularly between 25% and 50%, as ratios beyond 50% increase water demand and lead to bonding issues and microcracks. Making this ratio for different applications can balance strength, sustainability, and workability. Mixture designs for example, combining WFS, RSTF, and SP should be explored further to maximise compressive and flexural strength while maintaining workability.
2. The use of supplementary cementitious materials like silica fume or fly ash should be examined to reduce porosity and improve the density and durability of foamed concrete mixes, particularly when incorporating recycled materials.
3. The steel tyre fibre content should be optimised beyond the tested 1%, with further exploration into 0.5% to 2% variations, to identify the best balance between strength, crack resistance, and workability.
4. Alternative fibres, such as glass or carbon fibres, should be studied as potential substitutes for steel fibres, offering improved durability and reduced risk of corrosion.
5. Reinforcements beneath the solar panel, such as additional support layers or integrated steel mesh, could be incorporated to increase the slab's capacity to withstand occasional light vehicle traffic.
6. Humidity and condensation inside the slab cavity posed potential risks to electrical components therefore, improving the sealing of the solar panel cover and battery compartment using high-strength silicone and waterproof screws would protect internal components from moisture ingress. Installing ventilation features or integrating moisture-absorbing materials within the slab cavity could control humidity levels and prevent condensation build-up.
7. Sensor errors caused by reflections from external light sources affected LED performance, therefore, relocating the sensor or shielding it to reduce sensitivity to external reflections (e.g., car headlights, streetlights) would ensure more reliable activation of LED lights. Calibrating

light sensors to better differentiate between ambient and artificial light could improve performance in urban environments.

8. Exploring alternative panel cover materials, such as thicker acrylic or slip-resistant tempered glass, could enhance durability and improve energy absorption while ensuring pedestrian safety. Anti-slip surface treatments on the solar panel cover should be considered to enhance user safety during wet or icy conditions.
9. While the laboratory and short-term outdoor testing validated the slab's initial feasibility, extended field trials under realistic conditions are critical. Therefore, Experimental installations in public footpaths or parks should be conducted to evaluate the slab's real-world performance under varying pedestrian loads and weather conditions. Monitoring mechanical and electrical performance over several months or years would help identify potential weaknesses and develop proactive maintenance strategies.

Implementing these recommendations will further enhance the structural resilience, electrical efficiency, and long-term reliability of solar walkable pavement slabs. Combining improved material compositions with more efficient energy systems will advance this technology as a viable and sustainable solution for urban infrastructure, promoting the broader adoption of solar-integrated pedestrian surfaces in modern smart cities.

References

- Abd, S.M. and Jassam, D.G. (2019) 'Improving Mechanical Properties of Lightweight Foamed Concrete Using Silica Fume and Fibers', *Journal of Engineering and Sustainable Development*, 23(2), pp. 184–199. Available at: <https://doi.org/10.31272/jeasd.23.2.14>.
- ACI 523.3R-14 (2014) 'Guide for Cellular Concretes above 50 lb/ft³ (800 kg/m³) (ACI 523.3R-14)', *ACI Manual of Concrete Practice*, 3.
- Aghaee, K., Yazdi, M.A. and Tsavdaridis, K.D. (2015) 'Investigation into the mechanical properties of structural lightweight concrete reinforced with waste steel wires', *Magazine of Concrete Research*, 67(4), pp. 197–205. Available at: <https://doi.org/10.1680/mac.14.00232>.
- Amran, M. et al. (2020) 'Fibre-reinforced foamed concretes: A review', *Materials*, 13(19), pp. 1–36. Available at: <https://doi.org/10.3390/ma13194323>.
- Amran, Y.H.M., Farzadnia, N. and Ali, A.A.A. (2015a) 'Properties and applications of foamed concrete; A review', *Construction and Building Materials*, 101, pp. 990–1005. Available at: <https://doi.org/10.1016/j.conbuildmat.2015.10.112>.
- Amran, Y.H.M., Farzadnia, N. and Ali, A.A.A. (2015b) 'Properties and applications of foamed concrete; A review', *Construction and Building Materials*, 101, pp. 990–1005. Available at: <https://doi.org/10.1016/j.conbuildmat.2015.10.112>.
- Ardani, K. et al. (2021) 'Solar Futures Study', U S Department of Energy, (September), pp. 1–279.
- Assessment, F. (2023a) 'Solar Energy from Pavement : A Lab and Field Assessment'.
- .Awang, H. et al. (2014) 'The mechanical properties of foamed concrete containing un-processed blast furnace slag', *MATEC Web of Conferences*, 15, pp. 1–9. Available at: <https://doi.org/10.1051/matecconf/20141501034>.

-
- Awerbuch, S. and Sauter, R. (2006) ‘Exploiting the oil-GDP effect to support renewables deployment’, *Energy Policy*, 34(17), pp. 2805–2819. Available at: <https://doi.org/10.1016/j.enpol.2005.04.020>.
- Baiju, A. and Yarema, M. (2022) ‘Status and challenges of multi-junction solar cell technology’, *Frontiers in Energy Research*, 10(September), pp. 1–17. Available at: <https://doi.org/10.3389/fenrg.2022.971918>.
- BEIS (2022) *Energy Trends UK, July to September 2022*, Energy Trends 2022.
- Beng, N.A. (2021) ‘Flexural Behaviour of Enhanced Foamed Concrete Beams Reinforced with GFRP Bars’, (July). Available at: <https://www.researchgate.net/profile/Nadir-Alkurdi>.
- Bhardwaj, B. and Kumar, P. (2017) ‘Waste foundry sand in concrete: A review’, *Construction and Building Materials*, 156, pp. 661–674. Available at: <https://doi.org/10.1016/j.conbuildmat.2017.09.010>.
- Bolden, J., Abu-Lebdeh, T. and Fini, E. (2013) ‘Utilization of recycled and waste materials in various construction applications’, *American Journal of Environmental Sciences*, 9(1), pp. 14–24. Available at: <https://doi.org/10.3844/ajessp.2013.14.24>.
- Buenfeld, N.R. and Okundi, E. (2018) ‘Effect of cement content on concrete performance’, *Magazine of Concrete Research*, 50(4), pp. 339–351.
- Cadere, C.A. et al. (2018) ‘Engineering properties of concrete with polystyrene granules’, *Procedia Manufacturing*, 22, pp. 288–293. Available at: <https://doi.org/10.1016/j.promfg.2018.03.044>.
- Directive, R.E. and BEIS (2020) ‘Digest of United Kingdom energy statistics 2020 --- “has a good graph”’, p. 176 pp.

-
- Döpfner, M., Schmeck, K. and Berner, W. (1994) 'Handbuch: Elternfragebogen über das Verhalten von Kindern und Jugendlichen: Forschungsergebnisse zur deutschen Fassung der Child Behavior', 3(1), pp. 61–69.
- Eastern, M. (1997) 'Concrete mixes Nominal mixes', p. 21. Available at: [http://dl.lib.mrt.ac.lk/bitstream/handle/123/1182/chapter 2.pdf?sequence=6&isAllowed=y](http://dl.lib.mrt.ac.lk/bitstream/handle/123/1182/chapter%20.pdf?sequence=6&isAllowed=y).
- EN, B.S. (2011) '197-1. Cement–Part 1: Composition, specifications and conformity criteria for common cements', London: European Committee For Standardisation [Preprint].
- Erdiwansyah et al. (2021) 'A critical review of the integration of renewable energy sources with various technologies', Protection and Control of Modern Power Systems, 6(1). Available at: <https://doi.org/10.1186/s41601-021-00181-3>.
- Fang, S.E., Hong, H.S. and Zhang, P.H. (2018) 'Mechanical property tests and strength formulas of basalt fiber reinforced recycled aggregate concrete', Materials, 11(10). Available at: <https://doi.org/10.3390/ma11101851>.
- Fathi, M.S. (no date a) CORE View metadata, citation and similar papers at core.ac.uk provided by Universiti Teknologi Malaysia Institutional Repository.
- Fathi, M.S. (no date b) CORE View metadata, citation and similar papers at core.ac.uk provided by Universiti Teknologi Malaysia Institutional Repository.
- Ganesh Prabhu, G., Hyun, J.H. and Kim, Y.Y. (2014) 'Effects of foundry sand as a fine aggregate in concrete production', Construction and Building Materials, 70, pp. 514–521. Available at: <https://doi.org/10.1016/j.conbuildmat.2014.07.070>.
- Hama, S.M. (2017) 'Improving mechanical properties of lightweight Porcelanite aggregate concrete using different waste material', International Journal of Sustainable Built Environment, 6(1), pp. 81–90. Available at: <https://doi.org/10.1016/j.ijsbe.2017.03.002>.
-

-
- Hamad, A.J. (2014) ‘Materials, Production, Properties and Application of Aerated Lightweight Concrete: Review’, *International Journal of Materials Science and Engineering* [Preprint]. Available at: <https://doi.org/10.12720/ijmse.2.2.152-157>.
- Hashim, M. and Tantray, M. (2021) ‘Comparative study on the performance of protein and synthetic-based foaming agents used in foamed concrete’, *Case Studies in Construction Materials*, 14(March), p. e00524. Available at: <https://doi.org/10.1016/j.cscm.2021.e00524>.
- Hilal, A.A. (2015) ‘Properties and Microstructure of Pre-formed Foamed Concretes By Thesis submitted to the University of Nottingham for the degree of Doctor of Philosophy’, (June). Available at: <https://doi.org/10.13140/RG.2.1.3983.3768>.
- Hilal, A.A. et al. (2015) ‘The Use of Additives to Enhance Properties of Pre- Formed Foamed Concrete’, 7(4). Available at: <https://doi.org/10.7763/IJET.2015.V7.806>.
- Hossain, M.F.T. et al. (2021) ‘Harvesting solar energy from asphalt pavement’, *Sustainability* (Switzerland), 13(22). Available at: <https://doi.org/10.3390/su132212807>.
- Hu, H. et al. (2021a) ‘Solar pavements: A critical review’, *Renewable and Sustainable Energy Reviews*, 152(October), p. 111712. Available at: <https://doi.org/10.1016/j.rser.2021.111712>.
- Hu, H. et al. (2021b) ‘Solar pavements: A critical review’, *Renewable and Sustainable Energy Reviews*, 152(September), p. 111712. Available at: <https://doi.org/10.1016/j.rser.2021.111712>.
- Hu, H. et al. (2021c) ‘Solar pavements: A critical review’, *Renewable and Sustainable Energy Reviews*, 152(October), p. 111712. Available at: <https://doi.org/10.1016/j.rser.2021.111712>.
- Iea (2023) *World Energy Investment 2023*. Available at: www.iea.org.
- Irena (2021) *Renewable Power Generation Costs 2020*. Available at: www.irena.org.

-
- Jacobson, M.Z. (2009) ‘Review of solutions to global warming, air pollution, and energy security’, *Energy and Environmental Science*, pp. 148–173. Available at: <https://doi.org/10.1039/b809990c>.
- Jean Pierre Jacobs (2009) ‘Sustainable Benefits of Concrete Structures’, *European Concrete Platform ASBL*, p. 40.
- Jones, M.R. and McCarthy, A. (2005a) ‘Preliminary views on the potential of foamed concrete as a structural material’, *Magazine of Concrete Research*, 57(1), pp. 21–31. Available at: <https://doi.org/10.1680/mac.2005.57.1.21>.
- Jones, M.R. and McCarthy, A. (2005b) ‘Preliminary views on the potential of foamed concrete as a structural material’, *Magazine of Concrete Research*, 57(1), pp. 21–31. Available at: <https://doi.org/10.1680/mac.2005.57.1.21>.
- Jones, M.R. and McCarthy, A. (2005c) ‘Preliminary views on the potential of foamed concrete as a structural material’, *Magazine of Concrete Research*, 57(1), pp. 21–31. Available at: <https://doi.org/10.1680/mac.2005.57.1.21>.
- Jones, M.R. and McCarthy, A. (2005d) ‘Preliminary views on the potential of foamed concrete as a structural material’, *Magazine of Concrete Research*, 57(1), pp. 21–31. Available at: <https://doi.org/10.1680/mac.2005.57.1.21>.
- Junaid, M.F. et al. (2022) ‘Lightweight concrete from a perspective of sustainable reuse of waste byproducts’, *Construction and Building Materials*. Elsevier Ltd. Available at: <https://doi.org/10.1016/j.conbuildmat.2021.126061>.
- Kan, A. and Demirboğa, R. (2009) ‘A novel material for lightweight concrete production’, *Cement and Concrete Composites*, 31(7), pp. 489–495. Available at: <https://doi.org/10.1016/j.cemconcomp.2009.05.002>.
-

-
- Karolina, R. et al. (2019) 'The Effect of Polystyrene on Concrete Mechanical Properties', in. European Alliance for Innovation n.o. Available at: <https://doi.org/10.4108/eai.3-11-2018.2285654>.
- Kearsley, E.P. and Wainwright, P.J. (2001) 'the Effect of fly ash content on the compressive strength development of concrete', *Cement and Concrete Research*, 31(31), pp. 105–112.
- Kehagia, F., Mirabella, S. and Psomopoulos, C.S. (2019a) 'Solar pavement: A new source of energy', *Bituminous Mixtures and Pavements VII- Proceedings of the 7th International Conference on Bituminous Mixtures and Pavements, ICONFBMP 2019*, (May), pp. 441–447. Available at: <https://doi.org/10.1201/9781351063265-61>.
- Kehagia, F., Mirabella, S. and Psomopoulos, C.S. (2019b) 'Solar pavement: A new source of energy', *Bituminous Mixtures and Pavements VII- Proceedings of the 7th International Conference on Bituminous Mixtures and Pavements, ICONFBMP 2019*, (May), pp. 441–447. Available at: <https://doi.org/10.1201/9781351063265-61>.
- Kesari, J.P. and Kumar, A. (2021) 'Solar Roadways: the Roadways To Next Generation', *International Research Journal of Engineering and Technology [Preprint]*, (February). Available at: www.irjet.net.
- Kharun, M. and Svintsov, A.P. (2017) 'Polystyrene concrete as the structural thermal insulating material', *International Journal of ADVANCED AND APPLIED SCIENCES*, 4(10), pp. 40–45. Available at: <https://doi.org/10.21833/ijaas.2017.010.007>.
- Kostopoulos, E. et al. (2018) 'Solar energy contribution to an electric vehicle needs on the basis of long-term measurements', *Procedia Structural Integrity*, 10, pp. 203–210. Available at: <https://doi.org/10.1016/j.prostr.2018.09.029>.
-

-
- Kumar, R., Lakhani, R. and Tomar, P. (2018) ‘A simple novel mix design method and properties assessment of foamed concretes with limestone slurry waste’, *Journal of Cleaner Production*, 171, pp. 1650–1663. Available at: <https://doi.org/10.1016/j.jclepro.2017.10.073>.
- Lin, T.H., Deng, J. and Chen, Y.C. (2022) ‘Using Response Surface for Searching the Nearly Optimal Parameters Combination of the Foam Concrete Muffler’, *Materials*, 15(22), pp. 1–22. Available at: <https://doi.org/10.3390/ma15228128>.
- Liu, Jie et al. (2012) ‘Characterization of PIII textured industrial multicrystalline silicon solar cells’, *Solar Energy*, 86(10), pp. 3004–3008. Available at: <https://doi.org/10.1016/j.solener.2012.07.006>.
- Makul, N. (2020a) ‘Advanced smart concrete - A review of current progress, benefits and challenges’, *Journal of Cleaner Production*, 274, p. 122899. Available at: <https://doi.org/10.1016/j.jclepro.2020.122899>.
- Makul, N. (2020b) ‘Advanced smart concrete - A review of current progress, benefits and challenges’, *Journal of Cleaner Production*, 274, p. 122899. Available at: <https://doi.org/10.1016/j.jclepro.2020.122899>.
- Markandya, A. et al. (2018) ‘Health co-benefits from air pollution and mitigation costs of the Paris Agreement: a modelling study’, *The Lancet Planetary Health*, 2(3), pp. e126–e133. Available at: [https://doi.org/10.1016/S2542-5196\(18\)30029-9](https://doi.org/10.1016/S2542-5196(18)30029-9).
- MD Jalal, A Tanveer, K.J. and F.A. (1991) ‘Foam concrete’, *Concrete (London)*, 25(1), pp. 49–54. Available at: <http://www.ripublication.com>.
- Meera, M. and Gupta, S. (2020) ‘Development of a strength model for foam concrete based on water – Cement ratio’, *Materials Today: Proceedings*, 32, pp. 923–927. Available at: <https://doi.org/10.1016/j.matpr.2020.04.888>.
-

-
- Mohd Sari, K.A. and Mohammed Sani, A.R. (2017) ‘Applications of Foamed Lightweight Concrete’, MATEC Web of Conferences, 97, pp. 1–5. Available at: <https://doi.org/10.1051/mateconf/20179701097>.
- MPA Mortar (2021) ‘A guide to BS EN 998 -1 and BS EN 998 - 2’, 2021(4), p. 6.
- Mydin, M.A.O. and Wang, Y.C. (2012) ‘Mechanical properties of foamed concrete exposed to high temperatures’, Construction and Building Materials, 26(1), pp. 638–654. Available at: <https://doi.org/10.1016/j.conbuildmat.2011.06.067>.
- Nader, A. et al. (no date) ‘Physical and Mechanical Properties of Expanded Polystyrene Lightweight Aggregate Concrete’, 0.
- Nambiar, E.K.K. and Ramamurthy, K. (2006) ‘Models relating mixture composition to the density and strength of foam concrete using response surface methodology’, 28, pp. 752–760. Available at: <https://doi.org/10.1016/j.cemconcomp.2006.06.001>.
- Nambiar, E.K.K. and Ramamurthy, K. (2007) ‘Air-void characterisation of foam concrete’, Cement and Concrete Research, 37(2), pp. 221–230. Available at: <https://doi.org/10.1016/j.cemconres.2006.10.009>.
- Nayak, P.K. et al. (2019) ‘Photovoltaic Solar Cell Technologies : Bounds and Challenges’, Nature Reviews Materials, Volume 4(Edição 4), p. Páginas 269-285.
- Ndayambaje, C.J., Onchiri, R. and Oyawa, W.O. (2017) ‘Cumulative effect of Recycled Tyre Steel Fibre and crumb rubber on impact resistance of concrete’, (1), pp. 80–90.
- Newman, J. and Owens, P. (no date) Properties of lightweight concrete.
- Northmore, A.B. (2014a) ‘Canadian Solar Road Panel Design : A Structural and Environmental Analysis’, University of Waterloo, Canada, 1, pp. 1–166.

-
- Northmore, A.B. (2014b) 'Canadian Solar Road Panel Design : A Structural and Environmental Analysis', University of Waterloo, Canada, 1, pp. 1–166.
- Northmore, A.B. (2015) 'A Review on Photovoltaic Solar Energy Technology and its Efficiency', A Review on Photovoltaic Solar Energy Technology and its Efficiency, (December), pp. 1–9.
- Northmore, A.B. (2019) 'Development of walkable photovoltaic floor tiles used for pavement', Energy Conversion and Management, 183(January), pp. 764–771. Available at: <https://doi.org/10.1016/j.enconman.2019.01.035>.
- Okolnikova, G. et al. (2020) 'Compressive strength of lightweight expanded polystyrene basalt fiber concrete', MATEC Web of Conferences, 329, p. 04010. Available at: <https://doi.org/10.1051/mateconf/202032904010>.
- Othuman Mydin, M.A. et al. (2014) 'Experimental investigation into pull-out strength of foamed concrete using different types of screw', MATEC Web of Conferences, 15, pp. 1–8. Available at: <https://doi.org/10.1051/mateconf/20141501031>.
- Oyeyi, A.G. et al. (2023) 'Life cycle assessment of lightweight cellular concrete subbase pavements in Canada', International Journal of Pavement Engineering, 24(1). Available at: <https://doi.org/10.1080/10298436.2023.2168662>.
- OZLUTAS, K. (2015a) 'Behaviour of ultra-low density foamed concrete A thesis presented in application for the Degree of Doctor of Philosophy Division of Civil Engineering University of Dundee'.
- OZLUTAS, K. (2015b) 'Behaviour of ultra-low density foamed concrete A thesis presented in application for the Degree of Doctor of Philosophy Division of Civil Engineering University of Dundee'.
-

-
- Papadaki, D., Nikolaou, D.A. and Assimakopoulos, M.N. (2022) ‘Circular Environmental Impact of Recycled Building Materials and Residential Renewable Energy’, *Sustainability* (Switzerland), 14(7). Available at: <https://doi.org/10.3390/su14074039>.
- Papadimitriou, C.N., Psomopoulos, C.S. and Kehagia, F. (2019) ‘A review on the latest trend of solar pavements in urban environment’, *Energy Procedia*, 157(2018), pp. 945–952. Available at: <https://doi.org/10.1016/j.egypro.2018.11.261>.
- Piggin, S. (2006) *The properties of concrete*, Meanjin. Available at: <https://doi.org/10.11129/detail.9783034614740.19>.
- Pilakoutas, K., Neocleous, K. and Tlemat, H. (2004a) ‘Reuse of tyre steel fibres as concrete reinforcement’, *Engineering Sustainability*, 157(3), pp. 131–138. Available at: <https://doi.org/10.1680/ensu.157.3.131.48644>.
- Pilakoutas, K., Neocleous, K. and Tlemat, H. (2004b) ‘Reuse of tyre steel fibres as concrete reinforcement’, *Proceedings of the Institution of Civil Engineers: Engineering Sustainability*, 157(3), pp. 131–138. Available at: <https://doi.org/10.1680/ensu.2004.157.3.131>.
- Raj, A., Sathyan, D. and Mini, K.M. (2019) ‘Physical and functional characteristics of foam concrete: A review’, *Construction and Building Materials*, 221, pp. 787–799. Available at: <https://doi.org/10.1016/j.conbuildmat.2019.06.052>.
- Ramamurthy, K., Kunhanandan Nambiar, E.K. and Indu Siva Ranjani, G. (2009a) ‘A classification of studies on properties of foam concrete’, *Cement and Concrete Composites*, 31(6), pp. 388–396. Available at: <https://doi.org/10.1016/j.cemconcomp.2009.04.006>.
- Ramamurthy, K., Kunhanandan Nambiar, E.K. and Indu Siva Ranjani, G. (2009b) ‘A classification of studies on properties of foam concrete’, *Cement and Concrete Composites*, 31(6), pp. 388–396. Available at: <https://doi.org/10.1016/j.cemconcomp.2009.04.006>.
-

-
- Ranabhat, K. et al. (2016) ‘An introduction to solar cell technology’, *Journal of Applied Engineering Science*, 14(4), pp. 481–491. Available at: <https://doi.org/10.5937/jaes14-10879>.
- Renewable Energy Agency, I. (2020) RENEWABLE CAPACITY STATISTICS 2020 STATISTIQUES DE CAPACITÉ RENOUVELABLE 2020 ESTADÍSTICAS DE CAPACIDAD RENOVABLE 2020. Available at: www.irena.org.
- Renoald, J. et al. (2016) ‘Solar Roadways-The Future Rebuilding Infrastructure and Economy’, *International Journal of Electrical and Electronics Research*, 4(2), pp. 14–19. Available at: https://www.academia.edu/29381719/Solar_Roadways_The_Future_Rebuilding_Infrastructure_and_Economy.
- Shekhar, A. et al. (2015a) ‘Solar road operating efficiency and energy yield - An integrated approach towards inductive power transfer’, *Proceedings of the 31st European Photovoltaic Solar Energy Conference and Exhibition, Hamburg, 14-18 Sept., 2015; Authors version [Preprint]*, (January). Available at: <https://doi.org/10.4229/EUPVSEC20152015-6DP.2.2>.
- Shekhar, A. et al. (2015b) ‘Solar road operating efficiency and energy yield - An integrated approach towards inductive power transfer’, *Proceedings of the 31st European Photovoltaic Solar Energy Conference and Exhibition, Hamburg, 14-18 Sept., 2015; Authors version [Preprint]*, (January). Available at: <https://doi.org/10.4229/EUPVSEC20152015-6DP.2.2>.
- Smith, B.L. et al. (2021) ‘Photovoltaic (PV) Module Technologies : 2020 Benchmark Costs and Technology Evolution Framework Results. Golden, CO: National Renewable Energy Laboratory. NREL/TP-7A40-78173.’, (November).
- Taylor, W.H. (1967) ‘CONCRETE TECHNOLOGY AND PRACTICE, 4/E’.
- Thakur, S.S. et al. (2022) ‘Optimization of Different Mix-Proportions of Foam’, (August).

-
- Thienel, K.C., Haller, T. and Beuntner, N. (2020) 'Lightweight concrete-from basics to innovations', *Materials*, 13(5). Available at: <https://doi.org/10.3390/ma13051120>.
- Thomas, J. and Ramaswamy, A. (no date a) 'Mechanical Properties of Steel Fiber-Reinforced Concrete'. Available at: <https://doi.org/10.1061/ASCE0899-1561200719:5385>.
- Thomas, J. and Ramaswamy, A. (no date b) 'Mechanical Properties of Steel Fiber-Reinforced Concrete'. Available at: <https://doi.org/10.1061/ASCE0899-1561200719:5385>.
- Tyagi, V. V. et al. (2013) 'Progress in solar PV technology: Research and achievement', *Renewable and Sustainable Energy Reviews*, 20(April), pp. 443–461. Available at: <https://doi.org/10.1016/j.rser.2012.09.028>.
- Valore, R.C. (1954) 'Cellular concretes Part 1 composition and methods of preparation', in *Journal Proceedings*, pp. 773–796.
- Vandhiyan, R., Babu, R.B. and Nagarajan, M. (2016) 'A Study on Mechanical Properties of Concrete By Replacing Aggregate With Expanded Polystyrene Beads', *Global Journal of Engineering Science and Researches*, 3(11), pp. 7–13. Available at: <https://doi.org/10.5281/zenodo.192144>.
- Vizzari, D. et al. (2021) 'Pavement energy harvesting technologies: A critical review', *RILEM Technical Letters*, 6, pp. 93–104. Available at: <https://doi.org/10.21809/rilemtechlett.2021.131>.
- Wang, B. et al. (2021) 'A Comprehensive Review on Recycled Aggregate and Recycled Aggregate Concrete', *Resources, Conservation and Recycling*. Elsevier B.V. Available at: <https://doi.org/10.1016/j.resconrec.2021.105565>.
- Wee, T. et al. (2006) 'Air-Void System of Foamed Concrete and its Effect on Mechanical Properties', (103), pp. 45–53.
-

-
- Yang Hong-xing, B. (2016) 'Research and Development of Solar PV Pavement Panels for Application on the Green Deck (Final Report)', (January).
- Zhang, P. et al. (2022) 'A review on the properties of concrete reinforced with recycled steel fiber from waste tires', *Reviews on Advanced Materials Science*. Walter de Gruyter GmbH, pp. 276–291. Available at: <https://doi.org/10.1515/rams-2022-0029>.
- Zia, A. et al. (2022) 'A Comprehensive Review of Incorporating Steel Fibers of Waste Tires in Cement Composites and Its Applications', *Materials*. MDPI. Available at: <https://doi.org/10.3390/ma15217420>.
- Ziemińska-stolarska, A., Pietrzak, M. and Zbiciński, I. (2021) 'Application of LCA to determine environmental impact of concentrated photovoltaic solar panels—state-of-the-art', *Energies*, 14(11), pp. 1–20. Available at: <https://doi.org/10.3390/en14113143>.
- Hannah Ritchie, Max Roser and Pablo Rosado (2022) - "Energy". Published online at OurWorldInData.org. Retrieved from: '<https://ourworldindata.org/energy>' [Online Resource].
- Lee, H.-S., Ismail, M., Woo, Y.-J., Min, T.-B., Choi, H.-K., 2014. Fundamental Study on the Development of Structural Lightweight Concrete by Using Normal Coarse Aggregate and Foaming Agent. *Materials (Basel)*. 7, 4536–4554.
- Hashim, A.A., 2014. The Preparation of Foam Cement and Determining Some of Its Properties 3, 61–69.
- Jones, R., Mccarthy, A., Kharidu, S., Nicol, L., 2005. Foamed concrete developments and applications. *Concr.* 39, 41–43.
- BS EN-12390-5, 2000. Testing Hardend Concrete- Part 5: Flexural Stren- Gth of Test Specimens, British Standards Institution, London,.
- BS EN 12350-6, 2009. Testing fresh concrete - Part 6: Density.

-
- BS EN 12390-3, 2009. Testing hardened concrete- Part 3: Compressive strength of test specimens.
- BS EN 12390-5, 2009. Testing hardened concrete- part 5: Flexural Strength Test. *Constr. Stand.* 2, 1–14. <https://doi.org/10.1006/abio.1994.1569>
- BS EN12390-3, 2002. Testing hardened concrete—Compressive strength of test specimens. British European Standards Specifications.
- BS:EN:1008:2002, 2002. Mixing water for concrete. Specification for sampling, testing and assessing the suitability of water, including water recovered from processes in the concrete industry, as mixing water for concrete. BSI Stand. 3.
- Mohammad, M., 2011. Development of foamed concrete: enabling and supporting design.
- Mohammed, J.H., Hamad, A.J., 2014. A classification of lightweight concrete : materials , properties and application review 7, 52–57.
- Gurjar, A. & Chandak, R. (2013). Properties of Concrete Pavement Slabs. *Journal of Construction Engineering and Management*, 139(12), pp. 04013011-1-04013011-8.
- Neville, A.M. (2011). *Properties of Concrete*. 5th ed. London: Pearson Education Limited.
- Mindess, S., Young, J.F., and Darwin, D. (2003). *Concrete*. 2nd ed. Upper Saddle River, NJ: Prentice Hall.
- ACI Committee 213. (2003). *Guide for Structural Lightweight-Aggregate Concrete (ACI 213R-03)*. American Concrete Institute.
- Callister, W.D. and Rethwisch, D.G. (2018). *Materials Science and Engineering: An Introduction*. 10th ed. New York: John Wiley & Sons.
- Sperling, L.H. (2006). *Introduction to Physical Polymer Science*. 4th ed. Hoboken, NJ: Wiley-Interscience.
-

-
- Dominghaus, H. (2012). *Plastics for Engineers: Materials, Properties, Applications*. 2nd ed. Munich: Hanser Publishers.
- Dunkel, W. (2013). *Acrylic and its Applications*. Berlin: Springer.
- Jayaraman, K. (2003). *Polymeric Materials and their Applications*. Cambridge: Cambridge University Press.
- Dassault Systèmes. (2024). *ABAQUS/Standard User's Manual, Version 2024*. Providence, RI: Dassault Systèmes.
- Neville, A.M. (2011). *Properties of Concrete*. 5th ed. London: Pearson Education Limited.
- Jones, M.R. and McCarthy, A. (2005). "Preliminary views on the potential of foamed concrete as a structural material." *Magazine of Concrete Research*, 57(1), pp. 21-31.
- Dominghaus, H. (2012). *Plastics for Engineers: Materials, Properties, Applications*. Hanser Publishers.
- Hilal, A. A., Thom, N. H., & Dawson, A. R. (2015). The use of foamed concrete in construction: a review. *Proceedings of the Institution of Civil Engineers - Construction Materials*, 168(1), 3-13.
- Jones, M. R., & McCarthy, A. (2005). Preliminary views on the potential of foamed concrete as a structural material. *Magazine of Concrete Research*, 57(1), 21-31.
- Kearsley, E. P., & Wainwright, P. J. (2001). Porosity and permeability of foamed concrete. *Cement and Concrete Research*, 31(5), 805-812.
- Smith, W. F. (2003). *Acrylic Plastic: Properties and Applications*. *Journal of Applied Polymer Science*, 89(1), 56-63.
- Strong, A. B. (2006). *Plastics: Materials and Processing*. Pearson Prentice Hall.
- Yildirim, S. T. (2016). Evaluation of Slip Resistance for Different Pavement Surface Types. *International Journal of Pavement Research and Technology*, 9(3), 206-211.
-

-
- International Energy Agency (IEA). (2021). Cement. Retrieved from <https://www.iea.org/reports/cement>
- ISO 14040. (2006). Environmental management - Life cycle assessment - Principles and framework. International Organization for Standardization.
- Khatib, J. M., & Ellis, D. J. (2001). Mechanical properties of concrete containing foundry sand. ACI Special Publication, 200, 733-748.
- Khatib, J. M., Baig, M. A., Menadi, B., & Kenai, S. (2013). Waste foundry sand usage for building material production: A review. Proceedings of the Institution of Civil Engineers - Construction Materials, 166(6), 331-340.
- Peduzzi, P. (2014). Sand, rarer than one thinks. Environmental Development, 11, 208-218.
- Bathe, K.J. (1996). Finite Element Procedures. Prentice Hall.
- Belytschko, T., Liu, W.K., & Moran, B. (2000). Nonlinear Finite Elements for Continua and Structures. John Wiley & Sons.
- Crisfield, M.A. (1997). Non-linear Finite Element Analysis of Solids and Structures, Volume 1: Essentials. John Wiley & Sons.
- Wriggers, P. (2008). Nonlinear Finite Element Methods. Springer.
- Zienkiewicz, O.C., & Taylor, R.L. (2000). The Finite Element Method: Its Basis and Fundamentals (6th edition). Butterworth-Heinemann.
- Zienkiewicz, O. C. (1971). The Finite Element Method in Engineering Science. McGraw-Hill.
- Bathe, K. J. (1996). Finite Element Procedures in Engineering Analysis. Prentice Hall.
- Hughes, T. J. R. (1987). The Finite Element Method: Linear Static and Dynamic Finite Element Analysis. Prentice Hall.

-
- Zienkiewicz, O. C., & Taylor, R. L. (2005). *The Finite Element Method: Its Basis and Fundamentals*. Butterworth-Heinemann.
- Papadrakakis, M., & Lagaros, N. D. (2002). *Advances in Computational Structural Mechanics*. Saxe-Coburg Publications.
- Jones, M.R. & McCarthy, A. (2005) 'Preliminary views on the potential of foamed concrete as a structural material', *Magazine of Concrete Research*, 57(1), pp. 21-31. doi: 10.1680/macr.2005.57.1.21.
- Kearsley, E.P. & Wainwright, P.J. (2002) 'The effect of high fly ash content on the compressive strength of foamed concrete', *Cement and Concrete Research*, 32(2), pp. 241-246. doi: 10.1016/S0008-8846(01)00665-1.
- American Foundry Society. (2024). Safety Data Sheet for Spent Foundry Sand. Retrieved from American Foundry Society.
- Cioli, F., Abbà, A., Alias, C., & Sorlini, S. (2022). Reuse or Disposal of Waste Foundry Sand: An Insight into Environmental Aspects. *Applied Sciences*, 12(13), 6420. <https://doi.org/10.3390/app12136420>
- Elangovan, R. (2019). Strength properties of fibre-reinforced self-consolidating concrete with foundry waste sand. *International Journal of Innovative Technology and Exploring Engineering*, 8(10), 1530-1538.
- Sandhu, R. K., & Siddique, R. (2019). Strength properties and microstructural analysis of self-compacting concrete incorporating waste foundry sand. *Construction and Building Materials*, 225, 371-383.
- Zienkiewicz, O.C., Taylor, R.L. and Zhu, J.Z. (2013). *The Finite Element Method: Its Basis and Fundamentals*. 7th ed. Oxford: Butterworth-Heinemann.
-

-
- Liu, Y., & Zhang, W. (2023). The future of landscape lighting: An analysis of solar bricks as a sustainable solution. *Journal of Renewable Energy Research*, 15(3), 455-467.
- Patel, S., & Kumar, R. (2021). Challenges in the adoption of solar paver technologies: A comprehensive review. *International Journal of Sustainable Urban Development*, 12(1), 78-91.
- Sharma, R., Gupta, A., & Patel, S. (2022). Evaluating the effectiveness of solar garden lights in reducing energy consumption and carbon emissions. *International Journal of Sustainable Energy*, 10(2), 230-240
- Ardani, K., Davidson, C., Margolis, R., & Nobler, E. (2021). Challenges and opportunities for solar pavements: A review. *Renewable and Sustainable Energy Reviews*, 146, 111194.
- Baiju, S., & Yarema, N. (2022). Solar pavements: Integrating renewable energy technology into urban infrastructure. *Energy Reports*, 8, 123-135.
- Erdiwansyah, H., Sani, A., & Ridwan, D. (2020). The potential and development of solar pavement technology in urban environments. *Journal of Clean Energy Technologies*, 8(2), 99-107.
- Renewable Energy World. (2014). Netherlands debuts world's first solar bike path. Retrieved from Renewable Energy World.
- TNO. (2013). Solar road: An innovative energy solution. Retrieved from TNO.
- Neville, A. M. (2011). *Properties of Concrete* (5th ed.). Pearson Education Limited.
- Pacheco-Torgal, F., Cabeza, L. F., Labrincha, J., & de Magalhães, A. G. (2013). *Eco-Efficient Concrete*. Woodhead Publishing.
- Narayanan, N., & Ramamurthy, K. (2000). Structure and properties of aerated concrete: A review. *Cement and Concrete Composites*, 22(5), 321-329.
- Patel, S., & Kumar, R. (2021). Challenges in the adoption of solar paver technologies: A comprehensive review. *International Journal of Sustainable Urban Development*, 12(1), 78-91.
-

-
- Smith, J., & Lee, H. (2022). Design and performance constraints of solar paver systems in urban landscapes. *Energy and Environmental Design Journal*, 18(4), 299-310.
- Liu, Y., & Zhang, W. (2023). The future of landscape lighting: An analysis of solar bricks as a sustainable solution. *Journal of Renewable Energy Research*, 15(3), 455-467.
- Erdiwansyah, H., Sani, A., & Ridwan, D. (2020). The potential and development of solar pavement technology in urban environments. *Journal of Clean Energy Technologies*, 8(2), 99-107.
- Northmore, J. & Tighe, S. (2012). Innovative strategies for sustainable pavements: Integrating solar technology into pavement structures. *Transportation Research Record: Journal of the Transportation Research Board*, 2305(1), 21-28.
- Ardani, K., Davidson, C., Margolis, R., & Nobler, E. (2021). Challenges and opportunities for solar pavements: A review. *Renewable and Sustainable Energy Reviews*, 146, 111194.
- Baiju, S., & Yarema, N. (2022). Solar pavements: Integrating renewable energy technology into urban infrastructure. *Energy Reports*, 8, 123-135.
- Erdiwansyah, H., Sani, A., & Ridwan, D. (2020). The potential and development of solar pavement technology in urban environments. *Journal of Clean Energy Technologies*, 8(2), 99-107.
- Shekhar, R., Kumar, P., & Prakash, D. (2015). Evaluation of solar pavements in urban road infrastructure. *International Journal of Energy and Environmental Engineering*, 6(3), 213-220
- IPCC. (2021). *Climate Change 2021: The Physical Science Basis*. Intergovernmental Panel on Climate Change. Available at: <https://www.ipcc.ch/report/ar6/wg1/> [Accessed 27 August 2024].
- United States Environmental Protection Agency (EPA). (2022). *Air Pollution Emissions Overview*. Available at: <https://www.epa.gov/air-emissions-inventories/air-pollutant-emissions-trends-data> [Accessed 27 August 2024].
-

-
- World Health Organization (WHO). (2020). Ambient (Outdoor) Air Pollution. Available at: [https://www.who.int/news-room/fact-sheets/detail/ambient-\(outdoor\)-air-quality-and-health](https://www.who.int/news-room/fact-sheets/detail/ambient-(outdoor)-air-quality-and-health) [Accessed 27 August 2024].
- de Lima, C.H., Ghisolfi, R.D. and de Oliveira, L.B. (2020). 'Solar roadways and solar roofs: A comparative analysis of innovative ideas to integrate solar energy into the transportation infrastructure', *Renewable and Sustainable Energy Reviews*, 110, pp. 278-289.
- Energy Saving Trust. (2020). Solar panels (PV). Available at: <https://energysavingtrust.org.uk/advice/solar-panels/> [Accessed 27 August 2024].
- IEA. (2021). *Solar Energy: Mapping the Road Ahead*. International Energy Agency. Available at: <https://www.iea.org/reports/solar-energy>.
- IPCC. (2021). *Climate Change 2021: The Physical Science Basis*. Intergovernmental Panel on Climate Change. Available at: <https://www.ipcc.ch/report/ar6/wg1/>.
- IRENA. (2021). *Renewable Capacity Statistics 2021*. International Renewable Energy Agency. Available at: <https://www.irena.org/publications/2021/March/Renewable-Capacity-Statistics-2021>.
- REN21. (2022). *Renewables 2022 Global Status Report*. Renewable Energy Policy Network for the 21st Century. Available at: <https://www.ren21.net/reports/global-status-report>
- Schoenenberger, C.A. (2019). 'Innovative solar technologies for sustainable urban development', *Journal of Cleaner Production*, 235, pp. 1231-1240.
- United Nations Framework Convention on Climate Change (UNFCCC). (2015). *The Paris Agreement*. Available at: <https://unfccc.int/process-and-meetings/the-paris-agreement/the-paris-agreement>.
-

-
- Fthenakis, V., & Kim, H. C. (2019). 'Life cycle assessment of photovoltaic systems: Comparison of crystalline silicon and thin-film technologies', *Renewable and Sustainable Energy Reviews*, 13(3), pp. 1465-1475.
- International Energy Agency (IEA). (2021). *World Energy Outlook 2021*. Available at: <https://www.iea.org/reports/world-energy-outlook-2021> [Accessed 27 August 2024].
- Müller, A., Wambach, K., & Alsema, E. (2020). 'Recycling of photovoltaic panels: Current status and future perspectives', *Renewable Energy*, 41(1), pp. 9-15.
- Energy Saving Trust. (2023). *Benefits of Solar Panels*. Retrieved from <https://www.energysavingtrust.org.uk>
- International Energy Agency. (2020). *Renewables 2020: Analysis and Forecast to 2025*. Retrieved from <https://www.iea.org/reports/renewables-2020>
- International Renewable Energy Agency. (2021). *Renewable Power Generation Costs in 2021*. Retrieved from <https://www.irena.org/publications>
- Kalogirou, S. (2014). *Solar Energy Engineering: Processes and Systems*. 2nd ed. Academic Press.
- National Renewable Energy Laboratory. (2022). *The Environmental Benefits of Solar Energy*. Retrieved from <https://www.nrel.gov>
- Office of Energy Efficiency & Renewable Energy. (2020). *Solar Energy Technologies Office*. U.S. Department of Energy. Retrieved from <https://www.energy.gov/eere/solar/solar-energy-technologies-office>
- Sharma, P. (2019). *Large-Scale Solar Power System Design (GreenSource Books)*. McGraw Hill Professional.
- Solar Energy Industries Association. (2022). *Canopy Solar Panels: An Overview*. Retrieved from <https://www.seia.org>
-

U.S. Department of Energy. (2021). Solar Energy in the United States. Retrieved from <https://www.energy.gov/eere/solar/solar-energy-united-states>

Zillow. (2019). Solar Panels and Home Values: How They Impact the Market. Retrieved from <https://www.zillow.com/research/solar-panels-house-value-23798>

(Ali, K. A., Ahmad) M. I., & Yusup, Y. (2020). Issues, impacts, and mitigations of carbon dioxide emissions in the building sector. *Sustainability* (Switzerland), 12(18). <https://doi.org/10.3390/SU12187427>

BP. (2023). Statistical Review of World Energy 2023. Retrieved from <https://www.bp.com>

Global Alliance for Buildings and Construction. (2020). 2020 Global Status Report for Buildings and Construction. Retrieved from <https://globalabc.org>

Global Methane Initiative. (2020). Methane Emissions and Mitigation Opportunities. Retrieved from <https://www.globalmethane.org>

Intergovernmental Panel on Climate Change (IPCC). (2021). Climate Change 2021: The Physical Science Basis. Retrieved from <https://www.ipcc.ch>

International Energy Agency (IEA). (2020). Energy Technology Perspectives 2020. Retrieved from <https://www.iea.org/reports/energy-technology-perspectives-2020>

United Nations Environment Programme. (2021). 2021 Emissions Gap Report. Retrieved from <https://www.unep.org/resources/emissions-gap-report-2021>

BBC (2021) France's solar road experiment has not gone as planned. Available at: www.bbc.co.uk

Gao, X., Zhang, H. and Liu, J. (2018) 'Recent advances in solar energy applications in transportation infrastructure', *Sustainable Cities and Society*, 72, p. 103026.

International Energy Agency (IEA) (2021) Renewables 2021 Global Status Report. Available at: www.iea.org

-
- International Energy Agency (IEA) (2022) Solar PV Global Report. Available at: www.iea.org
- International Renewable Energy Agency (IRENA) (2021) World Energy Transitions Outlook 2021. Available at: www.irena.org
- Kostopoulos, E., Zygomalas, I. and Stathopoulos, T. (2018) 'Solar roads: Challenges, feasibility, and future applications', *Renewable and Sustainable Energy Reviews*, 97, pp. 38-50.
- Liu, C., Wang, C. and Zhang, Y. (2012) 'Photovoltaic road systems: Performance analysis and applications', *Energy and Buildings*, 49, pp. 429-436.
- Popular Mechanics (2019) France's ambitious solar road has turned into a colossal failure. Available at: www.popularmechanics.com
- Ranabhat, K., Shrestha, P. and Park, C. (2016) 'A review on the recent development of solar photovoltaic technologies', *Renewable and Sustainable Energy Reviews*, 67, pp. 1046-1060.
- Ritchie, H. and Roser, M. (2018) *Renewable Energy*. Available at: www.ourworldindata.org
- Smith, J., Patel, D. and Green, M. (2021) 'Advancements in high-efficiency solar panels and their implications for global energy generation', *Journal of Solar Energy Research*, 12(4), pp. 214-230.
- The Guardian (2016) France opens world's first solar panel road. Available at: www.theguardian.com
- Xie, H., Ma, S., Zhang, Q. and Sun, Y. (2019) 'Advances in solar-powered road technology: A review', *Energy Reports*, 5, pp. 822-836.
- Zhang, Y., Huang, Y. and Bird, R. (2020) 'Solar pavement technology: Current status and future prospects', *Transportation Research Part D: Transport and Environment*, 97, p. 102945.

-
- Ziemińska-Stolarska, A., Pietrzak, K. and Zbiciński, I. (2021) 'Analysis of environmental impacts of solar energy systems: A life cycle assessment approach', *Environmental Impact Assessment Review*, 91, p. 102383.
- Buswell, R. A., Soar, R. C., Gibb, A. G., & Thorpe, A. (2018) 'Freeform construction: Mega-scale rapid manufacturing for construction', *Automation in Construction*, 16(2), pp. 224-231.
- De Belie, N., Gruyaert, E., Al-Tabbaa, A., et al. (2018) 'A review on self-healing concrete for durable pavement applications', *Construction and Building Materials*, 197, pp. 1156-1171.
- Graybeal, B. (2014) *Ultra-High Performance Concrete*. Washington, DC: FHWA.
- Mehta, P. K. and Monteiro, P. J. M. (2014) *Concrete: Microstructure, Properties, and Materials*. 4th edn. New York: McGraw-Hill.
- Pomerantz, M., Akbari, H. and Harvey, J. (2000) 'Cool Pavements: Reflective Technologies', *Energy and Buildings*, 32(3), pp. 195-207.
- Tayabji, S. and Lim, S. (2006) *Concrete Pavement Technology and Research Program*. Federal Highway Administration.
- Van Dam, T., Taylor, P., Smith, K., et al. (2015) *Recycling Concrete Pavements*. National Concrete Pavement Technology Center.

Appendix A

The basic calculation for three mortar solid slabs in (Kg) and (Volume)

	The density of concrete mortar		2162		kg/m ³
	Plastic density of foamed concrete required =		1400		kg/m ³
	Concrete test slab	L	400		mm
		B	400		mm
		D	50		mm
Volume		8000000	mm ³ or	0.008	m ³
	Density = Mass /Volume ∴ Mass = D x V =	11.20	kg		
1. First calculate how much concrete is needed:					
Assume that 6 x solid slabs are needed only.					
	Volume of concrete needed	0.024	m ³	3	x solid slab
	∴ Mass of concrete needed = DxV =	33.60	kg		
	+ 0% wastage	0	kg	0%	
	∴ Total mass of concrete required	33.60	kg		

Concrete ratio	Cement (Kg)	Sand (Kg)	Water to cement ratio (mass)	Volume of 3 slabs (kg/m) ³	Typical weight of 3 slabs (Kg)
Mixing Ratio	1/3	2/3	0.17	N/A	N/A
Mass	11.20	22.40	5.60	N/A	33.60
Volume	0.008	0.016	0.0056	0.024	N/A
Material ratio (%)	Cement (kg)	Sand (kg)	Water to cement ratio (mass)	Recycle Materials (Kg)	slab (mass)
100%	11.20	22.40	5.6	0.00	33.60
50%	11.20	11.20	5.75	11.20	33.60

W/C	50%					
Specific cement gravity	3.15					
The specific gravity of sand	2.65					
Unit weight of water	1000	kg/m ³				
Unit weight of foam	45	kg/m ³				
Total mass of raw materials(0.024 m³ x 1200 kg/		0.024	1400		33.60	
Material	Weight	Calculation			Volume	
Cement	9.600	3622.6			0.0036	
Sand	19.200	7245.3			0.0072	
Water	4.800	4800			0.0048	
Total					0.0157	
Total volume of cement, water and sand					0.0157	
Air volume required			0.024	0.0157	0.0083	m ³
The air content in foam produced by Propump 26 foaming agent is			95%			
Therefore					8.7706	L
The amount of foaming agent required to produce 27L of foam is					0.0074	L
The amount of water required to produce 27L of foam is					0.3947	L
To make foam dilute Foaming Agent by 4% in water, e.g. 40 ml per 1 litre of water, to make a solution.						

Appendix B

Example Calculation of Carbon Footprint

For a mortar mixture containing 10 kg of waste foundry sand, 10 kg of river-washed sand, and 9 kg of Portland cement, calculate the carbon footprint using UK-specific data:

1. **Portland Cement:** Producing 1 kg of cement emits approximately 0.9 kg of CO₂ (International Energy Agency, 2021). Therefore, 9 kg of cement emits:

$$\underline{9 \text{ kg} \times 0.9 \text{ kg CO}_2/\text{kg} = 8.1 \text{ kg CO}_2}$$

2. **River-Washed Sand:** Assuming the extraction and processing of 1 kg of river-washed sand emits approximately 0.005 kg of CO₂ (based on general industry data). Therefore, 10 kg of sand emits:

$$\underline{10 \text{ kg} \times 0.005 \text{ kg CO}_2/\text{kg} = 0.05 \text{ kg CO}_2}$$

3. **Waste Foundry Sand:** Waste foundry sand, being a recycled by-product, has a much lower carbon footprint. Assuming it emits approximately 0.002 kg of CO₂ per kg:

$$\underline{10 \text{ kg} \times 0.002 \text{ kg CO}_2/\text{kg} = 0.02 \text{ kg CO}_2}$$

Total Carbon Footprint

$$8.1 \text{ kg CO}_2 \text{ (cement)} + 0.05 \text{ kg CO}_2 \text{ (river washed sand)} + 0.02 \text{ kg CO}_2 \text{ (waste foundry sand)} \\ = \underline{8.17 \text{ kg CO}_2}$$

This total carbon footprint of **8.17 kg CO₂** represents the emissions associated with producing the specified mortar mixture.

Appendix C

Solar panel manual energy production calculation

To determine if the Colossal 6V 9W Solar Panel can power a 3V Bright White LED Strip (120 cm) for 14 hours using the Adafruit Universal USB/ DC/ Solar Lithium Ion/Polymer Charger (bq24074), the RS PRO 3.7V Lithium-Ion Rechargeable Battery Pack (7.8Ah), and the Adafruit Trinket 3.3V MCU Development Board, follow these steps:

1. Solar Panel Output and Charging Efficiency

1. Solar Panel Output:

The solar panel provides 6V at 1.5A, resulting in 9W of power under optimal conditions.

2. Battery Charging Calculation

2. Daily Energy Production:

Assume the panel gets 5 peak sun hours per day (this can vary based on location):

Energy Produced Daily = $9W \times 5\text{hours} = 45Wh$

3. Charger Efficiency:

The bq24074 charger is quite efficient but not perfect. Assuming an efficiency of 90%:

Usable Energy = $45Wh \times 0.9 = 40.5Wh$

3. Battery Storage Calculation

To store this energy, we use the RS PRO 3.7V 7.8Ah battery pack. First, convert the energy to ampere-hours at 3.7V:

Energy in Ah = $40.5Wh / 3.7V = 10.95Ah$

The battery pack can store up to 7.8Ah, so in ideal conditions, it can be fully charged over multiple days, considering the daily energy input.

4. LED Strip Power Consumption

4. Power Requirement for 14 Hours:

The LED strip consumes 4.32W:

Total Energy Required = $4.32W \times 14h = 60.48Wh$

Convert this to ampere-hours at 3.7V:

Energy in Ah = $60.48Wh/3.7V = 16.35Ah$

5. Powering the LED Strip

To determine if the system can sustain the LED strip for 14 hours:

1. **Daily Charge Accumulation:** The solar panel provides 10.95Ah per day.
2. **Battery Capacity:** Each battery pack provides 7.8Ah, requiring 3 packs for 21.26Ah total capacity.

6. Conclusion

Daily Energy Balance:

- **Energy Produced Daily:** 40.5Wh
- **Daily Energy Needed:** 60.48Wh (for 14 hours of LED use)

Since the energy produced daily (40.5Wh) is less than the energy needed (60.48Wh), the system can only partially power the LED strip daily.

Sufficient Storage Capacity: However, with enough battery storage (21.26Ah total capacity from 3 battery packs), the LED strip can run for 14 hours:

- **Stored Energy:** 78.66Wh (21.26Ah * 3.7V)

This stored energy can power the LED strip for more than a day, but the system will need to accumulate this energy over multiple days of good sunlight to balance out the power consumption.

Appendix D

Waste foundry sans analysis form **William Lee Ltd** Callywhite Lane Dronfield

S18 2XU



Advanced Manufacturing Park,
Brunel Way, Rotherham, S60 5WG, UK
Tel: +44 (0)114 2541 144
UKAS Testing Laboratory No 0144

Analysis of foundry waste against:

Council of the European Union Decision (2003/33/EC)

Establishing criteria and procedures for the acceptance of
waste at landfills pursuant to Article 16
of and Annex II to Directive 1999/31/EC

for
William Lee Ltd

19 October 2018

Cti Ref: E69590

Customer ref: WL/24758-3.1

Jon Donohoe
Castings Technology International



Advanced Manufacturing Research Centre
Castings Technology International Ltd
Registered in England and Wales No 0521295

Page 1 of 2

Analysis of Waste Streams from William Lee Ltd

1. Introduction

These samples were taken by William Lee Ltd and submitted to Cti for analysis. The samples were analysed in accordance with the Waste Acceptance criteria both as received and to BSEN12457-3 for leachable materials in the waste stream.

2. Results of testing

2.1 HWS

2.1.1 Sample as received

Determination	Units	Analysis	Limit Value		
			Inert Waste Landfill	SNRHW in non-hazardous landfill ¹	Hazardous Waste Landfill
Total Organic Carbon	%	4.82*	3	5	6
Loss on ignition	%	6.15	-	-	10
BTEX	mg/kg	-	6	-	-
PCB	ug/kg	<0.021	1000	-	-
Mineral Oil	mg/kg	257	500	-	-
PAH	mg/kg	<10	100	-	-
pH	pH Units	9.94	-	>6	-

2.1.2 Leachates

Determination	Units	Analysis	Limit Value		
			Inert Waste Landfill	SNRHW in non-hazardous landfill ¹	Hazardous Waste Landfill
Antimony	mg/kg	<0.01	0.06	0.7	5
Arsenic	mg/kg	0.101	0.5	2	25
Barium	mg/kg	0.0273	20	100	300
Cadmium	mg/kg	<0.0008	0.04	1	5
Chromium	mg/kg	<0.01	0.5	10	70
Copper	mg/kg	0.0118	2	50	100
Lead	mg/kg	0.00294	0.5	10	50
Molybdenum	mg/kg	0.196	0.5	10	30
Nickel	mg/kg	<0.004	0.4	10	40
Selenium	mg/kg	<0.01	0.1	0.5	7
Zinc	mg/kg	0.0216	4	50	200
Mercury	mg/kg	0.000336	0.01	0.2	2
Chloride	mg/kg	111	800	15000	25000
Fluoride	mg/kg	19.9*	10	150	500
Sulphate	mg/kg	226	1000	20000	50000
Dissolved Organic Carbon	mg/kg	113	500	800	1000
Total Dissolved Solids	mg/kg	2700	4000	60000	100000
Phenols Monohydric	mg/kg	5.2*	1	-	-

* Exceeds Limit for inert waste
¹SNRHW is Stable, non-reactive, hazardous waste.

Jon Donohoe
 Manager: Cti Environmental
 19 October 2018